JYVÄSKYLÄ STUDIES IN COMPUTING
117

Keijo Mattila

Implementation Techniques for the Lattice Boltzmann Method

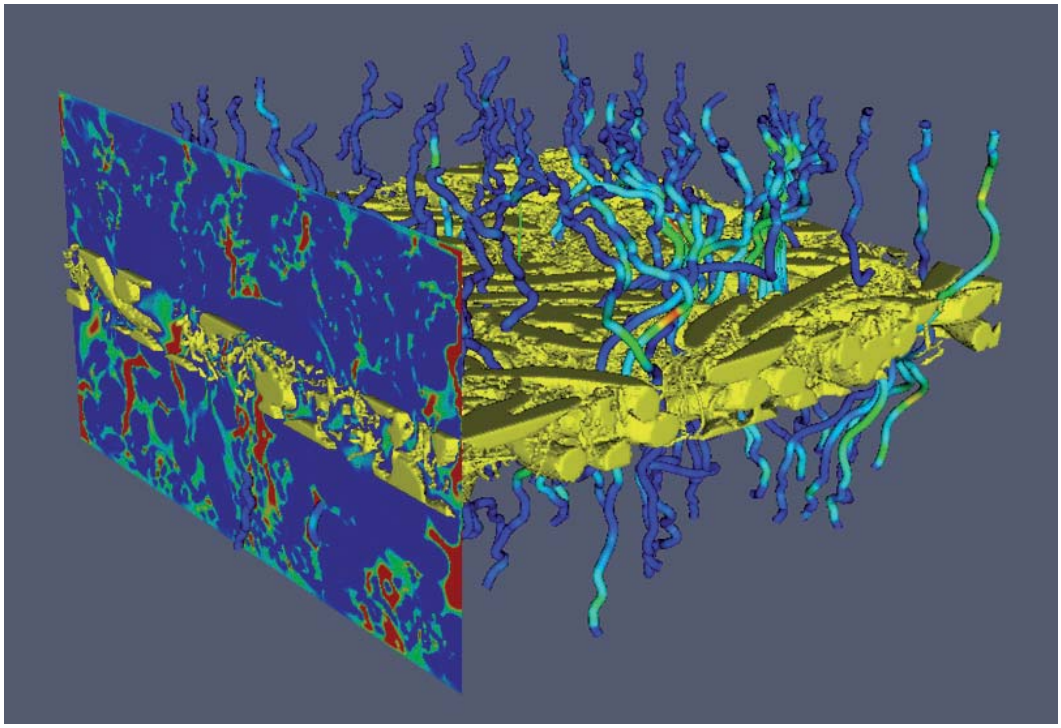

JYVÄSKYLÄN YLIOPISTO

JYVÄSKYLÄ STUDIES IN COMPUTING 117

Keijo Mattila

Implementation Techniques for the Lattice Boltzmann Method

Esitetään Jyväskylän yliopiston informaatioteknologian tiedekunnan suostumuksella
julkisesti tarkastettavaksi yliopiston vanhassa juhlasalissa S212
elokuun 28. päivänä 2010 kello 12.

Academic dissertation to be publicly discussed, by permission of
the Faculty of Information Technology of the University of Jyväskylä,
in Auditorium S212, on August 28, 2010 at 12 o'clock noon.

UNIVERSITY OF JYVÄSKYLÄ

JYVÄSKYLÄ 2010

Implementation Techniques for the Lattice Boltzmann Method

JYVÄSKYLÄ STUDIES IN COMPUTING 117

Keijo Mattila

Implementation Techniques for the Lattice Boltzmann Method

UNIVERSITY OF JYVÄSKYLÄ

JYVÄSKYLÄ 2010

Editor
Timo Männikkö
Department of Mathematical Information Technology, University of Jyväskylä
Pekka Olsbo, Sini Rainivaara
Publishing Unit, University Library of Jyväskylä

Cover picture: Velocity field of a simulated flow through a porous material.
Picture by Viivi Koivu and Keijo Mattila.

URN:ISBN:978-951-39-3991-5
ISBN 978-951-39-3991-5 (PDF)

ISBN 978-951-39-3973-1 (nid.)
ISSN 1456-5390

Jyväskylä University Printing House, Jyväskylä 2010

ABSTRACT

Mattila, Keijo
Implementation techniques for the lattice Boltzmann method
Jyväskylä: University of Jyväskylä, 2010, 177 p.(+included articles)
(Jyväskylä Studies in Computing
ISSN 1456-5390; 117)
ISBN 978-951-39-3991-5 (PDF), 978-951-39-3973-1 (nid.)
Finnish summary
Diss.

In the field of computational fluid dynamics, a variety of numerical methods have been constructed with the aim at computer simulations of flow phenomena. Some of these methods rely on a microscopic description of fluid flows, others are based on the macroscopic modelling perspective. The separation between these two extreme scales allows an intermediate, so-called mesoscopic description for the dynamic behaviour of fluids. The topic of this thesis, the lattice Boltzmann method, is a particular computational method based on a mesoscopic description. Equipped with a computer science perspective, we treat here specific aspects of the lattice Boltzmann method. Namely, we focus on boundary conditions and implementation techniques: the so-called mass-flux-based approach for boundary conditions, the swap-algorithm, and the bundle data layout, all of which have already been presented in our recent publications, are here reviewed. Moreover, we apply a systematic approach to implementing hydrodynamic boundary conditions for the method. This approach allows us to recover some of the well-known boundary condition implementations, as well as to derive alternative new implementations. A large part of this thesis is devoted to the physical background of the lattice Boltzmann method, as well as to a review of its basic properties.

Keywords: mathematical modelling, fluid dynamics, computer simulations, mesoscopic methods, kinetic theory of gases, the Boltzmann equation, the lattice Boltzmann method, boundary conditions, implementation techniques, high-performance computing, algorithms, data structures

Author

Keijo Mattila
Department of Mathematical Information Technology
University of Jyväskylä
Finland

Supervisors

Professor Tuomo Rossi
Department of Mathematical Information Technology
University of Jyväskylä
Finland

Professor Jussi Timonen
Department of Physics
University of Jyväskylä
Finland

Reviewers

Professor Mikko Karttunen
Department of Applied Mathematics
The University of Western Ontario
Canada

Priv. -Doz. Dr. Jens Harting
Department of Applied Physics
Eindhoven University of Technology
The Netherlands

Opponent

Professor Bastien Chopard
Department of Computer Science
University of Geneva
Switzerland

ACKNOWLEDGEMENTS

I started my graduate studies in February 2004. Ever since I have been working at the Department of Physics – an exciting environment for a computer scientist. Here I have been a member of the Soft Condensed Matter and Statistical Physics research group. As a member of the group, I have had the opportunity to work closely with physicists. For this opportunity I am grateful to my supervisors Professor Tuomo Rossi and Professor Jussi Timonen. Imagination and an enterprising frame of mind are characteristics of a scientist: this is the lesson which I will always remember from the two of you. During the period of past six years, my studies have been financially supported by the Finnish Funding Agency for Technology and Innovation (Tekes), Graduate School in Computing and Mathematical Sciences (COMAS), and Academy of Finland. The above funding is thankfully acknowledged.

Along the way, I have been influenced by many. I am indebted to Docent Antti Koponen, as well as to Dr. Pasi Raiskinmäki, for their guidance at the beginning of my studies. In the everyday research work, Dr. Jari Hyväluoma has been my tutor and a colleague. Jari, discussions with you have been important to me: thank you for everything! I am also grateful to Professor Timo Tiihonen for his constructive comments about the draft of this thesis. Collaborations with Professor Jan Westerholm, Dr. Mats Aspnäs, and Dr. Amos Folarin were definitely highlights of my research work. The research work has also involved conferences, courses, and seminars abroad. There I have met many interesting people: especially I like to mention Lilit, Luiz, Rodrigo, Yohei, and Jörg. Together we experienced the spectacular Hong Kong, visited the vineyard in Geneva, stood on the glacier in Banff, and sailed along the beaches of Florianópolis; these journeys gave me memories for life. Antti, Jari, Sami, Tuomas: thank you for travelling with me!

It has not been difficult to find friends in the the Department of Physics. Above all, Viivi, I have enjoyed working with you, but it is the sparkling temper of yours which is truly refreshing – your spirited presence is always a delight! All the members of rooms FL125 and FL348 have also been part of my life here: thank you for sharing the working days. But, at the end of the day, work is only the other side of my life. The time off I share, first and foremost, with my family. It is inspirational to me that, thanks to the happy encounter two years ago, my family is now bigger than ever before. Saara, you brought music into my life, and I like the melody.

Jyväskylä, August 2010

Keijo Mattila

LIST OF FIGURES

LIST OF TABLES

CONTENTS

LIST OF INCLUDED ARTICLES

PI Mattila K, Hyväluoma J, Rossi T, Aspnäs M, and Westerholm J. An efficient swap algorithm for the lattice Boltzmann method. *Computer Physics Communications*, **176** *(3): 200–210*, 2007.

PII Mattila K, Hyväluoma J, Timonen J, and Rossi T. Comparison of implementations of the lattice-Boltzmann method. *Computers and Mathematics with Applications*, **55** *(7): 1514–1524*, 2008.

PIII Mattila K, Hyväluoma J, Folarin AA, and Rossi T. A boundary condition for arbitrary shaped inlets in lattice-Boltzmann simulations. *International Journal for Numerical Methods in Fluids*, **63** *(5): 638–650*, 2010.

PIV Mattila K, Hyväluoma J, and Rossi T. Mass-flux-based outlet boundary conditions for the lattice Boltzmann method. *Journal of Statistical Mechanics: Theory and Experiment, P06015*, 2009.

The author of this thesis wrote the first drafts of the articles with the exception of the Code optimization section in the article [PI]. The author implemented the computational softwares related to the four articles, and carried out the numerical experiments – again with the exception of the aforementioned Code optimization section.

It's strange that by looking into yourself you really get an appreciation of the mystery of the universe. You don't by trying to find the laws of physics.

J. Backus

PREFACE

The world is a miracle. Its sheer existence tickles our curious mind. Questions related to the existence, however, are often so philosophical or abstract that many will refrain from the speculation. It is rather the small wonders around us, taking place everyday and everywhere, which truly poke our mind. Consider water in liquid state for example – we are surrounded by it. Whenever conditions are favourable, this vital substance can transform into solid ice or gaseuos vapour. The transformed substance is still water, but the state of the matter has changed: consequences to the properties of water are remarkable. We can drill holes to an ice cube or chop pieces from it, but the same actions are impossible for a volume of liquid water. Have you ever considered why? The next observation is baffling too: pure steam, meaning gaseuos water under specific conditions, occupies approximately 1600 times the volume of an equal mass of liquid water. Hence, when a large bucket of water, amounting to say twenty litres in volume, is converted into steam in normal conditions, the steam will occupy roughly 32 cubic metres of space – a roomful of gaseous water. The list of facts equally peculiar, but obvious at the same time, is endless.

As we acknowledge enough of cases like the ones above, we are compelled to ask a question. Is there a fundamental explanation for all the facts we have observed? The individuals most eager to understand will join the scientic community; they have an irresistible urge to seek answers. Unfortunately answers are hard to find, and scientists have to be both very persistent and imaginative since they will confront a paradox: every time an explanation is found, more profound questions are asked, and it appears as if our research takes us farther away from the ultimate truth, not closer. There is no need to be overly depressed by this vicious circle. Science is certainly more than a hunt for the Holy Grail of knowledge explaining everything. It is possible to find answers to problems in reality by an apparently simple procedure: first of all, commit to a particular level of analysis, then collect information on that level, use the information to develop a theory, and finally deduce immediate or subtle consequences of that theory. This *deduction from phenomena* is a way to practise science. In the materials science research scientists try to understand the composition of matter, and particularly its ramifications to the behaviour of matter in specific circumstances. We have indirectly taken part, with a minor role, in such a quest for knowledge.

We offer here an expedition to the frontier of science which, unknown to public and mysterious to most, has occupied our attention in recent times. Specifically, we explore the territory of the lattice Boltzmann method – a patch in the field of computational fluid dynamics. Scientists in the field of fluid dynamics devote their efforts to advance our understanding about fluid behaviour. When scientists harness computers for the same objective, by using computational methods as mediators between the man and a machine, they operate in the branch of computational fluid dynamics. Equipped with a computer science perspective, we have spent some time on investigating and further developing detailed as-

pects of the lattice Boltzmann method: a particular computational method. Here we elaborate these efforts and, above all, give them a context. Let us lay a foundation for the context by borrowing words so vividly stating the principle of modern science:

> The molecular hypothesis has been maintained, in one form or another, by various philosophers for the last 2300 years; but the reasoning of the ancients, on this subject at least, is so extremely subtle and nebolous that it has no value whatever for modern purposes. Nowadays the physicist requires us to state our assumption very clearly, and to deduce from them their necessary consequences. He will then compare these consequences with the observed facts, and if the two are in perfect agreement he will accept our assumptions provisionally, and will believe in our theory until some one can show that we overlooked some absurd things that could be deduced from our premises, or until somebody brings forward another theory that is just as good as ours, or perhaps better. Although this modern spirit of doubt is rather hard on the "man with a theory," it is nevertheless quite logical. It prevents us from being swamped by a multitude of unsound theories, and enables us to distinguish the grain from the chaff. You will agree with me, therefore, when I say that the real, healthy growth of the molecular theory of matter began when attempts were made to obtain *numerical results* from it.

Nothing needs to be added to or removed from this perceptive account. The writing is approximately one hundred years old dating back to the latest golden era of science; author *A.D. Risteen* wrote it at the beginning of his book *Molecules and the Molecular Theory of Matter*, published in 1895 [Ris95]. The message conveyed is deceptively trivial, at least for those involved with science. The truth of the matter is that the message is profound, rich, and deserves to be remembered at all times. It illustrates how resilient important philosophical ideas can be: they survive millennia. Simultaneously, it demonstrates how long it may take to advance from a philosophical hypothesis to a scientific theory. It also suggests that contemporary applications of science require evermore minute explanations for the nature.

The message continues: it makes a distinction between philosophy and science by implying that the latter ultimately strives for predictive power with concrete results, often numbers, whereas the former is rather oriented to improve our comprehension. It thus positions philosophy to a more abstract level of thinking, just adjacent to science (see Fig. 1). Finally it implies, rightfully, that in science 'laws of nature' are constantly proposed, extended, modified, and even cancelled. An author of a scientific theory is not shamed when the theory is outdated by subsequent findings. On the contrary, the author is honoured. Moreover, a successful scientific work does not necessarily have an immediate, direct or indirect, influence on real life. To expect the contrary is as naive as to presume moral statement from every book, to consider music not played for dancing purposeless, or to re-

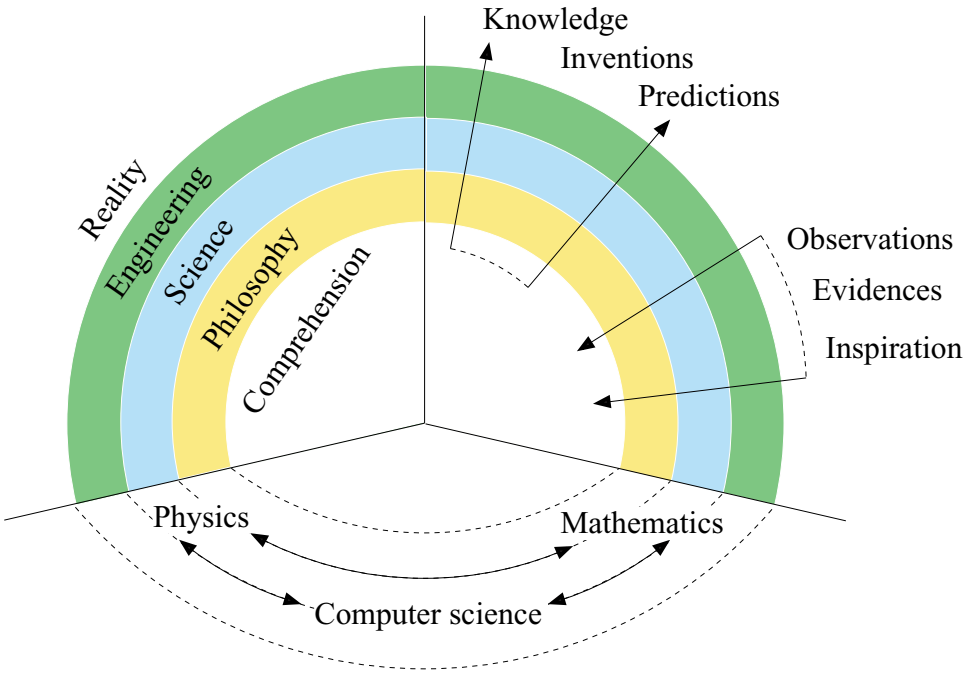

FIGURE 1 Science is a scheme of things: more abtract than engineering but less abstract than philosophy. The three disciplines, physics, mathematics, and computer science, can be practised with a mindset from any of the aforementioned abstraction levels.

gard only landscapes and portraits as fine art. Many scientific works are invisible to public, and remain so forever. Some works do not lead to progress at all, not even progress internal to science, but they can still be fruitful as they can exclude specific research directions from the set of promising ones. In short, the principal aim of science is to increase our understanding. In this role science is one of the three cultural pillars: it stands beside religion and art. It answers to the primitive urges of human race with equal conviction.

In a scientific work, we have to carefully state the kind of mental leaps required to follow our otherwise rigorous treatment of the subject, and we have to very precisely explain under which conditions our arguments are valid. That is, underlying hypotheses and fundamental assumptions related to our work must be unambiguously stated. This is exactly what we aim to do here. Our efforts with the lattice Boltzmann method can be categorised equally well into computational physics, applied mathematics, and scientific computing. They are nothing but names for the broad field of research where the three disciplines, physics, mathematics, and computer science, get together. In our efforts the perspective of computer science is emphasised more than the others. The three disciplines can all be practised at various levels of abstraction. Sometimes they are practised at a level which is closer to philosophy and every now and then the level is closer to engineering, as depicted in Fig. 1. As this treatise advances from the begin-

ning to the end, we will travel from the conceptual border between philosophy and science all the way to the vague border between science and engineering.

Jyväskylä, August 2010

Keijo Mattila

1 INTRODUCTION

When we are engaged with mathematical modelling of matter, or any other imaginable system of interest, we are immediately enforced to make the most fundamental choice; we have to choose the level of abstraction for our mathematical model. That is, a physical description can either include minute details of the system or it can operate on more general grounds. The esteemed scholar *Leo Kadanoff* phrased it elegantly [Kad86]:

> Some of the most interesting situations in physics, and indeed in other sciences as well, concern the connections between two "levels of reality".

In the context of fluid dynamics, our object of interest, these two levels correspond to the underlying world of atoms and molecules invisible to the eye, and to a continuum volume of fluid like we perceive it every day. The level of particles, atoms and molecules, is referred to as the microscopic scale and the bulk level as the macroscopic scale. The connection between these two extreme levels, a bridge of a kind, is an intermediate level appropriately referred to as the mesoscopic scale. Physical descriptions at the mesoscopic level essentially aim for a compromise between details and abstraction of the system.

Accordingly, fluid dynamical systems can be mathematically modelled with Hamilton's equations as well as with the Boltzmann and Navier-Stokes equations at the micro-, meso-, and macroscales, respectively. This is illustrated in Fig. 2. Here we are primarily interested in the mesoscopic descriptions, and particularly in the Boltzmann equation due to its direct connection with the lattice Boltzmann method. The Boltzmann equation is a statistical mechanical description for transport phenomena, and has an essential role in the kinetic theory of gases, among other disciplines. The kinetic theory of gases is founded on the fundamental hypothesis that all macroscopic observable properties of a gas can be deduced, at least in principle, from a knowledge of the forces of interaction and the internal structure of its molecules.

The topic of this thesis, the lattice Boltzmann method, is a particular computational method based on a mesoscopic description. We treat here specific aspects of the lattice Boltzmann method, namely boundary conditions and implementa-

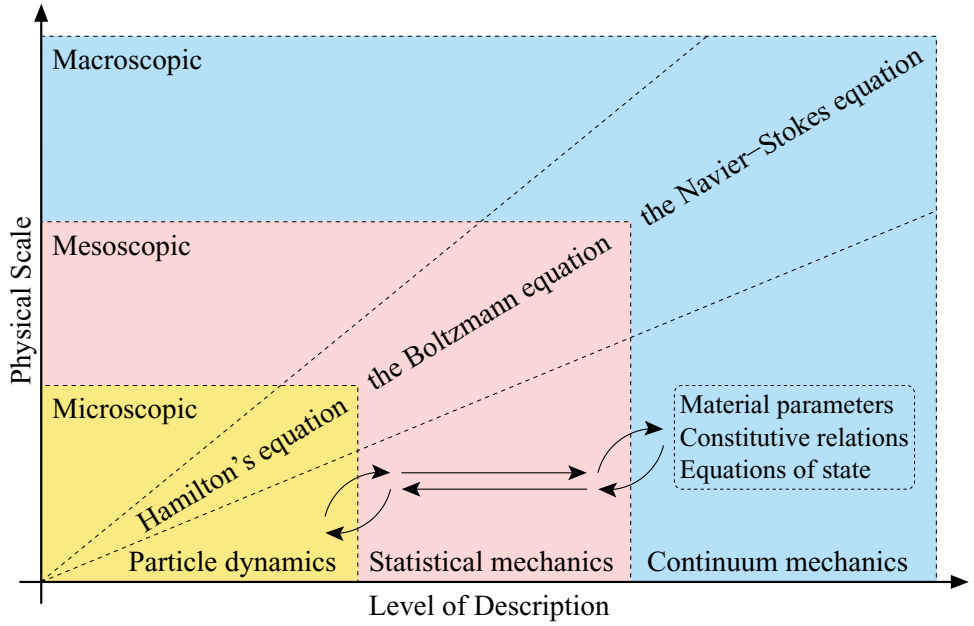

FIGURE 2 Physical systems can be described at various levels of abstraction. At the microscopic scale, the level of particles, the system is described in a very detailed way. At the macroscopic scale, the continuum level, the details are practically omitted and the description is very abstract. In between is the mesoscopic scale, an intermediate level, where a compromise is pursued. Accordingly, fluid dynamical systems can be mathematically modelled with Hamilton's equations as well as with the Boltzmann and Navier-Stokes equations.

tion techniques. While our main motivation is to review certain detailed and even technical developments related to the method, we also use this opportunity to portray the physical background of the lattice Boltzmann method. The physical exposition is intended especially for computer scientists as the associated discussion involves well-established concepts in physics. In fact, the aim is to provide such an introduction to the physical concepts that the published literature on the method, bulk of which is authored by physicists, becomes more accessible to computer scientists as well as to engineers and applied mathematicians. A large portion of the presented discussion is hence devoted to the basic concepts in mathematical modelling and computational methods. Therefore, let us return to the mathematical modelling of fluid dynamical systems.

Mathematical models, including the three equations mentioned above in their general form, are only occasionally amenable to analytical treatment, to the extent where concrete numerical results can be extracted for potentially interesting non-trivial fluid flow configurations – let us call this the 'pen and paper' style of computation. For this reason, the usual convention is to simplify or modify these models, in any conceivable way, in order to obtain new models for which

there exist some practical means to extract concrete results. Since the world where we are currently living has rushed into the digital era some while ago, perhaps the most practical or at least the most effective way of obtaining numerical results today is the 'software and computer' style of computation. To this end, so-called discrete counterparts are usually constructed for the original continuous models; the discrete models are constructed carefully with the purpose of producing results which approximate, in a consistent and predictable manner, the unattainable results of the original models. This is only a paradox, but of course it is not trivial to estimate the quality of approximations when the true results are generally unknown. From the perspective adopted in this thesis, the lattice Boltzmann equation is the best example of the above discussed discrete models: it is a discrete counterpart of the Boltzmann equation.

A numerical method includes not only the particular model equation, but also well-defined initial and boundary conditions, guaranteeing both the existence and uniqueness of the approximate solution for a particular flow configuration, as well as meaningful parameters for controlling the model properties. Furthermore, the method must include a theory for interpreting the obtained results, their accuracy, and dependence on the model parameters. In this context, an appropriate example is the lattice Boltzmann method. A computational scheme, in turn, is a concrete descendant of a particular numerical method. Its every aspect is defined to the extent which allows a straightforward computer implementation. For example, there is not one or two but many computational schemes corresponding to the lattice Boltzmann method, distinct in various ways and intended altogether for a rich set of fluid flows. Computer simulations of a physical system under investigation are then feasible simply by executing the computer program, a scientific software, implemented to compute approximate solutions of our original mathematical model.

There are notable exceptions among the variety of computational schemes, namely the Lattice-Gas Automata, for fluid flow simulations. They are exceptional since they are mathematical models and, at the same time, fully-fledged computational schemes. That is, the computational schemes involve no approximation or further discretisation whatsoever – they are precise schemes. This is due to the boolean computation inherent in the models. The boolean computation is of course a double-edged sword: boolean expressions indeed escape roundoff, plaguing floating-point computations so typical in other computational schemes, but a boolean model for the true observed fluid dynamics around us is most certainly a dramatic simplification and hardly realistic. Hence, it is remarkable that such simple models allow realistic fluid flow simulations. It is an illustration of how insensitive, at the macroscopic level, fluid flows can be for the fine microscopic details at the particle level. The physicist *Richard Feynman*, always a master of articulation, found simple words for conveying the idea of the simple automata [Hil89]:

> We have noticed in nature that the behavior of a fluid depends very little on the nature of the individual particles in that fluid. For example, the flow of sand is very similar to the flow of water or the flow of

> a pile of ball bearings. We have therefore taken advantage of this fact to invent a type of imaginary particle that is especially simple for us to simulate. This particle is a perfect ball bearing that can move at a single speed in one of the six directions. The flow of these particles on a large enough scale is very similar to the flow of natural fluids.

Moreover, the lattice Boltzmann method historically emerged as an improvement to the Lattice-Gas Automata. Because of the above reasons, we will spend some time in explaining the basics of the Lattice-Gas Automata – the same discussion will serve as an introduction to the concepts of the lattice Boltzmann method.

An important intermediate abstraction concept, namely an algorithm, not mentioned thus far, lies between a particular computational scheme and conforming computer implementation. It is a kind of recipe, a list of consecutive actions to be executed, for the implementation of a computational scheme. It collects all the essential steps of the scheme, while avoiding unnecessary details, into a procedure mechanical enough for computers. From the implementation point of view, algorithms are very convenient instruments for communicating the essence of a particular scheme. Just like there can be many schemes specifying a single numerical method, there can be, and usually is, many algorithms corresponding to a given scheme. The hierarchy is completed with the final description: there can be an arbitrary number of implementations for a specific algorithm – every chef has a personal way of following the recipe.

The four levels in the hierarchy, numerical method, computational scheme, algorithm, and implementation, all have a marked effect on the computer resources required for the execution of a computer simulation. Here we are particularly interested in how distinct algorithms and implementations, related to the lattice Boltzmann method, affect the computational efficiency. In Ref. [PI], we propose an algorithm for the implementation of a specific class of computational schemes specifying the lattice Boltzmann method. Furthermore, like mentioned above, even if an algorithm defines the main steps of a scheme, there is still typically plenty of freedom in many implementation points. In Ref. [PII] we have studied some of these implementation points as well as their effect on the computational efficiency. There, for example, we propose a particular data structure for the unknown dynamic variables of the lattice Boltzmann method.

Finally, in Refs [PIII, PIV] we propose an approach for enforcing boundary conditions for the simulation of fluid flows with the lattice Boltzmann method. More specifically, the approach is related to the inlets and outlets of flow domains. This issue is best explained with an academic flow configuration. Imagine an infinitely long straight pipe, full of fluid flowing steadily in one direction. That is, the pipe does not have a beginning nor an end, but instead continues forever in both directions – admittedly a very theoretical setting. But our computing resources are unfortunately not infinite; on the contrary, the computing resources are rather limited. Thus, computer simulation of an infinite system is not possible, not even in principle. We are enforced to simulate flow only in a finite segment of the pipe, and rather in a short than in a long segment. So, in order to obtain a finite segment, we cut the pipe at two points. The cross-sections of the

pipe at these two cutting points are now in a special role. They are called the inlet and outlet of the domain: the steady flow of fluid enters and exits the domain through these two cross sections. By imposing physical (or mathematical) restrictions to the flow at the inlet and outlet, the flow inside the finite pipe segment can be controlled. In other words, depending on what kind of a real pipe system we are trying to mimic with our computer simulation, we can enforce appropriate boundary conditions at the inlet and outlet. This portrays the context for Refs [PIII, PIV].

The body of this thesis begins with mathematical modelling of fluid dynamics, discussed in Chapter 2. It includes macroscopic as well as mesoscopic modelling approaches: specific attention will be paid to the kinetic theory of gases and to the Boltzmann equation. Chapter 3 gives a historical survey to the lattice Boltzmann method and, in addition, reviews its basic properties. A review of the boundary conditions for the method is presented in Chapter 4. Moreover, the chapter also recapitulates the fundamentals of the mass-flux-based approach for boundary conditions, originally treated in Refs [PIII, PIV]. Additionally, a systematic approach for implementing hydrodynamic LBM boundary conditions is presented. This approach is utilised in Chapter 4, and in Appendix 2, for recovering some of the well-known boundary condition implementations as well as to derive alternative new implementations. Chapter 5 considers implementation techniques for the lattice Boltzmann method. Specifically, it elaborates on some issues related to the swap algorithm and to the bundle data layout, originally presented in Refs [PI, PII]. Finally, some conclusions are given.

2 MATHEMATICAL MODELLING

Fluid flows provide nothing but opportunities for mathematical modelling. There are two basic reasons for these opportunities. First of all, fluid flows exhibit a vast range of relevant length and time scales. This fact is easily demonstrated by adopting a discrete perspective to the modelling: matter is divided into separate entities – like atoms. Following this atomistic view, fluid flow represents average motion in a massive collection of interacting particles. At this microscopic level of description the interplay between particles, either atoms or molecules, is of fundamental interest. Computational schemes, methods for simulation with computers, can be constructed based on this philosophy. A collective name for such constructions is Molecular Dynamics (MD). According to the current understanding, the diameter of an atom is of the order of one *Ångström* (1 Å = 0.1 nm = 1×10^{-10} m). Molecules are also very small. For example, in a methane molecule the hydrogen and carbon atoms are bonded with an average distance equal to 1.1 Å = 110 pm.

As (electrically neutral) atoms and molecules fly about, they exert interaction forces on each other from distances comparable to their size. The range of interaction, defined by the effective interaction radius r_μ, is typically limited to several particle diameters – for larger distances the force is virtually zero. The interaction radius is an appropriate characteristic measure for a given system of particles and thus defines the small end of the relevant length scales. In principle it would be possible to mimic nature in evermore larger scales by relying on the atomistic view with increasing number of particles. But in just a few grams of water there are approximately 10^{23} molecules! Thus, in practice, such a brute force strategy is quickly overpowered by limitations on the computing resources. One must thus rely on intellectual power in order to productively mimic larger scales in nature. In this chapter, we consider both macroscopic and mesoscopic models for fluid flows. The macroscopic models considered rely on the continuum approximation: it is basically assumed that the fluid completely fills the space it occupies. The fact that the matter is made of atoms, and ultimately is not continuous, is ignored; essentially, the modelling is carried out on length scales much greater than the range of interaction between atoms.

In the macroscopic scale, we concentrate on the model described by the Navier-Stokes equation. After a short discussion about the merits and shortcomings of the model, we advance to the mesoscopic modelling in fluid dynamics. In particular, we concentrate on the statistical mechanical approach, and on the kinetic theory of gases. Above all, we focus on the Boltzmann equation due to its direct connection with the lattice Boltzmann method.

2.1 Macroscopic description of fluid flows

To begin with, we resort to the continuum approximation. Let L denote the characteristic length scale related to a macroscopic flow configuration. For example, L can be associated with the diameter of a water pipe, length of a wing, or height of a building diverting wind. In that scale the fluid is now considered as a continuum, composed of infinitesimally small volume elements living side by side with no empty space in between. That is, fluid flow is examined at a scale much larger than L_Δ here associated with the volume elements: $L_\Delta \ll L$. But when compared to the atomistic world, the small fluid elements are rather huge – not small at all.

It is important to understand why continuum approximation requires these three well separated scales to coexist. To begin with, the continuum modelling of a fluid flow assumes hydrodynamic variables like density ρ, pressure p, temperature T, and velocity $\mathbf{u} = (u_x, u_y, u_z)^T$, as well as their gradients, to be meaningful at the scale of the elementary fluid elements; meaningful in the sense that the hydrodynamic variables can be considered as continuous functions of space $(\mathbf{r} = (r_x, r_y, r_z)^T)$ and time (t) coordinates. Here superscript T denotes the transpose of a matrix and should not be confused with temperature. It is typically also assumed that the gradients of the hydrodynamic variables are small rather than large, i.e. they are reasonably smooth functions. On the other hand, hydrodynamic variables represent average values computed from the true particle motion. Because it is intuitive, we here assume that the averages are computed over spatial space. Alternatively the domain for average computation could be time or even an ensemble of macroscopically equivalent, but microscopically distinct, flow configurations. In order to obtain reasonably smooth and continuous variables, the averages must be computed over large enough spatial domains. This in turn implies that $r_\mu \ll L_\Delta$.

The derivation of a macroscopic fluid flow description proceeds with the above assumptions, and culminates at general conservation equations for the elementary fluid elements:

$$\partial_t \rho + \nabla \cdot (\rho \mathbf{u}) = 0, \tag{1}$$

$$\partial_t (\rho \mathbf{u}) + \nabla \cdot \mathbf{\Pi} = 0. \tag{2}$$

The partial derivatives $\partial_t = \partial/\partial t$ and $\partial_\alpha = \partial/\partial r_\alpha$ express variation in quantities with respect to time and space; the divergence, for example $\nabla \cdot (\rho \mathbf{u}) \equiv \partial_\alpha \rho u_\alpha \equiv \partial_x \rho u_x + \partial_y \rho u_y + \partial_z \rho u_z$, measures net variation of a quantity in the spatial space. A

further notational remark is in order: in the index notation, the *Einstein summation convention* is implied by repeated indices in a single term, e.g. in $\partial_\alpha \rho u_\alpha$ above. The first and second equations enforce, in a differential form, conservation of mass and momentum for the elementary fluid elements, respectively; in this case there are no external forces acting on the elements. For example, the statement of Eq. (1) is blunt: temporal changes in total mass inside a fluid element must result from a mass flux through the element boundaries. That is, there are no mass sources or sinks. Furthermore, the momentum-flux tensor $\mathbf{\Pi} \equiv \Pi_{\alpha\beta}$ gives the flux of the α component of the momentum in the β direction. In general, the momentum-flux tensor can be decomposed into two terms,

$$\Pi_{\alpha\beta} = \rho u_\alpha u_\beta - \Pi^{str}_{\alpha\beta},$$

where the first term represents the convective momentum flux and $\Pi^{str}_{\alpha\beta}$ is the stress tensor of the fluid. Conventionally, the internal stresses of a fluid are divided into contributions arising from the pressure p and viscous stresses:

$$\Pi^{str}_{\alpha\beta} = -p\delta_{\alpha\beta} + \Pi^{visc}_{\alpha\beta}.$$

Whenever appropriate, Eqs (1) and (2) are supplemented with an equation enforcing conservation of energy. There is however a serious dilemma related to the general conservation equations. Namely, even if we assume a symmetric momentum-flux tensor $\mathbf{\Pi}$ in the three-dimensional case, Eqs (1) and (2) provide only four conditions for the ten dynamic variables: the density ρ, the three components of the velocity $\mathbf{u}$, and the six independent components of the tensor $\mathbf{\Pi}$. That is, the dynamical description is severely undetermined. In order to obtain a closed description for the fluid dynamics, additional resctrictions for the model must be imposed.

2.1.1 The incompressible Navier-Stokes equation

A physically apparent restriction assumes incompressible fluids, i.e. the fluid density is constant. This assumption, $\partial_t \rho \equiv \partial_\alpha \rho \equiv 0$, together with the above definitions, leads directly to special conservation equations:

$$\nabla \cdot \mathbf{u} = 0 \tag{3}$$

and

$$\rho \partial_t \mathbf{u} + \rho \mathbf{u} \cdot \nabla \mathbf{u} = -\nabla p + \nabla \cdot \mathbf{\Pi}^{visc} + \mathbf{F}, \tag{4}$$

where $\mathbf{F} = \rho \mathbf{a}$ refers to an external body force due to an additional acceleration $\mathbf{a}$ of a fluid element, representing e.g. gravity. The so-called continuity equation Eq. (3) enforces conservation of mass in an incompressible fluid. The conservation of momentum, enforced by Eq. (4), is actually also a manifestation of *Newton's Second Law*. This is apparent after a small rearrangement:

$$\rho(\partial_t u_\alpha + u_\beta \partial_\beta u_\alpha) = -\partial_\alpha p + \partial_\beta \Pi^{visc}_{\alpha\beta} + F_\alpha.$$

On the left is the inertia per volume, simply $\rho D_t u_\alpha$ with the material derivative $D_t := \partial_t + u_\beta \partial_\beta$, and the right-hand side sums up the forces exerted on the volume.

Nonetheless, the dynamical description is still as undetermined as before. Next, the number of dynamical variables is radically reduced with a specific constitutive relation for the viscous stresses. Namely, an additional assumption in the modelling defines a particularly simple expression for the components of the viscous stress tensor. Let us elaborate on this important modelling step. In the continuum mechanics philosophy, external forces on the fluid enforce motion which, in turn, causes volume element deformations. Strain is a geometrical measure of deformation. In a *Newtonian fluid*, named after *Isaac Newton*, it is assumed that the viscous stresses $\Pi^{visc}_{\alpha\beta}$ are linearly proportional to the strain rate defined as $S_{\gamma\delta} = (\partial_\delta u_\gamma + \partial_\gamma u_\delta)/2$:

$$\Pi^{visc}_{\alpha\beta} = \Phi_{\alpha\beta\gamma\delta} S_{\gamma\delta}. \tag{5}$$

The fourth-rank tensor $\Phi_{\alpha\beta\gamma\delta}$ with constant components measures the viscosity of the medium. That is, viscosity characterises how fluids react to strain rate or, rather informally, it is a measure for the internal friction of the fluid. Generally speaking, temperature has a strong effect and pressure a moderate if not negligible effect on viscosity [Whi03]. In isothermal flows temperature is constant, and all variations in viscosity due to temperature changes can be neglected. For simplicity, we here neglect also the effect of pressure induced changes in viscosity – a common approximation. Non-Newtonian fluids in general do not respect a linear relation, with constant coefficients, between the viscous stresses and strain rate.

The constitutive relation defined by Eq. (5) has effectively reduced the number of dynamic variables from ten to four: the pressure and the three components of the flow velocity. Equations (3) and (4) provide an equal number of conditions. In a general three-dimensional case, however, the fourth-rank tensor $\Phi_{\alpha\beta\gamma\delta}$ involves 81 undefined components – a staggering number from a practical point of view. Therefore, an additional reduction in model parameters is pursued by restricting the dynamic description to isotropic fluids. The definition of an isotropic fluid is straightforward: the tensor $\Phi_{\alpha\beta\gamma\delta}$ must be isotropic[1]. The most general form it may have is then

$$\Phi_{\alpha\beta\gamma\delta} = A\delta_{\alpha\beta}\delta_{\gamma\delta} + B\delta_{\alpha\gamma}\delta_{\beta\delta} + C\delta_{\alpha\delta}\delta_{\beta\gamma}, \tag{6}$$

where A, B, and C are arbitrary constants [Rot97]. Here $\delta_{\alpha\beta}$ is the *Kronecker delta*. By substituting this form into the relation Eq. (5), we find that

$$\Pi^{visc}_{\alpha\beta} = (B + C)S_{\alpha\beta} + A\delta_{\alpha\beta}S_{\gamma\gamma} = \mu(\partial_\beta u_\alpha + \partial_\alpha u_\beta) + \xi\delta_{\alpha\beta}\partial_\gamma u_\gamma.$$

The coefficient $\xi := A$ is related to the compression or bulk viscosity of the fluid whereas the dynamic viscosity coefficient $\mu := (B + C)/2$ is related to its shear viscosity.

[1] An isotropic tensor is a tensor whose components are unchanged by an orthogonal transformation of coordinates, i.e. by rotations and reflections.

TABLE 1 Material parameters for some fluids at 1 atm and 20°C [Whi03].

Fluid	Density ρ (kg/m^3)	Kin. visc. ν (m^2/s)
glycerin	1260	1.18×10^{-3}
SAE 10W oil	870	1.20×10^{-4}
air	1.20	1.50×10^{-5}
water	998	1.01×10^{-6}
mercury	13 550	1.15×10^{-7}

For incompressible fluids, the term related to compression is eliminated with the continuity equation Eq. (3). Finally, the internal forces emerging from the viscous stresses in the fluid are manifested with the source term

$$\nabla \cdot \mathbf{\Pi}^{visc} \equiv \partial_\beta \Pi^{visc}_{\alpha\beta} = \partial_\beta \mu (\partial_\beta u_\alpha + \partial_\alpha u_\beta) = \mu \partial_\beta \partial_\beta u_\alpha.$$

The last step involves again application of the continuity equation after changing the order of derivation. By substituting this source term into the momentum equation Eq. (4), we obtain the *Navier-Stokes equation* for an incompressible, isotropic Newtonian fluid:

$$\frac{\partial \mathbf{u}}{\partial t} + \mathbf{u} \cdot \nabla \mathbf{u} = -\frac{1}{\rho} \nabla p + \nu \nabla^2 \mathbf{u} + \mathbf{a}, \tag{7}$$

where $\nu = \mu/\rho$ is the kinematic viscosity. Here the viscous force term has an interesting mathematical interpretation. The term involving the vector laplacian of the velocity field, $\nu \nabla^2 \mathbf{u}$, represents diffusion of momentum, cf. diffusion of temperature in the heat equation. Then the kinematic viscosity ν is identified as the diffusion coefficient for momentum. The second term on the left, the so-called convective term, is the only nonlinear term. It is notorious as it prohibits analytical solutions except for a few cases. Thus, numerical methods are required to obtain approximate solutions for the coupled system of equations, i.e. for Eqs (3) and (7) together with given boundary conditions. On the other hand, the nonlinear term is very welcome as it is responsible for many interesting flow phenomena. For example, it gives rise to turbulence.

Microscopic details of the fluid are completely ignored in the Navier-Stokes equation. For example, the viscosity of a system is, from a fundamental point of view, a consequence of the interaction between particles at the atomic level. More often than not, macroscopic models ignore such connections: partly because the connections are irrelevant for many applications, and partly because there are no simple but correct expressions, e.g. for the viscosity, which would rely only on the atomistic details of the fluid. In the Navier-Stokes equation, the physical properties of the fluid are modelled with material parameters. That is, the density and kinematic viscosity are considered as input parameters for the model. Numerical values for these parameters are available from experimental measurements. Table 1 lists parameter values for some fluids. The minimum and maximum values

in the list, both for the density and kinematic viscosity, differ by four orders of magnitude. Furthermore, characteristic length scales for everyday flows range easily from millimeters to kilometers. The Navier-Stokes equation is celebrated because it is applicable to so many fluids under very diverse flow conditions.

In addition, the Navier-Stokes equation incorporates a very important mathematical property which has promoted its application – namely it defines *dynamic similarity* between fluid flows. Remarkably a single parameter can determine whether two fluid flows are dynamically similar. This parameter, perhaps the most important parameter in fluid dynamics, is the dimensionless Reynolds number R_e. We explain this important mathematical aspect further and write the Navier-Stokes equation in its dimensionless form. First we define the relevant dimensionless variables, and denote them by an asterisk:

$$r_\alpha^* = \frac{r_\alpha}{L}, \quad u_\alpha^* = \frac{u_\alpha}{U}, \quad t^* = t\frac{U}{L}, \quad P^* = P\frac{1}{U^2} \equiv \frac{p}{\rho}\frac{1}{U^2}, \quad a_\alpha^* = a_\alpha\frac{L}{U^2},$$

where L and U refer to the characteristic length scale and to the characteristic fluid flow velocity of the macroscopic system, respectively. Since the dimensional measures L and U are considered constant, the derivatives in the Navier-Stokes equation are easily transformed into dimensionless form. For example,

$$\frac{\partial u_\beta}{\partial r_\alpha} = \frac{\partial(u_\beta^* U)}{\partial(r_\alpha^* L)} = \frac{U}{L}\frac{\partial u_\beta^*}{\partial r_\alpha^*}.$$

Hence, by using the above definitions in Eq. (7), it is straightforward to obtain

$$\begin{aligned} \frac{U^2}{L}\frac{\partial \mathbf{u}^*}{\partial t^*} + \frac{U^2}{L}\mathbf{u}^*\cdot\nabla_*\mathbf{u}^* &= -\frac{U^2}{L}\nabla_* P^* + \nu\frac{U}{L^2}\nabla_*^2\mathbf{u}^* + \frac{U^2}{L}\mathbf{a}^* \\ \iff \frac{\partial \mathbf{u}^*}{\partial t^*} + \mathbf{u}^*\cdot\nabla_*\mathbf{u}^* &= -\nabla_* P^* + \frac{1}{R_e}\nabla_*^2\mathbf{u}^* + \mathbf{a}^*. \end{aligned} \tag{8}$$

The Reynolds number $R_e = LU/\nu$ provides an estimate for the ratio of inertial forces to viscous forces, quantifying their relative importance for given flow conditions. For example, low and high Reynolds numbers characterise laminar and turbulent flow, respectively. More importantly, the dimensionless Navier-Stokes equation Eq. (8) does not contain any scale, only a single dimensionless parameter R_e. Let us consider a particular flow configuration with given boundary conditions, say a flow past a sphere or a flow in a duct. That is to say, by fixing the geometry and the boundary conditions of the flow problem, we have a specific type of flow. Then all fluid flows of this type, but with different values of L, U, and ν, are described by one and the same dimensionless solution $(\mathbf{u}^*, P^*)$ if their Reynolds numbers are equal – the flows are said to be dynamically similar. This is the property which is treasured among the people applying the Navier-Stokes equation! The possibility to choose favourable values for L, U, and ν, while maintaining a desired value for R_e, is an immediate advantage in computer simulations and in experimental measurements.

2.1.2 Physical aspects of the continuum modelling

The conservation equations themself are universal, only the assumptions behind the modelling must be maintained. For example, the continuum approximation is considered valid in the regime of very small Knudsen number K_n; a condition $K_n \lesssim 10^{-2}$ is often quoted in the literature. Knudsen number is the ratio between the mean free path ℓ_m of a particle to a characteristic length scale L of the macroscopic flow configuration. Thus, $\ell_m \ll L$ implies a small value for K_n. Knudsen number can also be defined in terms of the mean collision interval and a characteristic time scale. With collisions we refer to the interaction events between two or more particles. For liquid flows the Knudsen number is typically smaller than for rarefied gas flows. The message is intuitive: particles in a liquid are in constant interaction with each other whereas in a gas the free flight of particles is occasionally interrupted by collisions. In fact, flow regimes are conveniently classified with the Knudsen number [Str05]:

- **The hydrodynamic regime** ($K_n \lesssim 0.01$) is very well described by the Navier-Stokes-Fourier equations[2].

- **The slip flow regime** ($0.01 \lesssim K_n \lesssim 0.1$) can still be described by the Navier-Stokes-Fourier equations, but the equations must be supplemented with boundary conditions which account for velocity slip and temperature jumps at the walls.

- **The transition regime** ($0.1 \lesssim K_n \lesssim 10$) is the domain where the Navier-Stokes-Fourier equations fail; the gas must be described in greater detail, or by extended macroscopic models.

- **Free molecular flow** ($K_n \gtrsim 10$) is dominated by particle-wall interactions, and collisions between the particles do not play an important role anymore.

The above classification is widely accepted, but sometimes with slightly different limits for K_n, see for example Ref. [Ree03]. Gases which are outside the hydrodynamic regime ($K_n \gtrsim 0.01$) are called *rarefied gases*. In the regime $0.01 \lesssim K_n \lesssim 1$ gas still behaves as a continuum, but the validity of the Navier-Stokes-Fourier equations is compromised and eventually broken: more refined sets of continuum equations are called for. Even when we commit ourselves to the hydrodynamic regime, the Navier-Stokes equation Eq. (7) is valid only for fluid flows with three more properties. These properties are their incompressibility, isotropy and Newtonian character. Mach number M_a is a measure of the compressibility of the fluid. It is the ratio of the characteristic fluid flow velocity U to the speed

[2] A coupled set of equations for the conservation of mass, momentum, and energy. Fourier's law, utilised in the energy equation, is a linear relation between the heat flux and temperature gradient: the coefficient of proportionality is called the thermal conductivity. Fourier's law is analogous to the linear relation between the viscous stresses and strain rate utilised in the momentum conservation equation for Newtonian fluids.

of sound c_s in the fluid: $M_a = U/c_s$. In general, the speed of sound for a fluid is given by

$$c_s = \sqrt{\frac{K}{\rho}}, \tag{9}$$

where the bulk modulus of compressibility K is related to fluid's resistance to uniform compression. K measures the pressure increase needed to cause a given relative decrease in volume, and its basic unit is Pascal. Ability to resist compression usually implies faster sound wave propagation in the medium. It is commonly stated that compressions in fluids are neglible when $M_a = U/c_s \leq 0.3$. In other words, subsonic flows are usually incompressible.

It is also very interesting to consider the Mach number as the ratio of inertial forces to the compressive forces which are proportional to KL^2 [Gra85]. This interpretation immediately leads to a conclusion: if the inertial forces are negligible in comparison to the compressive forces, i.e. the Mach number is very small, the variation of density due to the variation of the flow field is insignificant, and the fluid flow can be considered incompressible. There is also a relation between the Mach number and the Knudsen number [Bar91]:

$$K_n \sim \frac{M_a}{R_e}. \tag{10}$$

That is, the Knudsen number can also be viewed as the ratio between the viscous and compressive forces. According to the relation Eq. (10), in the hydrodynamic regime ($K_n \ll 1$) a finite Reynolds number must be compensated with a very small Mach number. This is the *incompressible limit*. Finally, a convincing argument for, or against, the isotropy and Newtonian character of a fluid requires empirical evidence.

2.1.3 Limitations of the Navier-Stokes equation

After all our praise, it is time to subject the Navier-Stokes equation, a nonlinear partial differential equation, to criticism: theoretical understanding of the solutions to this equation is still incomplete. This is an issue as such for mathematicians, but significant progress in the theoretical understanding would be a revolution for fluid mechanics. In the meantime, one could avoid the above criticism by adopting the common prerogative of applied scientist: the rigorous mathematical issues are neglected and the existence of solution to the equation is simply assumed. This is the spirit in which the Navier-Stokes equation, and that of Fourier if heat transfer is also considered, is routinely used by engineers and others. Unfortunately for applied scientists, but fortunately for the mankind, the Navier-Stokes equation is too simple to govern alone our complex world.

The equation is generally applicable only to the simplest of real fluid flows. It is an idealistic description for the behaviour of fluid pressure and velocity with respect to time; it incorporates many radical assumptions like the Newtonian character of the fluid. Everyday fluid flows can be overwhelmingly complex involving multiple phases (e.g. liquid and vapour), multiple components (e.g.

water and oil), and suspended matter (e.g. sand mixed with fluid). Any realistic description of such fluid flows, at a macroscopic scale, is far more complicated than the Navier-Stokes equation. Application and productive utilization of the complicated equations in experimental measurements or computer simulations can be very difficult. Mathematical difficulties certainly pile up and analytical solutions for any non-trivial setting can be even impossible to obtain. The above discussion portrays the second basic reason for the opportunities in mathematical modelling: there is practically no limit to the variety of fluid flows.

We conclude the treatment of macroscopic modelling with specific cases where the Navier-Stokes equation is no longer an appropriate description for the fluid flow. In the hydrodynamic regime, fluids are all the time very close to thermal equilibrium. The Knudsen number K_n indicates whether a fluid can maintain conditions of thermodynamic equilibrium. That is, K_n can also be used as a measure for departure from equilibrium. The process leading to a thermodynamic equilibrium is called thermalisation. For example, in a monoatomic gas the molecules need roughly three or four collisions to balance momentum and energy among themselves; the molecules reach thermal equilibrium through mutual interaction [Ree03]. In an equilibrium state, there are no unbalanced forces driving the fluid. The state can be global or local. In the latter case the balance is with an immediate surroundings of the point. Departures from equilibrium are attributed to two interrelated reasons: 1. in a rarefied gas molecules collide with solid boundaries more frequently than with each other, thus hindering thermalisation; 2. the fluid flow properties vary drastically at small scales. Both situations lead to a conflict with the continuum approximation: hydrodynamic variables, density ρ, pressure p, temperature T, velocity $\mathbf{u}$, or their gradients, are not smooth and continuous functions at the scale L_Δ associated with infinitesimally small fluid volume elements. According to Ref. [Str05], cases where the Navier-Stokes equation is not adequate for describing fluid flows include

- High altitude flight: space crafts need to manoeuvre at altitudes of 100 km where low gas pressure and density are manifested as the long mean free path of air molecules, $\ell_m \approx 0.1$ m, placing the flow well into the transition regime.

- Microscopic flows: the relevant macroscopic length scales L are very small, and hence the Knudsen number is not infinitesimal even at normal pressures and densities.

- Propagation of ultrasound: the frequency of sound wave is so high that the relevant Knudsen number cannot be considered as small.

- Shock waves: a flow changes from supersonic to subsonic over a few mean free paths, including drastic changes in temperature, pressure, and density, i.e. the gradients in the flow field are large.

- Boundary value problems at large Knudsen numbers: the presence of a wall will reduce the local mean free path in the near wall region. The Knudsen

layer is the limited non-equilibrium region, extending several mean free paths from the wall, where the linear constitutive relations for shear stress (and heat flux), assumed in the Navier-Stokes equation, are no longer valid. In addition to the nonlinear stress-strain relationship in the Knudsen layer, velocity and temperature of the gas may differ from those of the wall, i.e. temperature jumps and velocity slip can occur at solid boundaries.

To remedy shortcomings of the Navier-Stokes equation, extended hydrodynamic equations, more applicable to flows with a high K_n, can be constructed (e.g. Burnett and super-Burnett equations) [Ree03, Str05]. Extensions are typically accomplished with expressions for the stress tensor and heat flux containing higher-order (often nonlinear) terms in the velocity and temperature gradients than in the Navier-Stokes equation. Alternatively, an altogether distinct approach for modelling could be followed.

2.2 Mesoscopic description of fluid flows

Many macroscopically observable phenomena related to fluid dynamics have their origin in the underlying microscopic world. Surface tension is a prime example: cohesive (attractive) forces between molecules are responsible for phase separation in the macroscopic scale and hence for the emergent balancing forces maintaining an observed interface. Difficulties related to the modelling in macroscopic scale are often due to a particular mismatch: evolution equations, conforming to the phenomenon of interest, are sought for the macroscopic variables, say ρ, p, T, and $\mathbf{u}$, while the fundamental mechanisms giving rise to the phenomenon are rather related to a microscopic scale. This mismatch can make macroscopic descriptions cumbersome; more natural description might involve evolution equations for dynamic variables of microscopic character – not for the hydrodynamic ones. An enterprising scientist confronted with the above scenario will initiate a quest for an intermediate description, operating between microscopic and macroscopic worlds, pursuing an optimal compromise between details and abstraction. With an additional procedure, for example with averaging, hydrodynamic variables are then computed from the variables of intermediate scale. This alternative modelling philosophy is inherent in the mesoscopic description of fluid flows.

2.2.1 Microscopic origins of the mesoscopic modelling

The derivation of a mesoscopic description of fluid flows usually starts from the atomic perspective. So, let us return to the microscopic level. Suppose we have N particles in our three-dimensional system and the instantaneous state of each particle is reported with its position $\mathbf{r}_i$ and momentum $\mathbf{p}_i$, $i = 1, \ldots, N$. Instead of the momentum, we could altertanatively use the instantaneous velocity $\mathbf{c}_i = \mathbf{p}_i/m_i$ of the particle as a state variable. In what follows, we assume that the mass m_i

of the particle remains constant. Thus, we have a total of $6N$ degrees of freedom in our microscopic description of the particle system. Of course, N is usually a very large number: a realistic order of magnitude approximation is provided by the *Avogadro number* $N_A \cong 6.0221422 \times 10^{23}$ mol^{-1}. The equation of motion for the particles in the system is most conveniently given with the *Hamiltonian formulation*:

$$\frac{\partial \mathbf{r}_i}{\partial t} = \frac{\partial H}{\partial \mathbf{p}_i}, \quad \frac{\partial \mathbf{p}_i}{\partial t} = -\frac{\partial H}{\partial \mathbf{r}_i}, \quad i = 1, \cdots, N. \tag{11}$$

If there are no external fields enforcing the particle system, H is the total energy of the system including kinetic energy and any potential energy due to interaction forces between the particles.

It is possible to construct a phase space, denoted by $\mathbb{P}$, which has $6N$ mutually orthogonal axis, and where each axis is associated with a unique degree of freedom, i.e., with a position or momentum component of a particle. Then, the instantaneous state of the particle system is specified by a single point $\mathbf{q} \equiv (\mathbf{r}_1, \mathbf{p}_1, \ldots, \mathbf{r}_N, \mathbf{p}_N)$ in $\mathbb{P}$. Now suppose we specify the interaction forces between the particles; there exists quite a number of possibilities for these forces. With such a specification together with an initial condition, simply a point in the phase space, we can in theory use Eq. (11) to follow the time evolution of the system to any later or earlier instant. In other words, a trajectory for a particular system in the phase space can be computed with Eq. (11). In practice such a calculation is, of course, impossible. First, the total number of degrees of freedom in any macroscopically significant system overpowers any foreseeable computing resources – as we already stated at the very beginning. Moreover, for virtually every realistic system, like for a finite amount of gas, it is a practical impossibility to determine the initial conditions for each constituent molecule.

2.2.2 Classical kinetic theory of gases

The pioneering efforts to explain macroscopically observable features of a fluid with the properties of the underlying atomic configuration are now considered as the classical kinetic theory of gases, or kinetic theory of equilibrium gases. The focus was indeed on gases, rather than on liquids or some other states of matter, since from the beginning it was intuitively understood that it is easier to mathematically treat gases: mainly because the interactions between the constituent particles are practically limited to the rare occasions appropriately called collisions – an exciting hypothesis at the time. Due to the above discussed reasons, the early scientists did not derive their results from the detailed equations of motion for the individual particles, like from Eq. (11), but rather from the average properties of the system of particles. By doing so, they also established the statistical discipline for treating physical systems. In order to connect with the reality, and in order to grasp the statistical concepts of the classical kinetic theory, we consider an example of the properties of a real gas [McQ97, p.1032]:

> The number density of nitrogen gas at 25°C and one bar is $\rho_n = 2.43 \times 10^{25}/\mathrm{m}^3$. The average speed of N_2 molecules in the gas is 475 m/s.

> The collision frequency then is 7.3×10^9 collisions per second. Thus, at one bar and 25°C, the mean free flight time of a nitrogen molecule is 1.4×10^{-10} s – a fraction of a nanosecond. The mean free path is 65 nanometres, which is about 200 times the effective diameter of a nitrogen molecule.

The book by *A.D. Risteen* is an another enjoyable source for examples and approximations of gas properties [Ris95].

The classical kinetic theory of gases relies heavily on the concept of an ideal gas. It is a theoretical gas where point particles interact only through elastic collisions – molecular size and intermolecular attractions are completely neglected. In an elastic collision the total kinetic energy of the colliding particles is conserved; elastic collisions occur only if there is no net conversion of kinetic energy into other forms of energy. During the collision kinetic energy is first converted to potential energy: the particles approach each other against a repulsive force between them. As the particles start to travel apart, the potential energy is converted back to kinetic energy. If the gas is monoatomic, the constituent atoms have three translational degrees of freedom, namely the three components of velocity. Monoatomic molecules do not possess any other degrees of freedom. For example, they have zero degrees of rotational freedom because they have perfect three-dimensional symmetry. It is then sensible to expect elastic collisions in such a gas.

Other than monoatomic molecules, e.g. diatomic molecules such as oxygen (O_2) or nitrogen (N_2), three-atomic molecules such as water (H_2O) or carbon dioxcide (CO_2), or even larger molecules like methane (CH_4), have additional degrees of freedom due to rotation and vibration [Str05]. Thus, polyatomic molecules of a gas rarely experience perfectly elastic collisions because kinetic energy may be exchanged to energies associated with other, internal degrees of freedom. However, in a reasonable assumption half of the collisions are, at any one instant, inelastic to varying extent (the total kinetic energy of the colliding particles is reduced), and half of the collisions are super-elastic (the particle pair gains kinetic energy). Thereby, on average and with some assumptions, collisions between polyatomic molecules of a gas can be regarded as essentially elastic. This is confirmed by an observed fact: at normal ambient conditions, most real gases behave qualitatively like an ideal gas.

An ideal gas is a condition allowing particles to fly freely most of the time. The condition is expressed mathematically as

$$\frac{r_\mu}{\ell_m} \ll 1;$$

the effective interaction radius of particles must be much smaller than the mean free path. In an alternative expression, the mean time for a collision t_c must be small in comparison to the mean free flight time between collisions τ_m:

$$\frac{t_c}{\tau_m} \ll 1.$$

Furthermore, the interaction radius r_μ must be fixed to a distance above which the interaction potential, and thus the force, is sufficiently small. More precisely, the potential evaluated at distance r_μ must be small compared to the mean kinetic energy e_k of the particles. The last statement leads us to a third requirement for a gas to behave ideally [Str05]: the ratio between the average interaction potential ϕ and the mean kinetic energy must be small, i.e.,

$$\frac{\phi}{e_k} \ll 1.$$

Obviously, low density gases tend to be ideal as the size of the molecules becomes less significant compared to the empty space between them. In addition, the last condition above implies that a hot gas, where particle energies e_k are high, can behave ideally even at larger densities because the work performed by intermolecular forces is less significant. Conversely, the ideal gas model tends to fail at low temperatures or high pressures. Under such conditions intermolecular forces and molecular size become important. At some point, at low temperature or high pressure, real gases undergo a phase transition to a liquid or a solid. However, the ideal gas model does not describe or allow phase transitions, and therefore more complex modelling is then required. Yet another example of a gas which cannot be regarded as ideal is water vapour. Namely, in the gas phase of water the dipole structure of the molecules introduces long range electrostatic forces so that the interaction radius is considerable larger than the actual molecular diameter, and thus the ratio r_μ/ℓ_m cannot be considered small anymore [Str05].

The ideal gas law is a mathematical manifestation of the ideal gas model. It is a simplified equation of state, a constitutive equation in other words, which provides a relation between the state variables:

$$pV = n_m RT \quad \text{or} \quad pV = Nk_bT.$$

The macroscopic version of the ideal gas law is on the left and the microscopic version on the right; p is the pressure and V the volume of the gas. Moreover, n_m is the amount of gas measured in moles (mol), N is again the actual number of molecules, $R = 8.314472\,\mathrm{J/(K\cdot mol)}$ is the ideal gas constant, $k_b = 1.38065 \times 10^{-23}\,\mathrm{J/K}$ is the *Boltzmann constant*, and T is the absolute temperature measured in kelvins (K). The Boltzmann constant relates energy at the particle level with temperature at the bulk level and has the same units as entropy (joules divided by kelvins); the above constants are interrelated by equation $k_b = R/N_A$ or $Nk_b = n_mR$, where N_A is the Avogadro number. The number of moles n_m is equal to the total mass m_V in the volume divided by the molar mass M, i.e., $n_m = m_V/M$. This allows us to rewrite the ideal gas law in a very illuminative form,

$$p = \frac{R}{M}\rho T, \tag{12}$$

explicitly linking pressure, density $\rho = m_V/V$, and temperature. More sophisticated equations of state, like the *van der Waals equation*, allow more complex behaviour for the fluid – a phase transition for example. In the derivation of

these equations, the constituent molecules are typically considered particles with volume, not material points. Also, attractive forces between molecules, acting at a distance of several molecular diameters, are usually incorporated in the improved models.

There are more classical results for the properties of gases. An important statistical tool for obtaining these results is the *equipartition theorem* relating the temperature of the system with its average energies. The original theorem stated that, in thermal equilibrium, energy is divided equally among all of its degrees of freedom. For example there should be, in the equilibrium state and on the average, exactly the same amount of kinetic energy related to translational motion of molecules as is to their rotation. When a monatomic ideal gas is in thermal equilibrium at temperature T, equipartition predicts an average kinetic energy of $(3/2)k_BT$ per particle, attributed entirely to the translational motion – each velocity component degree of freedom contributes $(1/2)k_BT$. Thus, the heat capacity of an ideal gas of N particles is $(3/2)Nk_B$; the heat capacity of a mole of such gas particles is $(3/2)N_Ak_B = (3/2)R$. The heat capacity is a measure for the heat energy required to increase the temperature of the substance by a unit temperature. Furthermore in the equilibrium state, the most probable speed c_{mp}, that is the speed most likely to be possessed by any molecule, the mean speed c_{ms}, and the root mean square speed c_{rms} of the particles of a monoatomic ideal gas are respectively given by

$$c_{mp} = \sqrt{\frac{2k_bT}{m}} = \sqrt{\frac{2RT}{M}}, \quad c_{ms} = \sqrt{\frac{8k_bT}{\pi m}} = \sqrt{\frac{8RT}{\pi M}}, \quad c_{rms} = \sqrt{\frac{3k_BT}{m}} = \sqrt{\frac{3RT}{M}}.$$

These typical speeds are clearly functions of the gas temperature, specifically the average molecular kinetic energy is proportional to the absolute temperature. Moreover, the typical speeds are obviously interrelated so that $c_{mp} < c_{ms} < c_{rms}$.

The above expression for the root mean square speed, together with the ideal gas law Eq. (12), gives an interesting relation for the pressure:

$$p = \rho(c_{rms}^2/3). \tag{13}$$

It connects a macroscopic property, pressure, to a microscopic property, c_{rms}, which is proportional to the average kinetic energy per molecule. The kinetic theory of gases provides more such connections. Let us now consider the speed of sound in a gas, where the bulk modulus of compressibility K in Eq. (9) can be approximated by $K = \gamma p$. The speed of sound for an ideal gas is then

$$c_s = \sqrt{\frac{\gamma k_bT}{m}} = \sqrt{\frac{\gamma RT}{M}} = c_{ms}\sqrt{\frac{\gamma\pi}{8}}. \tag{14}$$

That is, for a given gas the speed of sound is simply a function of temperature or the mean speed of the molecules. The heat capacity ratio or the adiabatic index γ is the ratio of the heat capacity at constant pressure C_P to the heat capacity at constant volume C_V. For a monoatomic ideal gas with three degrees of freedom,

$\gamma = 5/3$. The expression for the mean free path ℓ_m in a monoatomic ideal gas is a function of temperature and pressure, or simply a function of density,

$$\ell_m = \frac{k_b T}{\sqrt{2}\pi d^2 p} = \frac{RT}{\sqrt{2}\pi d^2 p N_A} = \frac{1}{\sqrt{2}\pi d^2}\frac{M}{\rho N_A}, \tag{15}$$

where d is the effective diameter of molecules. According to the expression, higher temperatures as well as lower pressures, or densities, imply longer mean free paths.

By using relations $M/N_A = m_V/N$ and $\rho = m_V/V$, it is possible to write an even simpler expression for the mean free path

$$\ell_m = \frac{V}{\sqrt{2}\pi d^2 N}. \tag{16}$$

This expression most certainly conforms with our intuition: when the number of molecules N in the reference volume V decreases, the mean free path becomes longer. Finally, the dynamic viscosity of a monoatomic ideal gas in thermal equilibrium is

$$\mu = \frac{1}{2}\rho c_{ms}\ell_m \quad \Leftrightarrow \quad \ell_m = \frac{\mu}{\rho}\sqrt{\frac{\pi m}{2k_b T}}. \tag{17}$$

Because the mean free path is inversely proportional to the density, see Eq. (15), the viscosity μ depends only on temperature via the average speed of the molecules. Moreover, the viscosity of a gas increases together with the temperature. At the time of discovery, this was quite a surprising result.

To summarise the results presented thus far, the classical kinetic theory of gases has provided a great deal of knowledge about the properties of gases in equilibrium. Moreover, the classical kinetic theory is not restricted to monatomic gases, and it has been succesfully applied to a variety of physical systems including diatomic and polyatomic gases, mixtures, electrons in semiconductors, thermal radiation, and many others.

2.2.3 Statistical mechanics approach

While the classical kinetic theory has advanced our understanding about gases in equilibrium, general theories about gas properties in non-equilibrium are subjects of research even today. A very general basis for non-equilibrium kinetic theories is provided by the Liouville equation as well as by the BBGKY hierarchy of equations. In order to give a short introduction to these equations, let us return to the microscopic description of matter. The Hamiltonian formulation Eq. (11) for a system of N particles was presented in Sec. 2.2.1. There it was concluded that the instantaneous state of a particle system can, in principle, be described by a point in the so-called phase space, denoted by $\mathbb{P}$. The phase space has $6N$ mutually orthogonal axis and each axis is associated with a unique degree of freedom, i.e. with a position or momentum component of a particle.

In practice, however, it is simply impossible to associate any definitive point in the phase space to a given macroscopically observable state of a particle system. Hence, we must devise some alternative approach for studying dynamics

of such systems. Here we arrive at the point of departure of statistical and continuum mechanics. We have already considered the continuum fluid mechanics, now we follow a statistical approach. The Hamiltonian formulation of dynamics provides a convenient starting point for a statistical study of complex systems. Let us envisage a large number of distinct systems, $\mathcal{N}$, which macroscopically are equivalent to the actual system we are considering. That is, each of the $\mathcal{N}$ replicates have exactly the same hydrodynamic properties as the system of interest. However, the microscopic description for the target system is not specified, and we expect that the microscopic states differ greatly among the replicates: there is a large number of microscopic states corresponding to any given macroscopic state. This collection of replicate systems is referred to as the *Gibbs ensemble*.

Each replicate in the ensemble is represented by a point $\mathbf{q}^{(k)}$ in the phase space $\mathbb{P}$, $k = 1, \cdots, \mathcal{N}$. If we just assume a large enough value for $\mathcal{N}$, the representative points become quite dense in $\mathbb{P}$, and we can describe their distribution throughout the phase space by a continuous density function. The volume elements of the phase space $d\mathbf{q}$ defining the density must be sufficiently large to contain a significant number of points, but they must also be sufficiently small so that the density varies continuously [Tho04]. However, if we assume an ensemble involving an infinite number of replicate systems, a theoretical construction, the aforementioned volume elements $d\mathbf{q}$ are infinitesimal and the density function is then a continuous function even at the scales smaller than the particles. We can also normalise the density so that it is a probability density in $\mathbb{P}$: the resulting function will be denoted by $F_N \equiv F_N(\mathbf{q}, t) \equiv F_N(\mathbf{r}_1, \mathbf{p}_1, \ldots, \mathbf{r}_N, \mathbf{p}_N, t)$. The fraction of the $\mathcal{N}$ points which at time t lie within a $6N$ dimensional volume element $d\mathbf{q}$ of the phase space, centered about a point $\mathbf{q}$, is $F_N\, d\mathbf{q}$ with the notation $d\mathbf{q} \equiv d\mathbf{q}_1\, d\mathbf{q}_2 \cdots d\mathbf{q}_N$ and $d\mathbf{q}_i = d\mathbf{r}_i\, d\mathbf{p}_i$. It is important to make a distinction between N, the number of particles in a single system, and $\mathcal{N}$, the number of replicate systems in the ensemble. Furthermore, even if F_N is itself a probability, it evolves in a completely deterministic manner. The evolution is governed by the *Liouville's theorem* [Ale04]:

$$\frac{\partial F_N}{\partial t} + \sum_{i=1}^{N} \mathbf{c}_i \cdot \frac{\partial F_N}{\partial \mathbf{r}_i} + \sum_{i=1}^{N} \mathbf{F}_i \cdot \frac{\partial F_N}{\partial \mathbf{p}_i} = 0, \tag{18}$$

where $\mathbf{F}_i$ is the force acting on the ith particle. Equation (18) is in fact a conservation equation for the probability density, and the derivation involves application of the Hamilton's equation Eq. (11). According to the theorem, F_N remains constant along any trajectory in the phase space.

2.2.4 BBGKY hierarchy of equations

The progress made so far is purely formal: the evolution equation Eq. (18) involves just as many degrees of freedom as the original microscopic description – too many. We have to radically omit details in order to obtain a formulation with any potential for applications. Our next step is to contract the statistical mechanical description by directly utilising the ensemble formalism presented thus far.

Fortunately the macroscopic properties of greatest practical interest depend on averages taken with respect to the first few so-called reduced distribution functions. Let us define the R particle reduced distribution function with the following contraction:

$$F_R(\mathbf{r}_1, \mathbf{p}_1, \ldots, \mathbf{r}_R, \mathbf{p}_R, t) \equiv \int F_N(\mathbf{r}_1, \mathbf{p}_1, \ldots, \mathbf{r}_N, \mathbf{p}_N, t)\, d\mathbf{q}_{R+1} \cdots d\mathbf{q}_N.$$

Now, for example, $F_1\, d\mathbf{q}_1$ is the probability of finding particle 1 in the volume element $d\mathbf{q}_1$ about a given point at time t. Similarly, $F_2\, d\mathbf{q}_1\, d\mathbf{q}_2$ is the probability of finding particle 1 in the volume element $d\mathbf{q}_1$ and, at the same time, finding particle 2 in the volume element $d\mathbf{q}_2$. Furthermore, we can use the probability density to define a number density $f_N(\mathbf{r}_1, \mathbf{p}_1, t) = N \cdot F_1(\mathbf{r}_1, \mathbf{p}_1, t)$, and a mass density $f(\mathbf{r}_1, \mathbf{p}_1, t) = m \cdot N \cdot F_1(\mathbf{r}_1, \mathbf{p}_1, t)$, such that the expected number of particles and the expected mass within a volume element are $f_N\, d\mathbf{q}_1$ and $f\, d\mathbf{q}_1$, respectively [Har04]. In the definition of mass density we assumed, for simplicity, that all the particles are identical and $m_i \equiv m$ is the mass of a single particle.

The statistical treatment is still far from complete. In order to describe the temporal development of F_R, we start from the Liouville equation Eq. (18) by integrating it over the coordinates $\mathbf{q}_{R+1} \cdots \mathbf{q}_N$. Before giving away the well-known outcome of the integration, and subsequent mathematical manipulations, at least one detail must be explained. According to a common assumption in statistical mechanical description, the interaction forces between the particles are derivable from a two-particle potential. That is, the force exerted on the ith particle by the jth is derived from a potential $\phi_{i,j}$ which is a function of the distance between the particles. With this assumption, and in a system free from any other kinds of force, the net force $\mathbf{F}_i$ acting on the ith molecule is given by

$$\mathbf{F}_i = \sum_{j=1}^{N} \mathbf{F}_{i,j} := -\sum_{j=1}^{N} \frac{\partial\, \phi_{i,j}}{\partial \mathbf{r}_i}, \quad (\mathbf{F}_{i,\,i} \equiv 0).$$

In the case where no external forces act on the system, the famous equation for F_R is

$$\frac{\partial F_R}{\partial t} + \sum_{i=1}^{R} \mathbf{c}_i \cdot \frac{\partial F_R}{\partial \mathbf{r}_i} + \sum_{i,j=1}^{R} \mathbf{F}_{i,j} \cdot \frac{\partial F_R}{\partial \mathbf{p}_i} = (R - N) \sum_{i=1}^{R} \frac{\partial}{\partial \mathbf{p}_i} \cdot \int \mathbf{F}_{i,R+1}\, F_{R+1}\, d\mathbf{q}_{R+1}. \quad (19)$$

It is called the *BBGKY hierarchy of equations*, named after Bogoliubov, Born, Green, Kirkwood, and Yvon [Ale04]. Of particular interest are the first two equations of the hierarchy:

$$\frac{\partial F_1}{\partial t} + \mathbf{c}_1 \cdot \frac{\partial F_1}{\partial \mathbf{r}_1} = (1 - N) \frac{\partial}{\partial \mathbf{p}_1} \cdot \int \mathbf{F}_{1,2}\, F_2\, d\mathbf{q}_2 \quad (20)$$

and

$$\frac{\partial F_2}{\partial t} + \left(\mathbf{c}_1 \cdot \frac{\partial F_2}{\partial \mathbf{r}_1} + \mathbf{c}_2 \cdot \frac{\partial F_2}{\partial \mathbf{r}_2}\right) + \left(\mathbf{F}_{1,2} \cdot \frac{\partial F_2}{\partial \mathbf{p}_1} + \mathbf{F}_{2,1} \cdot \frac{\partial F_2}{\partial \mathbf{p}_2}\right)$$
$$= (2 - N)\left(\frac{\partial}{\partial \mathbf{p}_1} \cdot \int \mathbf{F}_{1,3}\, F_3\, d\mathbf{q}_3 + \frac{\partial}{\partial \mathbf{p}_2} \cdot \int \mathbf{F}_{2,3}\, F_3\, d\mathbf{q}_3\right).$$

Any attempt to apply the BBGKY hierarchy of equations encounters a completely new problem. Inspection of Eq. (19) reveals that it defines a never-ending chain of equations where reduced distribution functions are linked together: equation for F_R depends on F_{R+1}. In other words Eq. (19) is not closed. Specifically, equation for F_1 depends on F_2 – it is the equation of greatest interest. Now the major challenge is to remove the F_2 dependence, i.e., to make Eq. (20) self-contained in F_1.

2.3 Kinetic theory of non-equilibrium gases

The Liouville equation as well as the BBGKY hierarchy of equations are both very general descriptions for all states of matter: solid, liquid, gas, and even plasma. There is little or no hope of finding a general closure equation for F_1. Most amenable for further modelling has been the gas. The kinetic theory of gases attempts to explain macroscopic properties of gas, like pressure and temperature, with the statistical mechanics of constituent molecules. While in a liquid or solid the molecules are in constant 'contact' with each other, all the time exchanging energy and momentum, the molecules in a gas typically travel most of the time in a free flight, and only once in a while the flight is interrupted by relatively short interactions referred to as collisions [Str05].

2.3.1 The Boltzmann equation

It was 1872 when Boltzmann's closed equation for F_1 was published [Bol72]. It is a general non-equilibrium description intended for rarefied gas flows. Boltzmann obtained his equation in a phenomenological manner based on convincing physical arguments. His own forewords in the profound scientific contribution *Lectures on Gas Theory* were not an overstatement [Bol96]:

> I am conscious of being only an individual struggling weakly against the stream of time. But it still remains in my power to contribute in such a way that, when the theory of gases is again revived, not too much will have to be rediscovered.

Indeed, his work formed the basis for the kinetic theory of rarefied gases and not too much have been rediscovered.

Prior to Boltzmann, a decade or so, Maxwell had already started a new era in science by publishing his related discoveries [Max60a, Max60b]. These discoveries opened up an entirely new approach to physics, which led to statistical mechanics and to a proper understanding of thermodynamics. Maxwell presented the first statistical law in physics, now known as the Maxwell distribution of molecular velocities. Maxwell also predicted that the viscosity of a gas should be independent of density and should increase with increasing temperature, cf. Eq. (17). The latter prediction was a particularly surprising result since liquids

tend to behave in the opposite manner. Experiments confirmed these predictions and gave significant credence to the kinetic theory of gases. Among the most important papers of Maxwell is *On the Dynamical Theory of Gases* [Max67]. There, for example, he introduced the notion of relaxation time: the time it takes a system to return to a state of equilibrium after being disturbed – a concept now routinely used in science. Maxwell advanced kinetic theory to the very end of his life [Max79a, Max79b]. Boltzmann was impressed, and certainly influenced, by the work of his Scottish colleague. Fascinatingly enough, these two persons had almost opposite approaches for practising science: Maxwell advocated *deduction from the phenomena*, that is he gave empirical evidence a primary role in the formation of theories, whereas Boltzmann advocated *hypothetico-deductive method* with the preference for a theory to come first (as a mental picture to a hidden mechanism of reality) and only after its full completion he was willing to compare theoretical implications against empirical facts [Reg96].

Boltzmann did not derive his equation via Liouville equation nor BBGKY hierarchy of equations, both of which are very general descriptions for all matter. Instead, Boltzmann arrived at the closure equation with a more or less intuitive approach. Only much later have procedures been presented where the Boltzmann equation is rigorously derived all the way from the Liouville equation; a clarifying mathematical exposition is given by Grad [Gra58], who establishes very precisely the limit in which the equation is exact. This limit is called the *Boltzmann gas limit* or alternatively the *Boltzmann-Grad limit* (BGL). Here we are content with an informal, verbal declaration of the underlying assumptions [Vil02]:

1. The gas is dilute enough so that only binary collisions between constituent molecules need to be taken into account. This also implies that the interaction potential is of sufficiently short range, for even in a rarefied gas the concept of binary collisions is meaningless if the potential is of such long range that a given particle interacts with many particles at a particular instant.

2. The collisions are completed in a very limited domain both in space and time, that is they are purely local and virtually instantaneous events which occur at a given position $\mathbf{r}$ and a given time t. This means that the typical duration of a collision is very small compared to the typical time scale of the described flow.

3. Total mass, momentum, and kinetic energy are preserved in every collision. Hence, the collisions are elastic among other things.

4. The collisions are *microreversible*. This can be understood either in a purely deterministic way, meaning microscopic dynamics are time-reversible, or in a probabilistic way. That is, the probability that particles with velocities $\overline{\mathbf{c}}, \overline{\mathbf{c}}_R$ acquire velocities $\mathbf{c}, \mathbf{c}_R$ in a collision process is the same as the probability that the velocities $\mathbf{c}, \mathbf{c}_R$ change into $\overline{\mathbf{c}}, \overline{\mathbf{c}}_R$.

5. The state of molecular chaos is assumed before collisions. This assumption is also known as the collision number hypothesis, or *stosszahlansatz*, and it presumes that the velocities of two particles which are about to collide are uncorrelated, and independent of position.

For example, an ideal gas would definitively comply with the first three assumptions above, but the last two assumptions must be considered as additional and more elaborate conditions for the gas.

Like stated above, it is possible to carry out a derivation of Boltzmann's closed equation for the mass density distribution function $f = mNF_1$ in many ways: some emphasise physical argumentation more than mathematical techniques. We will simply present the equation. Here f is considered to be a function of time t, spatial coordinate $\mathbf{r}$, and velocity $\mathbf{c}$, instead of momentum. Furthermore, let $\mathbf{V}_R = \mathbf{c} - \mathbf{c}_R$ denote the relative velocity of two arbitrary particles (V_R is the corresponding speed). The Boltmann equation is founded on the concept of binary collision, i.e., two particles entering a collision will acquire new post-collisional velocities in the process. In a fruitful interpretation, the collision effectively deflects pre-collisional velocities, and the deflection is measured with a directional vector $\mathbf{b}(s, \epsilon, \theta)$. The parameters (s, ϵ, θ) are coordinates in a spherical coordinate system, typically set up as the scene of action for collisions. Then

$$\frac{\partial f}{\partial t} + \mathbf{c} \cdot \frac{\partial f}{\partial \mathbf{r}} + \mathbf{a} \cdot \frac{\partial f}{\partial \mathbf{c}} = \frac{1}{m} \int B(V_R, \theta)(\overline{f}\,\overline{f}_R - f\, f_R)\, d\epsilon\, d\theta\, d\mathbf{c}_R \tag{21}$$

is the celebrated *Boltzmann equation* with an external force $\mathbf{F}$ giving rise to the acceleration $\mathbf{a} = \mathbf{F}/m$; in addition, standard abbreviations have been utilised: $\overline{f} = f(\mathbf{r}, \overline{\mathbf{c}}, t)$, $\overline{f}_R = f(\mathbf{r}, \overline{\mathbf{c}}_R, t)$, $f_R = f(\mathbf{r}, \mathbf{c}_R, t)$. Here $\overline{\mathbf{c}}$ and $\overline{\mathbf{c}}_R$ are the particle velocities which become $\mathbf{c}$ and $\mathbf{c}_R$ in the process of binary collision.

The left hand side of the Boltzmann equation is referred to as the linear transport operator, and the right hand side as the nonlinear collision operator, here denoted by $\mathcal{J}(f)$. The collision operator $\mathcal{J}(f)$ presented in Eq. (21) is rigorously valid only for repulsive potentials. The original and general collision operator, applicable for interaction potentials which are both repulsive and attractive, is

$$\mathcal{J}(f) = \frac{1}{m} \int V_R(\overline{f}\,\overline{f}_R - f\, f_R)\, d\omega\, d\mathbf{c}_R, \tag{22}$$

where the collision process is now described in a polar coordinate system (s, ϵ), and $d\omega = s\, ds\, d\epsilon$ is an area element in a disk. The nonnegative function $B(V_R, \theta)$ in Eq. (21) is the *Boltzmann collision kernel* orchestrating binary collisions. The explicit form of $B(V_R, \theta)$ depends on the two-particle interaction potential $\phi_{i,j}$. A set of important collision models is provided by the inverse-power law potentials [Vil02],

$$\phi_{i,j}(r) \propto r^{-k+1}, \quad k > 2, \tag{23}$$

where r is the distance between two particles. Remember that the interaction force is computed as the derivative of the potential, with respect to the mutual distance. The collision kernel cannot be computed explicitly for the above potentials, but it has been shown that with a particular choice, $k = 5$, the kernel is no

longer dependent on the relative velocity between particles, i.e., $B(V_R, \theta) \rightarrow B(\theta)$. Particles obeying inverse-power law potentials with $k = 5$ are called *Maxwell molecules*. Both Maxwell and Boltzmann used frequently, but not exclusively, this admittedly theoretical model for particles – mainly because it allowed many explicit calculations.

From a mathematical perspective, Boltzmann's nonlinear integro-differential equation is anything but amenable for solution. Without solving it, Boltzmann was able to deduce immediately a very important result from his equation, namely the *H-Theorem*. It is a molecular-kinetic interpretation of the second law of thermodynamics, and in particular of the statistical meaning of the concept of entropy. In thermodynamics, the entropy is a direct measure for disorder or chaos of the fluid flow. Boltzmann discovered that it is possible to define the function

$$H = \int f \ln f \, d\mathbf{c}$$

which, if one assumes molecular chaos, must always decrease or remain constant in a closed system. Relation to the principle of increasing entropy is evident if the H-function is identified with the negative of entropy, $S = -k_b H + K$, where k_b is the Boltzmann constant and K an additional (here arbitrary) constant.

A molecular interpretation of the law of increasing entropy is thus intimately related to the assumption of molecular chaos and the relation between entropy and probability. The formula

$$S = k_b \ln W$$

connecting the entropy and the thermodynamic probability W (statistical weight of the macroscopic state of the system) is inscribed on Boltzmann's tombstone [Ale00]. Bolztmann's discovery culminated in the fact that function H remains constant only when the gas attains a special velocity distribution previously deduced by Maxwell in a more heuristic manner [Max60a, Max67]:

$$\begin{aligned} f^M(\mathbf{r}, \mathbf{c}, t; \rho, \mathbf{u}, T) &= \rho \left(\frac{m}{2\pi k_b T} \right)^{3/2} e^{-mv^2/2k_b T} \\ &= \rho \left(\frac{1}{\pi c_{mp}^2} \right)^{3/2} e^{-(v/c_{mp})^2}, \end{aligned} \tag{24}$$

where $\mathbf{v} = \mathbf{c} - \mathbf{u}$ is the thermal or relative or peculiar velocity, that is the particle velocity with respect to the macroscopic fluid flow velocity $\mathbf{u}$; $v^2 = v_\alpha v_\alpha = \mathbf{v} \cdot \mathbf{v}$. The local equilibrium state is provided by the local Maxwellian, Eq. (24), and accordingly $\mathcal{J}(f^M) = 0$. The Maxwellian distribution function f^M is also a mapping from hydrodynamic to mesoscopic description. In summary, Boltzmann presented an impressive bridge between microscopic and macroscopic mechanics.

The assumption of molecular chaos was a key element in Boltzmann's H-theorem, but it was initially unrecognised. It added, with no mechanical basis, another stochastic factor to the kinetic theory. Even if the velocities of colliding

particles are uncorrelated, they are correlated after the collision. By asserting that it was acceptable to ignore these correlations in the particle population at times after the initial time, Boltzmann had introduced an element of time asymmetry.

2.3.2 Hydrodynamic equations from the Boltzmann equation

The rationale for expressing fluid flow dynamics in terms of the mass density distribution function f is that we can relate the mesoscopic description so obtained to the macroscopic or fluid mechanical description. As a reminder, $f\,d\mathbf{r}\,d\mathbf{c}$ is the expected mass in the phase space volume element $d\mathbf{r}\,d\mathbf{c}$ about a given phase point $(\mathbf{r}, \mathbf{c})$. Thus, integration of f over its velocity argument will give an expression for the expected mass in the volume element $d\mathbf{r}$ about $\mathbf{r}$:

$$\rho(\mathbf{r}, t) = \int f(\mathbf{r}, \mathbf{c}, t)\, d\mathbf{c}.$$

In other words, ρ is the macroscopic fluid mass density. Furthermore,

$$\rho(\mathbf{r}, t)\mathbf{u}(\mathbf{r}, t) = \int \mathbf{c} f(\mathbf{r}, \mathbf{c}, t)\, d\mathbf{c}$$

defines the macroscopic fluid flow velocity $\mathbf{u}$. The density and momentum density presented above are zeroth and first order moments of f, respectively. Moments are easily defined up to an arbitrary order:

$$M_{\alpha\beta\cdots\nu} = \int c_\alpha c_\beta \cdots c_\nu f(\mathbf{r}, \mathbf{c}, t)\, d\mathbf{c}.$$

However, a physical interpretation is meaningful only for the low order moments. The second order moments are related to momentum transfer and energy density in the fluid. First of all, the total energy related to the molecules in an ideal gas is entirely due to their translational kinetic energy: $mc^2/2$. Thus, the energy density in a monoatomic ideal gas is

$$\rho(\mathbf{r}, t)e(\mathbf{r}, t) = \frac{1}{2}\int c_\alpha c_\alpha f(\mathbf{r}, \mathbf{c}, t)\, d\mathbf{c};$$

the particle mass m is already incorporated in the definition of mass density f. Next we will utilise the definition of the peculiar velocity $v_\alpha = c_\alpha - u_\alpha$. Evidently, the first moment of f over v_α vanishes. This fact allows us to write the energy density in the form

$$\rho e = \frac{1}{2}\int v_\alpha v_\alpha f(\mathbf{r}, \mathbf{c}, t)\, d\mathbf{c} + \frac{1}{2}\rho u^2 =: \rho\xi + \frac{1}{2}\rho u^2.$$

Above we have defined the internal or thermal energy of the gas $\rho\xi$, and $\rho u^2/2$ is the kinetic energy contributed to the macroscopic fluid motion. According to the equipartition theorem

$$\xi = \frac{3RT}{2M},$$

which establishes a relation between the internal energy and temperature of an ideal gas. Of course, the equipartition theorem applies strictly to an equilibrium situation, and hence strong deviations from the equilibrium may compromise the above relation.

The local Maxwellian, an equilibrium state, also produces the first few moments:

$$\rho = \int f^M \, d\mathbf{c}, \quad \rho u_\alpha = \int c_\alpha f^M \, d\mathbf{c}, \quad \rho\xi = \frac{1}{2}\int v^2 f^M \, d\mathbf{c} = \rho\frac{3RT}{2M}.$$

An another important fact is related to the collision operator $\mathcal{J}(f)$. Functions $1, c_\alpha$, and c^2 are eigenfunctions of the integral operator $\int \cdot \, \mathcal{J}(f) \, d\mathbf{c}$ having eigenvalue zero. That is,

$$\int 1 \, \mathcal{J}(f) \, d\mathbf{c} = \int c_\alpha \, \mathcal{J}(f) \, d\mathbf{c} = \int c^2 \, \mathcal{J}(f) \, d\mathbf{c} = 0.$$

This property has a simple physical interpretation: mass, momentum, and kinetic energy are conserved in the collisions. Of course, we should not be too astonished, because the conservation properties have been *a priori* assumed in the derivation of the collision operator.

The net momentum transfer in a flow is described by the second-rank tensor $\Pi_{\alpha\beta}$. Components of $\mathbf{\Pi}$ report the amount of momentum locally transported in each spatial direction. The tensor is a second order moment in the velocity space by definition

$$\Pi_{\alpha\beta} = \int c_\alpha c_\beta f \, d\mathbf{c} = \rho u_\alpha u_\beta + \int v_\alpha v_\beta f \, d\mathbf{c} =: \rho u_\alpha u_\beta - \Pi^{str}_{\alpha\beta},$$

where $\rho u_\alpha u_\beta$ accounts for the advected momentum. Obviously $\mathbf{\Pi}$ is symmetric, i.e. $\Pi_{\alpha\beta} = \Pi_{\beta\alpha}$. The stress tensor $\Pi^{str}_{\alpha\beta}$ describes momentum flux due to the microscopic particle motion in the frame of reference moving with the local macroscopic fluid flow velocity $\mathbf{u}$. Now, if we relate pressure p to the trace of the stress tensor, i.e. to the average of the diagonal components of $\mathbf{\Pi}^{str}$, we obtain an interesting relation:

$$p = -\frac{1}{3}\Pi^{str}_{\alpha\alpha} = \frac{1}{3}\int v_\alpha v_\alpha f \, d\mathbf{c} = \frac{2}{3}\rho\xi.$$

Therefore, if we accept the previously presented relation $\xi = 3RT/2M$ due to the equipartition theorem, we have

$$p = \frac{2}{3}\rho\xi = \rho\frac{RT}{M},$$

which is nothing but the ideal gas law! The recovery of the ideal gas law serves as a consistency check for the presented identifications of molecular quantities with the macroscopic variables. Finally, it is common practice to define the viscous stress tensor as the traceless part of the stress tensor:

$$\Pi^{visc}_{\alpha\beta} := \Pi^{str}_{\alpha\beta} - \frac{1}{3}\Pi^{str}_{\gamma\gamma}\delta_{\alpha\beta} = \Pi^{str}_{\alpha\beta} + p\delta_{\alpha\beta};$$

$p\delta_{\alpha\beta}$ is the so-called mean normal stress tensor and $\Pi^{visc}_{\alpha\beta}$ is the stress deviator tensor, or the viscous stress tensor. In the continuum mechanics interpretation, the former tends to change the volume of the stressed body and the latter tends to distort it.

When considering the transport of energy in a fluid flow, expressed with contracted third order moments in the velocity space, we distinguish between the net energy flow **E** and the heat flux **Q**. The net energy flow is the total kinetic energy flow per unit area through an imaginary fixed surface, whereas the heat flux is a similar quantity but through a surface moving with the local macroscopic fluid flow velocity [Har04]. Thus, the heat flux is only a component of the net energy flow:

$$\begin{aligned} Q_\alpha &= \int v_\alpha \frac{v^2}{2}\, d\mathbf{c}, \\ E_\alpha &= \int c_\alpha \frac{c^2}{2}\, d\mathbf{c} = \int \frac{1}{2}(v_\alpha + u_\alpha)(v^2 + 2v_\beta u_\beta + u^2)\, d\mathbf{c} \\ &= Q_\alpha - u_\beta \Pi^{str}_{\alpha\beta} + \rho u_\alpha (\xi + \frac{1}{2}u^2). \end{aligned}$$

Clearly, the total energy flow includes contributions from heat, work, and advected energy.

We are now able to connect the Boltzmann equation Eq. (21), a particular mesoscopic description, with macroscopic descriptions of fluid flows. In general, we can obtain an equation for the moment of an arbitrary order $M_{\alpha\beta\ldots\nu}$; we simply multiply the Boltzmann equation by $c_\alpha c_\beta \cdots c_\nu$ and then integrate it over $\mathbf{c}$. Again, we are particularly interested in the equations for the first few moments. We thus multiply Eq. (21) successively by $1, c_\alpha, c^2/2$ and then integrate the three equations over the velocity space. This gives us

$$\begin{gathered} \partial_t(\rho) + \partial_\alpha(\rho u_\alpha) = 0, \\ \partial_t(\rho u_\alpha) + \partial_\beta(\rho u_\alpha u_\beta - \Pi^{str}_{\alpha\beta}) = 0, \\ \partial_t\big[\rho(\xi + \frac{1}{2}u^2)\big] + \partial_\alpha\big[Q_\alpha - u_\beta \Pi^{str}_{\alpha\beta} + \rho u_\alpha(\xi + \frac{1}{2}u^2)\big] = 0, \end{gathered} \tag{25}$$

which are the usual equations of the macroscopic theory for mass, momentum, and energy conservation (cf. Eqs (1) and (2))! Above we have neglected the external force **F**, and in addition $\partial_\alpha \equiv \partial/\partial r_\alpha$. These equations elucidate the advantages of mesoscopic description in a transparent manner. Namely, there are five macroscopic equations for determining 13 independent hydrodynamic variables (density, three velocity components, six components of the symmetric tensor $\mathbf{\Pi}^{str}$, and three heat flux components). For this reason, the above hydrodynamic description is not self-contained. One is compelled to make various assumptions about the flow phenomena under investigation. These assumptions are then mathematically expressed with constitutive equations, relations between the hydrodynamic variables, which reduce the number of independent variables. In this way, one then obtains a closed set of specific equations, e.g. the Euler or Navier-Stokes

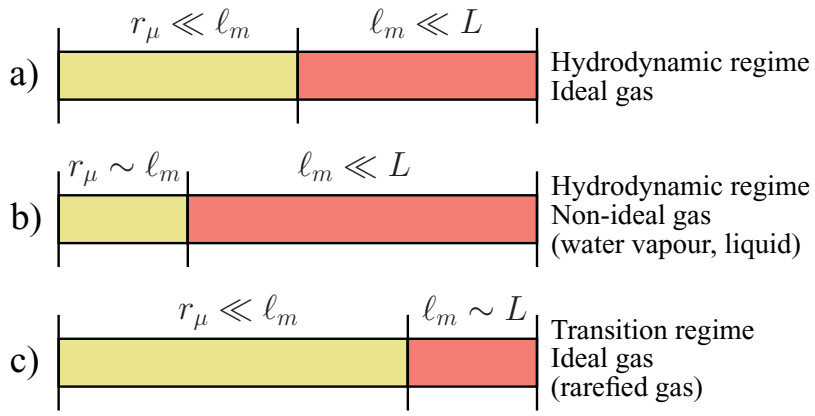

FIGURE 3 Fluid flows can be categorised in many ways. Here we use ratios of the effective interaction radius r_μ, the mean free path ℓ_m, and the characteristic hydrodynamic length L to define the hydrodynamic regime for a) ideal gases and b) non-ideal gases as well as c) the transition regime for ideal gases.

equations depending on the assumptions. From a mesoscopic point of view, these equations are always approximations.

The major advantage of the mesoscopic description is that there is no need to use macroscopic conservation equations for solving the space and time dependence of the hydrodynamic moment variables. Indeed, by directly solving the Boltzmann equation, the same information can be extracted from the solution f. Furthermore, the Boltzmann equation is applicable to infinitely high Knudsen number flows unlike, e.g., the Navier-Stokes equation – even though the BGL limit must be replaced in such cases with the so-called Knudsen limit. Because of the importance, we stress once more that there is no contradiction in modelling hydrodynamic fluid flows ($K_n \ll 1$) with the Boltzmann equation, provided there exists a clear scale separation: $r_\mu \ll \ell_m \ll L$, see Fig. 3. It is hard to miss the resemblance between scale separations required here and in the section of macroscopic modelling! The true limitation stems from the fact that the Boltzmann equation is invalid at the time scales of molecular interactions – collisions are considered instantaneous events. There are propositions for equations which are valid also in the interaction scales. They are collectively called generalised Boltzmann equations, see e.g. Refs [Ens22, Ale94, Ale00, Ale04]. Related to this discussion are general Boltzmann type models which can be constructed by requiring more independent parameters for the mass density distribution function f. These parameters, accompanying $\mathbf{r}, \mathbf{c}$, and t, can label e.g. additional internal states of the particles [Cha39, Arl02].

The two evolution mechanisms in Eq. (21), the linear transport and the nonlinear collision, are implicitly weighted by the Knudsen number. The Knudsen number appears directly in the Boltzmann equation when it is made dimensionless. Let us introduce dimensionless variables and denote them by asterisk

[Kel48, Str05]:

$$r_\alpha = L\, r^*_\alpha, \quad c_\alpha = c_{ms}\, c^*_\alpha, \quad t = \frac{L}{c_{ms}}\, t^*, \quad f = \frac{mN}{L^3 c^3_{ms}}\, f^*, \quad a_\alpha = \frac{c^2_{ms}}{L}\, a^*_\alpha,$$

$$d\omega = \pi\, d^2\, d\omega^*, \quad d\mathbf{c}_R = c^3_{ms}\, d\mathbf{c}^*_R, \quad V_R = V_{ave}\, V^*_R = (\sqrt{2}\, c_{ms})\, V^*_R, \tag{26}$$

where c_{ms} is the mean speed of the particles at a reference temperature T_0, the number of particles in the reference volume $V = L^3$ is N, the acceleration a_α is due to an external force, V_{ave} is the average of relative velocities between the particles, $d\omega$ and $d\mathbf{c}_R$ are related to the integrals in the binary collision operator $J(f)$, see Eq. (22), and d is the effective diameter of the particles – alternatively, the interaction radius r_μ could have been used instead of d. Just like in the case of the Navier-Stokes equation, the dimensional measures are considered constant, and hence the derivatives in the Boltzmann equation are easily transformed into dimensionless form. By using the above definitions in the Boltzmann equation, with the collision operator defined in Eq. (22), its dimensionless form is given by

$$\partial^*_t f^* + c^*_\alpha\, \partial^*_{r_\alpha} f^* + a^*_\alpha\, \partial^*_{c_\alpha} f^* = \frac{1}{K_n}\, J^*(f^*), \tag{27}$$

where we have utilised the expression Eq. (16) for the mean free path ℓ_m. This is a beautiful result: K_n explicitly measures relative importance of the linear transport operator (the left hand side) and the nonlinear collision operator (the right hand side). Since the right hand side must remain finite when $K_n \to 0$, it follows that simultaneously $J^*(f^*)$ must approach zero which, in turn, is an implicit statement for $f^* \to f^M_*$. The Knudsen number defines dynamic similarity between fluid flows with respect to the Boltzmann equation and after a particular interaction potential has been fixed, in the same way as the Reynolds number does with respect to the Navier-Stokes equation.

2.3.3 Approximate solutions of the Boltzmann equation

The large number of independent variables in the distribution function, seven in the general case considered here, together with the very complicated structure of the collision operator Eq. (22), lay a scene where the mathematical treatment of the Boltzmann equation is a formidable task. To prove theorems like the global existence and uniqueness of the solutions to this equation is certainly challenging. One of the earliest attacks on these issues was conducted, with a mathematical rigour, by Torsten Carleman – a swedish mathematician [Car33, Car57]. His famous publication on the topic dates back to the 1930's, when he considered solutions in very simple and specific cases. The string of mathematical developments thereafter is treated, for example, in Refs [Cer88, Cer94, Vil02, Cer09]. It is worth commenting that Ref. [Vil02] includes over 450 references accompanied by useful bibliographical notes, which help to orientate through the huge literature. As usual, instead of seeking for exact solutions to the Boltzmann equation, one may take an alternative approach, and seek for approximate solutions.

It was Maxwell himself who already proposed a technique for obtaining approximate solutions [Max67]. His proposal was based on the moments and on the moment equations called Maxwell's equations of transfer. Furthermore, Maxwell's procedure for approximate solutions relies on the Maxwell molecules, i.e. on the specific interaction potential between particles given by the Eq. (23) with $k = 5$. Nearly half a century later, in 1912, the great mathematician David Hilbert came forward with his proposal [Hil12]. He indicated how approximate solutions of the Boltzmann equation can be obtained by *a priori* expanding the distribution function f in a power series of a parameter inversely proportional to the gas density. For example, the Knudsen number can be used as a small expansion parameter:

$$f_H(\mathbf{r}, \mathbf{c}, t) := f^M + K_n f^{(1)} + K_n^2 f^{(2)} + \dots, \tag{28}$$

where the arguments of $f^{(i)}(\mathbf{r}, \mathbf{c}, t)$ are simply not written and the zeroth order approximation $f^{(0)}$ is identified as the Maxwellian distribution f^M. Few years later further progress was made when both Chapman and Enskog, independently but almost simultaneously (within about a year), obtained their approximate solutions of the Boltzmann equation [Cha16, Ens17]. Their results were identical from the practical point of view, but their procedures of computation were not identical– quite the contrary, their means were different with respect to the spirit as well as details.

Enskog basically generalised Hilbert's approach allowing a systematic construction of higher-order approximations; their respective treatment of the term $\partial f/\partial t$ in the Boltzmann equation is a particular point of disparity. At the same time, Chapman extended the procedure of Maxwell and, particularly, did not constrain himself to the theoretical gas of Maxwell molecules. He accomplished this by assuming, like Maxwell, a solution f deviating only slightly from the Maxwellian distribution:

$$f_C(\mathbf{r}, \mathbf{c}, t) := f^M(1 + \varphi(\mathbf{v})), \tag{29}$$

where φ is a general unknown function of small magnitude for which an expression is to be determined. Here Chapman deviated from Maxwell's path; he assumed a different form for the unknown function φ, and then used an infinite set of transfer equations to compute approximate solutions for it. By adhering to their choices, both Enskog and Chapman were able to compute expressions for the transport coefficients of fluid flows, i.e. for the viscosity, thermal conductivity, and diffusion coefficient. Notice that at a macroscopic level of description, the transport coefficients are typically considered as unknowns or modelling parameters.

Later on, Chapman and Cowling wrote their influential book *The Mathematical Theory of Non-Uniform Gases* [Cha39], where they adopted the method of Enskog. Since the book, dedicated gentlemanly to David Enskog, was more accessible to the general audience than the work published by Enskog, and since the two persons discovered identical expressions for the transport coefficients independently, the name Chapman-Enskog method is used today. Here we once

again have an example of simultaneous discovery which appears to be a persistent feature in the history of modern science. Chapman himself had a healthy attitude towards these incidents, as is clear from his statement [Bru72, pp.11]:

> If a discovery is highly abstract and complicated, the fact that two people simultaneously and independently publish the same result tends to produce much more confidence and acceptance of the result among other scientists who would not wish to follow through the details of the calculation; by helping to establish the validity of the discovery, the simultaneity benefits both discoverers at once.

For anyone interested in the related historical details, we cannot but advertise the sincere and warm-hearted memoir by Chapman – a delightfully personal account [Cha67].

The Chapman-Enskog method gives the Euler, Navier-Stokes-Fourier, and Burnett equations in successive levels of approximation with explicit expressions for the viscosity, among other transport coefficients. Furthermore, the explicit expressions depend on the specific interaction potential chosen for modelling the encounters between molecules. For example, Chapman and Enskog found that the expression for viscosity μ given in Eq. (17), reformulated as

$$\mu = \left(\frac{k_b T m}{\pi^3 d^4}\right)^{1/2},$$

is practically a perfect description, at the Navier-Stokes level of approximation, for a smooth rigid elastic spherical molecules of diameter d – corresponding to a repulsive force model of type $F = Kr^{-n}$, where K is an arbitrary coefficient and $n = \infty$. For Maxwell molecules, $n = 5$, their expression for viscosity agreed with that of Maxwell's. Generally speaking, all their expressions for viscosity, related to purely repulsive interaction models of the aforementioned type, are independent of density. The dependence of viscosity on temperature for the same models, according to Chapman and Enskog, is generally of the form $\mu \sim T^{(n+3)/2(n-1)}$. This agrees with the specific results, obtained already by Maxwell, namely $\mu \sim T^{1/2}$ (see the above expession) and $\mu \sim T$ for $n = \infty$ and $n = 5$, respectively. Above all, the Chapman-Enskog method allows computation of the viscosity coefficient for any interaction force law, in principle at least.

The fundamental assumption justifying the Maxwell-Chapman approach, as well as the Hilbert-Enskog approach, enforces consideration of approximate solutions almost equal to the local Maxwellian distribution f^M. That is, both approaches are limited to fluid flows in the small Knudsen number regime – a fact very evident from the expansion Eq. (28). Essentially these approaches assume normal solutions of the Boltzmann equation, implying that the distribution function f is uniquely determined by the five hydrodynamic variables ρ, $\mathbf{u}$, T and their first derivatives. In order to obtain solutions, not limited exclusively to the small Knudsen number regime, Harold Grad proposed a different kind of approximation procedure [Gra49a, Gra49b]. His formal idea was to expand f as a function

of microscopic velocity $\mathbf{c}$ in terms of the generalised Hermite polynomials $\mathcal{H}^{(n)}$:

$$f_G(\mathbf{r},\mathbf{c},t) := f^M\Big(1 + a^{(1)}\mathcal{H}^{(1)} + \frac{1}{2!}a^{(2)}\mathcal{H}^{(2)} + \frac{1}{3!}a^{(3)}\mathcal{H}^{(3)} + \dots\Big), \qquad (30)$$

where the generalised Hermite polynomials $\mathcal{H}^{(n)}$ are given tensors of rank n, and functions of the microscopic velocity only. For example,

$$\mathcal{H}^{(2)} \equiv \mathcal{H}^{(2)}_{\alpha\beta}(\mathbf{c}).$$

The coefficients $a^{(n)}$ of the Hermite polynomials are the primary unknowns, functions of the spatial coordinate $\mathbf{r}$ and time t only, and also tensors of rank n, e.g.

$$a^{(2)} \equiv a^{(2)}_{\alpha\beta}(\mathbf{r},t).$$

Note how the depence of the distribution function f_G on its arguments is reorganised in the expansion Eq. (30): the known component in the expansion contains the dependence on $\mathbf{c}$, and the unknown component contains the dependence on $\mathbf{r}$ and t. This is the *leitmotif* of the Grad expansion!

The true distribution function f is given by the Grad expansion with infinite number of terms. An approximation for f is obtained when only a finite number of terms are retained in the expansion. To obtain a definite expression for f_G, with only a finite number of terms in the expansion, the unknown coefficients $a^{(n)}$ of the Hermite polynomials must be found. The procedure of solving for the coefficients involves successively multiplying the expansion for f_G by Hermite polynomials, here the left hand side of Eq. (30) is formally taken to be equal to f. Since the depence of f_G on its arguments is decoupled, and since the generalised Hermite polynomials are orthogonal with respect to an inner product in the velocity space, the aforementioned procedure will immediately yield expressions for the unknown coefficients. In general, all the coefficients $a^{(n)}$ turn out to be linear combinations of the moments of f. Grad's procedure then continues with the construction of evolution equations for the now determined coefficients. The procedure is, at least in principle, able to produce non-normal solutions of the Boltzmann equation, i.e. solutions are not limited to the small Knudsen number regime. One of the advantages of Grad's approach is that the dependence of the approximate solution f on its moments is explicit. That is, moments of higher-order than $\rho, \mathbf{u}, T$ appear directly in the expansion. Probably the best-known approximation is Grad's system of 13 equations with the variables $\rho, \mathbf{u}, T, \mathbf{\Pi}, \mathbf{Q}$.

There is still one alternative, related to approximate solutions of the Boltzmann equation, which we would like to mention. The so-called linear Boltzmann equation is obtained with the assumption that the distribution function f varies around the Maxwellian distribution f^M such that

$$f_L(\mathbf{r},\mathbf{c},t) := f^M(1 + g(\mathbf{r},\mathbf{c},t)).$$

The above expression for f is then substituted into the Boltzmann equation, and only terms linear in perturbation g are retained, giving the linear collision operator

$$\mathcal{L}(g) := \frac{1}{m}\int B(V_R,\theta)(\overline{g}_R + \overline{g} - g - g_R)\, f^M(\mathbf{r},\mathbf{c}_R,t)\, d\epsilon\, d\theta\, d\mathbf{c}_R. \qquad (31)$$

It is of course an easier task to find solutions of the linear Boltzmann equation, both exact and approximate, than to tackle the true nonlinear Boltzmann equation. The perturbation function g is naturally small in magnitude, and hence the linear Boltzmann equation also describes processes not too far from the thermodynamic equilibrium.

2.3.4 Model Boltzmann equations

From an analytical treatment perspective, the most formidable barrier obstructing derivation of exact solutions to specific flow problems is the non-linear collision operator $\mathcal{J}(f)$ standing on the right-hand side of the Boltzmann equation Eq. (21). Even with the linearised Boltzmann equation Eq. (31), obtaining solutions to problems of interest still involves a great deal of painstaking labour. The most obvious shortcut for obtaining solutions is to replace the complex collision operator with a simpler expression. These expressions are called collision models, and any Boltzmann-like equation where $\mathcal{J}(f)$ is replaced by a simpler collision model is called a model Boltzmann equation or a kinetic model equation. The rationale behind this replacement is that the fine structures of the original binary collision model are not likely to influence significantly the values of many experimentally measured quantities. In essence, simpler models are blurred images of the original binary collision model, and retain only the qualitative and average properties of $\mathcal{J}(f)$. Let $\mathcal{M}(f)$ denote a simple collision model. Then $\mathcal{M}(f)$ should at least respect the most important properties of the original binary collision model:

1. Mass, momentum, and energy are conserved in the collisions. This is guaranteed if
$$\int 1\,\mathcal{M}(f)\,d\mathbf{c} = \int c_\alpha\,\mathcal{M}(f)\,d\mathbf{c} = \int c^2\,\mathcal{M}(f)\,d\mathbf{c} = 0.$$
2. The production of entropy in the collision process is always positive, i.e.
$$-\int \mathcal{M}(f)\ln f\,d\mathbf{c} \geq 0.$$
3. In an equilibrium state, the mass density distribution function f is given by the Maxwellian, or mathematically
$$\mathcal{M}(f) = 0 \quad \Rightarrow \quad f = f^M(\rho, \mathbf{u}, T).$$

The second property expresses the tendency of the gas to approach the Maxwellian distribution. This is the inspiration for a broad class of collision models. The simplest scheme of them all was proposed by Bhatnagar, Gross, and Krook, in the article published in 1954, and independently by Welander in the very same year [Bha54, Wel54]. In their proposal, collisions explicitly relax distribution functions towards the Maxwellian distribution, and the relaxation rate is controlled by the mean free flight time τ_m between the collisions:

$$\mathcal{M}_{BGK}(f) = \frac{1}{\tau_m}(f^M - f); \tag{32}$$

here the collision frequency $1/\tau_m$ is assumed constant, especially independent of the particle velocity $\mathbf{c}$, and it is generally treated as an adjustable parameter. This is a practical model, and the microscopic parameter τ_m conveniently tunes the Knudsen number. This single relaxation time scheme is usually called the *BGK model*, unfortunately ignoring Welander, and it respects the three properties presented above. On the other hand, the original binary collision model prescribes the transport coefficients μ and κ, viscosity and thermal conductivity, so that their ratio, i.e. the Prandtl number P_r is $2/3$. The BGK model differs in this respect since it enforces $P_r = 1$. Note also that the BGK model is deceptively simple and only apparently linear. The BGK model is actually highly non-linear because the Maxwellian is a complicated function of the hydrodynamic variables, which themself are moments of the mass density distribution functions in the velocity space.

A variant of the BGK model, where the collision frequency is velocity dependent, does prescribe transport coefficients so that $P_r = 2/3$. However, the variant is not too appealing for other physical reasons [Mie04]. Another modelling approach was presented by Holway [Hol66]: he suggested modifications to the simple model Eq. (32) by presenting an upgraded version, nowadays called the *ellipsoidal statistical BGK model* (ES-BGK). In the ES-BGK model, the Prandtl number can be controlled by a single model parameter. This property is provided with the replacement of the Maxwellian equilibrium distribution function (an isotropic Gaussian) by an anisotropic Gaussian [Mie04, Str05]:

$$\mathcal{M}_{ES}(f) = \frac{1}{\tau_m}(f^{ES} - f), \tag{33}$$

where

$$f^{ES} = \rho \left(\frac{1}{\det(2\pi\, T_{\alpha\beta})} \right)^{1/2} \exp(-\frac{1}{2} T^{-1}_{\alpha\beta}\, v_\alpha v_\beta)$$

includes the matrix

$$T_{\alpha\beta} = \frac{k_b T}{m}\delta_{\alpha\beta} + \frac{b}{\rho}\Pi^{visc}_{\alpha\beta};$$

the function $\det(\cdot)$ is the determinant, $\mathbf{\Pi}^{visc}$ is the traceless viscous stress tensor, and the inverse of matrix $\mathbf{T}$ is positive definite if $-1/2 \leq b \leq 1$. The ES-BGK model also respects the three properties presented above; the proof of the second property, increase of entropy, was presented very recently [And00, And01]. The parameter b can be adjusted to deliver the desired Prandtl number: $P_r = 1/(1-b)$. Obviously for $b = 0$, the ES-BGK model reduces to the standard BGK model. By using the definitions of the dimensionless variables, Eq. (26), the dimensionless form of the BGK model is

$$\partial^*_t f^* + c^*_\alpha\, \partial^*_{r_\alpha} f^* + a^*_\alpha\, \partial^*_{c_\alpha} f^* = \frac{1}{K_n}\,(f^M_* - f^*), \tag{34}$$

where we have utilised the definition $\tau_m = \ell_m / c_{ms}$. The dimensionless equation for the ES-BGK model is of equivalent form. Thus, the concept of dynamic similarity emerges once again, providing freedom to choose favourable modelling parameters as long as the desired value is maintained for K_n.

There is numerical evidence that the above models are accurate at the hydrodynamic regime, and are able to give qualitatively good results in the transition regime [And02, Mie04]. However, they fail to accurately describe flows at larger Knudsen numbers. This is not too surprising, because the models have a connection with the linearised Boltzmann equation, see Eq. (31), which describes processes where the distribution function f is always close to the Maxwellian distribution f^M [Gro59, Har04]. That is, the processes described do not include strong deviations from the thermodynamic equilibrium, and hence the Knudsen number must be small. Furthermore, the ES-BGK model is basically constructed for gases comprised of Maxwell molecules [Kos09]. A comprehensive survey on model equations is provided in Ref. [Zhe04] (see especially Table 2.1 in the reference). Finally, it is actually very intriguing to speculate under which conditions the BGK and ES-BGK models are strictly valid. For example, they do not involve, at least directly, an assumption of binary collisions. At the moment, we are not aware of publications describing efforts to derive e.g. the BGK model directly from the Liouville equation or alternatively from the BBGKY hierarchy of equations, rather than from the linearised Boltzmann equation.

2.3.5 Kinetic boundary conditions

When attention is focused to applications, it is immediately necessary to consider appropriate boundary conditions. In a typical scenario, fluid flow is either confined or diverted by solid boundaries – walls if you like. In the kinetic theory of gases, boundary conditions for such scenarios describe the interaction of the gas molecules with the solid walls. These interactions give rise to the drag and lift exerted by the gas on the solid body. They also account for heat transfer between the gas and the solid boudary. Realistic boundary conditions for e.g. the Boltzmann equation are, however, very difficult to formulate [Cer94]. In an optimal situation, we would have insight into the interaction mechanism combining aspects from both the kinetic theory of gases and solid-state physics. Unfortunately, our understanding even today about such a mechanism is very limited hindering new innovations on the topic. In general, it is not known how the molecules of a gas behave when they encounter a solid wall. Maxwell was well aware of the difficulties related to the modelling of gas dynamics in the close vicinity of solid walls, and made this known at the appendix of *On Stresses in Rarified Gases Arising from Inequalities of Temperature* published in 1879 [Max79a]:

> In the paper as sent in to the Royal Society, I made no attempt to express the conditions which must be satisfied by a gas in contact with a solid body, for I thought it very unlikely that any equations I could write down would be a satisfactory representation of the actual conditions, especially as it is almost certain that the stratum of gas nearest to a solid body is in a very different condition from the rest of the gas. One of the referees, however, pointed out that it was desirable to make the attempt, and indicated several hypothetical forms of surfaces which might be tried.

And sure enough, Maxwell makes the attempt in the very same appendix by presenting his ideas about boundary conditions at the interface between gas and solid. His idea was a combination of two boundary conditions. Let $\mathbf{n}(\mathbf{r})$ denote an outward unit normal at the solid boundary Γ_S, i.e. $\mathbf{n}$ points from the solid to the gas domain. The first and most natural boundary condition he considered was the *specular reflection law*:

$$f(\mathbf{r}, R\mathbf{c}, t) = f(\mathbf{r}, \mathbf{c}, t), \quad R\mathbf{c} = \mathbf{c} - 2\left[\mathbf{c} \cdot \mathbf{n}(\mathbf{r})\right] \mathbf{n}(\mathbf{r}), \quad \mathbf{r} \in \Gamma_S. \tag{35}$$

Here the tangential velocities of impinging molecules remain unchanged, but the normal components of the velocities are reversed. Since specular reflection implies zero friction in the tangential direction of the boundary, molecules so emitted to the gas do not impose drag on the solid body – there are no shear stresses acting on the wall. In reality solid walls do resist gas flows, and thus there has to be a mechanism responsible for friction at the boundary. Maxwell took this into consideration by introducing the *diffuse reflection law*:

$$f(\mathbf{r}, \mathbf{c}, t) = f^M(\rho_W, \mathbf{u}_W, T_W), \quad \mathbf{c} \cdot \mathbf{n}(\mathbf{r}) > 0, \quad \mathbf{r} \in \Gamma_S, \tag{36}$$

where $\mathbf{u}_W$ and T_W are the local wall velocity and temperature, respectively. The local density ρ_W is chosen carefully so that the wall does not accumulate or disperse molecules on that site. Here the colliding molecules interact strongly with the wall, and the emitted molecules leave the wall in a Maxwellian distribution determined by ρ_W, $\mathbf{u}_W$, and T_W. Finally, Maxwell proposed that a realistic boundary condition, at least to some degree, is a linear combination of the two conditions above: a portion χ of the incident molecules is specularly reflected and the rest $(1 - \chi)$ interact diffusively with the wall. This combination, with various expressions for the accommodation coefficient χ, is still a very popular boundary condition.

Nearly one hundred years after Maxwell's contribution, Schnute and Shinbrot presented their boundary condition [Sch73]. They proposed the *reverse reflection law*,

$$f(\mathbf{r}, -\mathbf{c}, t) = f(\mathbf{r}, \mathbf{c}, t), \quad \mathbf{r} \in \Gamma_S, \tag{37}$$

which implies zero fluid flow velocity at the boundary. It is an experimental fact that, in the hydrodynamic regime, most of the real gases in ordinary conditions effectively stick to a solid wall, i.e. they do not slip or, in other words, the relative velocity between the gas and the wall is zero at the boundary. Of course, fluids do slip to some extent when the Knudsen number for a flow is not neglible anymore. For example in the Maxwell's composite boundary condition, the slip can be adjusted with the accommodation coefficient χ. All this suggests that no-slip is an approximation, on a macroscopic level, to what actually happens at the boundary of a fluid. Unfortunately the distinction between the slip and no-slip boundary conditions is not so clear-cut as it may seem from the above discussion. Namely, the reverse reflection law was originally presented in the context of Liouville equation. Later, Cercignani studied solutions of the linearised Boltzmann

equation accompanied by the reverse reflection law for specific flow configurations [Cer89]. For a *Plane Poiseuille flow*, that is for a fluid flow between two parallel plates induced by a pressure gradient, the analytical solution he found for the velocity profile is a parabola. However, this parabola is shifted by a constant amount, proportional to the square of the Knudsen number. That is, although the reverse reflection law gives no microscopic slip at the boundary, it may distort the bulk flow by giving rise to a kind of effective macroscopic slip.

The three boundary conditions above all preserve the mass locally, and this enforces vanishing normal velocity at the boundary. In addition, the specular and reverse reflection laws are deterministic. The diffuse reflection on the other hand is a stochastic law, since the incident velocity of a molecule does not uniquely determine its velocity after wall encounter. It has also been shown that in the course of specular as well as reverse reflection, entropy remains constant [Shi78]. We conclude our treatment of the boundary conditions with a final remark: from the three boundary conditions just presented, only the diffuse reflection law allows control of temperature at the boundary.

2.4 Discrete kinetic theory of gases

The mass density distribution function f, the primary unknown object in the Boltzmann equation Eq. (21), depends on seven independent variables: three components of spatial coordinate $\mathbf{r}$, three components of microscopic particle velocity $\mathbf{c}$, and time t. In macroscopic descriptions, an unknown function of interest is typically dependent only on the spatial coordinate and time. Seeking solutions for unknown functions of four arguments, instead of seven, is a much easier task – in principle. This perspective immediately gives an idea of reducing the number of independent variables in f to, say, four. The reduction is feasible indeed, if only certain prescribed velocities are allowed for the particles. To this end, let q denote the finite number of admissible velocities; at any given instant, each of the particles in the system has a velocity from the set $\Psi_q = \{\mathbf{c}_0, \mathbf{c}_1, \ldots, \mathbf{c}_{q-1}\}$. Then the *discrete Boltzmann equation* is expressed as

$$\frac{\partial f_i}{\partial t} + \mathbf{c}_i \cdot \frac{\partial f_i}{\partial \mathbf{r}} + \mathbf{a} \cdot \frac{\partial f_i}{\partial \mathbf{c}_i} = \mathcal{J}_i(\vec{f}), \quad i = 0, 1, \ldots, q-1, \tag{38}$$

where $f_i \equiv f(\mathbf{r}, \mathbf{c}_i, t)$ and $\vec{f}$ is a shorthand for the vector $(f_0, f_1, \ldots, f_{q-1})^T$. In this discrete representation, the continuous binary collision operator $\mathcal{J}(f)$ involving integrals is replaced by a discrete counterpart $\mathcal{J}_i(\vec{f})$ involving summations, which is actually a considerable simplification. All in all, the single equation Eq. (21) for the unknown function f of seven independent variables is now replaced by the discrete Boltzmann equation Eq. (38) representing in fact a total of q coupled equations for the unknown function f_i of only four independent variables. The discrete Boltzmann equation is a generic nonlinear mathematical model, and the fundamental basis for the discrete kinetic theory of gases. Surveys

on the topic are available in Refs [Gat75, Gat77, Pla88, Bel91a, Mon91, Bel03], for example.

The first person to present a discrete Boltzmann equation is presumably Carleman [Car33, Car57]. His primary subjects of interest were mathematical aspects of the Boltzmann equation. Later in the 1960's, Broadwell proposed somewhat more realistic discrete velocity models, and applied them in studying specific fluid flow configurations [Bro64a, Bro64b]. His models included four velocities in two dimensional space, and six or eight velocities in three dimensions. It is rightfully argued that the work by Broadwell was the starting point for the discipline of the discrete kinetic theory of gases. Broadwell was immediately followed by Harris, who investigated properties of the discrete velocity models [Har66]. He, in turn, introduced a model with six velocities for two dimensional flows. Moreover, Broadwell and Harris both proposed expressions for the discrete collision operator $\mathcal{J}_i$ by considering collisions between two and even three particles. Let us now consider a four velocity model in two dimensions for illustration purposes. In the model credited to Gatignol, the velocities are along the two coordinate axes, both in the positive and negative directions, and the single speed related to the velocities is c [Mon91, p.43]:

$$\begin{cases} \partial_t f_0 + c\,\partial_x f_0 &= cS\,(f_1 f_3 - f_0 f_2), \\ \partial_t f_1 + c\,\partial_y f_1 &= cS\,(f_0 f_2 - f_1 f_3), \\ \partial_t f_2 - c\,\partial_x f_2 &= cS\,(f_1 f_3 - f_0 f_2), \\ \partial_t f_3 - c\,\partial_y f_3 &= cS\,(f_0 f_2 - f_1 f_3). \end{cases}$$

These four equations, for the four unknows, are clearly coupled in a nonlinear manner. Furthermore, the term S is obviously related to the particle collisions, and its explicit form depends on the the particular interaction potential chosen for the collisions. The above set of four equations is a concrete, albeit simple, example of discrete velocity models; it incorporates transparently all the main elements of the general model framework defined by the discrete Boltzmann equation Eq. (38). A closely related, but very distinctive, discretisation of the microscopic velocity space models a gas of particles having velocities with a finite number of magnitude but with a continuum of directions. Such a concept is represented with the so-called *semicontinuous Boltzmann equation*. It was first proposed in Ref. [Bel91b], and soon more publications followed [Lon93, Pre93, Pre97, Bel03].

The computation of hydrodynamic as well as non-hydrodynamic variables from the mass density distribution function f, as explained in the previous sections, involve weighted integrals over the velocity space, i.e. the variables are moments in that space. In the case of discrete velocity distribution functions f_i, the same variables are computed as weighted sums over the discrete velocity set Ψ_q. Now arises a question: to what extent the discrete velocity moments correspond or conform to the moments computed with the true integral expressions? In the same breath, what are the properties of the discrete collision operators and what are the governing evolution equations for the discrete velocity moments?

These are the questions, among others, for which answers are sought for in the discipline of discrete kinetic theory of gases [Bob95, Pal97, Cer00]. Apart from the theoretical issues, the discrete velocity models provide a convenient starting point for specific computational schemes [Mie00].

For two dimensional flows, Harris introduced a model with six velocities which correspond exactly with the six directional vectors connecting nodes in a hexagonal lattice. Interestingly enough, the hexagonal lattice was introduced two decades later for the Lattice-Gas Automata – an oversimplified particle model [Fri86]. Moreover, the expressions for the discrete collision operators proposed by Harris were adopted as collision rules (now expressions of mathematical logic) for the new automata. Subsequently, the lattice Boltzmann method was derived from this automata, and the very same collision rules, with slight modifications, were applied as presented by Harris – again in the role of discrete collision operators. From this perspective, it would have been natural to simply discretise space and time variables in the discrete velocity model of Harris in order to recover the lattice Boltzmann method. Frisch et al. were aware of this possibility, as is evident from their statement [Fri86]:

> There are many ways of building microscopic models that lead to a given set of continuum equations. It is known that one can build two- and three dimensional Boltzmann models, with a small number of velocity vectors, which, in the continuum limit, reproduce quite accurately major fluid dynamical features (e.g., shock waves in a dilute gas, etc.). Such Boltzmann models are fundamentally probabilistic, discrete only in velocity, but continuous in space and time. In contrast, we will use lattice-gas models, which have a completely discrete phase space and time and therefore may be viewed as made of "Boolean molecules".

But, hindsight is a luxury. There are no clear directions to be followed when new discoveries are pursued: science is a rogue traveller, it has paths of its own. After the work of Harris, the subsequent developments leading to the lattice Boltzmann method took a detour of more than twenty years.

3 THE LATTICE BOLTZMANN METHOD

Discrete simulation of fluid dynamics took a leap forward in 1986. The authors of this progress were Frisch, Hasslacher, and Pomeau: they introduced a modified version of the Lattice-Gas Automaton (LGA) for the Navier-Stokes equation [Fri86]. Reborn LGA adventured to simulate, now realistically, fluid flows with boolean microdynamics providing an exact computational scheme. Indeed, roundoff plagued floating-point computation is avoided in LGA by boolean expressions. This was not the end of good news: the extraordinary simple dynamics with local update rules was ideally suited for parallel computing. These technical aspect, together with the beautiful concept of digital machinery representing atomistic view of fluid flow, excited scientists and public [Hil85b, Kad86, Hil89]. Great expectations followed, even the possibility to unravel mysteries of turbulence. All took place in parallel with the commission of new type of general-purpose [Hil85a] and special-purpose [Tof84, Mar86, Mar87] computers. This further amplified the expectations. In the end the triumph was never really celebrated as further numerical studies set LGA among other numerical simulation schemes; limitations of LGA were soon understood. However, a new avenue for fluid flow simulation was opened.

Defects of LGA spurred scientists for improvements. McNamara and Zanetti proposed to replace the boolean variables with real numbers [McN88]. Their proposal in 1988 has been considered as the introduction of the lattice Boltzmann method (LBM). Rapidly a scientific community grew around this new numerical method and further developments took place. These developments are the topic of this chapter. In particular, the basic properties of LBM are here presented and, furthermore, special attentation is devoted to the so-called conventional lattice Boltzmann schemes. These schemes are specific yet embraced incarnations of LBM and have many exponents. Also, we demonstrate how lattice Boltzmann schemes can be derived from the discrete Boltzmann equation. Here the focus is exclusively on schemes intended for simulation of fluid flows macroscopically described by the Navier-Stokes equation. In order to elucidate how these hydrodynamic lattice Boltzmann schemes approximate the Navier-Stokes equation, we present a multiple-scale analysis of a specific scheme.

3.1 From the Lattice-Gas Automaton to LBM

Historically LBM emerged from LGA. In retrospect, the transtion from LGA to LBM was quite subtle. Originally many components of LGA, and many of its properties in consequence, were carried over to LBM as such. In this sense, the history of LGA is the prehistory of LBM. Therefore, let us first consider the major developments related to LGA.

Principal actors in the early stages of LGA were Hardy, Pomeau, and de Pazzis. In the beginning of the 1970's they investigated a rather simple system of particles in two dimensions [Har72, Har73]. They started off with a kind of restricted molecular dynamics: only few predefined velocities were allowed for the particles. That is, a set of particles follow constant trajectories (lines) and the particles, finite in number, interact only when their trajectories intersect. In free motion, positions of the particles evolve continuosly in time. In the first development stage, they prescribed explicit interaction laws for the particle collisions which conserve mass, momentum, and energy. Next, the above simple dynamics was made even simpler by allowing only discrete positions for the particles. In each unit of time Δt, particles hop, according to their velocity, from a site to another in a regular lattice, and suffer collisions with each other. This is the *modus operandi* of LGA.

An additional simplification, characteristic of LGA, was assumed from early on. Namely, the so-called exclusion principle is enforced: at any given time, particles sharing both the position and the velocity are not allowed to exist. One bit, here $b_i(\mathbf{r}, t)$, is hence enough to state whether a location $\mathbf{r}$ is occupied at time t by a particle with a prescribed velocity $\mathbf{c}_i$. This principle facilitates relatively simple collision rules; both propagation and collision of particles can be coded with boolean expressions – unconditional stability is a give away. The exclusion principle also leads to Fermi-Dirac type equilibrium distributions for mean occupation numbers, not to the Maxwellian distribution. The general evolution equation for the occupation variables is

$$b_i(\mathbf{r} + \Delta t \mathbf{c}_i, t + \Delta t) = b_i(\mathbf{r}, t) + \Omega_i^b(\mathbf{r}, t), \tag{39}$$

where the collision operator Ω_i^b is a boolean expression representing change in the occupation variable due to particle collisions; coordinates $(\mathbf{r} + \Delta t \mathbf{c}_i)$ coincide with the nodes of a lattice. The above equation is a convenient definition for LGA. A two-dimensional computational procedure with a specification for Ω_i^b, known as the HPP model, was presented in the appendix of Ref. [Har76] – see the illustration in Fig. 4.

All so far seems too easy, and in a way it is. A critical question is justified when a computational scheme built upon a discrete system of particles with fictitious interaction laws is presented: what kind of equations or laws govern the collective motion of particles? That is, what kind of a system we are simulating in a macroscopic sense? Is there even enough particles in the discrete system so that the collective motion and the macroscopic sense are meaningful concepts? Before

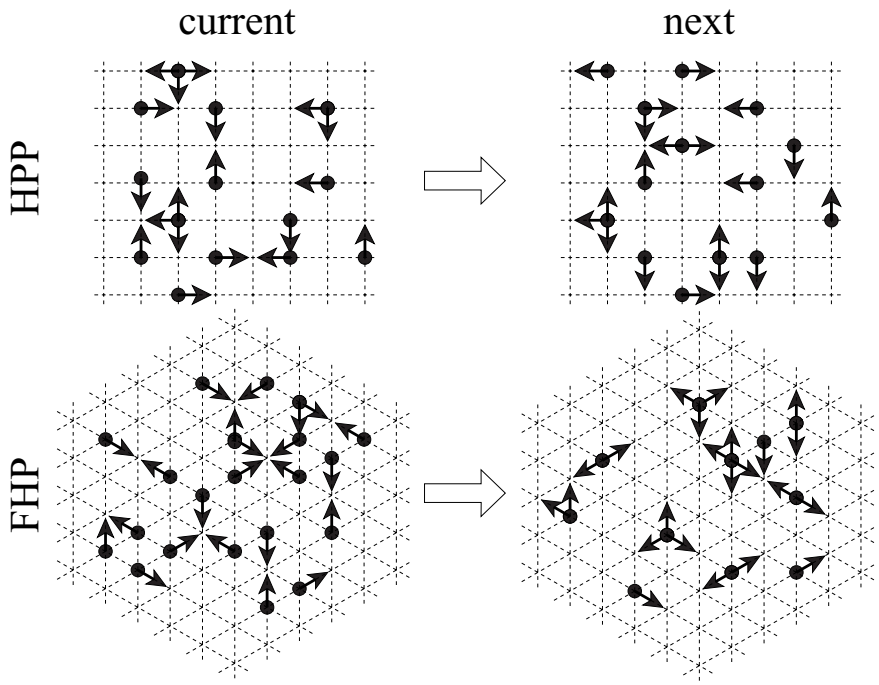

FIGURE 4 A sketch of particle dynamics in two LGA models. In the HPP and FHP models, particles live in a square and hexagonal lattices, respectively. During a discrete time step, the particles first propagate, according to their velocity, from their current positions (on the left). Then, during the same time step but after the propagation, particles collide at their new locations and acquire new velocities (on the right). Here the particles obey collision rules presented in Ref. [Fri87].

answering, a measure that characterises physical flows is needed. One measure is provided by the dimensionless Knudsen number K_n. Dense fluid flows and rarefied gas flows are typically described by small and large Knudsen numbers, respectively. Furthermore, the Navier-Stokes equation is assumed valid in the regime of small Knudsen numbers [Raa04]. Now a more refined question is appropriate: given a computational particle-based scheme and a simulation configuration with small K_n, can we simulate solutions of the Navier-Stokes equation? From the beginning it was known that the answer is no for the HPP model [Har72].

In the asymptotic limit, the HPP model does not comply with the Navier-Stokes equation. Two main obstacles are insufficient Galilean invariance and insufficient isotropy. Term insufficient is meaningful since discrete models can be upgraded to evermore invariant and isotropic. It is noteworthy that developments related to LBM have often been propelled by identification of sources breaking either Galilean invariance or isotropy. The HPP model breaks the principle of Galilean invariance at the lowest order since e.g. the pressure turns out to

be dependent on the average (macroscopic) velocity.[1] But even more severe is the low symmetry of the discretised microscopic velocity space; there are only four allowed velocities for the particles (cf. Fig. 4). Thus the HPP model is invariant under $\pi/2$ rotations, which is not sufficient to ensure the isotropy of a certain fourth-rank tensor formed from the discrete velocities and related to the momentum flux. Unfortunately, the momentum flux tensor computed according to the HPP model does not agree with its counterpart in the Navier-Stokes equation.

Frisch, Hasslacher, and Pomeau set out to remedy the insufficient isotropy. They presented a version of LGA, the FHP model, with six allowed velocities for particles [Fri86]. In two dimensions, this set of velocities provides enough symmetry; the FHP model was an immediate success since it was shown to conform with the Navier-Stokes equation in the asymptotic limit. The new model was exciting especially because adequate isotropy was achieved with six velocity vectors each connecting a node in a hexagonal lattice to one of its neighbours (see Fig. 4). Thus, the computational scheme remained exact as the particles continued to hop between lattice sites. Other discrepancies of the original LGA relative to the Navier-Stokes equation were still present. Mass and momentum conserving collision rules, with a random element, were adopted for the FHP model from the discrete velocity model presented by Harris (see discussion in Sec. 2.4). Frisch et al. also presented the possibility to have particles with zero velocity in the model, i.e. the so-called rest particles.

Taking LGA from two dimensions to three dimensions is not as straightforward as one would expect at first. Due to computational reasons, two components were supposed to be married. A set of discrete velocities, possessing sufficient symmetry properties, were sought for a regular lattice. These two components would live in harmony, if every velocity vector connects two sites of the lattice. In three dimensions, such a combination cannot be found for any discrete velocity set with only one non-zero speed. A seminal article proposed two alternative solutions for this problem [d'Hu86a]. In a multi-speed solution, a cubic lattice is used together with 19 discrete velocities connecting lattice sites: the number of velocities having speed $0, 1$, and $\sqrt{2}$ are $1, 6$, and 12, respectively. This model has precisely the velocity set of the so-called D3Q19 model, later proposed for LBM. A corresponding proposal was made also for two dimensions involving square lattice with 9 velocities – later known as the D2Q9 model. Multi-speed solution required elaborate conditions to be satisfied; implementations enforcing these conditions were not presented. The second solution is more exotic, but readily amenable to implementation. It is a pseudo 3D model operating actually in a 4D face-centered hyper-cubic lattice – hence the name FCHC model. Exactly the same two opportunities for progress were also recognised by Wolfram [Wol86].

Variants of the original LGA models started to emerge. Particularly, new models came with modified collision rules [d'Hu86b, Hén87a, d'Hu87a]. In LGA, the kinematic viscosity is determined by the density[2] and the collision rules. The

[1] Galilean invariance generally means that equations describing the physics involved are independed of the inertial frame of reference.

[2] Here the average number of particles per lattice site, assigned in the system initialisation.

tuning of collision rules, typically by increasing the number of particle collisions with additional collision arrangements, strives for a lower viscosity or ultimately for a higher Reynolds number in simulations. The logic comes from the kinetic theory of gases: the more collisions there are, the shorter the mean free path is, and the smaller the viscosity is – provided the number of particles is kept constant at the same time, cf. Eq. (17). Pioneering work in optimising collision rules for minimum viscosity was done by Hénon [Hén87b]. He also proposed a general recipe, utilising the molecular chaos assumption, for computing viscosity directly from the collision rules. Wolfram had used the same approximation in his notable publication when computing transport coefficients, e.g. viscosity, for LGA models [Wol86]. Expressions for viscosity so obtained are approximations by construction, but nevertheless valuable in the analysis and theoretical work. More stringent values for viscosity, important on the practical side, are obtained by measuring viscosity with computational experiments – a kind of computational viscometer is set up. Such measurements are described with enjoyable clarity of presentation by Kadanoff et al. [Kad87].

At the same time a comprehensive study summarising theoretical aspects of various LGA models was published [Fri87]. There the main analytical results thus far were recapitulated: the Navier-Stokes equation is recovered in the asymptotic limit with the low Mach number assumption; the discrete velocity set must be chosen so that any tensor up to fourth degree formed from the velocities is isotropic. The equation obtained as such bears a close resemblance to the Navier-Stokes equation, but is polluted by terms breaking the principle of Galilean invariance. Specifically there are two problems. The first problem is that an additional coefficient emerges in front of the convective term. This coefficient is not necessarily equal to unity, as it should be in a physical system. Ultimately this is a consequence of the Fermi-Dirac type equilibrium. For constant density single-phase flows, this problem can be tackled by a density-dependent rescaling of time, viscosity, and pressure. This rescaling typically decreases the Reynolds number. In consequence, more computational resources are required for high Reynolds number simulations. The second problem is related to the equation of state. That is, for simple fluids the pressure should depend only on the density and temperature (see the ideal gas law Eq. (12) in Sec. 2.2.2). However, LGA models with just one non-zero microscopic speed simulate systems with pressure depending also on the macroscopic flow velocity. The correct physical equation of state is recovered with LGA models having at least two non-zero particle speeds [Cho88, Che89b, Che89c, Mol89].

Single-speed LGA models with certain collision rules have an additional peculiarity, potentially leading to dynamical behaviour not described by the Navier-Stokes equation. These models accommodate so-called spurious invariants. That is, the models conserve quantities prescribed for them, i.e. mass and momentum, but also others. These extra invariants show up in the equations describing the macroscopic behaviour of the automata. Spurious invariants are avoided by appropriate collision rules or by utilising multi-speed models [Wol86, Zan89, Kad89, d'Hu89, Fah91]. More on the practical side, inherent noise and compress-

ibility related to the hydrodynamic variables extracted from LGA simulation permit a rather limited domain for simulation parameters yielding the behaviour of an incompressible Navier-Stokes fluid [Dah87, Che89d]. One equipped with a positive mind can look at the bright side: such parameters exist! Also, the inherent noise can be seen as an advantage. With large LGA simulations it is possible to reproduce the full dynamical scale, all the way from the nonlinear Navier-Stokes dynamics to the small-scale dissipation effects embedded in the noisy pseudo-molecular fluctuations of the automaton [Lad88, Suc88].

Nonetheless, it was gradually becoming clear that LGA offered no particular advantage over conventional approaches in high Reynolds number simulations [Ors86, Fri87, Suc88, Zal89]. Actually, LGA turned out be rather limited with respect to the Reynolds number – killing the high hopes for rapid advancement in turbulence research. An interesting case study of a particular 3D simulation with the FCHC model was presented by Rivet et al., illustrating the difficulty of reaching low viscosity in LGA simulations [Riv88]. With the benefit of hindsight, modelling the collision process with a set of enumerated collision rules, especially in three dimensions, had become the burden for LGA. Even so, considerable effort was still invested in enhancing the collision rules [Dub88, Hén89, Rot89a, Som90, Dub90]. Along the way of the aforementioned developments, a wonderfully rich world of low Reynolds number flows was discovered suitable for simulation with LGA.

Possibility to simulate complex phenomena such as magnetohydrodynamics [Mon87, Che87], fluid flow in porous media [Bal87, Rot88a], fluids with interfaces and multicomponent flows [Bur87, Bur88, Rot88b, Rot89b], multiphase flows [Che89a, App90], reactive flows [d'Hu87b, Cla88, Sea89], dispersion [Bau89], and particles suspended in a fluid [Lad88, Lad90] stirred new excitement. These are often appointed, due to the typical length and time scales involved, as prime examples of mesoscopic flow phenomena – naturally suited for simulation also with LBM. Many of the above flow phenomena involve complex boundaries, and hence boundary conditions often determine whether computer simulations of the phenomena are feasible. Particularly in this respect, LGA equipped with simple and operational, albeit crude, boundary conditions is an attractive computational scheme. This aspect is true also for LBM. Perhaps the most accurate, or the most rigorous, treatment of the boundary conditions for LGA is presented in Ref. [Cor91], including reverse and specular reflection laws (see Sec. 2.3.5). In the context of LGA, as well as LBM, the reverse and specular reflection laws are commonly referred to as the bounce-back and bounce-forward boundary conditions.

Finally it appeared as if all major theoretical improvements were squeezed out of LGA; more technically oriented improvements were still pursued. For example, Refs [Hén92, Som92, Adl95, Kob03], published after the golden age of LGA, provide an interesting account of the high-performance implementation issues related to computations with the FCHC model. For those interested in more general accounts, thorough and insightful reviews of LGA are available e.g. in Refs [Has87, Vic89, Boo91, Che91b, Som91]. The history of LGA, as seen today, portrays a scientific rush where scientists vigorously seek improvements one af-

ter the other. Soon new improvements became harder to come by, and the rush gradually lost its momentum. Or actually, as described below, the momentum was diverted into a new direction.

3.2 Conventional lattice Boltzmann schemes

Numerical analysis of the properties of LGA requires formal computation of averages for the boolean occupation variables $b_i(\mathbf{r}, t)$. In this context, several authors presented the lattice Boltzmann equation (LBE) as an intermediate analysis tool [Wol86, Fri87, Hén87b]:

$$f_i(\mathbf{r} + \Delta t \mathbf{c}_i, t + \Delta t) = f_i(\mathbf{r}, t) + \Omega_i(\mathbf{r}, t); \tag{40}$$

it was commissioned to govern evolution of the formal averages. The above equation is equivalent with the LGA equation Eq. (39) except that all boolean variables have now been replaced with floating-point variables. The function $f_i(\mathbf{r}, t)$ is referred to as the single-particle distribution funtion indicating the probability of finding a particle at site $\mathbf{r}$ at time t with velocity $\mathbf{c}_i$. The last term on the right, $\Omega_i(\mathbf{r}, t)$, is the discrete collision operator representing change in the distributions due to the interactions between particles.

Instead of using LBE merely as an analysis tool, McNamara and Zanetti utilised the same equation as a numerical tool for computer simulations [McN88]. Their motivation was to eliminate the inherent noise plaguing LGA simulations; the collision rules of LGA were still utilised for describing the discrete collision operator Ω_i and thus other peculiarities of LGA remained. Their article on the topic, published in 1988, established LBM – a numerical method for transport phenomena. McNamara and Zanetti also presented an estimate according to which the new method is computationally efficient in the region of intermediate to low Reynolds number. As it happens, this is the region where LBM is nowadays most often applied. In parallel with McNamara and Zanetti, Higuera and Jiménez also discovered the opportunity to use LBE as a simulation tool [Hig89a, Hig89b, Hig89c, Hig89d] – apparently their first article on the topic was delayed because of the publication process. Higuera and Jiménez understood that, while suppressing the noise present in LGA simulations, a numerical method based on LBE allowed much more freedom in constructing discrete collision operators and handling the required symmetries of the distribution functions.

3.2.1 LBGK

By modelling the collision term $\Omega_i(\mathbf{r}, t)$ in Eq. (40) with a linearised expression, then referred to as *the enhanced collision*, Higuera et al. took LBM further apart from LGA [Hig89d]. The departure from LGA was completed when not one but three independent parties simultaneously proposed a scheme for hydrodynamic

fluid flow simulations where the collision term in LBE is modelled with a simple relaxation process involving a single parameter [Koe91, Che91a, Che92, Qia92]. Specifically, a scheme was proposed for the simulation of such incompressible isothermal fluid flows which are described by the Navier-Stokes equation. This can be regarded as the true breakthrough moment for LBM mainly because of two reasons: the single relaxation parameter directly controls viscosity and, like proposed by Qian et al., this simple scheme is a discrete counterpart for the BGK model defined in Eq. (32). Qian et al. used the descriptive name lattice BGK scheme (LBGK) when they proposed the evolution equation

$$f_i(\mathbf{r} + \Delta t \mathbf{c}_i, t + \Delta t) = f_i(\mathbf{r}, t) - \omega \Big(f_i(\mathbf{r}, t) - f_i^{eq}(\mathbf{r}, t) \Big); \tag{41}$$

the discrete equilibrium function f_i^{eq} is an approximation for the true Maxwellian Eq. (24), and the dimensionless relaxation parameter ω is of the order of unity, i.e. $\omega \sim \mathcal{O}(1)$. Simplicity immediately made LBGK a popular scheme and the connection to the kinetic theory of gases made it plausible.

In fact, Qian et al. proposed a family of lattice BGK schemes. These schemes, also referred to as models, share a common discrete equilibrium function:

$$f_i^{eq}(\rho(\mathbf{r}, t), \mathbf{u}(\mathbf{r}, t)) \equiv f_i^{eq}(\rho, \mathbf{u}) := w_i \, \rho \left(1 + \frac{c_{i\alpha} u_\alpha}{\theta} + \frac{c_{i\alpha} u_\alpha c_{i\beta} u_\beta}{2\theta^2} - \frac{u_\alpha u_\alpha}{2\theta} \right). \tag{42}$$

The discrete weight coefficients w_i, and the parameter θ, are model dependent. The arguments of f_i^{eq} are the local density ρ and the flow velocity $\mathbf{u}$. These hydrodynamic variables are defined as the zeroth and first order moments of the discrete distribution function in the microscopic velocity space; they are computed as weighted sums over the discrete velocities:

$$\rho(\mathbf{r}, t) = \sum_i f_i(\mathbf{r}, t), \tag{43}$$

$$\rho(\mathbf{r}, t) u_\alpha(\mathbf{r}, t) = \sum_i c_{i\alpha} f_i(\mathbf{r}, t). \tag{44}$$

Note that the moments of continuous distributions $f(\mathbf{r}, \mathbf{c}, t)$ are defined as integrals over the continuous velocity space (see Sec. 2.3.2). Thus the discrete distribution functions $f_i(\mathbf{r}, t)$ and the continuous distribution function $f(\mathbf{r}, \mathbf{c}, t)$ necessarily differ in units – otherwise definitions of the moments do not make sence. Specifically, $f_i(\mathbf{r}, t)$ is defined in units of density alone, but $f(\mathbf{r}, \mathbf{c}, t)$ is defined in units of density divided by velocity cubed.

Specific lattice BGK models emerge when the spatial dimension and the set of discrete velocities is fixed. For example, the so-called D2Q9 model operates on a two-dimensional square lattice with nine discrete velocities [Qia92]. Qian et al. enumerated their models with notation the DdQq, where d and q refer to the spatial dimension and number of discrete velocities, respectively. The discrete velocity set Ψ_9 involves three speeds: the number of velocities having speed $0, c_r$, and $\sqrt{2}\, c_r$ are $1, 4$, and 4, respectively (see Fig. 5). In conventional lattice

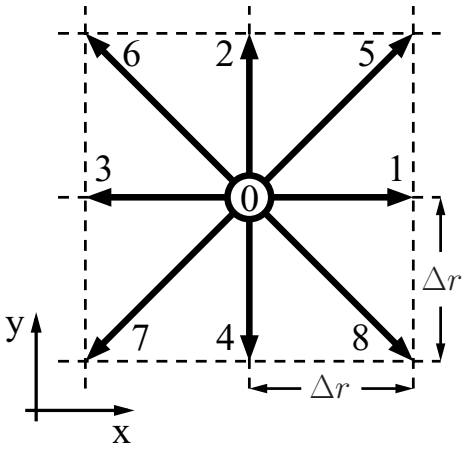

$$\begin{aligned}
\mathbf{c}_0 &= (0 \quad , \quad 0) \\
\mathbf{c}_1 &= (c_r \quad , \quad 0) \\
\mathbf{c}_2 &= (0 \quad , \quad c_r) \\
\mathbf{c}_3 &= (-c_r, \quad 0) \\
\mathbf{c}_4 &= (0 \quad , -c_r) \\
\mathbf{c}_5 &= (c_r \quad , \quad c_r) \\
\mathbf{c}_6 &= (-c_r, \quad c_r) \\
\mathbf{c}_7 &= (-c_r, -c_r) \\
\mathbf{c}_8 &= (\quad c_r, -c_r)
\end{aligned}$$

FIGURE 5 The set of nine discrete velocities Ψ_9 in the D2Q9 lattice Boltzmann model. The lattice spacing of the two-dimensional square lattice is Δr. In conventional schemes, the lattice spacing, the reference speed c_r, and the discrete time step Δt are interconnected by the relation $\Delta r = \Delta t\, c_r$; the components $c_{i\alpha}$ are equal to the reference speed c_r multiplied by an integer. The set Ψ_9 includes three speeds: $0, c_r$, and $\sqrt{2}\, c_r$. The numbers of velocities having these speeds are 1, 4, and 4, respectively.

Boltzmann schemes the underlying lattice is uniform, e.g. a square lattice in the D2Q9 model, and moreover the reference speed c_r is intimately connected to the lattice spacing Δr and to the discrete time step Δt: $\Delta r = \Delta t\, c_r$. Furthermore, the components $c_{i\alpha}$ of the discrete velocity vectors are equal to the reference speed c_r multiplied by an integer. Or in other words, in a conventional scheme vectors $\Delta t\, \mathbf{c}_i$ serve as exact links between the nodes of a uniform lattice.

The models are completely specified when the equilibrium weights w_i, and the parameter θ, are determined. Usually it is assumed that a weight w_i depends only on the speed of the associated microscopic velocity $\mathbf{c}_i$; for every speed in a discrete velocity set there is a prescribed weight value W_p. In the case of the D2Q9 model, values W_0, W_1, and W_2 are prescribed for the three speeds. That is, $w_0 = W_0$, $w_1 = w_2 = w_3 = w_4 = W_1$, and $w_5 = w_6 = w_7 = w_8 = W_2$. These values, as presented by Qian et al. [Qia92], are given in Table 2. Other lattice BGK models are specified in the same table. The family of lattice BGK schemes presented by Qian et al. have a common expression for the viscosity:

$$\nu = \theta\left(\frac{1}{\omega} - \frac{1}{2}\right)\Delta t. \tag{45}$$

Also, the relation $\theta = c_r^2/3$ is true for each of the models. This expression for the viscosity can be obtained via Chapman-Enskog analysis (see Sec.3.4.1). The same

TABLE 2 Various lattice BGK models as presented by Qian et al. [Qia92]. They enumerate the models with the notation DdQq, where d and q refer to the spatial dimension and number of discrete velocities, respectively. The relation $\theta = c_r^2/3$ is true for each model. Likewise, the models have a common expression for the viscosity: $\nu = \theta(1/\omega - 1/2)\Delta t$.

Model	W_0	W_1	W_2	W_3
D1Q3	2/3	1/6	0	0
D2Q9	4/9	1/9	1/36	0
D3Q15	2/9	1/9	0	1/72
D3Q19	1/3	1/18	1/36	0
D4Q25	1/3	1/36	0	0

analysis shows that an appropriate equation of state for these schemes is $p = \theta\rho$. Because in classical mechanics the speed of sound c_s is commonly defined with the relation

$$c_s^2 = \frac{\partial p}{\partial \rho},$$

our parameter θ can be identified with the speed of sound squared.

By comparing the equation of state $p = (c_r^2/3)\rho$ with the equation of state Eq. (13) introduced in the classical kinetic theory of gases, we immediately identify the reference speed c_r with the root mean square speed c_{rms} proportional to the average molecular kinetic energy which, in turn, is proportional to the absolute temperature. This connection is an indicator of physical consistency for the schemes. Now, if we utilise a conventional lattice Boltzmann scheme and furthermore fix the lattice spacing $\Delta r = \Delta t\, c_r$ in a particular flow simulation, we are left with two options:

1. either we fix θ (with T_0) which then determines c_r (or c_{rms}), and thereby the discrete time step Δt is implicitly assigned,

2. or we fix, *a priori*, the discrete time step Δt which determines c_r and so, in turn, the reference temperature T_0 is indirectly prescribed.

It is a matter of convenience which of the two ways is chosen for configuring a simulation. Of course, the expression Eq. (45) for viscosity is also a coupling of simulation parameters. At the implementation level, the actual units are typically hidden; usually for lattice BGK schemes, the discrete equilibrium function Eq. (42) is implemented with dimensionless variables such that:

$$f_i^{eq}(\rho, \mathbf{u}) \equiv w_i\, \rho \left(1 + 3c_{i\alpha}^* u_\alpha^* + \frac{9}{2} c_{i\alpha}^* u_\alpha^* c_{i\beta}^* u_\beta^* - \frac{3}{2} u_\alpha^* u_\alpha^* \right), \tag{46}$$

where variables denoted by an asterisk are dimensionless, i.e. $c_{i\alpha} = c_r\, c_{i\alpha}^*$ and $u_\alpha = c_r\, u_\alpha^*$. In addition, the schemes are sometimes defined and implemented with dimensionless distribution functions: $f_i = \rho_0\, f_i^*$ and $f_i^{eq} = \rho_0\, f_i^{eq*}$, where ρ_0 is a reference density.

3.2.2 Derivation of the discrete equilibrium function

From a computer science perspective, construction of specific lattice Boltzmann schemes is a very interesting topic. Because the discrete equilibrium function is the key component of many schemes, it is instructive to follow through a derivation of a particular f_i^{eq}. Thus, let us focus on a scheme for incompressible isothermal flow simulations of Newtonian fluids in the hydrodynamic regime – macroscopically described by the Navier-Stokes equation.

Since we are here dealing with an isothermal flow, temperature is not an unknown variable, but instead a material parameter. Typically in isothermal lattice Boltzmann schemes, the temperature $T(\mathbf{r}, t)$ is actually not a constant. In the *de facto* approach, the temperature is fixed in the equilibrium function with a reference temperature T_0 – a kind of heat bath is envisaged. Inevitably, there will be a discrepancy between the local temperature T and the reference temperature T_0. This discrepancy is simply neglected because the temperature is not a quantity of interest in isothermal flow simulations. At first sight, it would appear that similar treatment is possible also for the density in incompressible fluids. However, such a straightforward approach is not feasible. It turns out that the basic schemes obey the ideal gas law: pressure is directly proportional to the density. Since pressure variations are essential in hydrodynamics, the basic schemes must in some way allow small density variations. Therefore, it is the responsibility of the simulation configuration to quarantee that the density variations are very small, with respect to both space and time.

In the next step, we define a constant $\theta := (k_b T_0)/m$ and rewrite the local Maxwellian Eq. (24) in the form

$$\begin{aligned} f^{eq}(\mathbf{c}, \rho, \mathbf{u}) &:= f^M(\mathbf{c}, \rho(\mathbf{r}, t), \mathbf{u}(\mathbf{r}, t), T_0) = \rho\,(2\theta\pi)^{-d/2}\,\mathrm{e}(-v_\alpha v_\alpha/2\theta) \\ &= \rho\,\underbrace{(2\theta\pi)^{-d/2}\,\mathrm{e}(-c_\alpha c_\alpha/2\theta)}_{=:w_b(c_\alpha)} \cdot \underbrace{\mathrm{e}(c_\alpha u_\alpha/\theta)}_{=:B(c_\alpha,u_\alpha)} \cdot \underbrace{\mathrm{e}(-u_\alpha u_\alpha/2\theta)}_{=:C(u_\alpha)}, \end{aligned} \quad (47)$$

where d is the spatial dimension, $\mathrm{e}(\cdot)$ the exponential function, and $v_\alpha = c_\alpha - u_\alpha$ the peculiar or relative velocity. The variable $\sqrt{\theta}$, here constant, is often referred to as the thermal speed, and in our discrete model it will be identified with the speed of sound. Before proceeding, we will recall the Taylor series expansion of the exponential function:

$$e^x = \sum_{n=0}^{\infty} \frac{x^n}{n!} = 1 + x + \frac{x^2}{2!} + \frac{x^3}{3!} + \dots .$$

We utilise this expansion for the two exponential functions B and C, defined above in Eq. (47):

$$\begin{aligned} B(c_\alpha, u_\alpha) &= 1 + \left(\frac{c_\alpha u_\alpha}{\theta}\right) + \frac{1}{2}\left(\frac{c_\alpha u_\alpha}{\theta}\right)^2 + \dots \quad , \\ C(u_\alpha) &= 1 - \left(\frac{u_\alpha u_\alpha}{2\theta}\right) + \frac{1}{2}\left(\frac{u_\alpha u_\alpha}{2\theta}\right)^2 + \dots \quad . \end{aligned}$$

The above expressions are regarded as expansions with respect to the Mach number, because $M_a \sim u_\alpha/\sqrt{\theta}$ and $c_\alpha \sim \sqrt{\theta}$. By inserting these expansions into the equilibrium function Eq. (47), and by retaining only terms up to second order in M_a (low Mach number assumption), we obtain an approximate equilibrium function:

$$\widetilde{f}^{eq}(\mathbf{c},\rho,\mathbf{u}) := w_b(c_\alpha)\,\rho\left(1+\frac{c_\alpha u_\alpha}{\theta}+\frac{c_\alpha u_\alpha c_\beta u_\beta}{2\theta^2}-\frac{u_\alpha u_\alpha}{2\theta}\right).$$

In the final step, the velocity space is discretised, i.e. a finite set of microscopic velocities $\Psi_q = \{c_{0\alpha}, c_{1\alpha}, \ldots, c_{(q-1)\alpha}\}$ is introduced for representing the velocity space. Simultaneously, the continuous weight function $w_b(c_\alpha)$ is replaced with discrete weight coefficients w_i, where subscript i refers to a microscopic velocity. Note that here the function $w_b(c_\alpha)$ is really discarded. In other words, coefficients w_i are not directly determined by $w_b(c_{i\alpha})$, but rather left unspecified at the moment. As presented already in Ref. [Qia92], we then arrive at the general discrete equilibrium function given in Eq. (42). By simply considering the zeroth moment of the discrete equilibrium, which should give the density ρ, it is evident that the coefficients w_i are necessarily dimensionless. Hence, even the units of $w_b(c_\alpha)$ and w_i are different

3.2.3 Construction of lattice BGK schemes

To obtain a specific lattice Boltzmann scheme, the equilibrium weight coefficients w_i must be specified. The coefficients are model dependent, i.e. they must be determined separately for each set of discrete velocities Ψ_q. One approach to determine the coefficients is to require that the moments of the discrete equilibrium functions correspond, up to some order, to the moments of the continuous Maxwellian distribution function. Actually, it turns out that in order to simulate solutions of the incompressible Navier-Stokes equation Eq. (7), in the asymptotic limit with the low Mach number assumption, the moments must match up to the fourth order. This can be guaranteed, when the conditions below are enforced [Koe91, Wol00]:

$$\sum_i w_i = 1 = \int w_b(\mathbf{c})\,d\mathbf{c}, \tag{48}$$

$$\sum_i w_i c_{i\alpha} c_{i\beta} = \theta\,\delta_{\alpha\beta} = \int w_b(\mathbf{c}) c_\alpha c_\beta\,d\mathbf{c}, \tag{49}$$

$$\sum_i w_i c_{i\alpha} c_{i\beta} c_{i\gamma} c_{i\delta} = \theta^2(\delta_{\alpha\beta}\delta_{\gamma\delta}+\delta_{\alpha\gamma}\delta_{\beta\delta}+\delta_{\alpha\delta}\delta_{\beta\gamma}) = \int w_b(\mathbf{c}) c_\alpha c_\beta c_\gamma c_\delta\,d\mathbf{c}. \tag{50}$$

These can be perceived as isotropy conditions for the even-rank tensors defined in the equations. Note that the last isotropy condition Eq. (50) for the fourth-rank tensor is slightly more stringent than the general isotropy condition Eq. (6).

In addition, we assume a symmetric set of discrete velocities Ψ_q in the sence that for every non-zero velocity $\mathbf{c}_i$ there exists an opposite velocity $\mathbf{c}_j$, i.e. $\mathbf{c}_j = -\mathbf{c}_i$; the associated weights are assumed equal, i.e. $w_i = w_j$. These assumptions

have an important consequence: the odd-rank tensors, defined in the same way as the even-rank tensors above, are identically zero. Whenever the odd-rank tensors vanish, and the isotropy conditions Eqs (48) – (50) are satisfied, the first four moments of the discrete equilibrium function Eq. (42) are

$$\sum_i f_i^{eq}(\rho, \mathbf{u}) = \rho, \tag{51}$$

$$\sum_i c_{i\alpha} f_i^{eq}(\rho, \mathbf{u}) = \rho u_\alpha, \tag{52}$$

$$\sum_i c_{i\alpha} c_{i\beta} f_i^{eq}(\rho, \mathbf{u}) = \theta\rho\delta_{\alpha\beta} + \rho u_\alpha u_\beta, \tag{53}$$

$$\sum_i c_{i\alpha} c_{i\beta} c_{i\gamma} f_i^{eq}(\rho, \mathbf{u}) = \theta\rho(u_\alpha\delta_{\beta\gamma} + u_\beta\delta_{\alpha\gamma} + u_\gamma\delta_{\alpha\beta}). \tag{54}$$

Let us now consider a concrete case study, which illustrates how the equilibrium weights w_i can be determined, and thus, how a particular lattice Boltzmann scheme is specified. We concentrate on the D2Q9 model introduced in Sec. 3.2.1 (see Fig. 5). In summary, the D2Q9 model operates on a two-dimensional square lattice with nine discrete velocities. Furthermore, it is assumed that an equilibrium weight w_i depends only on the speed of the microscopic velocity $\mathbf{c}_i$. Hence in the D2Q9 model, the weights w_i are prescribed with the three values: W_0, W_1, and W_2. That is, $w_0 = W_0$, $w_1 = w_2 = w_3 = w_4 = W_1$, and $w_5 = w_6 = w_7 = w_8 = W_2$. Now the isotropy condition for the zeroth-rank tensor Eq. (48) requires that

$$\sum_{i=0}^{8} w_i = W_0 + 4W_1 + 4W_2 = 1. \tag{55}$$

The off-diagonal elements of the second-rank tensor in the condition Eq. (49) are identically zero and hence do not contribute equations to the unknown weights. However, the diagonal elements are equal to each other, and must fulfil

$$\sum_{i=0}^{8} w_i c_{ix} c_{ix} = \sum_{i=0}^{8} w_i c_{iy} c_{iy} = 2c_r^2 W_1 + 4c_r^2 W_2 = \theta. \tag{56}$$

The isotropy conditions Eq. (50) for the off-diagonal elements of the fourth-rank tensor also do not contribute equations to the unknown weights, except for

$$\sum_{i=0}^{8} w_i c_{ix} c_{ix} c_{iy} c_{iy} = 4c_r^4 W_2 = \theta^2. \tag{57}$$

The conditions for the diagonal elements of the fourth-rank tensor require that

$$\sum_{i=0}^{8} w_i c_{ix} c_{ix} c_{ix} c_{ix} = \sum_{i=0}^{8} w_i c_{iy} c_{iy} c_{iy} c_{iy} = 2c_r^4 W_1 + 4c_r^4 W_2 = 3\theta^2. \tag{58}$$

We have now four equations Eqs (55) – (58) for the three unknowns W_0, W_1, and W_2. We use the extra equation for defining a relation between θ and c_r. The solution is

$$W_0 = \frac{4}{9}, \quad W_1 = \frac{1}{9}, \quad W_2 = \frac{1}{36}, \quad \theta = \frac{c_r^2}{3}. \tag{59}$$

Generally speaking, a solution respecting the isotropy conditions can always be found, if a large enough discrete velocity set is chosen. In their article, Qian et al. present various lattice BGK models [Qia92] – here listed in Table 2.

3.3 LBM based on the kinetic theory

Historically, LBM was introduced as an improvement to LGA. In the first lattice Boltzmann scheme, the boolean occupation variables of LGA were simply replaced by mean occupation variables. The lattice BGK scheme was proposed soon after and this, at the latest, established LBM as a simulation tool (see Secs 3.1 and 3.2). In the historical approach, also called the bottom-up or particle-based approach, LBM is constructed directly from discrete particle systems like LGA. Such an approach highlights the connection to the underlying particles: the particle interpretation can sometimes help to perceive the concepts of LBM, and it has definitively inspired many extensions to the conventional schemes. Furthermore, during the historical developments, a great deal of understanding, knowledge, and concrete tools for analytical work were transferred from LGA to LBM.

But, there is an alternative to the bottom-up approach: LBM can be derived also from the Boltzmann equation, or model Boltzmann equations like the BGK-model. A mathematically rigorous connection with the kinetic theory of gases was established in the late 1990's, when several publications presented top-down or statistical mechanical approaches for the derivation of lattice Boltzmann schemes directly from the Boltzmann equation [Abe97, He97a, He97b, Sha98]. The distinctive stage, discretisation of the microscopic velocity space, involves application of the *Gauss-Hermite quadratures* for approximating the moment integrals in the velocity space – the abscissas of the quadratures are identified as the discrete velocities. Higher-order quadratures enable accurate approximations of higher-order moments. Depending on the hydrodynamic equations ultimately pursued, e.g. the Navier-Stokes equation, an appropriate order is chosen for the quadratures. Discretisation of the velocity space leads to a discrete Boltzmann equation (DBE) or, as some prefer, to a discrete velocity model (DVM), see Eq. (38). In the last step of the top-down approach, the partial derivatives in the model equation are discretised – a typical step in the construction of computational schemes in general. A derivation of the lattice BGK scheme from DBE is presented in Sec. 3.3.1.

The two routes to LBM are illustrated in Fig. 6. They represent two altogether different philosophies for the construction of computational methods. Namely, the bottom-up approach is a kind of reverse-engineering approach where a discrete particle system with fictious interaction rules is carefully set up; the particle system must obey prescribed dynamics at a macroscopic scale. The top-down approach, on the other hand, is a very general and traditional strategy in computational sciences. Ideally, it is only a mathematical discretisation of the

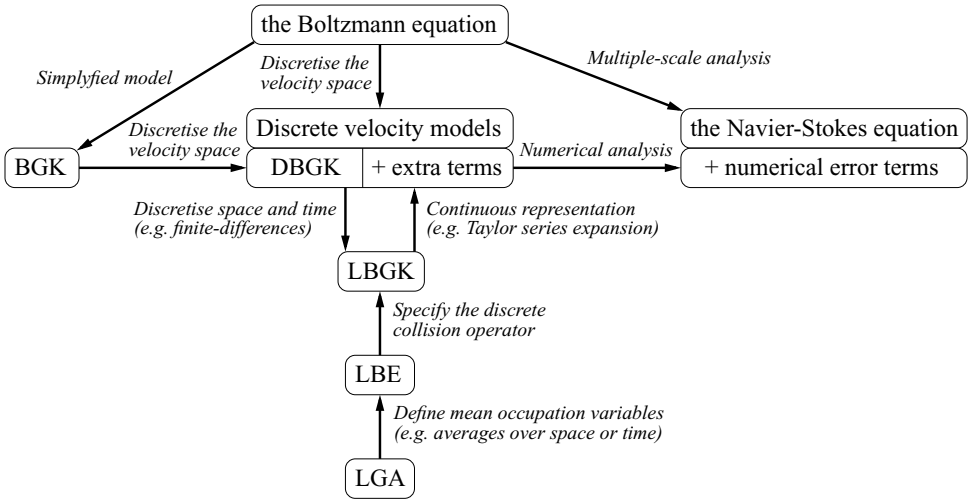

FIGURE 6 The basic concepts and elements related to LBM are illustrated with a graph. Above all, the graph describes the two routes to LBM. That is, lattice Boltzmann schemes can be derived either from the continuous Boltzmann equation, or model Boltzmann equations (e.g. the BGK-model), with a sequence of discretisation steps; alternatively, lattice Boltzmann schemes can be constructed upon discrete particle systems encompassing simplyfied interaction dynamics – LGA is a prime example of a fictitious particle system. These two routes are referred to as the top-down and bottom-up approaches, respectively.

model equation while all physical considerations have already been incorporated at the modelling stage. The possibility to follow two completely separate routes in the construction of LBM can be regarded as a major asset of the method. Due to these two routes, a quite disparate set of lattice Boltzmann schemes have already been proposed – some of the schemes do not even include a lattice. Hence, it is very difficult to give a coherent definition for LBM. The bottom-up approach, and the convetional lattice Boltzmann schemes, suggest a naive but tempting definition: *LBM represents a class of schemes where the explicit evolution equation is of LBE-type, the discrete collision operator is liable for the correct physical description at a macroscopic scale (whenever the set of microscopic velocity vectors possess sufficient symmetry properties), and the velocity vectors* $\Delta t\, \mathbf{c}_i$ *serve as exact links between the nodes of a uniform lattice.*

However, by following the top-down approach, lattice Boltzmann schemes not conforming with the above definition arise naturally. For example, such computational schemes, usually classified as lattice Boltzmann schemes, which involve nonuniform grids supplemented with an interpolation procedure [He96], finite-element treatments [Lee01, Shi03, Li04, Düs06], and finite-volume discretisations [Nan92, Pen99, Xi99, Ube04, Ros05, Sti06, Ube06, Ube08, Pat09] have been proposed. From the top-down approach perspective, LBM is closely related to

DBE (or DVM). Even so, LBM and DBE have sprout two quite separate scientific communities. The difference in philosophy, advocated by the two communities, is well captured by *Sauro Succi* [Suc01a]:

> Surely DVM and LBE are very close relatives in mathematical terms, since they both are based on grid-bound particles moving along a set of discrete speeds.
>
> However, as far as we can judge, they depart significantly in their practical aim. DVM is genuinely concerned with kinetic theory, the main aim being to develop stylised Boltzmann equations possibly amenable to analytical solutions, or theorem demonstration. Computer simulation is also in focus, but with no particular obsession on reaching the hydrodynamic scales.
>
> LBE is less and more ambitious at the same time.
>
> Less ambitious, because the idea of a faithful description of kinetic phenomena is not pursued at all. More, because it challenges the Lion King in his own den, aiming as it does at capturing hydrodynamic phenomena (and beyond) more effectively than continuum models themselves! As we shall see, such a daring task often meets with significant success.

The above is rather a manifesto than a definition for LBM, but nevertheless it encompasses the spirit of LBM which we acknowledge: instead of a faithful description of kinetic phenomena, prescribed macroscopic dynamics are pursued with computational schemes which are based on or inspired by kinetic dynamics. Accordingly, it is then critical to expose the exact macroscopic equations for which approximations are computed with the lattice Boltzmann schemes, and to estimate the accuracy of these approximations. In Sec. 3.4 we utilise a multiple-scale analysis when investigating the hydrodynamic properties of LBGK .

3.3.1 LBGK from the discrete Boltzmann equation

In Sec. 3.2, the construction of lattice Boltzmann schemes was based on LBE, Eq. (40). Here we present how LBE, and specifically LBGK, can be obtained from the discrete Boltzmann equation (DBE). For simplicity, in our presentation we omit the term involving an external acceleration. Even without this simplification, DBE Eq. (38) is a set of constant coefficient first-order hyperbolic partial differential balance equations or, more narrowly, a set of linear advection equations with non-linear source terms [LeV02].

To begin with, we recall the discrete Boltzmann equation Eq. (38) without an external acceleration,

$$\frac{\partial f_i}{\partial t} + \mathbf{c}_i \cdot \frac{\partial f_i}{\partial \mathbf{r}} = \mathcal{J}_i(\vec{f}), \quad i = 0, 1, \ldots, q-1,$$

and continue with the discretisation of the remaining derivative terms, i.e. $\partial_t f_i$ and $c_{i\alpha}\partial_\alpha f_i$, by finite differences. The philosophy here is to carry out the discreti-

sation in a macroscopic frame of reference. That is, the small expansion parameters Δr and Δt below are perceived small at a macroscopic level rather than at a microscopic level. In fact, the parameters are large numbers in the microscopic frame of reference. Again, ∂_α refers to differentiation with respect to r_α. From the Taylor series expansion

$$f_i(\mathbf{r}, t + \Delta t) = f_i(\mathbf{r}, t) + \Delta t \partial_t f_i(\mathbf{r}, t) + \frac{\Delta t^2}{2} \partial_t^2 f_i(\mathbf{r}, t) + \ldots$$

we find the first-order forward-difference approximation for the time derivative:

$$\partial_t f_i(\mathbf{r}, t) = \frac{f_i(\mathbf{r}, t + \Delta t) - f_i(\mathbf{r}, t)}{\Delta t} + \mathcal{O}(\Delta t), \tag{60}$$

where $\mathcal{O}(\Delta t)$ represents all the terms neglected in the approximation of the derivative; the order of the leading error term is Δt. Similarly, from

$$f_i(\mathbf{r} + \Delta t \mathbf{c}_i, t) = f_i(\mathbf{r}, t) + \Delta t c_{i\alpha} \partial_\alpha f_i(\mathbf{r}, t) + \frac{\Delta t^2 c_{i\alpha} c_{i\beta}}{2} \partial_\alpha \partial_\beta f_i(\mathbf{r}, t) + \ldots$$

we find the first-order forward-difference approximation for the convective derivative:

$$c_{i\alpha} \partial_\alpha f_i(\mathbf{r}, t) = \frac{f_i(\mathbf{r} + \Delta t \mathbf{c}_i, t) - f_i(\mathbf{r}, t)}{\Delta t} + \mathcal{O}(\Delta t\, c_r^2). \tag{61}$$

In the next step, we rearrange the simplified DBE in such a way that only $\partial_t f_i$ is left on the left hand side of the equation. In addition, we apply the above forward difference for the time derivative and find that

$$\frac{f_i(\mathbf{r}, t + \Delta t) - f_i(\mathbf{r}, t)}{\Delta t} = -c_{i\alpha} \partial_\alpha f_i(\mathbf{r}, t) + \mathcal{J}_i(\mathbf{r}, t), \quad i = 0, 1, \ldots, q - 1. \tag{62}$$

The discrete collision operator $\mathcal{J}_i$ models change in the distribution function f_i due to particle interactions in the underlying microworld. The purpose of this rearrangement is to highlight an essential decision: when pursuing LBE in the discretisation, i.e. the evolution equation Eq. (40), everything on the right hand side is subjected to an upwind treatment. The general principle in upwind-based schemes is to utilise, or emphasise, the information propagating from the upwind direction. This is a common approach especially for linear advection equations [LeV02]. An upwind scheme is stable if the so-called Courant number C_o satisfies the *Courant-Friedrichs-Lewy* condition [Cou28]:

$$C_o = \frac{c_r \Delta t}{\Delta r} \leq 1.$$

The relation $\Delta r = \Delta t c_r$ enforces $C_o = 1$ in conventional lattice Boltzmann schemes, and thus the condition is satisfied at the limit. The upwind treatment as presented here is a reminiscence of LGA, where the particles explicitly carry information. Various finite-difference schemes, distinct from LBE, can be obtained by applying more elaborate approximations for the derivatives and by selectively adhering to the upwind principle [Rei95, Cao97, McN95, McN97, He98a, Lee03, Sof03]. At the

hydrodynamic level, these schemes typically differ at least in their expressions for the viscosity.

In the context of DBE, the microscopic velocities $\mathbf{c}_i$ naturally define upwind as well as downwind directions; a characteristic line is defined by $\mathbf{c}_i$. The upwind treatment here then means that, in Eq. (62), the two terms on the right are both evaluated at an upwind location $(\mathbf{r} - \Delta t\mathbf{c}_i)$ at time t. From there the information then propagates along the characteristic line and, in one discrete time step Δt, arrives at the location of interest $\mathbf{r}$. That is,

$$\frac{f_i(\mathbf{r}, t + \Delta t) - f_i(\mathbf{r}, t)}{\Delta t} = -c_{i\alpha}\partial_\alpha f_i(\mathbf{r} - \Delta t\mathbf{c}_i, t) + \mathcal{J}_i(\mathbf{r} - \Delta t\mathbf{c}_i, t).$$

In this equation, we approximate the convective derivative with the first-order forward difference Eq. (61). Note that the described discretisation procedure for the convective derivative is equivalent to the first-order backward-difference approximation of $c_{i\alpha}\partial_\alpha f_i(\mathbf{r}, t)$. Finally, in the resulting equation we formally replace $\mathbf{r}$ with $\mathbf{r} + \Delta t\mathbf{c}_i$:

$$\begin{aligned}\frac{f_i(\mathbf{r} + \Delta t\mathbf{c}_i, t + \Delta t) - f_i(\mathbf{r} + \Delta t\mathbf{c}_i, t)}{\Delta t} &= -\frac{f_i(\mathbf{r} + \Delta t\mathbf{c}_i, t) - f_i(\mathbf{r}, t)}{\Delta t} + \mathcal{J}_i(\mathbf{r}, t) \\ \Leftrightarrow f_i(\mathbf{r} + \Delta t\mathbf{c}_i, t + \Delta t) &= f_i(\mathbf{r}, t) + \Delta t\, \mathcal{J}_i(\mathbf{r}, t). \end{aligned} \tag{63}$$

The above equation conforms to LBE when $\Delta t\, \mathcal{J}_i$ is identified with Ω_i.

In order to obtain a particular scheme, instead of a general evolution equation, the collision operator $\mathcal{J}_i$ must be specified. Here our aim is to obtain LBGK from the discrete kinetic theory. Hence, we introduce a discrete counterpart for the BGK model Eq. (32):

$$\mathcal{J}_i(\mathbf{r}, t; \tau_m, \lambda) = -\frac{\lambda}{\tau_m} f_i^{neq}(\mathbf{r}, t), \tag{64}$$

where $f_i^{neq} \equiv f_i - f_i^{eq}$; the discrete equilibrium function f_i^{eq} is defined in Eq. (42). The discrete BGK model includes now two parameters: τ_m and λ. The mean free flight time between molecular collisions τ_m is a material parameter, and the characteristic time at a microscopic scale. The dimensionless parameter λ is an additional simulation parameter. The interpretation of Eq. (64) is straightforward: the change in f_i due to particle interactions is $-\lambda f_i^{neq}$ during one period of τ_m, or per one collision. By applying this collision operator in Eq. (63), we find that

$$f_i(\mathbf{r} + \Delta t\mathbf{c}_i, t + \Delta t) = f_i(\mathbf{r}, t) - \frac{\lambda \Delta t}{\tau_m} f_i^{neq}(\mathbf{r}, t). \tag{65}$$

An important note is now in order. When we exclusively commit to hydrodynamic fluid flow simulations, and to nothing else, the lattice spacing Δr and the discrete time step Δt provide the lower limits for the characteristic length and time scales at a macroscopic level, respectively. That is, for a particular fluid flow simulation, they indicate the smallest scales in which the variation of hydrodynamic variables can be meaningfully differentiated. For example, the characteristic macroscopic length scale in a fluid flow simulation must be defined as

$L = L^* \Delta r$, where $L^* > 1$. At the microscopic level, the characteristic length scale is given by the mean free path ℓ_m. Furthermore, $\ell_m / \tau_m = c_{ms} \sim \mathcal{O}(c_r)$. The Knudsen number is small in the hydrodynamic regime , $K_n \ll 1$, and then the most stringent definitions of Knudsen number, $K_n = \ell_m / \Delta r$ and $K_n = \tau_m / \Delta t$, require $\ell_m \ll \Delta r$ and $\tau_m \ll \Delta t$, respectively. Evidently, our target equation Eq. (41), LBGK, is obtained from the above equation by setting $\lambda \equiv \omega \tau_m / \Delta t = \omega K_n$, where $\omega \sim \mathcal{O}(1)$. We arrive at the same equation directly with the discrete collision operator

$$\mathcal{J}_i(\mathbf{r}, t; \Delta t, \omega) = K_n \cdot \mathcal{J}_i(\mathbf{r}, t; \tau_m, \omega).$$

The above equation is illuminative: the original BGK model Eq. (32) must be multiplied by the Knudsen number, a very small number in the hydrodynamic regime, in order to arrive at the evolution equation for LBGK.

From a modelling perspective this can be interpreted in many ways. First of all, locally the fluid is close to a thermodynamic equilibrium due to the small Knudsen number assumption. However, the small deviations from the equilibrium are apparently persistent, i.e. the process of thermalisation is very slow in comparison to the original BGK model. Informally speaking, since τ_m must be small with respect to Δt, a great number of collisions is required to reach a local equilibrium. For example, we may consider that the average interaction potential is very weak, again in comparison to the original BGK model. Hence, comparatively small mean kinetic energies still fulfil the condition of an ideal gas (see Sec. 2.2.2). Remember that the reference velocity c_r is associated with the average molecular kinetic energy. Be that as it may, the computational interpretation is clear: whatever value is assigned for the macroscopic time step Δt, the microscopic time step τ_m is always perceived as much smaller, i.e. $\tau_m = K_n \Delta t$. Whether this small Knudsen number assumption is physically sensible, depends on the simulation configuration. Nonetheless, the approach taken is consistent and pragmatic for hydrodynamic fluid flow simulations. With the choices made above, the scheme does not depend directly on the Knudsen number any more, and any deviations in simulation results from the hydrodynamic solution are attributed to computational errors.

3.4 Hydrodynamic equations from LBGK

A lattice Boltzmann scheme provides means to compute time evolution of the discrete distribution functions f_i. Since hydrodynamic variables, e.g. density and flow velocity, are moments of f_i in the microscopic velocity space, their time evolution is indirectly computed by the same scheme. This raises a question: what equations govern the time evolution of the hydrodynamic variables at a macroscopic level? That is, are there physically meaningful hydrodynamic equations to which our simulated flow field provides an approximate solution? In what follows, we use LBGK as an example and show that, with suitable assumptions, it produces approximate solutions to the Navier-Stokes equation.

In the previous section, we used Taylor series expansion in order to get finite-difference approximations for the derivatives at a macroscopic level. Now we use the same approach again, but in an opposite manner. Namely, from Taylor series expansions we find that

$$f_i(\mathbf{r}+\Delta t\mathbf{c}_i, t+\Delta t) = f_i(\mathbf{r}, t+\Delta t) + \Delta t c_{i\alpha}\partial_\alpha f_i(\mathbf{r}, t+\Delta t) + \frac{\Delta t^2 c_{i\alpha}c_{i\beta}}{2}\,\partial_\alpha\partial_\beta f_i(\mathbf{r}, t+\Delta t) + \ldots$$

and

$$f_i(\mathbf{r}, t+\Delta t) = f_i(\mathbf{r}, t) + \Delta t\partial_t f_i(\mathbf{r}, t) + \frac{\Delta t^2}{2}\partial_t^2 f_i(\mathbf{r}, t) + \ldots \quad .$$

The expansion parameters $\Delta r = \Delta t\, c_r$ and Δt are still considered small at a macroscopic scale and, at the same time, large at a microscopic scale. Next we combine these two expansions, and retain derivatives only up to second order:

$$f_i(\mathbf{r}+\Delta t\mathbf{c}_i, t+\Delta t) = f_i(\mathbf{r}, t) + \Delta t\partial_t f_i(\mathbf{r}, t) + \frac{\Delta t^2}{2}\partial_t^2 f_i(\mathbf{r}, t) + \Delta t c_{i\alpha}\partial_\alpha f_i(\mathbf{r}, t) + \Delta t^2 c_{i\alpha}\partial_\alpha\partial_t f_i(\mathbf{r}, t) + \frac{\Delta t^2 c_{i\alpha}c_{i\beta}}{2}\,\partial_\alpha\partial_\beta f_i(\mathbf{r}, t).$$

This expression is then substituted into the left hand side of the LBGK evolution equation Eq. (41). In the resulting equation, the distribution functions all have exactly the same arguments, viz. the spatial coordinate $\mathbf{r}$ and time t. For simplicity, the arguments are omitted below, e.g. $f_i \equiv f_i(\mathbf{r}, t)$:

$$\Delta t\partial_t f_i + \frac{\Delta t^2}{2}\partial_t^2 f_i + \Delta t c_{i\alpha}\partial_\alpha f_i + \Delta t^2 c_{i\alpha}\partial_\alpha\partial_t f_i + \frac{\Delta t^2 c_{i\alpha}c_{i\beta}}{2}\,\partial_\alpha\partial_\beta f_i = -\omega f_i^{neq}. \quad (66)$$

In the limit of very small Δr and Δt, this is a second-order continuum description of LBGK. In order to proceed, we utilise a particular analysis procedure.

3.4.1 Chapman-Enskog analysis

Hydrodynamic equations which conform to a lattice Boltzmann scheme can be obtained by resorting to a multiple-scale analysis. Specifically, we assume that the dynamical description above Eq. (66) involves two relevant hydrodynamic time scales: the convective (fast) $\mathcal{T}_1$ and the diffusive (slow) $\mathcal{T}_2$ scales. We introduce a small parameter ϵ which relates these two scales to the discrete time step Δt: $\mathcal{T}_1 = \epsilon^{-1}\Delta t$ and $\mathcal{T}_2 = \epsilon^{-2}\Delta t$. In other words, the small parameter is the ratio between the computational time step and the characteristic convective time scale, i.e. $\epsilon = \Delta t/\mathcal{T}_1$. Moreover, these definitions imply $\mathcal{T}_2 = \epsilon^{-1}\mathcal{T}_1$; the scale $\mathcal{T}_2$ is indeed long in comparison to $\mathcal{T}_1$. Let t_1 and t_2 denote the time variables which act on the two scales, respectively. That is, $t_1 = t_1^*\mathcal{T}_1$ and $t_2 = t_2^*\mathcal{T}_2$, where t_1^* and t_2^* are dimensionless time variables of the order of $\mathcal{O}(1)$.

The essence of the multiple-scale analysis is captured when we assert that the distribution functions depend on two independent time variables instead of

one: $f_i(\mathbf{r}, t) \rightarrow f_i(\mathbf{r}, t_1, t_2)$. The time derivative is redefined accordingly:

$$\partial_t := \frac{\partial}{\partial t_1} + \frac{\partial}{\partial t_2} \equiv \partial_t^{(1)} + \partial_t^{(2)}. \tag{67}$$

In a moment, we continue with a Chapman-Enskog style of analysis. It is a peculiarity of the Chapman-Enskog analysis that the spatial variable is not subjected to a two-scale expansion. The single characteristic length scale is associated with the convective time scale, i.e. $L = c_r \mathcal{T}_1$. A simple dimensional analysis reveals the order of magnitudes for the relevant partial derivatives:

$$\begin{aligned} \Delta t \partial_t &= \Delta t \left(\frac{\partial}{\partial t_1^* \mathcal{T}_1} + \frac{\partial}{\partial t_2^* \mathcal{T}_2} \right) = \epsilon \frac{\partial}{\partial t_1^*} + \epsilon^2 \frac{\partial}{\partial t_2^*}, \\ \Delta t c_{i\alpha} \partial_\alpha &= \Delta t c_{i\alpha}^* c_r \frac{\partial}{\partial r_\alpha^* L} = \Delta t c_{i\alpha}^* c_r \frac{\partial}{\partial r_\alpha^* c_r \mathcal{T}_1} = \epsilon c_{i\alpha}^* \frac{\partial}{\partial r_\alpha^*}. \end{aligned} \tag{68}$$

In the subsequent presentation, we use notation $\partial_\alpha \equiv \partial_\alpha^{(1)}$ whenever it is appropriate.

In the spirit of multiple-scale analysis, the above time scale expansion is supplemented with an additional expansion for the target function, here the distribution function f_i. The section 2.3.3 already included a discussion about how approximate solutions of the Boltzmann equation can be obtained by expanding the distribution function in a power series in terms of a parameter inversely proportional to the gas density. The parameter might as well be the Knudsen number K_n, like in the expansion Eq. (28). Here our objective is different: we pursue hydrodynamic equations which conform to our computational scheme. Particularly, our aim is to understand how these hydrodynamic equations are affected by our computational parameters; the most important parameters are the time step Δt, the lattice spacing Δr, and the relaxation parameter ω. Thus, we use $\epsilon = \Delta t / \mathcal{T}_1$ as the expansion parameter in the power series, i.e.

$$f_i := f_i^{(0)} + \epsilon f_i^{(1)} + \epsilon^2 f_i^{(2)} + \dots \quad . \tag{69}$$

Alternatively, we could have defined the parameter ϵ as the ratio of the lattice spacing to the convective length scale. Note the philosophical difference: instead of using the multiple-scale analysis for investigating macroscopic properties of a discrete mathematical model controlled by physical parameters, e.g. by the Knudsen number, we investigate numerical properties of a computational scheme for hydrodynamic fluid flow simulations where the properties depend on the discretisation parameters. There is an another tacit, if not insignificant, difference with the previously presented expansion Eq. (28): the first term is not automatically identified with the equilibrium function.

When we substitute the expansion Eq. (69) into Eq. (66), together with the assumption of two time-scales, we only retain terms up to second-order in the

small parameter ϵ – recall the order of magnitudes from Eq. (68). Thus,

$$\Delta t\left(\partial_t^{(1)} f_i^{(0)} + \partial_t^{(2)} f_i^{(0)} + \epsilon\partial_t^{(1)} f_i^{(1)}\right) + \frac{\Delta t^2}{2}\partial_t^{(1)}\partial_t^{(1)} f_i^{(0)} + \Delta t c_{i\alpha}\left(\partial_\alpha^{(1)} f_i^{(0)} + \epsilon\partial_\alpha^{(1)} f_i^{(1)}\right) + \Delta t^2 c_{i\alpha}\partial_\alpha^{(1)}\partial_t^{(1)} f_i^{(0)} + \frac{\Delta t^2 c_{i\alpha}c_{i\beta}}{2}\partial_\alpha^{(1)}\partial_\beta^{(1)} f_i^{(0)} = -\omega\left(f_i^{(0)} + \epsilon f_i^{(1)} + \epsilon^2 f_i^{(2)} - f_i^{eq}\right). \quad (70)$$

The fundamental idea in a multiple-scale analysis is to equate terms order by order. Here the order is defined by the small parameter ϵ. Equipped with this perspective, we simply assort the terms in Eq. (70). Remembering that $\omega \sim \mathcal{O}(1)$ we find

$$\mathcal{O}(\epsilon^0): \quad 0 = -\omega\left(f_i^{(0)} - f_i^{eq}\right), \quad (71)$$

$$\mathcal{O}(\epsilon^1): \quad \Delta t\partial_t^{(1)} f_i^{(0)} + \Delta t c_{i\alpha}\partial_\alpha^{(1)} f_i^{(0)} = -\omega\epsilon f_i^{(1)}, \quad (72)$$

$$\mathcal{O}(\epsilon^2): \quad \Delta t\left(\partial_t^{(2)} f_i^{(0)} + \epsilon\partial_t^{(1)} f_i^{(1)} + \epsilon c_{i\alpha}\partial_\alpha^{(1)} f_i^{(1)}\right) + \frac{\Delta t^2}{2}\left(\partial_t^{(1)}\partial_t^{(1)} + 2c_{i\alpha}\partial_\alpha^{(1)}\partial_t^{(1)} + c_{i\alpha}c_{i\beta}\partial_\alpha^{(1)}\partial_\beta^{(1)}\right) f_i^{(0)} = -\omega\epsilon^2 f_i^{(2)}. \quad (73)$$

From the first equation Eq. (71) we can immediately identify $f_i^{(0)}$ with f_i^{eq}. Furthermore, by utilising Eq. (72) twice in Eq. (73), we find that

$$\mathcal{O}(\epsilon^0): \quad f_i^{(0)} = f_i^{eq}, \quad (74)$$

$$\mathcal{O}(\epsilon^1): \quad \partial_t^{(1)} f_i^{(0)} + c_{i\alpha}\partial_\alpha^{(1)} f_i^{(0)} = -\frac{\omega\epsilon}{\Delta t} f_i^{(1)}, \quad (75)$$

$$\mathcal{O}(\epsilon^2): \quad \partial_t^{(2)} f_i^{(0)} + \epsilon\left(1 - \frac{\omega}{2}\right)\left(\partial_t^{(1)} f_i^{(1)} + c_{i\alpha}\partial_\alpha^{(1)} f_i^{(1)}\right) = -\frac{\omega\epsilon^2}{\Delta t} f_i^{(2)}. \quad (76)$$

With the identification $f_i^{(0)} \equiv f_i^{eq}$, and by neglecting all the terms higher than second order in ϵ, the first hydrodynamic moments of the expansion Eq. (69) become

$$\sum_i f_i^{neq} \equiv \sum_i \left(\epsilon f_i^{(1)} + \epsilon^2 f_i^{(2)}\right) = 0 \;\Rightarrow\; \sum_i f_i^{(1)} = -\epsilon\sum_i f_i^{(2)}, \quad (77)$$

$$\sum_i c_{i\alpha} f_i^{neq} \equiv \sum_i c_{i\alpha}\left(\epsilon f_i^{(1)} + \epsilon^2 f_i^{(2)}\right) = 0 \;\Rightarrow\; \sum_i c_{i\alpha} f_i^{(1)} = -\epsilon\sum_i c_{i\alpha} f_i^{(2)}. \quad (78)$$

Note that these moment equations do not correspond to the formal constraints usually exploited in the analysis:

$$\sum_i f_i^{(k)} = 0, \quad \sum_i c_{i\alpha} f_i^{(k)} = 0, \quad k \geq 1. \quad (79)$$

The formal constraints are appropriate when approximate solutions of the Boltzmann equation are pursued with an analytical procedure. However, when

the objective is to understand the behaviour of a computational scheme, it seems more appropriate instead to incorporate Eqs (77) and (78) into the procedure – especially since these equations are fulfilled at the computational level. Another related aspect is the *Chapman-Enskog ansatz*: it asserts that the distribution function f_i depends implicitly on time via the hydrodynamic variables, here ρ and $\mathbf{u}$. That is, f_i is not a function of time t directly, but rathet a functional of $\rho(\mathbf{r}, t)$ and $\mathbf{u}(\mathbf{r}, t)$ [Har04]. Formally then

$$f_i(\mathbf{r}, t) \to f_i(\mathbf{r}; \rho(\mathbf{r}, t), \mathbf{u}(\mathbf{r}, t))$$

or actually

$$f_i(\mathbf{r}, t_1, t_2) \to f_i(\mathbf{r}; \rho(\mathbf{r}, t_1, t_2), \mathbf{u}(\mathbf{r}, t_1, t_2)).$$

Then, due to the implicit dependence, the time derivative of f_i is computed with the chain rule:

$$\frac{\partial f_i}{\partial t} = \frac{\partial f_i}{\partial \rho}\frac{\partial \rho}{\partial t} + \frac{\partial f_i}{\partial u_\alpha}\frac{\partial u_\alpha}{\partial t}.$$

A similar assertion can be postulated for the dependence of the distribution function f_i on the spatial variable $\mathbf{r}$. In what follows, however, we do not explicitly utilise the Chapman-Enskog ansatz.

In the next step of the analysis, we compute moments of Eqs (75) and (76). The lowest order moments of the first order equation Eq. (75) are

$$\sum_i \quad \to \quad \partial_t^{(1)}\rho + \partial_\alpha^{(1)}\rho u_\alpha = -\frac{\omega\epsilon}{\Delta t}\rho^{(1)}, \tag{80}$$

$$\sum_i c_{i\alpha} \quad \to \quad \partial_t^{(1)}\rho u_\alpha + \partial_\beta^{(1)}\Pi_{\alpha\beta}^{(0)} = -\frac{\omega\epsilon}{\Delta t}j_\alpha^{(1)}, \tag{81}$$

$$\sum_i c_{i\alpha}c_{i\beta} \quad \to \quad \partial_t^{(1)}\Pi_{\alpha\beta}^{(0)} + \partial_\gamma^{(1)}S_{\alpha\beta\gamma}^{(0)} = -\frac{\omega\epsilon}{\Delta t}\Pi_{\alpha\beta}^{(1)}, \tag{82}$$

where

$$\Pi_{\alpha\beta}^{(0)} := \sum_i c_{i\alpha}c_{i\beta}f_i^{eq} = \theta\rho\delta_{\alpha\beta} + \rho u_\alpha u_\beta, \tag{83}$$

$$S_{\alpha\beta\gamma}^{(0)} := \sum_i c_{i\alpha}c_{i\beta}c_{i\gamma}f_i^{eq} = \theta\rho(u_\alpha\delta_{\beta\gamma} + u_\beta\delta_{\alpha\gamma} + u_\gamma\delta_{\alpha\beta}), \tag{84}$$

$$\rho^{(1)} := \sum_i f_i^{(1)}, \quad j_\alpha^{(1)} := \sum_i c_{i\alpha}f_i^{(1)}, \quad \Pi_{\alpha\beta}^{(1)} := \sum_i c_{i\alpha}c_{i\beta}f_i^{(1)}. \tag{85}$$

Here we have used Eqs (51) – (54). Similarly, the zeroth and first order moments of the second order equation Eq. (76) are

$$\sum_i \quad \to \quad \partial_t^{(2)}\rho + \epsilon\left(1 - \frac{\omega}{2}\right)\left(\partial_t^{(1)}\rho^{(1)} + \partial_\alpha^{(1)}j_\alpha^{(1)}\right) = -\frac{\omega\epsilon^2}{\Delta t}\rho^{(2)}, \tag{86}$$

$$\sum_i c_{i\alpha} \quad \to \quad \partial_t^{(2)}\rho u_\alpha + \epsilon\left(1 - \frac{\omega}{2}\right)\left(\partial_t^{(1)}j_\alpha^{(1)} + \partial_\beta^{(1)}\Pi_{\alpha\beta}^{(1)}\right) = -\frac{\omega\epsilon^2}{\Delta t}j_\alpha^{(2)}. \tag{87}$$

Now we add up moment equations of equal order; first we sum the zeroth order moment equations Eqs (80) and (86) and find

$$\left(\partial_t^{(1)} + \partial_t^{(2)}\right)\rho + \partial_\alpha^{(1)}\rho u_\alpha + \epsilon\left(1 - \frac{\omega}{2}\right)\left(\partial_t^{(1)}\rho^{(1)} + \partial_\alpha^{(1)} j_\alpha^{(1)}\right) = -\frac{\omega}{\Delta t}\left(\epsilon\rho^{(1)} + \epsilon^2\rho^{(2)}\right).$$

The left hand side is simplified with the definition of the time derivative, i.e. with Eq. (67). And according to Eq. (77), the right hand side is zero, if we neglect the terms higher than second-order in the expansion Eq. (69). We thus find that

$$\partial_t\rho + \partial_\alpha\rho u_\alpha = -\epsilon\left(1 - \frac{\omega}{2}\right)\left(\partial_t^{(1)}\rho^{(1)} + \partial_\alpha^{(1)} j_\alpha^{(1)}\right). \tag{88}$$

If the awkward terms on the right are ignored, the equation obtained is the mass conservation equation for a compressible fluid. If we furthermore assume a very low Mach number flow, the density variations in the fluid are negligible and we get the continuity equation of an incompressible fluid – see the discussion around Eq. (9). Note that the low Mach number assumption here is consistent with the Taylor series expansion of the exponential function, i.e. the equilibrium function, presented in Sec. 3.2.1.

There are many arguments for ignoring the additional terms in Eq. (88). If the formal moment constraints are acknowledged, as defined in Eq. (79), all the terms on the right hand side vanish automatically. On the other hand, one could neglect the second order terms in the expansion Eq. (69), and obtain a first order approximation:

$$f_i := f_i^{(0)} + \epsilon f_i^{(1)}.$$

Then the formal constraints Eq. (79) would be true for $f_i^{(1)}$. This purpose-oriented approach is also factitious since our multiple-scale analysis necessarily involves terms of the order $\mathcal{O}(\epsilon^2)$; the omission of the second order terms from the expansion Eq. (69) does not correspond to the analytical framework nor to the computational reality. In fact, we are not aware of a single argument which would rigorously eliminate the additional terms. Without better means, we content to the following approximation. First we employ Eqs (77) and (78):

$$\partial_t\rho + \partial_\alpha\rho u_\alpha = \epsilon^2\left(1 - \frac{\omega}{2}\right)\left(\partial_t^{(1)}\rho^{(2)} + \partial_\alpha^{(1)} j_\alpha^{(2)}\right) =: E_0\left(\omega, \epsilon^2, f_i^{(2)}\right).$$

The error function E_0 defined here now incorporates all the unwanted terms. By neglecting the error function, we have the approximation

$$\partial_t\rho + \partial_\alpha\rho u_\alpha \simeq 0 \tag{89}$$

which, in the incompressible limit where $\partial_t\rho \to 0$ and $\partial_\alpha\rho \to 0$, gives

$$\partial_\alpha u_\alpha \approx 0. \tag{90}$$

After obtaining the mass conservation equation, we proceed to the evolution equation for the momentum. We advance by summing the first order moment equations, namely Eqs (81) and (87):

$$\partial_t \rho u_\alpha + \partial_\beta(\rho u_\alpha u_\beta) = -\partial_\alpha(\theta\rho) - \epsilon\left(1-\frac{\omega}{2}\right)\partial_\beta \Pi^{(1)}_{\alpha\beta} - \epsilon\left(1-\frac{\omega}{2}\right)\partial_t^{(1)} j_\alpha^{(1)} - \frac{\omega}{\Delta t}\left(\epsilon j_\alpha^{(1)} + \epsilon^2 j_\alpha^{(2)}\right).$$

We can identify the first term on the right with the pressure gradient by adopting the equation of state $p = \theta\rho$, i.e. the ideal gas law. In addition, on the left hand side we utilise the approximation Eq. (89), and the last term on the right vanishes with the approximation Eq. (78). Thus, we are left with

$$\rho\partial_t u_\alpha + \rho u_\beta\,\partial_\beta u_\alpha = -\partial_\alpha p - \epsilon\left(1-\frac{\omega}{2}\right)\partial_\beta \Pi^{(1)}_{\alpha\beta} - \epsilon\left(1-\frac{\omega}{2}\right)\partial_t^{(1)} j_\alpha^{(1)}. \tag{91}$$

The last term on the right is eventually embedded into an another error function. Now we concentrate on the first order tensor on the right; it will be related to the viscous stress tensor. We use Eq. (82) together with Eqs (80) and (81) to derive an expression for it. The details of the derivation are presented in Appendix 1. With the expression for the tensor,

$$\begin{aligned}\Pi^{(1)}_{\alpha\beta} &= -\frac{\Delta t}{\omega\epsilon}\left(\theta\rho\left(\partial_\beta^{(1)} u_\alpha + \partial_\alpha^{(1)} u_\beta\right) - \partial_\gamma^{(1)}\rho u_\alpha u_\beta u_\gamma\right) \\ &\quad + \left(\delta_{\alpha\beta}\theta\rho^{(1)} + u_\beta\, j_\alpha^{(1)} + u_\alpha\, j_\beta^{(1)} - u_\alpha u_\beta\,\rho^{(1)}\right),\end{aligned} \tag{92}$$

we find that

$$\begin{aligned}\rho\partial_t u_\alpha + \rho u_\beta\,\partial_\beta u_\alpha = -\partial_\alpha p + \theta\left(\frac{1}{\omega}-\frac{1}{2}\right)\Delta t\,\partial_\beta\left(\rho\left(\partial_\beta u_\alpha + \partial_\alpha u_\beta\right) - \partial_\gamma\rho u_\alpha u_\beta u_\gamma\right) \\ - \epsilon\left(1-\frac{\omega}{2}\right)\left(\partial_t^{(1)} j_\alpha^{(1)} + \partial_\alpha\theta\rho^{(1)} + \partial_\beta u_\beta\, j_\alpha^{(1)} + \partial_\beta u_\alpha\, j_\beta^{(1)} - \partial_\beta u_\alpha u_\beta\,\rho^{(1)}\right).\end{aligned}$$

From the above equation we can identify the kinematic viscosity $\nu = \mu/\rho$, i.e.

$$\nu := \theta\left(\frac{1}{\omega}-\frac{1}{2}\right)\Delta t;$$

this expression was presented already in Eq. (45). Furthermore, after the application of Eqs (77) and (78), the last terms are incorporated into an error function

$$E_1\left(\omega,\epsilon^2,f_i^{(2)}\right) := \epsilon^2\left(1-\frac{\omega}{2}\right)\left(\partial_t^{(1)} j_\alpha^{(2)} + \partial_\alpha\theta\rho^{(2)} + \partial_\beta u_\beta\, j_\alpha^{(2)} + \partial_\beta u_\alpha\, j_\beta^{(2)} - \partial_\beta u_\alpha u_\beta\,\rho^{(2)}\right). \tag{93}$$

Then,

$$\rho\partial_t u_\alpha + \rho u_\beta\,\partial_\beta u_\alpha = -\partial_\alpha p + \nu\,\partial_\beta\Big(\rho\big(\partial_\beta u_\alpha + \partial_\alpha u_\beta\big) - \partial_\gamma \rho u_\alpha u_\beta u_\gamma\Big) + E_1\big(\omega, \epsilon^2, f_i^{(2)}\big).$$

Next we discard the error function E_1. In addition, the usual convention is to neglect the term involving velocity cubed, $u_\alpha u_\beta u_\gamma$, because it shoud be negligible due to the low Mach number assumption; recall that in the Taylor series expansion of the exponential function, presented in Sec. 3.2.1, only terms up to second-order in u were retained. This all leads to the approximation

$$\rho\partial_t u_\alpha + \rho u_\beta\,\partial_\beta u_\alpha \simeq -\partial_\alpha p + \nu\,\partial_\beta \rho\big(\partial_\beta u_\alpha + \partial_\alpha u_\beta\big).$$

The last term remaining on the right encompasses the so-called strain rate tensor $S_{\alpha\beta} := \big(\partial_\beta u_\alpha + \partial_\alpha u_\beta\big)/2$, see Sec. 2.1. In a Newtonian fluid, the viscous stresses are linearly proportional to the strain rate. This linear approximation assumes, particularly, very small strain rates. According to the product rule of derivation,

$$\partial_\beta \rho\big(\partial_\beta u_\alpha + \partial_\alpha u_\beta\big) = \rho\partial_\beta\big(\partial_\beta u_\alpha + \partial_\alpha u_\beta\big) + \big(\partial_\beta u_\alpha + \partial_\alpha u_\beta\big)\partial_\beta \rho. \tag{94}$$

Now, in the incompressible limit, the spatial variations of density must be very small. Thus, the last term in Eq. (94) is a product of two small terms, and it will be neglected in the approximation

$$\partial_\beta \rho\big(\partial_\beta u_\alpha + \partial_\alpha u_\beta\big) \simeq \rho\partial_\beta\big(\partial_\beta u_\alpha + \partial_\alpha u_\beta\big) = \rho\partial_\beta\partial_\beta u_\alpha + \rho\partial_\alpha\partial_\beta u_\beta.$$

Once again, in the incompressible limit, the last term on the right vanishes with the approximation Eq. (90). This leads to our final result,

$$\rho\partial_t u_\alpha + \rho u_\beta \partial_\beta u_\alpha = -\partial_\alpha p + \nu\rho\partial_\beta\partial_\beta u_\alpha,$$

which is the Navier-Stokes equation without an external acceleration, cf. Eq. (7). In summary, the presented (rather lengthy) multiple-scale analysis procedure yields the hydrodynamic equations which conform to LBGK. Along the way, several assumptions as well as approximations were made. Perhaps the most essential assumption, from a physical perspective, is the assumption of an almost incompressible fluid. At the computational level, this assumption is not enforced at all; it must be maintained with the simulation configuration. Whenever the assumption is compromised, so-called compressibility errors arise [Sko93, Rei95, Hou95, Del01, Ház03, Del03]. The approximation neglecting the term involving velocity cubed is both mathematical and physical in character, and is related to the low Mach number assumption. There are publications addressing this approximation [Qia93a, Che94, Qia98, Ház06, Nie08a, Pra09]. The error functions E_0 and E_1 are considered as numerical errors of the computational scheme for hydrodynamic fluid flow simulations; they are not discarded on the grounds of a physically meaningful argument. Finally, the presented Chapman-Enskog style multiple-scale analysis is just one approach to investigating hydrodynamic properties of lattice Boltzmann schemes: there are other ways of analysis [Swi96, Ina97, Hol04, Jun05a, Sbr06, Jun08a, Cai09].

3.5 Various lattice Boltzmann schemes

So far we have consider only the lattice Boltzmann scheme which is based on the BGK collision operator, i.e. LBGK. It is perhaps the simplest of the lattice Boltzmann schemes, and it has been a convenient representative when illustrating general or typical aspects and concepts related to the lattice Boltzmann method. However, LBM has spurred scientist to develop a whole family of schemes. The schemes do not address a single issue. Quite the contrary, they have been motivated by a rich set of interesting problems. For example, some of the schemes have a different definition for the discrete collision operator Ω_i, for whatever reason, others try to remedy compressibility errors, and many incorporate additional physical mechanisms, usually via the equilibrium function or body force, in order to simulate complex flows like multiphase flows and magnetohydrodynamics. Here we list some of these schemes.

3.5.1 TRT

Most of the definitions for the discrete collision operator Ω_i rely on a relaxation-based procedure. That is, typically the collision operators enforce distribution functions towards the local equilibrium, and the relaxation rate is controlled by simulation parameters. The simplest example is LBGK Eq. (41), where the linear relaxation rate of the non-equilibrium part is controlled by the single parameter ω. The so-called two-relaxation-time scheme (TRT), perhaps the second simplest relaxation scheme, also involves linear relaxation, but now controlled by two parameters [Gin05, Gin07, Gin08a, Ser08]. Before presenting the scheme in a compact form, we need to present some definitions. First of all, let index $-i$ denote such a microscopic velocity vector for which $\mathbf{c}_i = -\mathbf{c}_{-i}$. Then, the symmetric and antisymmetric distribution functions are defined as

$$\widehat{f}_i := \frac{1}{2}(f_i + f_{-i}), \quad \widetilde{f}_i := \frac{1}{2}(f_i - f_{-i}),$$

respectively. These distribution functions fulfil the relations

$$f_i = \widehat{f}_i + \widetilde{f}_i, \quad f_{-i} = \widehat{f}_i - \widetilde{f}_i, \quad \widehat{f}_i = \widehat{f}_{-i}, \quad \widetilde{f}_i = -\widetilde{f}_{-i}.$$

The last two relations expose the fundamental property incorporated in TRT: odd moments of the symmetric function vanish, as well as even moments of the anti-symmetric function. Accordingly, the symmetric and anti-symmetric functions are also called the even and odd parts of the distribution function f_i, respectively.

With the above definitions, TRT is described by the equation

$$\begin{aligned} f_i(\mathbf{r} + \Delta t\mathbf{c}_i, t + \Delta t) &= f_i(\mathbf{r}, t) - \omega_e \widehat{f}_i^{neq}(\mathbf{r}, t) - \omega_o \widetilde{f}_i^{neq}(\mathbf{r}, t) \\ &= f_i(\mathbf{r}, t) - \frac{1}{2}(\omega_e + \omega_o) f_i^{neq}(\mathbf{r}, t) - \frac{1}{2}(\omega_e - \omega_o) f_{-i}^{neq}(\mathbf{r}, t). \end{aligned} \quad (95)$$

Clearly, TRT is a special version of a general two-relaxation-time scheme:

$$f_i(\mathbf{r} + \Delta t \mathbf{c}_i, t + \Delta t) = f_i(\mathbf{r}, t) - \omega_1 f_i^{neq}(\mathbf{r}, t) - \omega_2 f_{-i}^{neq}(\mathbf{r}, t).$$

This scheme, in turn, is a very simple incarnation of the linear multi-relaxation-time scheme:

$$f_i(\mathbf{r} + \Delta t \mathbf{c}_i, t + \Delta t) = f_i(\mathbf{r}, t) - \Lambda_{ij} f_j^{neq}(\mathbf{r}, t), \tag{96}$$

where Λ_{ij} is a generic collision matrix carrying all the relaxation parameters. However, it is difficult to treat, in a physically meaningful manner, all the degrees of freedom present in such a generic formulation. Hence, simpler schemes are defined for practical purposes. For examle in TRT, the relaxation parameter ω_e tunes viscosity, which is obviously related to the viscous stresses which themself are prescribed by a second-order (even) moment of the distribution function. In TRT, the expression for viscosity is the same as in LBGK, see Eq. (45). The other relaxation parameter ω_o, connected to odd moments of f_i, provides an additional degree of freedom. Usually it is chosen so as to minimise the viscosity dependence of the slip velocity – a numerical peculiarity of LBM. The viscosity-dependence is minimised, at least in a simple Poiseuille flow, by choosing $\omega_o = 8(2 - \omega_e)/(8 - \omega_e)$ [Gin03, Gin08a, Gin08b, Ver09a, d'Hu09].

3.5.2 MRT

As discussed above, the problem with the general multi-relaxation-time scheme Eq. (96) is related to the treatment of the large number of degrees of freedom present. That is, in general, there are $q \times q$ adjustable relaxation parameters in the matrix Λ_{ij}, q being the number of discrete velocity vectors. A particular solution for the oversupply of freedom is to consider relaxation of moments towards their equilibrium values, instead of directly considering relaxation of the distribution functions [d'Hu92, Bou01a, d'Hu01, d'Hu02]. Here we give only a very brief explanation of the basic idea. For more details, see the above references.

To begin with, moments are simply linear combinations of f_i. It is thus possible to define a set of linearly independent moments $m_i = M_{ij} f_j$ with a linear transformation M_{ij}, where $i, j = 0, \ldots, q-1$. If the moments m_i are defined suitably, the transformation $\mathbf{M}$ is orthogonal or even orthonormal. The moments can be categorised into hydrodynamic and non-hydrodynamic moments, meaning that the former have a physical interpretation, from a hydrodynamic perspective, whereas the latter do not. Furthermore, some of the moments are conserved quantities, like density and momentum, and they remain unaltered in the relaxation procedure. The others are relaxed towards their equilibrium values m_i^{eq}; the non-equilibrium parts of the non-conserved quantities are reduced by $-\omega_k m_i^{neq}$. The relaxation can also be written with a diagonal matrix $\mathbf{R}$ specifying the relaxation parameters ω_k, i.e. the non-equilibrium parts are reduced by $-R_{ij} m_j^{neq}$. This is the essence of the multi-relaxation-time scheme (MRT) under discussion: it is easier to associate a physical meaning, at least in principle and in a hydrodynamic sense, for the individual relaxation parameters – the moments, or some of them, have a hydrodynamic interpretation.

Finally, the change in the distribution functions f_i, due to relaxation of the moments, is obtained with the inverse transformation ($f_i = M_{ij}^{-1} m_j$). In summary, MRT is governed by the evolution equation

$$f_i(\mathbf{r} + \Delta t \mathbf{c}_i, t + \Delta t) = f_i(\mathbf{r}, t) - \Lambda_{ij} f_j^{neq}(\mathbf{r}, t)$$

with $\mathbf{\Lambda} := \mathbf{M}^{-1}\mathbf{R}\mathbf{M}$. Properties of MRT are investigated, for example, in Refs [Lal00, Del03]. Besides MRT, also the so-called regularisation schemes, and alike, naturally fit the general collision matrix framework defined in Eq. (96) [Lad94a, McN95, Lad01, Che06a, Lät06, Zha06, Zha07].

3.5.3 Incompressible lattice Boltzmann schemes

The macroscopic equations describing hydrodynamic behaviour of LBGK were derived in Sec. 3.4. These equations are similar, but not identical, to the Navier-Stokes equation for incompressible fluid flows. Specifically, the derived equations involve spatial and temporal gradients of density, which can give rise to the so-called compressibility errors. For this reason, there have been efforts to construct incompressible lattice Boltzmann schemes where the compressibility errors are effectively reduced [Fri87, Ale93, Zou95a, Lin96, He97c, Guo00]. Here we present the incompressible scheme proposed in Ref. [He97c].

The first step in the proposed scheme is to decompose the density into a constant and fluctuating part: $\rho = \rho_0 + \delta\rho$. Then it is argued that the fluctuations $\delta\rho$ should be of the order of $\mathcal{O}(M_a^2)$ in the incompressible limit, i.e. when $M_a \to 0$. The essence of the model is to neglect all the terms proportional to $\delta\rho(u/c_r)$ and $\delta\rho(u/c_r)^2$, which are of the order of $\mathcal{O}(M_a^3)$ or higher. In particular, the above mentioned terms are neglected in the equilibrium distribution function after substituting the expression for the fluctuating density. When the procedure described is applied to the equilibrium function Eq. (42), we find that

$$f_i^{eq}(\rho, \mathbf{u}) = w_i \left(\rho + \rho_0 \left[\frac{c_{i\alpha} u_\alpha}{\theta} + \frac{c_{i\alpha} u_\alpha c_{i\beta} u_\beta}{2\theta^2} - \frac{u_\alpha u_\alpha}{2\theta} \right] \right). \tag{97}$$

The second modification is related to computation of the macroscopic fluid flow velocity. That is, originally the basic hydrodynamic variables, the mass density ρ and the momentum density ρu_α, are calculated from the zeroth and first moments of the distribution functions such that

$$\rho = \sum_i f_i, \quad \rho u_\alpha = \sum_i c_{i\alpha} f_i.$$

However, the momentum density, and thus the velocity, is redefined in the incompressible scheme [He97c]:

$$\rho_0 u_\alpha := \sum_i c_{i\alpha} f_i.$$

3.6 LBM as a computational method

We have treated LBM as a numerical method for hydrodynamic fluid flow simulations. Indeed, the most successful lattice Boltzmann schemes are constructed for simulation of incompressible, isothermal Newtonian fluids – the Knudsen number must be very small. The Boltzmann equation, on the other hand, applies for fluid flows with arbitrary Knudsen number. Because LBM can be derived from the Boltzmann equation, directly or via the discrete Boltzmann equation, many features of the Boltzmann equation have been abandoned in favour of computational feasibility. The distinctive stage in the derivation involves discretisation of the microscopic velocity space such that the chosen set of discrete velocities is enough for recovering appropriate hydrodynamic equations in the continuum limit [Che94, Abe97, He97a, He97b, Pav98, Qia98, Sha98, Chi06a, Phi06, Sha06, Che08, Chi08, Nie08a, Rub08, Chi09, Kar10].

Computational properties of the hydrodynamical lattice Boltzmann schemes, e.g. stability, have been investigated by many authors [Anc94, Beh94, Ste96, Wor97, Töl98, Lal00, Wol00, Bog01, Bou01a, Aok02, Set02, Lal03a, Ban06, Bro07, Sie08, Yon09]. In the case of LBGK, for example, these investigations conclude an experimentally observed fact: stability is compromised when the relaxation parameter ω approaches 2, i.e. when the viscosity approaches zero. From a physical point of view, stability issues are related to the H-theorem; an unconditional stability would be guaranteed by the H-theorem. However, unlike for the Boltzmann equation and for the BGK model, there is no H-theorem for relaxation-based schemes with a polynomial equilibrium like Eq. (42) – certainly not for the standard LBGK [Wag98, Luo00b, Yon03, Yon05]. For this reason, there have been efforts to construct lattice Boltzmann schemes which admit an H-theorem [Kar98a, Kar98b, Ren98, Kar99, Bog01, Suc02, Ans03, Bog03, Bog04a, Bog04b, Ans05, Kea07, Asi09]. Actually, Koelman can be regarded as a pioneer also in this respect, since he derived his equilibrium function with the principle of maximising the local entropy [Koe91]. Not surprisingly, also the entropic schemes have drawbacks [Del02, Yon03]. Another attempt to enhance stability is the so-called cascaded lattice Boltzmann automaton [Gei06, Gei09]. Moreover, it is worth remarking that the stability issues are manifested particularly in thermal flows. There has been considerable interest in developing lattice Boltzmann schemes for fluid flows with temparature variation [Ale93, McN93, Qia93b, Che94, Che95a, McN95, Che97a, McN97, He98a, Ren98, Soe98, Pen04, Guo07, Pra07, Nie08b, Sbr09]. So far the success has been limited, but since some of the above references are very recent, the current state of affairs remains to be settled.

The formal accuracy of the conventional lattice Boltzmann schemes is second-order both in space and time [Sko93, Anc94, Rei95, Ste96, Hol04]. This somewhat surprising property results from the interpretation of certain numerical errors as physics. Namely, numerical errors have been incorporated in the definition of viscosity: this is manifested by the term $-1/2$ in Eq. (45). However, in practise the realisable accuracy is only first-order with respect to time because of the

compressibility errors (the discrete time step Δt must decrease faster than the lattice spacing Δr due to consistency reasons) [Rei95, Jun01, Hol04]. In fact, the compressibility errors are suppressed with the diffusive scaling of numerical parameters, i.e. the discrete time step Δt should scale like $(\Delta r)^2$. In the role of a computational method for hydrodynamics, LBM has been compared with other numerical methods. Comparisons have been conceptual [Anc94, Xu98, Jun01], and with respect to accuracy as well as computational efficiency [Mar94, Rei95, Hou95, Nob96, Ber99, Kan99a, Lai01, He02, Xu03, Gel06a, Mar09]. According to these comparisons, LBM appears to be a competitive alternative for computational fluid dynamics (CFD), especially for transient low-Reynolds number flows.

The low Reynolds number, $R_e = UL/\nu$, is almost inherent in the conventional schemes where $\Delta r = \Delta t c_r$. Namely, the characteristic velocity U must be small due to the compressibility errors (low Mach number) and, on the other hand, the viscosity ν cannot be too small due to stability issues. Then, the only way to increase the Reynolds number in the simulations is to configure a large number of lattice spacings per characteristic length scale L – which is of course computationally expensive [He96, He97a, He97d]. This is one of the reasons why scientists have pursued alternative discretisations of the discrete Boltzmann equation Eq. (38). These efforts include nonuniform grids supplemented with an interpolation procedure [He96], finite-element treatments [Lee01, Shi03, Li04, Düs06], and finite-volume discretisations [Nan92, Pen99, Xi99, Ube04, Ros05, Sti06, Ube06, Ube08, Pat09].

In conclusion, LBM has been most successful in simulations of complex flows in the low-Reynolds number regime – just like LGA. Pioneering work in complex flow simulations was done soon after the emergence of LBM: magnetohydrodynamics [Che91a], multiphase and multicomponent fluids [Gun91, Gru93, Sha93, Sha94, Swi95], reactive flows [Che95b], fluid flow in porous media [Suc89, Can90, Kop98], and suspension flows [Lad93, Lad94a, Lad94b, Aid95]. A prime example of complex flow simulations with LBM is the multicomponent flow in porous media [Gun93, Fer95, Mar96] – a very difficult problem for any computational method. There are five main reasons why LBM has been successful in simulations of complex flows:

1. The conventional lattice Boltzmann schemes are easy to implement because of the uniform lattice and because of the simple relaxation-based time stepping.

2. The conventional lattice Boltzmann schemes involve a discrete evolution equation which is explicit in time and highly local in space; the schemes are ideal for parallel computing.

3. The conservation of relevant hydrodynamic quantities is exact, both locally and globally. This compliance to basic physical principles is not only a theoretical issue; for example, even a slight drainage of mass per one discrete time step would severely hinder very long fluid flow simulations.

4. There are simple, albeit crude, boundary conditions which are feasible even in arbitrarily complex domains.

5. It is relatively easy to extend the schemes with additional physical mechanisms. These supplementary mechanisms are naturally included via body force or modified equilibrium functions.

The body force, mentioned in the last point above, is not trivial to impose, but many practical implementations for it have been proposed [He98a, He98b, Luo98, Mar98, Luo00a, Bui00, Wol00, Lad01, Guo02a, Sha06]. The above reasons are all individually important but, even so, they are really not that exceptional features. The true merit is that the above features are all harmoniously packed into LBM. Finally, if we were compelled to pick up one of the features above the others, we would choose the last one. It is clear that by doing so we agree with *Sauro Succi*; we conclude our general treatment of LBM with his statement [Suc08]:

> In this work, we have brought up three examples of LB schemes for complex flows across scales, from macroscopic turbulence down to nanofluids of biological interest. The interesting point, from a statistical mechanical perspective, is that each of these examples calls for a significant extension of the original LB scheme for Navier-Stokes hydrodynamics. Far from being the result of numerical thinking alone, these extensions are deeply rooted into the basic physical principles governing the phenomena they are meant to desribe. This is why, in our opinion, LB should most appropriately be viewed not just as a smart Navier-Stokes solver in disguise, but rather like a fully-fledged simulation strategy for complex flows across scales, well grounded into the basic principles of non-equilibrium statistical physics. It is remarkable that such a broad variety of complex fluid phenomena can be mould within a common mathematical framework, and actually with relatively minor changes of the original computational architecture. This is a major asset, deeply rooted in the stream-collide mathematical structure of kinetic theory.

4 BOUNDARY CONDITIONS

A mathematical model including a partial differential equation for the unknown quantity, like a conservation or balance equation, is incomplete. From a mathematical point of view, the governing equation imposes restrictions on the function describing the unknown quantity – flow velocity for example. Or, the same statement rephrased, the undetermined function must conform with the rules set by the partial differential equation. But, in general, there are an infinite number of functions which obey the given rules. Thus, it is necessary to impose more restrictions on the undetermined function so as to single out a particular function which then is the solution and determines the quantity of interest. Additional restrictions can be enforced by boundary conditions. The number of boundary conditions required depends on the governing equation. All this applies for computational methods as well. For example, all the lattice Boltzmann schemes discussed in the previous section must be supplemented with an appropriate number of boundary conditions before they can be used for computer simulations.

Boundary conditions appear in many ways. Initial conditions further restrict the undetermined functions at a given instant: a solution for the unknown quantity is then pursued at times later than the initial instant. In the LBM context, initial conditions have been treated e.g. in Refs [Sko93, Cai05, Mei06, Lee09]. On the other hand, spatial boundary conditions are typically associated with interfaces. For example, envisage a solid body submerged in a fluid. In addition, the body is stationary at all times and unpermeable for the fluid. Then, the surface of the body constitutes a fluid-solid interface. If we are interested e.g. in the flow of fluid around the body, the local flow velocity, here the quantity of interest, is meaningfully defined only in the domain exterior to the body. Hence, it is necessary to define a boundary condition for the flow velocity at the fluid-solid interface: typical choices include the so-called no-slip and slip conditions. At the interface, the former enforces equal velocities for the fluid and solid component, and the latter enforces equal normal velocities but allows friction-free flow in the tangential direction.

Boundary conditions of a third type are inherent for computational methods. Namely, mathematical models can in principle operate in infinite domains.

For instance, consider our above example involving the submerged body. In a theoretical investigation, the domain exterior to the body can extend infinitely far away from the fluid-solid interface. Obviously, in computer simulations such a configuration is not possible due to the limited computing resources. Thus, the domain must be somehow truncated for computational purposes, and the conditions enforced at the edge of the truncated domain are often called articial, absorbing, open, or free boundary conditions – depending on the physical system under investigation and on the purposes of the conditions.

From a technical point of view, the role of spatial boundary conditions in LBM is clear. Consider a lattice node located close to a boundary, or even exactly at the boundary. Let us refer to it as a boundary node; whether the boundary is an edge of the computational domain, an open boundary, or a fluid-solid interface, does not matter here. In the course of time evolution, the distribution functions at the boundary node, as well as everywhere else in the domain, must be updated. The update procedure involves distribution functions from the neighbouring lattice nodes but, for the boundary nodes, some of these neighbours reside outside of the computational domain. That is, some of the distribution functions needed for the update procedure at a boundary node are unknown. Pictorially speaking, the unknown distribution functions depart from the exterior of the domain and propagate to the boundary nodes. Therefore, the role of spatial boundary conditions in LBM is to provide expressions for these unknown distribution functions.

From a physical point of view, however, the role of spatial boundary conditions in LBM is not so clear. Namely, the expressions for the unknown distribution functions provided by the boundary condition may be constructed either upon microscopic, mesoscopic, or macroscopic considerations. That is, the expressions may be derived from particle dynamics, statistical mechanics, or from hydrodynamics. Nevertheless, once the unknown distribution functions at the boundary are determined, hydrodynamic variables are readily available as the first few moments of the distribution functions. The analytical computation of these moments, or approximation when appropriate, gives the *hydrodynamic interpretation* for a boundary condition – regardless of the physical origins of the expressions. For hydrodynamic lattice Boltzmann schemes this is of course a critical point. Accordingly, in a pragmatic strategy for imposing boundary conditions, the hydrodynamic variables or their derivatives are first prescribed at the boundary and then, in the second step, this information is utilised in the expressions for the unknown distribution functions. We say that the expressions enforce the given conditions whenever the moments agree with the prescribed hydrodynamic information. Or, in computer science parlance, *the expressions provide an implementation for the prescribed hydrodynamic condition*. Implementations of hydrodynamic boundary conditions for LBM is the topic considered in Sec. 4.3 as well as in Appendix 2.

The open boundary conditions and the fluid-solid interface conditions typically differ with respect to the hydrodynamic information available at the boundary. Namely, the local fluid velocities are typically known (or prescribed) at the fluid-solid interfaces but the local densities, which are directly proportional to

the local pressures via the ideal gas law, almost necessarily remain unknown. At the open boundaries, on the other hand, such discrimination is not natural. Whether the local velocities, densities, or their derivatives are considered unknown at the open boundary, depends entirely on the simulation configuration and on the purpose of the open boundary condition. In Sec. 4.2 we elaborate on a particular approach to the problem of using LBM for simulating physical flow systems involving open boundaries. There we focus on the so-called mass-flux-based approach for the inlet and outlet boundary conditions. The approach is somewhat unconventional as it relies on a global condition imposed at the open boundary – a fixed average velocity at the inlet is an example of a global condition. Prior to the treatment of the mass-flux-based approach, we review the boundary conditions proposed in the literature for LBM at fluid-solid interfaces.

4.1 A survey of LBM boundary conditions

Due to their prominent status, the discussion must start from the so-called bounce-back and bounce-forward schemes: they are the prototype solutions for implementing no-slip and slip conditions, respectively. These two boundary condition schemes were utilised in LGA from the very beginning [Fri86, Wol86], and were immediately carried over to LBM. At the same time, they are incarnations of the kinetic boundary conditions, the reverse and specular reflection laws, presented already in Sec. 2.3.5. The reverse and specular reflection laws can be appropriately classified as mathematical models describing the macroscopic effects of the true underlying microscopic dynamics at the fluid-solid interace. These models are readily amenable to mathematical analysis of their properties [Sch73], and hence it is not entirely fair to state that boundary schemes based directly on these models are simply heuristic – as is sometimes proclaimed.

It is, however, fair to state that the bounce-back and bounce-forward schemes are the icons of LBM boundary conditions – their simplicity, even for arbitrarily complex interfaces, is an allure which has arguably promoted application of LBM. The bounce-back boundary scheme became even more appealing when *Anthony Ladd* presented his modification of the scheme for moving interfaces [Lad94a]: a simple expression alters the values of the reflected distribution functions so as to mimic additional momentum transfer at the interface. Similar boundary conditions had already been proposed for LGA [Lad88, Rem89]. However, the simplicity is of course also the weakness of the reflection schemes. From early on it was understood that the bounce-back and bounce-forward schemes have deficiencies. For example, the simulated flow velocities at the interfaces are affected by the simulation parameters in an undesirable manner: e.g. slip velocities may be observed when no-slip conditions are pursued [Cor91, Lav91, Zie93, Zou95b]. This issue was briefly touched upon in Sec. 3.5.1. Above all, the simple schemes degrade the spatial accuracy of LBM, and only first-order accuracy is obtained in general configurations [Cor91, Gin94, Gal97]. A particular version

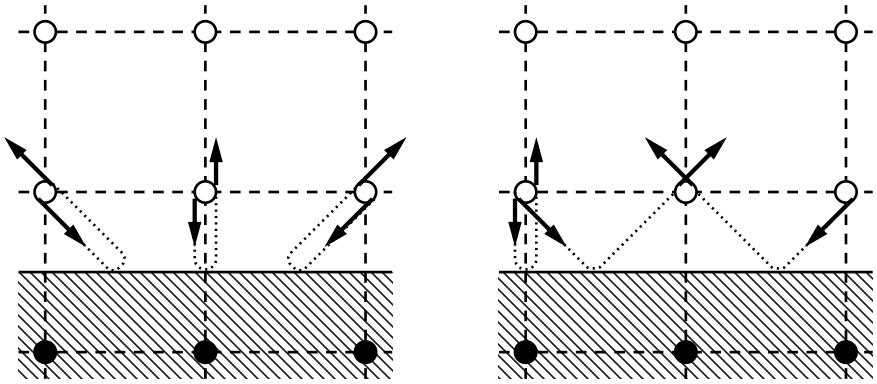

FIGURE 7 Schematic descriptions of halfway reflection boundary conditions for LBM. The fluid-solid interface is located halfway between the fluid and solid nodes. The halfway bounce-back and bounce-forward schemes are depicted on the left and on the right, respectively. In the course of streaming, the values of the distribution functions, associated with the discrete velocities represented by the arrows, propagate along the paths indicated by the dotted lines – at every discrete time step. Note that in the standard versions, the values of the distribution functions involved remain unaltered: the values are simply associated with different discrete velocities before and after the reflection – possibly at a new location.

of the reflection boundary conditions provides some remedy [Rem89, Cor91]: so-called halfway bounce-back and bounce-forward schemes can deliver second-order spatial accuracy in specific flow configurations, e.g. in the case of a plane Poiseuille flow – the peculiar slip velocity dependence on the simulation parameters still remained [He97e, Sbr05]. The halfway reflection schemes are illustrated in Fig. 7. In conclusion, our major point here is that the above discussed deficiencies have encouraged scientist to devise alternative, improved boundary conditions.

During the years, various approaches for constructing boundary conditions have been adopted. A simple strategy, in principle, is to directly use hydrodynamic variables prescribed at the boundary, and their derivatives, for approximating the unknown distribution functions one by one. Let us assume that the boundary node is located exactly at a boundary for which the hydrodynamic variables are known. Then we can use the decomposition $f_i = f_i^{eq} + f_i^{neq}$ for reconstructing the unknown distribution functions. The equilibrium part can be computed directly and, by using multiple-scale analysis, approximations involving derivatives of the hydrodynamic variables can be deviced for the non-equilibrium part [Kin92, Sko93]. If necessary, the derivatives can be computed e.g. with finite differences. Unfortunately, this reconstruction strategy immedi-

ately encounters two major difficulties: 1. the densities are usually unknown as discussed above, at least for the fluid-solid interfaces, and thus the computation of the equilibrium part is possible only if the density is also somehow approximated; 2. finite-difference approximations of the derivatives at the boundaries may not be practical, certainly not when the boundary has a complex shape. These two aspects have suppressed application of the above direct reconstruction schemes.

A particularly notable approach for constructing hydrodynamic boundary conditions was presented by *Noble et al.* [Nob95a]. They presented their approach for the hexagonal FHP model, and assumed that the boundary nodes lie exactly at a straight boundary for which the local flow velocities are known; this is the setting for which also *D. Ziegler* presented his boundary condition [Zie93]. The fundamental idea of the approach is to utilise definitions of the moments as conditions for the unknown variables. In particular, the density and the momentum density are zeroth and first order moments of the discrete distribution functions, see Eqs (43) and (44). In two dimensions, their definitions provide three equations. In the two-dimensional setting considered by Noble et al., there is locally three unknown variables: two distribution functions and the density. In this special case, the number of independent equations and the number of unknown variables agree, and a solution is available. This was demonstrated with simulations of Poiseuille flow and machine accuracy was attained independently of the imposed viscosity and pressure gradient. However, when the boundary is not straight, or when the lattice Boltzmann scheme involves more discrete velocities, as in D2Q9, the number of equations and unknown variables do not match in general. Then some additional constraints, approximations of some sort, must be imposed so as to obtain a linear system of equations which can be solved.

For example, in Ref. [Nob95b] Noble et al. use the above approach to construct a hydrodynamic boundary condition for the D2Q9 model – the boundary configuration is exactly the same. In this case, the number of unknown variables is four, three distribution functions and the local density, and hence they use energy considerations to provide an additional constraint. That is, they enforce a fixed internal energy at the boundary in order to provide the fourth equation for the unknown variables. Since the internal energy is not a conserved quantity in the athermal D2Q9 model – it is rather a free variable – this constraint is only an approximation. For the same D2Q9 model, and for the same boundary configuration, *Zou and He* proposed a different approximation: they used bounce-back of the non-equilibrium part for one unknown distribution function, which provides the fourth equation [Zou97]. For the D3Q15 model, now 6 unknowns and 4 equations, they utilised bounce-back of the non-equilibrium part for all unknown distribution functions. In addition, they introduced so-called correction terms for some of the unknown distribution functions so as to enforce correct tangential velocities at the boundary. This strategy is relatively straightforward to apply e.g. for the D3Q19 model [PIV, Hec10]. Bounce-back of the non-equilibrium part is an intermediate step also in the regularisation boundary scheme [Lät08].

Perhaps the most elaborate scheme for determining the unknown distribu-

tion functions from a linear system of equations, at least among the pioneering works, was presented by *Ginzburg and d'Humières* [Gin96]. They utilise not only the prescribed velocity at the boundary, but also known derivatives of the boundary velocities to construct approximations for the distribution functions, as in Refs [Kin92, Sko93]. All this information is used to set up a linear system of equations which is then solved. It is noteworthy that, unlike in Refs [Kin92, Sko93], derivatives of the velocities are not approximated with finite differences – their values are simply deduced from the physical setting, e.g. the derivatives along the boundary are identically zero whenever the boundary velocity is spatially uniform. The strategy proposed by Ginzburg and d'Humières for constructing boundary schemes was later recognised and adapted by *Halliday et al.* [Hal02, Hol06, Hol08].

On the other hand, the approach for the D3Q15 model presented in Ref. [Zou97] is actually very similar to the boundary condition scheme presented earlier by *Maier et al.* [Mai96]. They also considered boundary nodes exactly at the wall and proposed two versions. First, in the velocity boundary condition, the bounce-back procedure gives provisional values for the unknown distribution functions: this defines the local density at the wall and enforces zero normal momentum. In the second step, mass is redistributed among the reflected distribution functions so as to enforce the prescribed tangential momentum. In general interfaces, where the boundary is not straight, i.e. the interface includes edges and corners, special approximations must be included. For the open boundaries, they again propose a two-step procedure. To begin with, provisional values for the unknown distribution functions are computed by a first-order extrapolation. Then the values are adjusted to satisfy the prescribed density and velocity constraints. A somewhat similar boundary scheme was presented by *Behrend* [Beh95]: bounce-back at the boundary together with a velocity-correction term.

At the same time, *Chen et al.* proposed a boundary scheme for arbitrarily complex boundaries [Che96]: the unknown distribution functions are obtained by extrapolating along the characteristics. In addition to the extrapolation, prescribed boundary densities and velocities are used in the equilibrium function – also here the boundary nodes reside exactly at the boundary. This scheme was later extended for the treatment of curved boundaries [Guo02b]. The problem of treating curved boundaries is related to the fact that, in general, nodes of a regular lattice do not coincide with the boundary. The distance from the boundary nodes to the curved boundary is arbitary, as the boundary resides somewhere between two adjacent lattice nodes.

Another strategy for imposing velocity boundary condition was presented by *Inamuro et al.* [Ina95]. Their approach was inspired by the Maxwell's diffusive reflection boundary condition, see Sec. 2.3.5. Specifically, they presented a scheme where the unknown distribution functions are determined by the equilibrium distribution function which, in turn, is evaluated with a so-called counter-slip velocity. The essence is then to compute the counter-slip velocity so that the local flow velocity corresponds to the wall velocity. The scheme was demonstrated with simulations of Poiseuille flow: machine accuracy was attained in-

dependently of the relaxation parameter. Their scheme can be applied for models with an arbitrary number of discrete velocities, but only for straight walls. Also, mass conservation at the boundary is not guaranteed, as pointed out in Ref. [Cho03].

Actually, many boundary schemes are similarly imperfect – for example the extrapolation scheme presented above do not guarantee mass conservation. Motivated by the conservation of mass, *Chopard et al.* proposed a boundary condition scheme of their own [Cho03]: for the case of a straight wall and D2Q9 model, a system of 6 unknowns and three equations was set up. They argued that, in principle, the extra degrees of freedom can then be used to tune the accuracy of the simulations. However, a systematic procedure for tuning the extra degrees of freedom in general simulation configurations was not presented. In addition to the boundary scheme by *Inamuro et al.* [Ina95], a boundary scheme presented by *Ansumali et al.* is also based on the diffusive reflection boundary condition [Ans02]. A similar, kinetically inspired diffusive boundary scheme was soon there after presented for thermal flows [Sof05, Sof06].

The problem of treating curved boundaries, or actually any off-lattice interfaces, was mentioned above. In order to accurately treat curved boundaries, *Filippova and Hänel* proposed a boundary-fitting scheme together with local grid refinement [Fil97, Fil98]. The boundary-fitting scheme was soon improved by *Mei et al.* [Mei99, Mei00]. A well-known boundary scheme for curved boundaries involves combination of the bounce-back and spatial interpolation of the distribution functions along the characteristics [Bou01b]. Both linear and quadratic interpolations were proposed, and the scheme can be modified for treating moving boundaries [Bou01b, Lal03b]. The approach based on combining the bounce-back and interpolation along the characteristics was later generalised in Ref. [Gin03]; the *multireflection boundary condition* was also presented in the same publication. Unfortunately, the schemes discussed above, i.e. [Fil97, Mei99, Bou01b, Gin03], do not conserve mass in general.

Another distinctive class of boundary schemes is provided by the so-called volumetric approaches [Che98a, Che98b, Ver00, Ver01, Roh02]. A kind of volumetric approach was proposed by Noble and Torczynski [Nob98]. In their approach, the percentage of volume occupied by a solid is determined for each cell in the lattice. If the solids represent moving obstacles, like suspended particles in a fluid, the percentages are recomputed at every discrete time step. An additional term, a function of the local solid volume percentage, is then introduced to a lattice Boltzmann scheme to account for the fluid-solid interactions within each cell. This approach is especially appealing for dynamic geometries, since a relatively simple implementation can provide smooth fluid-solid interaction dynamics. This is in contrast to e.g. the bounce-back scheme, where the coarse, staircase description of the moving solid boundaries inherently produces abrupt or fluctuating dynamics. Later this approach was considered as an immersed boundary method [Coo04, Str07], and it has been applied to suspension flows [Han07, Fen10]. Other immersed boundary methods for LBM are presented e.g. in Refs [Fen04, Niu06, Shu07, Dup08, Wu09, Hao10, Lia10]. External bound-

ary force schemes are closely related to the immersed boundary methods, and have been proposed also for LBM [Wu10a, Wu10b]. Moreover, the volumetric approach proposed by Noble and Torczynski bears a resemblance to the partial bounce-back schemes [Gao94, Dar98a, Dar98b, Wal09].

In addition, a diverse set of boundary schemes has been proposed over the years, see e.g. Refs [Kim00, Roh03, Jun05b, Jun05c, Chu07, Bao08, Kao08, Cha09, Ver09b, Izq10, Jeo10]. The literature addressing LBM boundary schemes is apparently broad and expanding. The interest in the topic is due to the quest for an ideal boundary scheme. Such a scheme would fulfil an impressive list of requirements:

1. Second-order spatial accuracy is guaranteed, which conforms with the formal accuracy of LBM.

2. The second-order spatial accuracy is obtained even for curved, general boundaries.

3. Implementation of the second-order accurate scheme is feasible in an arbitrary complex geometry.

4. The scheme is not limited to a particular discrete velocity set, and it is applicable in a three-dimensional setting.

5. The scheme provides accurate transient solutions, not only steady-state flow fields.

6. The scheme provides smooth dynamics for moving fluid-solid interfaces.

7. The scheme is accurate in the above sense independent of the remaining simulation parameters; for example, there are no unphysical slip-velocity peculiarities.

8. Conservation of mass is always guaranteed.

9. The scheme is explicit in time.

10. The scheme is numerically stable.

11. The update procedure at the boundary allows simulation of multiphase flows, or other complex fluids.

12. The scheme can be applied, or at least extended, to thermal flows.

At present, a scheme complying with all of the above requirements remains to be discovered. Whether an optimal scheme can be found or not is an open issue. In the meantime, application of a compromise scheme depending on the simulation setting is mandatory.

4.2 Mass-flux-based open boundary conditions

After the fluid-solid interface conditions, we concentrate on open boundary conditions for LBM – periodic boundary conditions are excluded from the discussion. We begin with a brief review of the topic. Ladd's approach for moving interfaces can be employed at the open boundaries with prescribed velocities [Lad94a]. This approach involves bounce-back supplemented with a simple expression altering the values of the reflected distribution functions. Extrapolation-based boundary schemes for inlets and outlets were presented in Refs [Che96, Mai96]. The open boundary scheme proposed by *Zou and He* provides the unknown distribution functions by solving a linear system of equations [Zou97] – the scheme involves bounce-back of the non-equilibrium part.

In the approach proposed by *Yu et al.*, the local densities and velocities are given at the inlet boundary which, in general, is not located exactly at the lattice nodes [Yu05]. Then interpolation, together with the bounce-back of the non-equilibrium part, is used to compute the unknown distribution functions. A boundary scheme based on a reconstruction of the unknown distribution functions from approximate hydrodynamic moments was presented in Ref. [Chi06b]. Implementation of several Navier-Stokes outflow boundary conditions in the LBM context was presented by *Junk and Yang* [Jun08b, Jun09]. Finally, some of the above schemes were analysed and compared in Ref. [Izq09]. Many other boundary schemes originally intended for fluid-solid interfaces can also be applied at the open boundaries – at least after some modification. Such schemes are presented e.g. in Refs [Gin96, Hal02, Hol06, Hol08]. Typically in these schemes, the local velocities, and sometimes even the densities, are considered as given values at the boundary.

Here we elaborate on a different kind of approach to the problem of using LBM for simulating physical flow systems that involve open boundaries. Namely, we propose a mass-flux-based framework for the inlet and outlet boundary conditions in LBM simulations. The framework includes three distinctive steps:

1. A global condition is imposed for an inlet or outlet boundary. For example, the condition can enforce a mass flow rate over the inlet or, as in Ref. [PIII], an average velocity at the inlet.

2. At the boundary, the local densities and velocities are deduced by utilising the global condition together with the locally known distribution functions. The deduction involves additional assumptions about the flow configuration.

3. The unknown distribution functions are approximated based on the above determined local densities and velocities. The expressions for the unknown distribution functions can be assigned independently of the first two steps; Sec. 4.3 and Appendix 2 provide a discussion on this topic.

4.2.1 A global condition at the open boundary

Indeed, the mass-flux-based approach is motivated by a practical property: by utilising additional assumptions, the local hydrodynamic variables can be computed from a given global condition – they are not prescribed *a priori*. Therefore, we first focus on global conditions at the open boundary. For example, let us consider a case where the mass flow rate $Q(t)$ is controlled at the inlet Γ. The area of the inlet is A_{in}, and the inlet is located at x=0. We choose to utilise the incompressible lattice Boltzmann scheme presented in Sec. 3.5.3 [He97c]. Then an appropriate definition for the mass flow rate is

$$Q(t) := \int_{\Gamma} \rho_0 \mathbf{u}(\mathbf{r}, t) \cdot \mathbf{n} \, dA \equiv A_{in} \cdot \rho_0 u_a(t), \tag{98}$$

where ρ_0 is the average or reference density and $\mathbf{n}$ is the unit, inward normal vector. Let us further assume a unidirectional inflow in the x-direction; the inflow is perpendicular to the inlet Γ which lies on the yz-plane (cf. Fig. 8). Therefore, $\mathbf{u} \cdot \mathbf{n} = u_x$, and accordingly u_a is the average inlet velocity in the x-direction. When the simulation geometry is represented in a discrete lattice, and the fluid-solid interface is located halfway between the fluid and solid nodes (again, see Fig. 8), the inlet area is directly available from the number of lattice nodes N_{in} at the inlet, i.e. $A_{in} = N_{in} \cdot \Delta r^2$. It is evident from Eq. (98) that, by controlling the average inlet velocity, the mass flow rate is also controlled. In this demonstration, let u_a be our single boundary scheme parameter. For simplicity, it is considered independent of time.

On the other hand, if we take a glance at the underlying microscopic world, there are constantly particles leaving and entering our computational domain. Thus, the macroscopic mass flow rate actually emerges from the imbalance between the two sets of particles. It is hence sensible to view the net mass flow rate Q at the inlet as the difference between the mass inflow rate Q_+ and the mass outflow rate Q_-, i.e. $Q(t) = Q_+(t) - Q_-(t)$. This decomposition is most fruitful in the LBM context. Namely, the conventional lattice Boltzmann schemes in fact allow computation of Q_-. This opportunity, together with the predetermined Q, gives us an expression for the mass inflow rate: $Q_+(t) = Q + Q_-(t)$. The expression for Q_+ is essential when we set out to determine the local densities and velocities at the boundary.

Let us first explain why Q_- can be computed, or actually measured. The time evolution in conventional lattice Boltzmann schemes can be decomposed into two steps: streaming and collision of distribution functions. At time step t, the instant after a streaming step, and hence immediately before the next collision step, is denoted by t^*. At the boundary, some of the velocity vectors point into the computational domain, and some point out of the domain. In the case of D3Q19, illustrated in Fig. 8, there are five inbound as well as outbound velocities; the remaining nine velocities point along the inlet plane. After the streaming step, all the distribution functions are known at the boundary, except those associated with the inbound velocities. Hence, the mass outflow rate $Q_-(t^*)$ can be com-

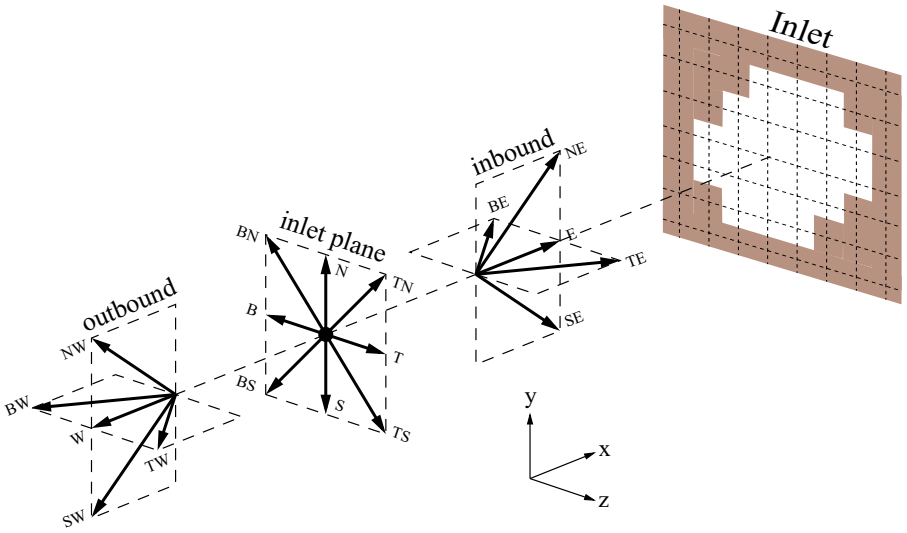

FIGURE 8 An arbitrarily shaped inlet: here unidirectional inflow in the x-direction is envisaged; the inflow is perpendicular to the inlet which lies in the yz-plane. The fluid-solid interface is located halfway between the fluid and solid nodes. Velocity vectors of the D3Q19 model are also presented and enumerated. The logic of the enumeration is as follows: east (E) and west (W) denote positive and negative directions along the x-axis, respectively; similarly, north (N) and south (S) denote positive and negative directions along the y-axis; finally, top (T) and bottom (B) denote positive and negative directions along the z-axis. Not shown is the symbol C which refers to the zero velocity vector. At the inlet boundary, the eastbound velocities point into the computational domain, whereas the westbound velocities point out of the domain. Thus, at the boundary, there are five inbound as well as outbound velocities. The remaining nine velocities point along the inlet plane. From the open boundary condition perspective, the distribution functions associated with the inbound velocities are considered as the primary unknowns and expressions must be assigned to them.

puted from the distribution functions associated with the outbound velocities:

$$Q_-(t^*) := -\sum_{\mathbf{r}\in\Gamma} \Delta r^2 \left(\sum_{i\in I_-} c_{ix} f_i(\mathbf{r}, t^*) \right) = \Delta r^2 \sum_{\mathbf{r}\in\Gamma} q_-(\mathbf{r}, t^*).$$

Above the first summation is over the lattice nodes at the inlet, and the second summation is over the outbound velocities denoted by index set I_-. Furthermore, the above defined quantity $q_-(\mathbf{r}, t)$ is the local mass outflux, i.e. the rate of mass flow across a unit area. There is a minus sign in front of the first sum because we prefer to define q_- and Q_- as positive values: the x-components c_{ix} of the outbound velocity vectors are negative due to our choice of the inlet boundary (located at x=0) – distribution functions f_i are by definition positive. The mass flux has the same units as the momentum density, here denoted by

$j_\alpha(\mathbf{r}, t)$. In LBM, the momentum density is the first-order moment in the microscopic velocity space, and specifically the momentum density in the x-direction is $j_x(\mathbf{r}, t) := \rho_0 u_x(\mathbf{r}, t) = q_+(\mathbf{r}, t) - q_-(\mathbf{r}, t)$; the local mass influx q_+ is defined in the same way as q_-.

4.2.2 Local hydrodynamic variables from a global condition

As presented in the previous section, an expression for Q_+ can be derived from an appropriately defined global condition. This expression is essential in the next step where we set out to determine the local densities $\rho(\mathbf{r}, t^*)$ and momentum densities $j_x(\mathbf{r}, t^*)$ – they are unknown variables before the collision step. This task is accomplished by determining $q_+(\mathbf{r}, t^*)$, as demonstrated below. Let us start off by decomposing also the local density into two parts:

$$\rho(\mathbf{r}, t^*) = \sum_{i \in I_{kn}} f_i(\mathbf{r}, t^*) + \sum_{i \in I_+} f_i(\mathbf{r}, t^*) =: \rho_{kn}(\mathbf{r}, t^*) + \rho_+(\mathbf{r}, t^*), \tag{99}$$

where the index set $I_{kn} := I \setminus I_+$ denotes all the discrete velocities for which the distribution functions are known after the streaming step, i.e. the inbound velocities I_+ are excluded; $\rho_+(\mathbf{r}, t^*)$ is an unknown quantity at the inlet. Now we make an additional assumption. Namely, we assume that

$$c_{ix} = -c_r,\ i \in I_- \quad \text{and} \quad c_{ix} = c_r,\ i \in I_+,$$

i.e. the x-components of the outbound and inbound velocity vectors are equal in magnitude to c_r. All standard lattice-Boltzmann models, e.g. D2Q9, D3Q15, D3Q19, and D3Q27, fulfil this condition. With this assumption, we can directly relate the two unknown local quantities: $\rho_+(\mathbf{r}, t^*) = q_+(\mathbf{r}, t^*)/c_r$.

There is only one intermediate step remaining, and it requires computation of the average density $\rho_c(t^*)$ at the inlet:

$$\rho_c(t^*) = \frac{1}{N_{in}} \sum_{\mathbf{r} \in \Gamma} \rho(\mathbf{r}, t^*) = \frac{1}{N_{in}} \sum_{\mathbf{r} \in \Gamma} \Big(\rho_{kn}(\mathbf{r}, t^*) + \rho_+(\mathbf{r}, t^*) \Big) = \overline{\rho}_{kn}(t^*) + \frac{1}{c_r} \overline{q}_+(t^*),$$

where the overbar denotes an average computed over the inlet boundary. The average mass influx $\overline{q}_+$ is computed from the expression for Q_+:

$$\overline{q}_+(t^*) = \frac{1}{A_{in}} Q_+(t^*) = \rho_0 u_a + \frac{1}{A_{in}} Q_-(t^*) = \rho_0 u_a + \overline{q}_-(t^*).$$

Since we assumed an inflow perpendicular to the inlet boundary, there cannot be any pressure gradients along (parallel to) the boundary. Due to the ideal gas law, $p = c_s^2 \rho$, this implies constant density along the boundary. This constant density is now available in the form of the average density and, furthermore, an expression for ρ_+ is obtained from Eq. (99):

$$\rho_+(\mathbf{r}, t^*) = \rho_c(t^*) - \rho_{kn}(\mathbf{r}, t^*) = \overline{\rho}_{kn}(t^*) - \rho_{kn}(\mathbf{r}, t^*) + \frac{1}{c_r} \Big(\rho_0 u_a + \overline{q}_-(t^*) \Big).$$

With the above results, and assumptions, the local inlet velocities are also immediately available ($u_y = u_z = 0$):

$$q_+(\mathbf{r}, t^*) = c_r \cdot \rho_+(\mathbf{r}, t^*) \quad \Rightarrow \quad u_x(\mathbf{r}, t^*) = \frac{1}{\rho_0}\Big(q_+(\mathbf{r}, t^*) - q_-(\mathbf{r}, t^*)\Big).$$

Hence, at this point, we have time-dependent expressions for the local densities and velocities at the inlet. Now it remains to enforce these local hydrodynamic variables by assigning values for the unknown distribution functions. The local hydrodynamic variables can be enforced for example with the boundary schemes presented in the following section. Note that the mass-flux-based approach just presented is not too restricted: it can be applied in conjunction with many lattice Boltzmann schemes involving different relaxation schemes. The approach is, however, somewhat unconventional as it involves a global condition at the open boundary, and the time-dependent expression for $Q_+(t)$ introduces a kind of feedback mechanism to the flow system.

4.3 Implementations of hydrodynamic boundary conditions

As discussed in the introduction of this chapter, hydrodynamic boundary conditions for LBM involve two steps. First the hydrodynamic variables, or possibly their derivatives, are prescribed at the boundary. Then the prescribed information is utilised in the expressions for the unknown distribution functions. That is, the expressions must be defined in such a way that, when the relevant hydrodynamic moments are computed from the distribution functions, the results agree with the prescribed hydrodynamic information – the expressions enforce the given hydrodynamic condition. Or in other words, the expressions provide an implementation for the prescribed hydrodynamic condition. Some implementations, referred to as boundary schemes, are presented in this section.

Specifically, we present here various boundary schemes that provide expressions for the unknown distribution functions of the D2Q9 model. The two-dimensional model allows us to demonstrate the relevant issues in a more transparent way – at least the formulae along the way are simpler to read. Boundary schemes that provide expressions for the unknown distribution functions of the D3Q19 model are given in Appendix 2. The two-dimensional setting for which we are about to present the boundary schemes is illustrated in Fig. 9. Specifically for this setting, the index sets introduced in the previous section are used: $I_+ = \{SE, E, NE\}$, $I_- = \{SW, W, NW\}$, and $I_{kn} = \{SW, W, NW, S, C, N\}$. That is, the unknown distribution functions after the streaming step are f_{SE}, f_E, f_{NE}.

We utilise below the incompressible lattice Boltzmann scheme with the discrete equilibrium function given in Eq. (97). The equilibrium coefficients for the D2Q9 model are given in Table 2 ($W_0 = 16/36, W_1 = 4/36, W_2 = 1/36$). Furthermore, the speed of sound for the D2Q9 model is defined by the relation $\theta = c_s^2 = c_r^2/3$. Perhaps the most straightforward boundary scheme at the inlet is

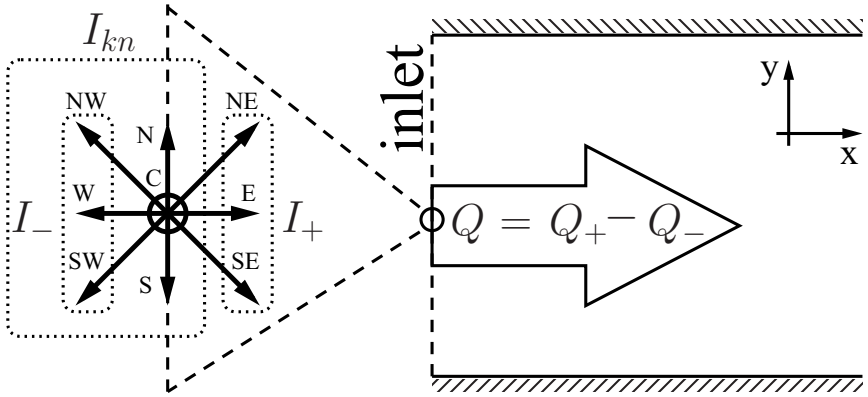

FIGURE 9 A simple two-dimensional flow geometry. The flow is in the x-direction and perpendicular to the inlet. In addition, an enumeration for the velocity vectors of the D2Q9 model is presented. The logic of the enumeration is the same as in Fig. 8: east (E), west (W), north (N), and south (S) denote positive and negative directions along the x- and y-axis. Moreover, center (C) refers to the zero-velocity vector. At the inlet, the eastbound and westbound velocities point into and out of the computational domain, respectively. Thus, at the boundary, there are three inbound as well as outbound velocities. The remaining three velocities point along the inlet plane. The distribution functions associated with the inbound velocities are considered as the primary unknowns and expressions must be assigned to them.

to compute the values of the equilibrium distribution functions, and then simply assign these values to the unknown distributions:

$$f_{SE}(\mathbf{r}, t^*) = f_{SE}^{eq}(\rho_c, \mathbf{u}), \quad f_E(\mathbf{r}, t^*) = f_E^{eq}(\rho_c, \mathbf{u}), \quad f_{NE}(\mathbf{r}, t^*) = f_{NE}^{eq}(\rho_c, \mathbf{u});$$

here the local densities and velocities are considered available after the streaming step. However, this scheme does not enforce the desired hydrodynamic variables at the inlet. That is, if we compute the zeroth and first-order moments of the distribution functions after we have assigned the equilibrium function values, they do not correspond to the prescribed ρ_c and $\mathbf{u}$. Therefore, more elaborate expressions for the unknown distribution functions must be pursued.

4.3.1 Bounce-back of the non-equilibrium part

In what follows, we simplify further the notation. Namely, we omit the arguments from the distribution functions whenever they are obvious, e.g. $f_{SE} \equiv f_{SE}(\mathbf{r}, t^*)$ and $f_{SE}^{eq} \equiv f_{SE}^{eq}(\rho_c, \mathbf{u})$. An intuitive improvement supplements the simple equilibrium scheme with the bounce-back of the non-equilibrium part,

$$f_{SE} = f_{SE}^{eq} + f_{NW}^{neq}, \quad f_E = f_E^{eq} + f_W^{neq}, \quad f_{NE} = f_{NE}^{eq} + f_{SW}^{neq}.$$

With the incompressible equilibrium function Eq. (97), this is equivalent to

$$f_{SE} = f_{NW} + 2W_2\,\rho_0 \frac{\mathbf{c}_{SE}\cdot\mathbf{u}}{\theta},$$
$$f_E = f_W + 2W_1\,\rho_0 \frac{\mathbf{c}_E\cdot\mathbf{u}}{\theta}, \quad f_{NE} = f_{SW} + 2W_2\,\rho_0 \frac{\mathbf{c}_{NE}\cdot\mathbf{u}}{\theta}. \quad (100)$$

In fact, exactly the same expressions were proposed by *Ladd* for the treatment of moving fluid-solid interaces [Lad94a]: bounce-back with an additional term related to the local non-zero velocity at the interface. The difference to Ladd's scheme is minor: first and foremost, Ladd considered interfaces located halfway between the lattice nodes.

Now we have to check whether this scheme enforces the prescribed hydrodynamic variables. We start from the definition of density:

$$\sum_i f_i = (\overbrace{f_{SW} + f_W + f_{NW} + f_S + f_C + f_N}^{\rho_{kn}=\rho_c-\rho_+}) + \overbrace{f_{NW} + f_W + f_{SW}}^{=\rho_-}$$
$$+ \underbrace{6W_2}_{=1/6}\frac{\rho_0 u_x}{c_r} + \underbrace{6W_1}_{=4/6}\frac{\rho_0 u_x}{c_r} + \underbrace{6W_2}_{=1/6}\frac{\rho_0 u_x}{c_r}$$

$$\Leftrightarrow \sum_i f_i = \rho_c - \rho_+ + \rho_- + \frac{\rho_0 u_x}{c_r} = \rho_c - \rho_+ + \rho_- + \frac{1}{c_r}(q_+ - q_-) = \rho_c.$$

Indeed, the correct density is recovered. Next we check the momentum density in the x-direction. Some intermediate steps which were explicitly presented in the above verification of density are now skipped:

$$\sum_i c_{ix} f_i = c_r\big(f_{SE} + f_E + f_{NE} - f_{SW} - f_W - f_{NW}\big) = c_r\big(\rho_- + \frac{\rho_0 u_x}{c_r} - \rho_-\big) = \rho_0 u_x.$$

The correct momentum in the x-direction is hence recovered. Finally, let us check the momentum density in the y-direction. Remember that we have prescribed $u_y = 0$ which, however, is not relevant – we could prescribe any other value for u_y as well:

$$\sum_i c_{iy} f_i = c_r\big(f_{NW} + f_N + f_{NE} - f_{SW} - f_S - f_{SE}\big)$$
$$= c_r\big(f_N + 6W_2\frac{\rho_0 u_x}{c_r} - f_S - 6W_2\frac{\rho_0 u_x}{c_r}\big) = c_r\big(f_N - f_S\big).$$

In general, the y-component is not zero! Therefore, with this boundary scheme we cannot guarantee correct velocities in the transverse y-direction. Hence, an even more elaborate boundary scheme is desired.

Before presenting an improved boundary scheme, an explanation is in order. Why did the simple bounce-back of the non-equilibrium part recover both the correct density as well as the velocity in the normal direction? First of all, let us forget the above bounce-back of the non-equilibrium part scheme for a moment, and simply consider $f^u_{SE}, f^u_E, f^u_{NE}$ as unknown variables at the inlet – here

the extra superscript u further highlights the unknown variables. In addition, the distribution functions at the inlet (the known and unknown together) must respect the prescribed hydrodynamic variables. Here it suffices to concentrate on the density, ρ_c, and the x-component, $\rho_0 u_x$, of the momentum density. In other words, the moments of the distribution functions must match with these hydrodynamic variables. Mathematically, the distribution functions must fulfil two linear equations:

$$\begin{cases} f_{SW} + f_W + f_{NW} + f_S + f_C + f_N + f^u_{SE} + f^u_E + f^u_{NE} = \rho_c, \\ c_r\left(f^u_{SE} + f^u_E + f^u_{NE} - f_{SW} - f_W - f_{NW}\right) = \rho_0 u_x \end{cases}$$

$$\Leftrightarrow \begin{cases} f^u_{SE} + f^u_E + f^u_{NE} = \rho_c - \rho_{kn} = \rho_+, \\ f^u_{SE} + f^u_E + f^u_{NE} = (\rho_0 u_x)/c_r + \rho_- = \rho_+. \end{cases}$$

The two moment equations provide exactly the same condition for the three unknown variables! Thus, enforcing a given density necessarily enforces the corresponding normal momentum, and vice versa.

In more general terms, the two moment equations for the density and the x-component of the momentum density are linearly dependent for the predetermined unknown variables $f^u_{SE}, f^u_E, f^u_{NE}$. This is the key point here: the set of unknown variables determines whether the moment equations are linearly independent or not. For example, let us reinterpret the bounce-back of the non-equilibrium part scheme. First of all, we *postulate* a bounce-back scheme supplemented with additional terms:

$$f_{SE} = f_{NW} + a, \quad f_E = f_W + 4a, \quad f_{NE} = f_{SW} + a, \tag{101}$$

where a is an unknown variable to be determined and the $4a$ term for the distribution function f_E is motivated by the ratio between the equilibrium coeffients ($W_1/W_2 = 4$). It is easily verified that for the only unknown variable, a, the moment equations for the density and for the x-component of the momentum density provide exactly the same condition – just like above. That is, we have a single equation for one unknown. This linear system of equations is trivially solved:

$$a = \frac{\rho_0 u_x}{6c_r} \quad \Rightarrow \quad f_{SE} = f_{NW} + \frac{\rho_0 u_x}{6c_r}, \; f_E = f_W + \frac{4\rho_0 u_x}{6c_r}, \; f_{NE} = f_{SW} + \frac{\rho_0 u_x}{6c_r}.$$

These expressions were presented already in Eq. (100). In summary, the bounce-back of the non-equilibrium part scheme provides the prescribed density ρ_c and normal momentum density $\rho_0 u_x$, but fails to provide the correct transverse momentum density, or the velocity component parallel to the inlet boundary.

4.3.2 A scheme for the D2Q9 model: enforcing 1+2 moments

With an intuitive extension to the boundary scheme formulation Eq. (101), it is possible to correctly reproduce the three hydrodynamic variables, the density ρ_c

(the zeroth-order moment) as well as the momentum density components $\rho_0 u_x$ and $\rho_0 u_y$ (the two first-order moments). Namely, we introduce another unknown variable b, and postulate a bounce-back scheme:

$$f_{NE} = f_{SW} + a + b, \quad f_E = f_W + 4a, \quad f_{SE} = f_{NW} + a - b. \tag{102}$$

Then, we set up a linear system of equations by utilising the definitions of the hydrodynamics variables ρ_c, $\rho_0 u_x$, $\rho_0 u_y$, i.e. the zeroth and first-order moment equations.

Since the equations for ρ_c and $\rho_0 u_x$ again provide exactly the same condition, we have two equations for the two unknown variables. By solving this system, we obtain

$$a = \frac{\rho_0 u_x}{6c_r}, \quad b = -\frac{1}{2}(f_N - f_S) + \frac{\rho_0 u_y}{2c_r};$$

the expressions for the unknown distribution functions are

$$\begin{aligned} f_E &= f_W + \frac{2\rho_0 u_x}{3c_r}, \\ f_{NE} &= f_{SW} + \frac{\rho_0 u_x}{6c_r} - \frac{1}{2}(f_N - f_S) + \frac{\rho_0 u_y}{2c_r}, \\ f_{SE} &= f_{NW} + \frac{\rho_0 u_x}{6c_r} + \frac{1}{2}(f_N - f_S) - \frac{\rho_0 u_y}{2c_r}. \end{aligned}$$

These are exactly the same expressions as presented by *Zou and He* [Zou97]; the right hand sides involve only known variables. For example, in the simple two-dimensional flow configuration presented in Fig. 9, we assign $u_y = 0$ and u_x is computed with the mass-flux-based approach.

It is interesting to note that there appears to be no unique way of constructing this boundary scheme. That is, the unknown variables a and b can be defined in various ways. For example, instead of relying on Eq. (102), we could have based our boundary scheme construction on

$$f_{NE} = a, \quad f_E = f_E^{eq} + f_W^{neq}, \quad f_{SE} = b,$$

or

$$f_{NE} = f_{NE}^{eq} + a, \quad f_E = f_E^{eq} + f_W^{neq}, \quad f_{SE} = f_{SE}^{eq} + b. \tag{103}$$

All these formulations provide the same solution. However, the last formulation above is especially fruitful since it will guide us to even more precise boundary schemes.

4.3.3 A second-order upgrade: enforcing 1+2+1 moments

The problem of assigning values to the unknown distribution functions is a delicate matter. When pursuing hydrodynamic fluid flow simulations, the fundamental idea is deceptively simple: the aim is to incorporate information about the local hydrodynamic state into the unknown distribution functions – the state

is described by a suitable set of hydrodynamic variables. On the other hand, the moment equations serve as kinetic definitions for the hydrodynamic variables. That is, the values of the hydrodynamic variables can be computed directly from the distribution functions. Therefore, it is essential that the information about the hydrodynamic state is incorporated in a very precise way: the reverse computation must recover exactly the prescribed values, i.e. the values computed from the moment equations must match with the prescribed values. Otherwise there is a mismatch, and the distribution functions do not carry information about the true hydrodynamic state.

In the previous section, we presented a scheme which correctly incorporated information about the local densities and velocities into the unknown distribution functions. However, those three variables do not provide a complete description about the local hydrodynamic state. In particular, information about the viscous stresses is not included and hence, from the hydrodynamic point of view, the assigned distribution functions are underspecified. Here we present a boundary scheme which incorporates information about the viscous stresses. First of all, we utilise an approximative relation between the viscous stresses and the second-order moments of the non-equilibrium functions:

$$\sum_i c_{i\alpha} c_{i\beta} f_i^{neq} = \Pi_{\alpha\beta}^{neq} \approx \Pi_{\alpha\beta}^{(1)} \approx -\frac{2\Delta t \theta \rho_0}{\omega} S_{\alpha\beta} =: \Pi_{\alpha\beta}^{visc}, \tag{104}$$

where $S_{\alpha\beta} = (\partial_\beta u_\alpha + \partial_\alpha u_\beta)/2$ is the strain rate tensor, and we have used ρ_0 in order to be consistent with the incompressible lattice Boltzmann scheme. This approximation is based on the Chapman-Enskog analysis, see Eqs (91) and (92) or Appendix 1, and has been employed in the construction of boundary schemes for example by *Halliday et al.* [Hal02].

Since the tensors in the relation Eq. (104) are symmetric, they involve three independent components in two dimensions. Hence, we get three conditions for the non-equilibrium functions:

$$\begin{aligned}
\Pi_{xx}^{neq}: &\quad c_r^2 \left(f_{NE}^{neq} + f_E^{neq} + f_{SE}^{neq} + f_{NW}^{neq} + f_W^{neq} + f_{SW}^{neq} \right) = \Pi_{xx}^{visc}, \\
\Pi_{xy}^{neq}: &\quad c_r^2 \left(f_{NE}^{neq} - f_{SE}^{neq} - f_{NW}^{neq} + f_{SW}^{neq} \right) = \Pi_{xy}^{visc}, \\
\Pi_{yy}^{neq}: &\quad c_r^2 \left(f_{NE}^{neq} + f_N^{neq} + f_{NW}^{neq} + f_{SE}^{neq} + f_S^{neq} + f_{SW}^{neq} \right) = \Pi_{yy}^{visc}.
\end{aligned}$$

The above three equations are actually very useful since, as demonstrated in the formulation Eq. (103), we can construct a boundary scheme by treating non-equilibrium parts as the unknown variables. Therefore, the above three conditions provide equations for our unknown variables.

We can immediately obtain three more equations for the non-equilibrium functions. Namely, in order to enforce the prescribed density and momentum density, we require that the zeroth and first moments of the non-equilibrium parts

are identically zero:

$$\begin{aligned}
\rho: &\quad f_{NE}^{neq} + f_{E}^{neq} + f_{SE}^{neq} + f_{N}^{neq} + f_{C}^{neq} + f_{S}^{neq} + f_{NW}^{neq} + f_{W}^{neq} + f_{SW}^{neq} = 0, \\
\rho_0 u_x: &\quad c_r \left(f_{NE}^{neq} + f_{E}^{neq} + f_{SE}^{neq} - f_{NW}^{neq} - f_{W}^{neq} - f_{SW}^{neq} \right) = 0, \\
\rho_0 u_y: &\quad c_r \left(f_{NE}^{neq} + f_{N}^{neq} + f_{NW}^{neq} - f_{SE}^{neq} - f_{S}^{neq} - f_{SW}^{neq} \right) = 0.
\end{aligned}$$

In summary, we have a total of six equations for the non-equilibrium functions. However, the number of independent equations is not six in general, but depends on the unknown variables we choose for our boundary scheme. For example, if we straightforwardly choose the non-equilibrium parts of the inbound velocities as our unknown variables, i.e. $f_{NE}^{neq}, f_{E}^{neq}$, and f_{SE}^{neq}, we recognise that the equations provided by $\rho, \rho_0 u_x$, and Π_{xx}^{neq} are linearly dependent and cannot be fulfilled simultaneously. Similarly, the equations provided by $\rho_0 u_y$ and Π_{xy}^{neq} are also linearly dependent. Although there actually are three linearly independent equations for the three unknowns in this example, we cannot obtain a solution which would simultaneously guarantee the prescribed values for ρ and $\rho_0 u_x$.

From the kinetic theory point of view, a consistent strategy for constructing boundary schemes first guarantees correct values for the low-order moments, here density and momentum density, and then attempts to enforce higher-order moments. We utilise this strategy with the observation that there are discrete velocity vectors pointing along the open boundary. Distribution functions associated with these velocities, some or all of them, are quite naturally treated as unknown variables. In our two-dimensional setting, the non-equilibrium distribution functions associated with the vectors pointing along the boundary are f_{N}^{neq}, f_{S}^{neq}, and f_{C}^{neq}, see Fig. 9. We choose the last one, f_{C}^{neq}, as our fourth unknown variable. To be more precise, the philosophy we propose is as follows: f_C is actually known after the streaming step. Thus, it can be used e.g. in the mass-flux-based approach for computing the local densities and flow velocities. However, after the hydrodynamic variables have been determined, and we decide to enforce them together with the viscous stresses, we choose to replace f_{C}^{neq} with the value presented in this boundary scheme.

Hence, the four unknown variables for the present boundary scheme are

$$f_C = f_{C}^{eq} + a, \quad f_{NE} = f_{NE}^{eq} + b, \quad f_E = f_{E}^{eq} + c, \quad f_{SE} = f_{SE}^{eq} + d. \tag{105}$$

Then, after some rearranging, the previously presented six conditions for the non-

equilibrium functions are

$$\rho: \quad a+b+c+d = -\left(f_{NW}^{neq}+f_{N}^{neq}+f_{S}^{neq}+f_{W}^{neq}+f_{SW}^{neq}\right), \tag{106}$$

$$\rho_0 u_x: \qquad b+c+d = \quad \left(f_{NW}^{neq}+f_{W}^{neq}+f_{SW}^{neq}\right), \tag{107}$$

$$\rho_0 u_y: \qquad b \quad -d = -\left(f_{NW}^{neq}+f_{N}^{neq}-f_{S}^{neq}-f_{SW}^{neq}\right), \tag{108}$$

$$\Pi_{xx}^{neq}: \qquad b+c+d = -\left(f_{NW}^{neq}+f_{W}^{neq}+f_{SW}^{neq}\right)+\frac{1}{c_r^2}\Pi_{xx}^{visc}, \tag{109}$$

$$\Pi_{xy}^{neq}: \qquad b \quad -d = \quad \left(f_{NW}^{neq}-f_{SW}^{neq}\right)+\frac{1}{c_r^2}\Pi_{xy}^{visc}, \tag{110}$$

$$\Pi_{yy}^{neq}: \qquad b \quad +d = -\left(f_{NW}^{neq}+f_{N}^{neq}+f_{S}^{neq}+f_{SW}^{neq}\right)+\frac{1}{c_r^2}\Pi_{yy}^{visc}. \tag{111}$$

Clearly, the equations above provided by $\rho_0 u_x$ and Π_{xx}^{neq}, as well as by $\rho_0 u_y$ and Π_{xy}^{neq}, are linearly dependent. In these kinds of cases, we resolve the conflict by always utilising the equation from the lowest order moment. Accordingly, we utilise here the four linearly independent equations provided by the moments $\rho, \rho_0 u_x, \rho_0 u_y$, and Π_{yy}^{neq} to determine expressions for the four unknown variables:

$$\begin{aligned}
a &= -\left(2f_{NW}^{neq}+f_{N}^{neq}+f_{S}^{neq}+2f_{W}^{neq}+2f_{SW}^{neq}\right),\\
b &= -\left(f_{NW}^{neq}+f_{N}^{neq}\right)+\frac{1}{2c_r^2}\Pi_{yy}^{visc},\\
c &= \quad \left(2f_{NW}^{neq}+f_{N}^{neq}+f_{S}^{neq}+f_{W}^{neq}+2f_{SW}^{neq}\right)-\frac{1}{c_r^2}\Pi_{yy}^{visc},\\
d &= -\left(f_{S}^{neq}+f_{SW}^{neq}\right)+\frac{1}{2c_r^2}\Pi_{yy}^{visc}.
\end{aligned}$$

Notice that in our simple inlet flow configuration, the component S_{yy} of the strain rate tensor is identically zero implying $\Pi_{yy}^{visc}=0$. Hence, we do not need to use e.g. finite-difference schemes for the approximation of $\partial_y u_y$.

4.3.4 A further improvement: enforcing 1+2+2 moments

By comparing Eq. (108) provided by $\rho_0 u_y$ and Eq. (110) provided by Π_{xy}^{neq}, we observe that these equations become linearly independent if even one the two remaining non-equilibrium distribution functions propagating along the inlet boundary, f_N^{neq} or f_S^{neq}, is treated as an unknown variable – in the sense explained in the previous section. Here we choose to treat f_N^{neq} as an additional unknown. Then we have a total of five unknown variables,

$$f_C = f_C^{eq}+a,\ f_{NE}=f_{NE}^{eq}+b,\ f_E=f_E^{eq}+c,\ f_{SE}=f_{SE}^{eq}+d,\ f_N=f_N^{eq}+e, \tag{112}$$

for which we have five linearly independent equations:

$$\begin{aligned}
\rho: \quad & a+b+c+d+e = -\left(f_{NW}^{neq}+f_{S}^{neq}+f_{W}^{neq}+f_{SW}^{neq}\right),\\
\rho_0 u_x: \quad & b+c+d \quad = \quad \left(f_{NW}^{neq}+f_{W}^{neq}+f_{SW}^{neq}\right),\\
\rho_0 u_y: \quad & b \quad -d+e = -\left(f_{NW}^{neq}-f_{S}^{neq}-f_{SW}^{neq}\right),\\
\Pi_{xy}^{neq}: \quad & b \quad -d \quad = \quad \left(f_{NW}^{neq}-f_{SW}^{neq}\right)+\frac{1}{c_r^2}\Pi_{xy}^{visc},\\
\Pi_{yy}^{neq}: \quad & b \quad +d+e = -\left(f_{NW}^{neq}+f_{S}^{neq}+f_{SW}^{neq}\right)+\frac{1}{c_r^2}\Pi_{yy}^{visc}.
\end{aligned}$$

The solution to this linear system of equations is given by

$$\begin{aligned}
a &= -\left(2f_{S}^{neq}+2f_{W}^{neq}+4f_{SW}^{neq}\right)+\frac{1}{c_r^2}\Pi_{xy}^{visc},\\
b &= \left(f_{NW}^{neq}-f_{S}^{neq}-2f_{SW}^{neq}\right)+\frac{1}{c_r^2}\Pi_{xy}^{visc}+\frac{1}{2c_r^2}\Pi_{yy}^{visc},\\
c &= \left(2f_{S}^{neq}+f_{W}^{neq}+4f_{SW}^{neq}\right)-\frac{1}{c_r^2}\Pi_{xy}^{visc}-\frac{1}{c_r^2}\Pi_{yy}^{visc},\\
d &= -\left(f_{S}^{neq}+f_{SW}^{neq}\right)+\frac{1}{2c_r^2}\Pi_{yy}^{visc},\\
e &= -\left(2f_{NW}^{neq}-f_{S}^{neq}-2f_{SW}^{neq}\right)-\frac{1}{c_r^2}\Pi_{xy}^{visc}.
\end{aligned}$$

The off-diagonal component Π_{xy}^{visc} involves partial derivatives $\partial_x u_y$ and $\partial_y u_x$. It is relatively easy to approximate the latter: finite-difference schemes along the inlet boundary are not difficult to implement. For example, second-order accurate (biased) central-difference schemes presented in Appendix 3 can be applied. That is, $\partial_y u_x$ can be conveniently measured and then utilised. The partial derivative $\partial_x u_y$ can also be measured, but now forward finite-differences must be used. Alternatively, we could impose an additional hydrodynamic boundary condition by requiring that $\partial_x u_y \equiv 0$ at the inlet.

4.3.5 Enforcing hydrodynamic moments up to second order

For the boundary scheme presented here, we assume that there is information available about the complete viscous stress tensor at the open boundary – here the tensor has three independent components. The information is either measured, approximated e.g. with finite-differences, or it is provided by additional boundary conditions, for example $\partial_x u_x \equiv 0$. We start off just like in the previous section. By comparing Eq. (107) provided by $\rho_0 u_x$ and Eq. (109) provided by Π_{xx}^{neq}, we observe that these equations become linearly independent if any of the

non-equilibrium distribution functions associated with the three outbound velocity vectors, $f_{NW}^{neq}, f_{W}^{neq}$, or f_{SW}^{neq}, is treated as an unknown variable – the meaning of this treatment has already been explained. Here we choose to treat f_{W}^{neq} as the sixth unknown variable:

$$\begin{aligned} f_C &= f_C^{eq} + a, \quad f_{NE} = f_{NE}^{eq} + b, \quad f_E = f_E^{eq} + c, \\ f_{SE} &= f_{SE}^{eq} + d, \quad f_N = f_N^{eq} + e, \quad f_W = f_W^{eq} + g. \end{aligned} \tag{113}$$

For this set of unknown variables we have six linearly independent equations:

$$\begin{aligned}
\rho: &\quad a+b+c+d+e+g = -\left(f_{NW}^{neq} + f_{S}^{neq} + f_{SW}^{neq}\right), \\
\rho_0 u_x: &\quad b+c+d \quad -g = \left(f_{NW}^{neq} + f_{SW}^{neq}\right), \\
\rho_0 u_y: &\quad b \quad -d+e \quad = -\left(f_{NW}^{neq} - f_{S}^{neq} - f_{SW}^{neq}\right), \\
\Pi_{xx}^{neq}: &\quad b+c+d \quad +g = -\left(f_{NW}^{neq} + f_{SW}^{neq}\right) + \frac{1}{c_r^2}\Pi_{xx}^{visc}, \\
\Pi_{xy}^{neq}: &\quad b \quad -d \quad = \left(f_{NW}^{neq} - f_{SW}^{neq}\right) + \frac{1}{c_r^2}\Pi_{xy}^{visc}, \\
\Pi_{yy}^{neq}: &\quad b \quad +d+e \quad = -\left(f_{NW}^{neq} + f_{S}^{neq} + f_{SW}^{neq}\right) + \frac{1}{c_r^2}\Pi_{yy}^{visc}.
\end{aligned}$$

The solution to this linear system of equations is given by

$$\begin{aligned}
a &= \left(2f_{NW}^{neq} - 2f_{S}^{neq} - 2f_{SW}^{neq}\right) - \frac{1}{c_r^2}\Pi_{xx}^{visc} + \frac{1}{c_r^2}\Pi_{xy}^{visc}, \\
b &= \left(f_{NW}^{neq} - f_{S}^{neq} - 2f_{SW}^{neq}\right) + \frac{1}{c_r^2}\Pi_{xy}^{visc} + \frac{1}{2c_r^2}\Pi_{yy}^{visc}, \\
c &= -\left(f_{NW}^{neq} - 2f_{S}^{neq} - 3f_{SW}^{neq}\right) + \frac{1}{2c_r^2}\Pi_{xx}^{visc} - \frac{1}{c_r^2}\Pi_{xy}^{visc} - \frac{1}{c_r^2}\Pi_{yy}^{visc}, \\
d &= -\left(f_{S}^{neq} + f_{SW}^{neq}\right) + \frac{1}{2c_r^2}\Pi_{yy}^{visc}, \\
e &= -\left(2f_{NW}^{neq} - f_{S}^{neq} - 2f_{SW}^{neq}\right) - \frac{1}{c_r^2}\Pi_{xy}^{visc}, \\
g &= -\left(f_{NW}^{neq} + f_{SW}^{neq}\right) + \frac{1}{2c_r^2}\Pi_{xx}^{visc}.
\end{aligned}$$

This concludes our treatment of boundary schemes. With the same approach as adopted here, we present boundary schemes for the D3Q19 model in Appendix 2. In summary, the above presented scheme is almost equivalent to the one presented by *Halliday et al.* [Hal02]. The schemes differ in their sets of unknown variables. With their parlance and our two-dimensional setting, Halliday et al. consider $f_{C}^{neq}, f_{SW}^{neq}$, and f_{W}^{neq} as the so-called free variables in their scheme;

the corresponding variables in our scheme are f_S^{neq}, f_{SW}^{neq}, and f_{NW}^{neq} – there are many other viable choices for the free variables. Whether this difference in the set of unknown variables has some consequences on hydrodynamic fluid flow simulations, is a matter which we leave open here. Computationally the two schemes are equally demanding. They involve similar expressions for the unknown variables; the hydrodynamic information for the expressions may require approximation of the partial derivatives of the local flow velocities with e.g. finite differences. Also, the two schemes both utilise information propagating from the interior of the flow domain to the same extent. Finally, the boundary schemes presented here and in Ref. [Hal02] are both asymmetric to some degree: with this remark we refer to the fact that, for example, in our scheme the non-equilibrium function f_N^{neq} is considered as one of the unknown variables but the function f_S^{neq} is not. This arbitrary choice discriminates the two opposite directions, and hence introduces a kind of asymmetry to the scheme. However, some degree of asymmetry is unavoidable in the selected approach.

5 IMPLEMENTATION TECHNIQUES

Generally speaking, the discussion presented thus far has covered mathematical modelling of physical phenomena, as well as discretisation of the resulting models. Discretisation aims at computational schemes which can be implemented and ultimately executed on computers. For example, the discretisation procedure replaces such mathematical operators as integrals and derivatives with approximations that involve only elementary operations, i.e. summation, multiplication, and division – computers compute with elementary operations. The approximation of mathematical operators is inherently related to the essential step in the discretisation procedure: continuous variables are replaced by the corresponding discrete variables defined e.g. at the nodes of the lattice. An approximative solution for the original mathematical model is then pursued by solving the associated discrete problem with a computational scheme constructed for the purpose.

Nevertheless, from the programming point of view, the mathematical description of a computational scheme is still quite abstract, and leaves many issues undetermined. With the implementation of a computational scheme we refer to the treatment of the remaining issues as well as to the concrete programming. The final outcome of the implementation is a source code, written with a programming language, which is then compiled into a computational software. Finally, computer simulation of a physical phenomenon concretely means that we command execution of the program on a computer: a suitable set of parameters is introduced for controlling the simulation configuration. Here we consider aspects related to the implementation of the lattice Boltzmann schemes. By doing so, we enter the territory of computer science and of high-performance computing (HPC) in particular.

The objective in HPC is to economically utilise the always limited computing resources; HPC focuses on the efficient execution of computational schemes on modern computers. Several arguments can be given for why HPC has emerged as a distinctive discipline:

- The developed solutions provide an immediate practical gain: limited computing resources are utilised to their full extent.

- There is an intellectual charm in developing the fastest, or most frugal, computer implementation of a computational scheme – the most elegant solutions inspire people.
- Often the solutions are like operational principles, and the principles may find applications in unexpected domains – not only in the domain where they were initially presented.
- In order to reach high effiency with an implementation, it is often necessary to have understanding of computer hardware. Thus, HPC promotes the knowledge of contemporary hardware among the people implementing computational software.

Indeed, the understanding of computer hardware is often essential when tackling challenges in HPC. For example, today most of the modern computers involve a memory interface which transmits data between the main memory and the central processing unit (CPU) of the computer. The technical development of computer hardware has led to a situation where the memory interface struggles with an enormous data traffic. Nowadays it is even typical that the efficiency of an implementation is limited by the capability of the interface: the interface constitutes the so-called *von Neumann bottleneck*, coined by *John Backus* in his ACM Turing Award Lecture [Bac78]. In order to relieve some of the burden from the interface, auxiliary hardware components have been introduced. Most notably a hierarchy of cache memories have been mounted between the main memory and CPU: typically the hierarchy includes L1, L2, and even L3 cache memories. The property of the hierarchy is that the cache memories grow in size from L1 to L3. The counterbalance is that the time it takes to transfer data between CPU and the cache memories gets longer from L1 to L3. Actually, the data transferred between CPU and L3 usually travels via L1 and L2. Nonetheless, even the L3 cache memory is much smaller in size than the main memory, and also significantly faster with regard to the data transfer speed. Therefore, a common problem in the field of HPC is to find a way to maximally exploit the small but fast cache memories in an implementation of a given computational scheme. Basic cache utilisation techniques are reviewed e.g. in Ref. [Kow03].

There are at least three apparent ways to relieve some of the burden from the memory interface, and to promote efficient utilisation of the cache memory hierarchy:

1. An implementation of a computational scheme should use data per unit task as little as possible. This will directly reduce the data traffic between the main memory and CPU.
2. Surplus data traffic must be avoided. For example, when data are retrieved from the main memory, they are typically transferred in blocks or lines, e.g. a block includes not one but many floating-point numbers. It is desirable that all the data in a block will participate in the computations. That is, there should be a minimal amount of data which pointlessly stow away in the blocks.

3. Once data are retrieved from the main memory to CPU, or actually to one of the cache memories, they should be exploited as many times as possible. Otherwise the data must be retrieved from the main memory separately for every occasion where they are needed – retrieving data from the cache memory is much faster.

Here, and in Refs [PI, PII], we consider implementation techniques which were motivated by the above three, rather general principles. Implementation techniques for the lattice Boltzmann schemes, directly concerning efficient utilisation of the cache memory hierarchy, have also been treated e.g. in Refs [Poh03, Vel04, Wel06, Zei08]. In addition, the brute-force strategy of high-performance computing relies on parallel computing. Various parallel computing aspects related to LBM have been treated e.g. in Refs [Pun94, Kan98, Dup00, Bel02, Sch02, Mas02, Pan04, Wan05, Axn08, Zei08, Vid10]. The so-called grid-refinement techniques, on the other hand, utilise non-uniform grids in an attempt to intelligently allocate computing resources to the spatial regions of the computational domain where large gradients are expected to arise: for example, a fine grid spacing is pursued in the vicinity of fluid-solid interfaces whereas a coarser spacing serves the purpose in the regions far away from the interfaces – the battle is between accuracy and limited computing resources. Grid-refinement techniques for LBM have been consider for example in Refs [Fil98, Töl98, Fil00, Kan00, Lin00, Suc01b, Yu02, Cro03, Dup03, Rei05, Che06b, Gel06b, Roh06, Töl06]. Also, several techniques for accelerating steady-state fluid flow simulations with the lattice Boltzmann method have been proposed [Töl98, Kan99b, Ver99, Ber01, Kan01, Ber02, Töl02, Ber03, Lee03, Guo04, Ima05, Mav06, Liu08, Pre09].

5.1 Algorithms

From the programming point of view, as already stated, many issues not addressed by the mathematical description of a computational scheme must be determined at the implementation stage. An algorithm provides a bridge between the description of a computational scheme and its realisation on a computer. That is, an algorithm is an intermediate abstraction concept: it collects all the essential steps of the scheme, while avoiding unnecessary details, into a procedure mechanical enough for computers. Essentially, an algorithm is a step towards the programming language manifestation of the scheme. One of the main issues addressed by the algorithms for the lattice Boltzmann schemes, and schemes in general, is the data dependence. This issue is particularly common in schemes that involve time evolution of the dynamic variables, here the distribution functions.

Consider for example the LBE Eq. (40): it explicitly states that the distribution function $f_i(\mathbf{r} + \Delta t\mathbf{c}_i, t + \Delta t)$ depends on the distribution function $f_i(\mathbf{r}, t)$ together with the collision term $\Omega_i(\mathbf{r}, t)$. Similarly, the distribution function $f_i(\mathbf{r}, t + \Delta t)$ depends on $f_i(\mathbf{r} - \Delta t\mathbf{c}_i, t)$, and so forth. When the scheme is executed on a computer, the distribution functions must be concretely stored in the main mem-

ory. Let us assume that in the implementation stage we allocate two virtual memory locations for the distribution functions $f_i(\mathbf{r} + \Delta t\mathbf{c}_i, t)$ and $f_i(\mathbf{r}, t)$. During the time evolution, the distribution value stored at the location for $f_i(\mathbf{r}, t)$ must be replaced with the value of $f_i(\mathbf{r}, t + \Delta t)$ computed according to LBE – basically the value $f_i(\mathbf{r}, t)$ is overwritten. Hence, the data needed for the update of $f_i(\mathbf{r} + \Delta t\mathbf{c}_i, t)$ are lost, i.e. the value $f_i(\mathbf{r} + \Delta t\mathbf{c}_i, t + \Delta t)$ cannot be computed anymore.

It turns out that the simple data dependence introduced by LBE can be handled in many ways. In fact, the data dependence in LBE Eq. (40) is *the simplest of all dependences* – excluding of course the case of no dependence at all! Namely, the distribution functions are dependent along the characteristics only and, moreover, the dependence is on the upwind-direction to the nearest neighbour – it is a one-to-one dependence. This favourable state of affairs is compromised in such specific lattice Boltzmann schemes where only the hydrodynamic moments are stored into the main memory instead of the actual distribution functions. Such schemes, together with appropriate implementation techniques for the treatment of the more compex data dependences, are presented e.g. in Refs [Mar02, Arg04]. There are at least five algorithms for handling the simple data dependence: the two-lattice, two-step, shift (or compressed grid) [Poh03], swap [PI], and lagrangian [Mas02] algorithms all operate in a distinct way. The operational principles of the two-lattice and shift algorithms are illustrated in Fig. 10. In a similar way, the essence of the two-step as well as the swap algorithm is presented in Fig. 11. For simplicity, the figures present a purely synthetic setting composed of a one-dimensional lattice and a lattice Boltzmann scheme with two discrete velocities pointing to the left and right.

Essentially, just like the two-lattice and shift algorithms, the swap algorithm allows execution of both the streaming and collision steps for a single node at a time. In practice, this is computationally more efficient than iterating the lattice at least twice, as is done in the two-step algorithm. In addition, the swap and shift algorithms enable the fused streaming and collision step without the second lattice – the single lattice must however be extended in the shift algorithm. The usage of only a single lattice directly reduces the memory consumption and, hence, also the memory traffic by striving for minimal amount of data per unit task. Moreover, due to the relocation of the distribution values by the swapping operation, the memory access pattern in the swap algorithm has potential for reducing surplus memory traffic and, therefore, it may promote efficient utilisation of the cache memory hierarchy.

5.2 Data layouts

The data dependence is just one of the many technical points which must be addressed in the implementation of a lattice Boltzmann scheme. For example, it is possible to implement the schemes by first executing the streaming step which

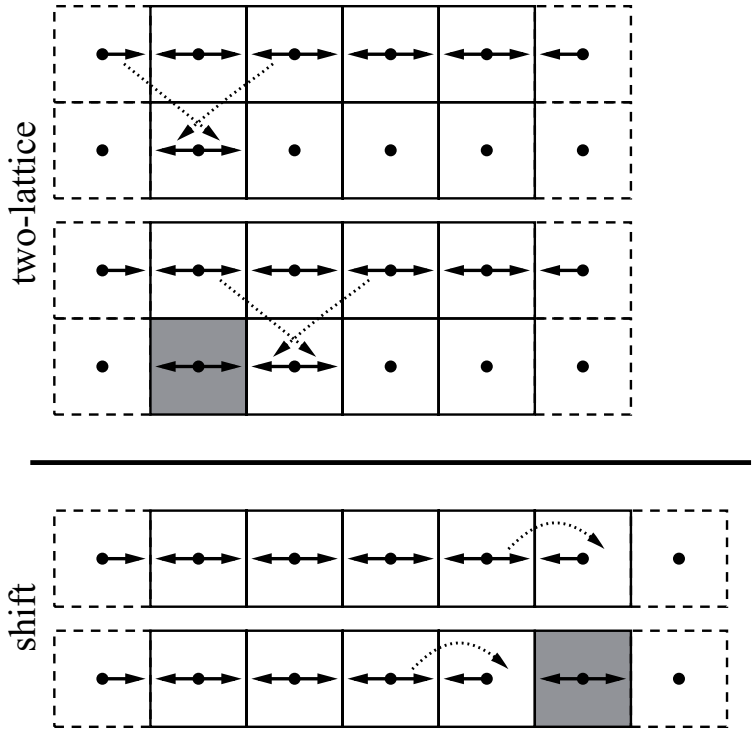

FIGURE 10 Operational principles of the two-lattice and shift algorithms presented in a one-dimensional setting with the D1Q2 model. The 1D cells of the lattice are represented with squares only for graphical reasons. The extreme cells of the 1D lattice, represented with the dashed squares, are so-called ghost or halo or buffer cells facilitating implementation of the streaming step together with e.g. periodic boundary conditions. The solid arrows represent the distribution functions associated with the two discrete velocities pointing to the left and right. The dashed arrows illustrate how the values of the distribution functions are shuffled in the virtual memory during a streaming step. The grey cells indicate that both the streaming and collision steps have already been executed at the corresponding lattice node. In the two-lattice algorithm, the distribution functions are retrieved from a given lattice, and stored into the other one. The roles of the two lattices are exchanged between the time steps. The shift algorithm operates with a single lattice which, however, is appropriately extended – here one extra cell for the 1D lattice is enough. The extension is carefully utilised: again, the values of the distribution functions are retrieved and stored into different virtual memory locations. During a given time step in the shift algorithm, the lattice nodes are iterated from the last node to the first, as above, and during the next time step, the iteration proceeds in the opposite direction.

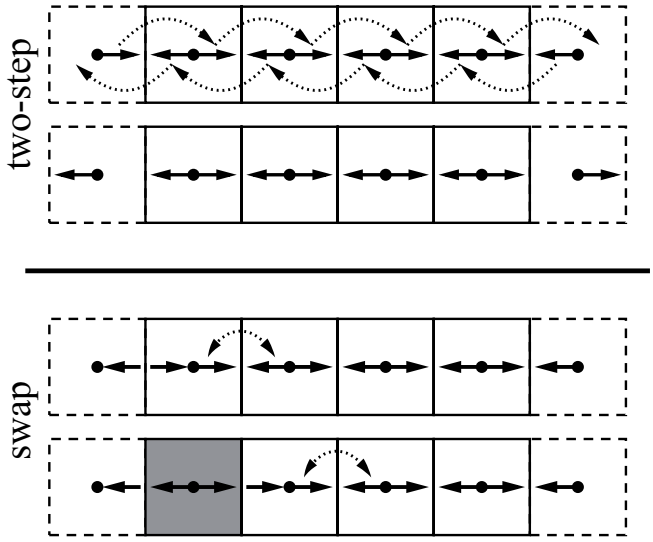

FIGURE 11 Operational principles of the two-step and swap algorithms presented in a one-dimensional setting with the D1Q2 model. The caption of Fig. 10 explains the imagery. In the two-step algorithm, all the distribution values are first carefully propagated along the characteristics, i.e. the streaming step is first executed for the whole lattice. Thereafter, the whole lattice is iterated again in order to execute the collision step. The swap algorithm, on the other hand, operates in a manner which allows execution of both the streaming and collision step for a single node at a time. Namely, while the lattice nodes are traversed, some of the distribution values are explicitly exchanged or swapped between the neighbours – the data dependence between neighbouring nodes is consequently broken. Note that in the swap algorithm, the lattice iteration must be initialised: here the initialisation has exchanged the distribution values between the ghost node and the first node of the lattice.

is then followed by the collision step, or the order of execution can be reversed. These two approaches are referred to as the 'pull' and 'push' update procedures, respectively [Wel06]. Furthermore, let us consider iteration of the lattice nodes during the update of the distribution functions: it is necessary to determine in which order the nodes are iterated. An order can be defined by enumerating the nodes; the enumeration numbers can either be computed on the fly, e.g. from the integer coordinates of a node, (i, j, k) in the three-dimensional setting, or they can be predetermined by a given procedure and the numbers are actually stored into the main memory. A natural numbering for the nodes of a two-dimensional lattice is presented in Fig. 12(a): the numbering advances first in the x-direction.

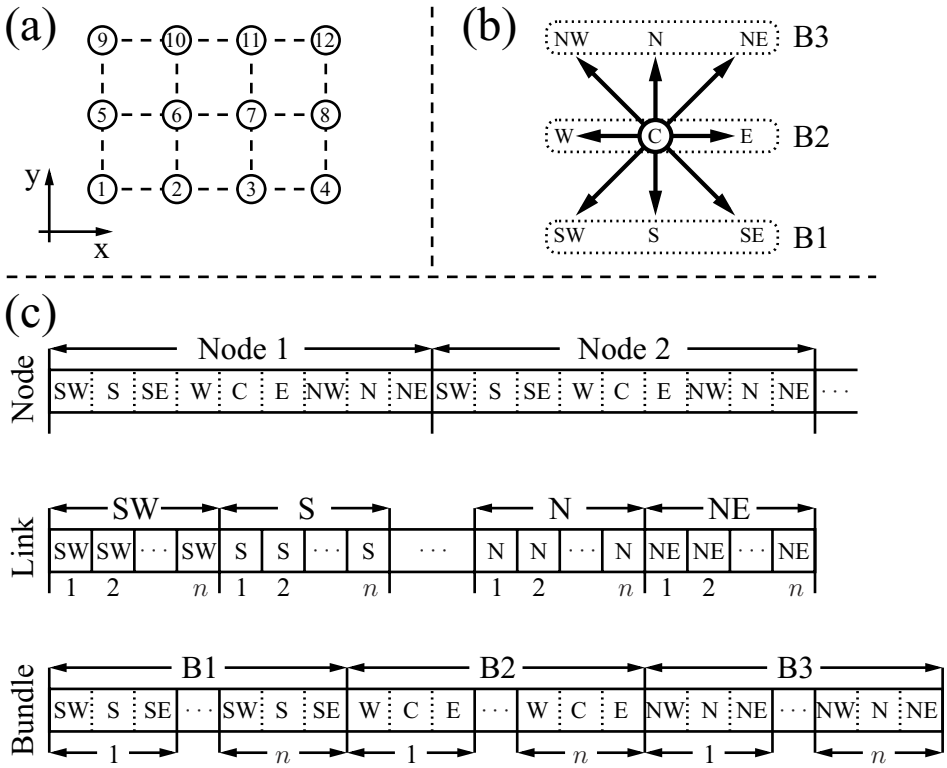

FIGURE 12 An illustration of data layouts and related concepts. In part (a), an enumeration for the nodes of a two-dimensional lattice is defined with natural numbering. Part (b) presents a definition of the so-called distribution function bundles, here B1,B2, and B3; the logic behind the definitions is explained in the text. Finally, three alternative data layouts for storing the values of the distribution functions into a single one-dimensional array are presented in part (c). These three data layouts store the distribution values node-wise, link-wise, and bundle-wise.

It is also necessary to resolve the manner in which the distribution functions are stored into the memory. One choice is to store all the distribution functions into a long, one-dimensional array. However, this choice does not completely determine the issue: it is still necessary to specify how exactly the distribution functions are stored in the 1D array – the specification is referred to as the data layout. There are two almost opposite alternatives: in the so-called collision optimised data layout, all the distribution functions of a single node are assembled and stored consecutively into the 1D array, whereas in the propagation optimised layout, all the distribution functions associated to a discrete velocity vector are assembled from the whole lattice and stored consecutively into the array [Wel06].

That is, in the collision and propagation data layouts, the distribution functions are stored node-wise and link-wise, respectively. This is illustrated in Fig. 12(c). A particular compromise between the two alternatives was proposed in Ref. [PII]: in the so-called bundle data layout, the distribution functions are grouped into small bundles which are then assembled from the whole lattice and stored consecutively into the 1D array. The small bundles are defined in Fig. 12(b) for the D2Q9 model; Fig. 12(c) illustrates how these bundles are assembled and stored.

The logic of defining the small bundles is actually quite simple, and moreover intimately related to the order in which the lattice nodes are iterated during the update procedure. Specifically, let us consider the two-dimensional lattice presented in Fig. 12(a) together with the natural numbering of lattice nodes – the numbering defines the order of iteration for the nodes. In addition, let us assume that, during the update procedure, the iteration has advanced to node 6. The update of f_{NW} at node 6 requires the value of f_{NW} at node 3. Once all the distribution functions of node 6 are updated, the iteration proceeds to node 7, where the update of f_N requires the value of f_N at node 3. Similarly, the update of f_{NE} at node 8 requires the value of f_{NE} at node 3. In other words, the values of the distribution functions f_{NW}, f_N, and f_{NE} at node 3 are required for the update of nodes 6,7, and 8, respectively. Hence, in order to reduce redundant memory traffic and also to promote efficient utilisation of the cache memory hierarchy, it is sensible to fetch the values of the three distribution functions all at once. This is the logic behind the definition of bundle B3, presented in Fig. 12(b) – the bundles B1 and B2 are defined with a similar logic.

5.3 Arithmetic precision

The swap algorithm and the bundle data layout both try to reduce the unnecessary memory traffic in a very detailed manner. According to the current trends in computing hardware, a detailed control of the memory traffic is likely to be even more important than before – not less. Such a conclusion is at least tempting from the publications concerning implementations of LBM on graphics processing units (GPU), see Refs [Zha08, Töl08, Ber09, Kau09, Rie09, Ber10, Kuz10, Töl10]. Related to the implementation of LBM on GPU, there is an issue which deserves some consideration. Namely, the implementation of a lattice Boltzmann scheme with single-precision floating-point arithmetic, instead of double-precision, results in significant memory savings and, therefore, reduces memory traffic and promotes efficient utilisation of the cache memories; today, single-precision floating-point arithmetic is the default in GPU rather than double-precision.

However, a straightforward single-precision implementation of LBM is vulnerable to numerical roundoff during the arithmetic operations. The reason for the potential roundoff problems lies in the discrete equilibrium function f_i^{eq}. That is, consider Eq. (42): since θ has been indentified as the speed of sound squared, c_s^2, the terms inside the parentheses are evidently of the order of $\mathcal{O}(1), \mathcal{O}(M_a)$,

and $\mathcal{O}(M_a^2)$. In order to simulate such fluid flows with LBM which obey the incompressible Navier-Stokes equation, the Mach number M_a must be small. On the other hand, in the simulation configurations where M_a gets smaller and smaller, the terms in f_i^{eq} become more and more disparate in size. Unfortunately, the basic arithmetic operations on computers, particularly summation, are prone to numerical roundoffs whenever the two operands are of very different size.

A particular remedy for the problem was proposed in Ref. [Sko93] (see also Ref. [Del03]). Basically, simulations are carried out with distribution functions redefined by a simple algebraic transformation:

$$g_i := f_i - w_i\rho_0, \quad g_i^{eq} := f_i^{eq} - w_i\rho_0 = w_i\left(\delta\rho + \rho\left[\frac{c_{i\alpha}u_\alpha}{\theta} + \frac{c_{i\alpha}u_\alpha c_{i\beta}u_\beta}{2\theta^2} - \frac{u_\alpha u_\alpha}{2\theta}\right]\right),$$

where ρ_0 is the reference or average density; the fluctuating part of the density $\delta\rho = \rho - \rho_0$ is of the order of $\mathcal{O}(M_a^2)$, as already discussed in Sec. 3.5.3. Hence, the terms in the redefined equilibrium function g_i^{eq} are of the order of $\mathcal{O}(M_a)$ and $\mathcal{O}(M_a^2)$, which is an improvement to the original state of affairs from the computer arithmetic point of view. Note that the first moments of the redefined distribution functions are

$$\sum_i g_i = \sum_i g_i^{eq} = \delta\rho, \quad \sum_i c_{i\alpha}\, g_i = \sum_i c_{i\alpha} g_i^{eq} = \rho u_\alpha,$$
$$\sum_i c_{i\alpha}c_{i\beta}\, g_i = \Pi_{\alpha\beta} - \rho_0\theta\delta_{\alpha\beta}, \quad \sum_i c_{i\alpha}c_{i\beta}\, g_i^{eq} = \delta\rho\theta\delta_{\alpha\beta} + \rho u_\alpha u_\beta.$$

The incompressible lattice Boltzmann scheme, together with the modified equilibrium function Eq. (97), can be redefined in a similar manner.

This concludes our treatment of the implementation techniques for lattice Boltzmann schemes. A concrete implementation example for the collision step of the D3Q19 model is given in Appendix 4. In the example, written in C/C++ -style, the collision operator is modelled with the standard single-relaxation-time BGK model.

6 CONCLUSION

With the string of chapters presented here, we have advanced from the very abstract to the most concrete. Along the way, the chapters covered special topics such as mathematical modelling in fluid dynamics, computational methods, boundary conditions, and implementation of computational schemes. A large portion of the presented discussion was devoted to the physical background of the lattice Boltzmann method. The physical exposition was intended especially for computer scientists as the associated discussion involved well-established concepts in physics. Although the lattice Boltzmann method, a mesoscopic method for the computer simulation of fluid flow phenomena, has attracted scientists and engineers in many fields, it has occasionally been referred to as the 'method of physicist'. Be that as it may, this playful statement embodies a true tone reflecting the physical origins of the method.

It is a well-worn claim in the literature that the lattice Boltzmann method is increasingly recognised among the scientific community at large due to its favourable properties: simplicity in coding, amenable for parallel computing, simple boundary conditions facilitating simulations in even arbitrarily complex domains, and so forth. While many of the above properties are individually appealing, they are really not that exceptional and often even compromise other desirable properties, for example accuracy. The true merit of the method is that it harmoniously combines many computationally exploitable features enabling simulations of many difficult flow problems on the whole. The same pattern repeats when the lattice Boltzmann method is investigated from a scientific computing point of view. The standard version of the method is derived by discretising the Boltzmann equation in several consecutive steps, many of which involve rather rudimentary techniques such as first-order upwind finite-difference schemes. Nevertheless, the combined effect of all the discretisation steps together is that the resulting computational scheme is formally second-order accurate both in space and time. Moreover, the discretisation of the velocity space is perhaps a distinctive step in the derivation of the method but, from the numerical analysis point of view, it lacks certain charm due to the indirect manner in which the discretisation is usually carried out. Namely, a set of discrete velocities is

constructed by matching the moments with the continuous model up to a given order. A direct discretisation of the velocity space, for example with some conceivable basis functions, is a strategy not yet considered in the lattice Boltzmann method literature – at least to our knowledge.

Hence, we argue, the profound appeal of the lattice Boltzmann method indeed stems from the physics considerations. The method is based on a mesoscopic description of fluid dynamics, and on the kinetic theory of gases in particular. From the modern perspective, kinetic theory of gases is the *tour de force* of statistical mechanics. It provides an original description for the dynamic behaviour of fluid flows and, at the same time, it establishes physically relevant connections between the alternative descriptions operating at the microscopic and macroscopic scales. These inherent connections truly separate kinetic theory of gases from many other modelling approaches. Moreover, the connections are eventually carried over into the lattice Boltzmann method, where they constitute its true asset. In other words, the natural connections to the microscopic and macroscopic worlds enable relatively effortless extensions of lattice Boltzmann schemes. These extensions usually have physically transparent origins and may incorporate, e.g., additional interaction mechanisms that allow simulation of complex phenomena like multiphase flows.

Here, in this thesis, we have recapitulated some of our recent, already published efforts related to LBM. Specifically, we have presented the mass-flux-based approach to open boundary conditions in Sec. 4.2 as well as the swap algorithm for the implementation of lattice Boltzmann schemes in Sec. 5.1. The bundle data layout was presented in Sec. 5.2: it is a detailed description for the manner in which the distribution functions are stored into the main memory of the computer. The mass-flux-based approach is based on a global condition imposed, e.g., at the inlet of a computational domain. A fixed average velocity at the inlet is an example of a global condition. Arguably, the application of a global condition is a somewhat unconventional strategy in computational fluid dynamics. Moreover, the mass-flux-based approach operates in a way which introduces a kind of feedback mechanism to the flow system. This aspect suggests that the approach is perhaps best suited for steady-state fluid flow simulations.

The most restricting assumption in the presented approach is the flow perpendicular to the boundary, i.e. there are no pressure gradients along the boundary which in turn implies, together with the equation of state of an ideal gas, a constant density along the boundary. In the current presentation, this fact is explicitly utilised in the derivation of expressions for the unknown, local hydrodynamic variables. In the future, it would be interesting to investigate whether the mass-flux-based approach could be extended to configurations where the inflow is, for example, unidirectional at the boundary, instead of perpendicular to the boundary. This would facilitate simulations of fluid flows in, e.g., inclined channels and pipes. Furthermore, no explicit boundary conditions for the local hydrodynamic variables have been presented which would conform to the mass-flux-based approach specified with, e.g., a prescribed average velocity at the inlet. Such formulations could be a topic for future work.

The two other contributions, the swap algorithm and the bundle data layout, both belong conceptually to the territory of high-performance computing. In essence, they try to reduce the unnecessary memory traffic between CPU and the main memory of the computer in a very detailed manner. Particularly, they aim at efficient utilisation of the small but fast cache memories in the implementations of lattice Boltzmann schemes. According to the current trends in computing hardware, a detailed control of the memory traffic is likely to be even more important than before. Such a conclusion is indicated by the recent publications concerning implementations of LBM on graphics processing units (GPU). It would be a relevent study to investigate how the swap algorithm and the bundle data layout affect computational efficiency of the implementations on new, emerging computer architectures like the promising general purpose graphics processing units (GP-GPU). In addition, efficient implementation of lattice Boltzmann schemes with a relatively large number of discrete velocities is an interesting topic for future work – even schemes such as D3Q125 have been proposed. Due to their inherent properties, the swap algorithm and the bundle data layout are promising candidates for such implementations.

In addition to the above discussed contributions, we have here introduced particular implementations of hydrodynamic LBM boundary conditions. These implementations, not previously published, enforce a given number of prescribed moments at straight boundaries. The most elaborate implementations presented enforce hydrodynamic moments up to second order (six and ten moments in two and three dimensions, respectively). Specifically, in Sec. 4.3 we present boundary condition implementations for the D2Q9 model, and in Appendix 2 for the D3Q19 model. As is evident from these presentations, and from the summary at the end of Sec. 4.3, these implementations are not unique: there is plenty of freedom in the implementation of hydrodynamic boundary conditions. That is, with the approach adopted here, a number of distinct implementations can be derived which all enforce the same prescribed moments. It remains to be investigated whether these distinct implementations differ in their numerical properties. Numerical validations for the presented implementations were not given here; validations are left as a work for the future.

APPENDIX 1 THE FIRST-ORDER MOMENTUM TRANSFER TENSOR

In the context of a multiple-scale analysis (Sec. 3.4.1), where hydrodynamic equations conforming to a lattice Boltzmann scheme are sought for, a second-rank tensor is encountered. This tensor is apparently related to viscous momentum transfer in the momentum conservation equation, see for example Eq. (91). Here we derive, in detail, an expression for the above mentioned tensor, i.e.

$$\Pi^{(1)}_{\alpha\beta} := \sum_i c_{i\alpha} c_{i\beta} f_i^{(1)}.$$

The derivation is based on the repeated usage of Eqs (80) and (81). Also, an operation from tensor calculus is frequently applied: the Kronecker delta symbol $\delta_{\alpha\beta}$ changes indices, e.g. $\delta_{\alpha\beta}\,\partial_\beta \equiv \partial_\alpha$. Since all the partial derivatives involved are of the first order in magnitude with respect to the small expansion parameter ϵ, we omit the superscripts (1) carrying this information – the superscripts are reintroduced in the final expression. With the underbraces we denote the equation which will be used when the associated term is substituted. We start from the moment equation Eq. (82), and immediately apply Eq. (83) as well as Eq. (84):

$$\begin{aligned}
-\frac{\omega\epsilon}{\Delta t}\Pi^{(1)}_{\alpha\beta} &= \partial_t \Pi^{(0)}_{\alpha\beta} + \partial_\gamma S^{(0)}_{\alpha\beta\gamma} \\
&= \partial_t\left(\theta\rho\delta_{\alpha\beta} + \rho u_\alpha u_\beta\right) + \partial_\gamma \theta\rho\left(u_\alpha\delta_{\beta\gamma} + u_\beta\delta_{\alpha\gamma} + u_\gamma\delta_{\alpha\beta}\right) \\
&= u_\beta \underbrace{\partial_t \rho u_\alpha}_{(81)} + \rho u_\alpha \partial_t u_\beta + \theta\partial_\beta \rho u_\alpha + \theta\partial_\alpha \rho u_\beta + \delta_{\alpha\beta}\theta\big(\underbrace{\partial_t\rho}_{(80)} + \partial_\gamma \rho u_\gamma\big) \\
&= -u_\beta \partial_\gamma \Pi^{(0)}_{\alpha\gamma} + \rho u_\alpha \partial_t u_\beta + \theta\partial_\beta \rho u_\alpha + \theta\partial_\alpha \rho u_\beta \\
&\quad -\frac{\omega\epsilon}{\Delta t}\left(\delta_{\alpha\beta}\theta\rho^{(1)} + u_\beta\, j^{(1)}_\alpha\right).
\end{aligned}$$

The expression for the tensor is not yet completed, but let us simplify the notation in the subsequent intermediate expressions. The last two terms, multiplied by the coefficient $\omega\epsilon/\Delta t$, will remain unaltered to the very end of the derivation. Furthermore, eventually these terms will be embedded in an error term, and ultimately neglected in the final approximation for the momentum conservation equation. So, let us not carry these terms through the intermediate steps; we acknowledge their presence, but omit them from the equations along the way. These terms will be reintroduced at the final expression. With this in mind, we proceed such that

$$\begin{aligned}
-\frac{\omega\epsilon}{\Delta t}\Pi^{(1)}_{\alpha\beta} &= -u_\beta\partial_\gamma\left(\theta\rho\delta_{\alpha\gamma} + \rho u_\alpha u_\gamma\right) + \rho u_\alpha \partial_t u_\beta + \theta\partial_\beta \rho u_\alpha + \theta\partial_\alpha \rho u_\beta \\
&= -\theta u_\beta \partial_\alpha \rho - u_\beta \partial_\gamma \rho u_\alpha u_\gamma + \rho u_\alpha \partial_t u_\beta + \theta\partial_\beta \rho u_\alpha + \theta u_\beta \partial_\alpha \rho + \theta\rho\partial_\alpha u_\beta \\
&= -u_\beta \partial_\gamma \rho u_\alpha u_\gamma + (u_\alpha \underbrace{\partial_t \rho u_\beta}_{(81)} - u_\alpha u_\beta \underbrace{\partial_t \rho}_{(80)}) + \theta\partial_\beta \rho u_\alpha + \theta\rho\partial_\alpha u_\beta
\end{aligned}$$

$$\Leftrightarrow -\frac{\omega\epsilon}{\Delta t}\Pi^{(1)}_{\alpha\beta} = -u_\beta\partial_\gamma\rho u_\alpha u_\gamma - u_\alpha\partial_\gamma\Pi^{(0)}_{\beta\gamma} + u_\alpha u_\beta\partial_\gamma\rho u_\gamma + \theta\partial_\beta\rho u_\alpha + \theta\rho\partial_\alpha u_\beta - \frac{\omega\epsilon}{\Delta t}\left(u_\alpha\, j^{(1)}_\beta - u_\alpha u_\beta\,\rho^{(1)}\right).$$

Again, the last two terms on the right are considered unwanted, and hence they are embedded in the error term. Thus, these two terms are omitted from the subsequent intermediate expressions. As discussed above, these terms will be reintroduced at the final expression. Let us proceed:

$$\begin{aligned}
-\frac{\omega\epsilon}{\Delta t}\Pi^{(1)}_{\alpha\beta} &= -\left(\partial_\gamma\rho u_\alpha u_\beta u_\gamma - \rho u_\alpha u_\gamma\partial_\gamma u_\beta\right) - u_\alpha\partial_\gamma\left(\theta\rho\delta_{\beta\gamma} + \rho u_\beta u_\gamma\right) \\
&\quad + u_\alpha u_\beta\partial_\gamma\rho u_\gamma + \theta\partial_\beta\rho u_\alpha + \theta\rho\partial_\alpha u_\beta \\
&= \rho u_\alpha u_\gamma\partial_\gamma u_\beta - \theta u_\alpha\partial_\beta\rho - u_\alpha\partial_\gamma\rho u_\beta u_\gamma + u_\alpha u_\beta\partial_\gamma\rho u_\gamma \\
&\quad + \theta\left(\rho\partial_\beta u_\alpha + u_\alpha\partial_\beta\rho\right) + \theta\rho\partial_\alpha u_\beta - \partial_\gamma\rho u_\alpha u_\beta u_\gamma \\
&= u_\alpha\left(\rho u_\gamma\partial_\gamma u_\beta + u_\beta\partial_\gamma\rho u_\gamma - \partial_\gamma\rho u_\beta u_\gamma\right) \\
&\quad + \theta\rho\left(\partial_\beta u_\alpha + \partial_\alpha u_\beta\right) - \partial_\gamma\rho u_\alpha u_\beta u_\gamma \\
&= \theta\rho\left(\partial_\beta u_\alpha + \partial_\alpha u_\beta\right) - \partial_\gamma\rho u_\alpha u_\beta u_\gamma.
\end{aligned}$$

The first term on the right now involves the so-called strain rate tensor $S_{\alpha\beta} := \left(\partial_\beta u_\alpha + \partial_\alpha u_\beta\right)/2$, see Sec. 2.1. The second term is usually neglected because it involves the velocity cubed, u^3, which shoud be negligible due to the low Mach number assumption; recall that in the Taylor series expansion of the exponential function, presented in Sec. 3.2.1, only terms up to second order in u were retained. Nonetheless, the complete expression is

$$\Pi^{(1)}_{\alpha\beta} = -\frac{\Delta t}{\omega\epsilon}\left(\theta\rho\left(\partial^{(1)}_\beta u_\alpha + \partial^{(1)}_\alpha u_\beta\right) - \partial^{(1)}_\gamma\rho u_\alpha u_\beta u_\gamma\right) + \left(\delta_{\alpha\beta}\theta\rho^{(1)} + u_\beta\, j^{(1)}_\alpha + u_\alpha\, j^{(1)}_\beta - u_\alpha u_\beta\,\rho^{(1)}\right).$$

APPENDIX 2 BOUNDARY SCHEMES FOR THE D3Q19 MODEL

In the context of hydrodynamic boundary conditions for LBM, we derive and present boundary schemes that provide expressions for the unknown distribution functions of the D3Q19 model. The presentation here is a catalogue of boundary schemes rather than a comprehensive discussion; Chapter 4, and especially Section 4.3, should be consulted whenever more elaborate explanations are desired. For example, the enumeration used for the velocity vectors of the D3Q19 model is explained in Fig. 8. The three-dimensional setting considered here involves a flat boundary for which the local density ρ and momentum density $\rho_0\mathbf{u}$ are available.

Let the boundary be located at x=0, i.e. it is parallel to the yz-plane. Then at the boundary nodes (also located at x=0), the index set $\{SE, BE, E, TE, NE\}$ refers to the five velocity vectors which point into the computational domain (eastbound or inbound velocities). The index set $\{SW, BW, W, TW, NW\}$ refers to the five velocity vectors which point out of the computational domain (westbound or outbound velocities). The remaining nine velocity vectors point along the boundary (inplane velocities): $\{BS, S, TS, B, C, T, BN, N, TN\}$. The distribution functions associated with the inbound velocities are considered as the primary unknown variables, after the streaming step, and expressions must be assigned to them.

We utilise the incompressible discrete equilibrium function given in Eq. (97): $W_0 = 12/36, W_1 = 2/36$, and $W_2 = 1/36$ are the equilibrium coefficients for the D3Q19 model, see Table 2. The speed of sound for the D3Q19 model is defined by the relation $\theta = c_s^2 = c_r^2/3$. In the most straightforward boundary scheme, the values of the equilibrium distribution functions are computed, and then these values are simply assigned to the unknown distributions. However, this procedure does not enforce the desired hydrodynamic variables at the inlet. Therefore, more elaborate expressions for the unknown distribution functions must be pursued.

APPENDIX 2.1 Bounce-back of the non-equilibrium part

An intuitive improvement supplements the simple equilibrium scheme with the bounce-back of the non-equilibrium part. With the incompressible equilibrium function Eq. (97), this is equivalent to

$$f_{SE} = f_{NW} + \frac{\rho_0(u_x - u_y)}{6c_r}, \quad f_{BE} = f_{TW} + \frac{\rho_0(u_x - u_z)}{6c_r}, \quad f_E = f_W + \frac{2\rho_0 u_x}{6c_r},$$
$$f_{TE} = f_{BW} + \frac{\rho_0(u_x + u_z)}{6c_r}, \quad f_{NE} = f_{SW} + \frac{\rho_0(u_x + u_y)}{6c_r}.$$

This boundary scheme guarantees prescribed density and momentum density in the x-direction, but it does not enforce correct transverse velocities at the bound-

ary. That is, the scheme does not enforce the prescribed y-component of the momentum density, nor the z-component. Specifically, in a general case,

$$\sum_i c_{iy} f_i = c_r\left(f_{BN} + f_N + f_{TN} - f_{BS} - f_S - f_{TS} + \frac{\rho_0 u_y}{3c_r}\right) \neq \rho_0 u_y,$$
$$\sum_i c_{iz} f_i = c_r\left(f_{TS} + f_T + f_{TN} - f_{BS} - f_B - f_{BN} + \frac{\rho_0 u_z}{3c_r}\right) \neq \rho_0 u_z.$$

With the boundary scheme presented next, this discrepancy is corrected.

APPENDIX 2.2 Enforcing density and momentum density

It is possible to construct a boundary scheme which correctly reproduces the four hydrodynamic variables, the density ρ (the zeroth-order moment) as well as the momentum density components $\rho_0 u_x, \rho_0 u_y$, and $\rho_0 u_z$ (the three first-order moments). Namely, we postulate a bounce-back scheme with three unknown variables (a, b, and c):

$$f_{NE} = f_{SW} + a + b, \quad f_{SE} = f_{NW} + a - b, \quad f_E = f_E^{eq} + f_W^{neq},$$
$$f_{TE} = f_{BW} + a + c, \quad f_{BE} = f_{TW} + a - c.$$

Then we impose conditions for the unknown variables by demanding that the zeroth and first-order moment equations yield the prescribed hydrodynamic variables (four equations in total):

$$\sum_i f_i = \rho, \quad \sum_i c_{ix} f_i = \rho_0 u_x, \quad \sum_i c_{iy} f_i = \rho_0 u_y, \quad \sum_i c_{iz} f_i = \rho_0 u_z.$$

Since the moment equations for ρ and $\rho_0 u_x$ provide exactly the same condition for the postulated scheme, we have three linearly independent equations for the three unknown variables. By solving the system of equations, we obtain the following expressions for the unknown distribution functions:

$$f_E = f_W + \frac{\rho_0 u_x}{3c_r},$$
$$f_{NE} = f_{SW} + \frac{\rho_0 u_x}{6c_r} - \frac{1}{2}(f_{BN} + f_N + f_{TN} - f_{BS} - f_S - f_{TS}) + \frac{\rho_0 u_y}{2c_r},$$
$$f_{SE} = f_{NW} + \frac{\rho_0 u_x}{6c_r} + \frac{1}{2}(f_{BN} + f_N + f_{TN} - f_{BS} - f_S - f_{TS}) - \frac{\rho_0 u_y}{2c_r},$$
$$f_{TE} = f_{BW} + \frac{\rho_0 u_x}{6c_r} - \frac{1}{2}(f_{TS} + f_T + f_{TN} - f_{BS} - f_B - f_{BN}) + \frac{\rho_0 u_z}{2c_r},$$
$$f_{BE} = f_{TW} + \frac{\rho_0 u_x}{6c_r} + \frac{1}{2}(f_{TS} + f_T + f_{TN} - f_{BS} - f_B - f_{BN}) - \frac{\rho_0 u_z}{2c_r}.$$

This is the boundary scheme proposed by *Zou and He* [Zou97]. By using their approach, explicit expressions for the unknown distribution functions of the D3Q19

model have been presented at least in Refs [Kut06, PIV, Hec10]. Unfortunately, expressions presented in Ref. [Kut06] are incorrect. Also the expressions presented in Ref. [Hec10] appear to include a small mistake: the transverse velocity component terms in the expressions are divided by 3. They should be divided by 2 (cf. the above expressions). The above expressions were presented in Ref. [PIV] for the special case of $u_y = u_z = 0$. There the use of dimensionless flow velocities was manifested with $c_r = 1$.

APPENDIX 2.3 An upgrade: enforcing six hydrodynamic moments

In the previous section, we presented a scheme which correctly incorporated information about the local densities and velocities into the unknown distribution functions. However, these four variables do not provide a complete description for the local hydrodynamic state. In particular, information about the viscous stresses were not included. Here we present a boundary scheme which incorporates information about the viscous stresses. We utilise an approximative relation between the viscous stresses and the second-order moments of the non-equilibrium functions:

$$\sum_i c_{i\alpha} c_{i\beta} f_i^{neq} = \Pi_{\alpha\beta}^{neq} \approx \Pi_{\alpha\beta}^{(1)} \approx -\frac{2\Delta t \theta \rho_0}{\omega} S_{\alpha\beta} =: \Pi_{\alpha\beta}^{visc},$$

where $S_{\alpha\beta}$ is the strain rate tensor, and ρ_0 is used in order to be consistent with the incompressible lattice Boltzmann scheme.

Since the tensors in the above relation are symmetric, they involve six independent components in three dimensions. Hence, we get six conditions for the non-equilibrium functions:

$$\begin{aligned}
f_{NE}^{neq} + f_{BE}^{neq} + f_{E}^{neq} + f_{TE}^{neq} + f_{SE}^{neq} + f_{NW}^{neq} + f_{BW}^{neq} + f_{W}^{neq} + f_{TW}^{neq} + f_{SW}^{neq} &= \frac{1}{c_r^2}\Pi_{xx}^{visc}, \\
f_{NW}^{neq} + f_{BN}^{neq} + f_{N}^{neq} + f_{TN}^{neq} + f_{NE}^{neq} + f_{SW}^{neq} + f_{BS}^{neq} + f_{S}^{neq} + f_{TS}^{neq} + f_{SE}^{neq} &= \frac{1}{c_r^2}\Pi_{yy}^{visc}, \\
f_{TW}^{neq} + f_{TS}^{neq} + f_{T}^{neq} + f_{TN}^{neq} + f_{TE}^{neq} + f_{BW}^{neq} + f_{BS}^{neq} + f_{B}^{neq} + f_{BN}^{neq} + f_{BE}^{neq} &= \frac{1}{c_r^2}\Pi_{zz}^{visc}, \\
f_{NE}^{neq} - f_{SE}^{neq} - f_{NW}^{neq} + f_{SW}^{neq} &= \frac{1}{c_r^2}\Pi_{xy}^{visc}, \\
f_{TE}^{neq} - f_{BE}^{neq} - f_{TW}^{neq} + f_{BW}^{neq} &= \frac{1}{c_r^2}\Pi_{xz}^{visc}, \\
f_{TN}^{neq} - f_{BN}^{neq} - f_{TS}^{neq} + f_{BS}^{neq} &= \frac{1}{c_r^2}\Pi_{yz}^{visc}.
\end{aligned}$$

In addition, we require that the zeroth and first-order moments of the non-equilibrium functions are identically zero. This provides four additional conditions:

$$\sum_i f_i^{neq} = \rho, \quad \sum_i c_{ix} f_i^{neq} = 0, \quad \sum_i c_{iy} f_i^{neq} = 0, \quad \sum_i c_{iz} f_i^{neq} = 0.$$

Thus, we have a total of ten conditions for the 19 non-equilibrium functions.

Here we construct a boundary scheme which enforce six hydrodynamic moments. To begin with, we postulate a scheme with six unknown variables:

$$\begin{aligned} f_C &= f_C^{eq} + a, \quad f_{NE} = f_{NE}^{eq} + b, \quad f_{BE} = f_{BE}^{eq} + c, \\ f_E &= f_E^{eq} + d, \quad f_{TE} = f_{TE}^{eq} + e, \quad f_{SE} = f_{SE}^{eq} + g. \end{aligned} \tag{114}$$

In order to obtain equations for the unknown variables a, b, c, d, e, and g, we rewrite the ten conditions for the non-equilibrium functions such that

$$\begin{aligned}
\rho : a+b+c+d+e+g &= -\Big(f_{NW}^{neq}+f_{BW}^{neq}+f_{W}^{neq}+f_{TW}^{neq}+f_{SW}^{neq}+f_{BS}^{neq}+f_{S}^{neq}+f_{TS}^{neq} \\
&\quad +f_{B}^{neq}+f_{T}^{neq}+f_{BN}^{neq}+f_{N}^{neq}+f_{TN}^{neq}\Big), \\
\rho_0 u_x : \quad b+c+d+e+g &= \Big(f_{NW}^{neq}+f_{BW}^{neq}+f_{W}^{neq}+f_{TW}^{neq}+f_{SW}^{neq}\Big), \\
\rho_0 u_y : \quad b \qquad\quad -g &= -\Big(f_{NW}^{neq}+f_{BN}^{neq}+f_{N}^{neq}+f_{TN}^{neq}-f_{SW}^{neq}-f_{BS}^{neq}-f_{S}^{neq}-f_{TS}^{neq}\Big), \\
\rho_0 u_z : \quad -c \quad +e \quad &= -\Big(f_{TW}^{neq}+f_{TS}^{neq}+f_{T}^{neq}+f_{TN}^{neq}-f_{BW}^{neq}-f_{BS}^{neq}-f_{B}^{neq}-f_{BN}^{neq}\Big), \\
\Pi_{xx}^{neq} : \quad b+c+d+e+g &= -\Big(f_{NW}^{neq}+f_{BW}^{neq}+f_{W}^{neq}+f_{TW}^{neq}+f_{SW}^{neq}\Big)+\frac{1}{c_r^2}\Pi_{xx}^{visc}, \\
\Pi_{yy}^{neq} : \quad b \qquad\quad +g &= -\Big(f_{NW}^{neq}+f_{BN}^{neq}+f_{N}^{neq}+f_{TN}^{neq}+f_{SW}^{neq}+f_{BS}^{neq}+f_{S}^{neq}+f_{TS}^{neq}\Big)+\frac{1}{c_r^2}\Pi_{yy}^{visc}, \\
\Pi_{zz}^{neq} : \quad +c \quad +e \quad &= -\Big(f_{TW}^{neq}+f_{TS}^{neq}+f_{T}^{neq}+f_{TN}^{neq}+f_{BW}^{neq}+f_{BS}^{neq}+f_{B}^{neq}+f_{BN}^{neq}\Big)+\frac{1}{c_r^2}\Pi_{zz}^{visc}, \\
\Pi_{xy}^{neq} : \quad b \qquad\quad -g &= \Big(f_{NW}^{neq}-f_{SW}^{neq}\Big)+\frac{1}{c_r^2}\Pi_{xy}^{visc}, \\
\Pi_{xz}^{neq} : \quad -c \quad +e \quad &= \Big(f_{TW}^{neq}-f_{BW}^{neq}\Big)+\frac{1}{c_r^2}\Pi_{xz}^{visc}, \\
\Pi_{yz}^{neq} : \quad 0 &= -\Big(f_{TN}^{neq}-f_{BN}^{neq}-f_{TS}^{neq}+f_{BS}^{neq}\Big)+\frac{1}{c_r^2}\Pi_{yz}^{visc}.
\end{aligned}$$

We immediately observe that the moment equations provided by $\rho_0 u_x$ and Π_{xx}^{neq} are linearly dependent. Likewise, the moment equations provided by $\rho_0 u_y$ and Π_{xy}^{neq} as well as by $\rho_0 u_z$ and Π_{xz}^{neq} are linearly dependent. In these kinds of conflict, we always utilise the equations from the lowest order moments. Furthermore, the moment equation provided by Π_{yz}^{neq} does not involve any of the unknown variables.

Hence, the moments $\rho, \rho_0 u_x, \rho_0 u_y, \rho_0 u_z, \Pi_{yy}^{neq}$, and Π_{zz}^{neq} provide six linearly independent equations for the six unknown variables. This system of equations is relatively easy to solve. For example, by subtracting the equation enforcing $\rho_0 u_x$ from the equation enforcing ρ, an expression for a is obtained. Moreover, by adding up the moment equations provided by $\rho_0 u_y$ and Π_{yy}^{neq}, an expression is obtained for b, and hence also for g. Similarly, by adding up the moment equations provided by $\rho_0 u_z$ and Π_{zz}^{neq}, an expression is obtained for e and c. The solution of the linear system of equations defines the boundary scheme under construction such that

$$
\begin{aligned}
a = &-\left(f_{BS}^{neq} + f_{S}^{neq} + f_{TS}^{neq} + f_{B}^{neq} + f_{T}^{neq} + f_{BN}^{neq} + f_{N}^{neq} + f_{TN}^{neq}\right) \\
&- 2\left(f_{NW}^{neq} + f_{BW}^{neq} + f_{W}^{neq} + f_{TW}^{neq} + f_{SW}^{neq}\right), \\
b = &-\left(f_{NW}^{neq} + f_{BN}^{neq} + f_{N}^{neq} + f_{TN}^{neq}\right) + \frac{1}{2c_r^2}\Pi_{yy}^{visc}, \\
c = &-\left(f_{BW}^{neq} + f_{BS}^{neq} + f_{B}^{neq} + f_{BN}^{neq}\right) + \frac{1}{2c_r^2}\Pi_{zz}^{visc}, \\
d = &\ 2\left(f_{NW}^{neq} + f_{BW}^{neq} + f_{TW}^{neq} + f_{SW}^{neq} + f_{BS}^{neq} + f_{TS}^{neq} + f_{BN}^{neq} + f_{TN}^{neq}\right) \\
&+ \left(f_{W}^{neq} + f_{N}^{neq} + f_{S}^{neq} + f_{T}^{neq} + f_{B}^{neq}\right) - \frac{1}{c_r^2}\Pi_{yy}^{visc} - \frac{1}{c_r^2}\Pi_{zz}^{visc}, \\
e = &-\left(f_{TW}^{neq} + f_{TS}^{neq} + f_{T}^{neq} + f_{TN}^{neq}\right) + \frac{1}{2c_r^2}\Pi_{zz}^{visc}, \\
g = &-\left(f_{SW}^{neq} + f_{BS}^{neq} + f_{S}^{neq} + f_{TS}^{neq}\right) + \frac{1}{2c_r^2}\Pi_{yy}^{visc}.
\end{aligned}
$$

The partial derivatives $\partial_y u_y$ and $\partial_z u_z$ included in the definitions of Π_{yy}^{visc} and Π_{zz}^{visc}, respectively, are either approximated by e.g. finite differences or they are given by a boundary condition, e.g. $\partial_y u_y = \partial_z u_z = 0$. Which of the two alternatives is more appropriate depends on the interface and on the simulation configuration.

Note also that f_C^{neq} is, in principle, known after the streaming step. As explained in Sec. 4.3, the procedure proposed here actually involves two steps: first, the value of f_C after the streaming step can be used e.g. in the mass-flux-based approach for computing the local densities and flow velocities. Then, in the second step, we choose to replace f_C^{neq} with the value presented in this boundary scheme – a kind of reconstruction is executed.

APPENDIX 2.4 A further improvement: enforcing seven hydrodynamic moments

Since we are considering a flat boundary, where the y- and z-directions are in-plane or tangential directions, it might be of practical importance to consider special boundary schemes enforcing only those second-order moments which involve partial derivatives along the boundary. For example, if the prescribed velocity components at the boundary are constant, e.g. zero velocity at a no-slip boundary, partial derivatives along the boundary vanish automatically: $\partial_y u_x = \partial_y u_y = \partial_y u_z = 0$ and $\partial_z u_x = \partial_z u_y = \partial_z u_z = 0$. The second-order moments which involve partial derivatives only along the boundary are $\Pi^{visc}_{yy}, \Pi^{visc}_{zz}$, and Π^{visc}_{yz}. The first two are enforced by the boundary scheme presented in the previous section. The last moment, Π^{visc}_{yz}, can be enforced in two ways. First of all, we could proceed exactly as before; we could increase the number of unknowns with a new variable h:

$$\begin{aligned} f_C = f^{eq}_C + a, \quad f_{NE} = f^{eq}_{NE} + b, \quad f_{BE} = f^{eq}_{BE} + c, \quad f_E = f^{eq}_E + d, \\ f_{TE} = f^{eq}_{TE} + e, \quad f_{SE} = f^{eq}_{SE} + g, \quad f_{TN} = f^{eq}_{TN} + h. \end{aligned} \tag{115}$$

We could equally well associate the variable h with $f^{neq}_{BN}, f^{neq}_{TS}$, or f^{neq}_{BS}. The ten conditions for the non-equilibrium functions provide seven linearly independent equations for these seven unknown variables. The system of equations can be solved, and a boundary scheme is so defined.

However, there is an attractive alternative. By inspecting the moment equation enforcing Π^{visc}_{yz},

$$f^{neq}_{TN} - f^{neq}_{BN} - f^{neq}_{TS} + f^{neq}_{BS} = \frac{1}{c_r^2}\Pi^{visc}_{yz},$$

we realise that the equation is fulfilled if we assign

$$f^{neq}_{TN} = f^{neq}_{BS} = \frac{1}{4c_r^2}\Pi^{visc}_{yz}, \quad f^{neq}_{TS} = f^{neq}_{BN} = -\frac{1}{4c_r^2}\Pi^{visc}_{yz}. \tag{116}$$

That is, we reconstruct the four non-equilibrium functions in the sense explained in the previous section (and in Sec. 4.3). This is a very convenient approach since these four non-equilibrium functions appear in the other nine conditions in such a way that, with this reconstruction, they always cancel each other – resulting in a null contribution to the other conditions.

In summary, we propose a boundary scheme which enforces seven hydrodynamic moments: $\rho, \rho_0 u_x, \rho_0 u_y, \rho_0 u_z, \Pi^{neq}_{yy}, \Pi^{neq}_{zz}$, and Π^{neq}_{yz}. This is accomplished with the reconstruction presented in Eq. (116) together with the expressions for the six unknown variables presented in the previous section. In conjunction with

Eq. (116), these expressions are

$$
\begin{aligned}
a &= -\left(f_S^{neq} + f_B^{neq} + f_T^{neq} + f_N^{neq}\right) - 2\left(f_{NW}^{neq} + f_{BW}^{neq} + f_W^{neq} + f_{TW}^{neq} + f_{SW}^{neq}\right), \\
b &= -\left(f_{NW}^{neq} + f_N^{neq}\right) + \frac{1}{2c_r^2}\Pi_{yy}^{visc}, \\
c &= -\left(f_{BW}^{neq} + f_B^{neq}\right) + \frac{1}{2c_r^2}\Pi_{zz}^{visc}, \\
d &= 2\left(f_{NW}^{neq} + f_{BW}^{neq} + f_{TW}^{neq} + f_{SW}^{neq}\right) \\
&\quad + \left(f_W^{neq} + f_N^{neq} + f_S^{neq} + f_T^{neq} + f_B^{neq}\right) - \frac{1}{c_r^2}\Pi_{yy}^{visc} - \frac{1}{c_r^2}\Pi_{zz}^{visc}, \\
e &= -\left(f_{TW}^{neq} + f_T^{neq}\right) + \frac{1}{2c_r^2}\Pi_{zz}^{visc}, \\
g &= -\left(f_{SW}^{neq} + f_S^{neq}\right) + \frac{1}{2c_r^2}\Pi_{yy}^{visc}.
\end{aligned}
$$

APPENDIX 2.5 Enforcing hydrodynamic moments up to second order

The last boundary scheme here proposed for the D3Q19 model enforces a total of ten hydrodynamic moments: one zeroth-order moment (ρ), three first-order moments ($\rho_0 u_x, \rho_0 u_y, \rho_0 u_z$), and the six second-order moments related to the viscous stresses ($\Pi_{xx}^{neq}, \Pi_{xy}^{neq}, \Pi_{xz}^{neq}, \Pi_{yy}^{neq}, \Pi_{zz}^{neq}, \Pi_{yz}^{neq}$). We propose a scheme which is a specific extension of the schemes presented in the previous sections. Particularly, this scheme enforces also the three second-order moments which involve partial derivatives in the normal direction (i.e. in the x-direction): $\Pi_{xx}^{visc}, \Pi_{xy}^{visc}$, and Π_{xz}^{visc}. To begin with, we utilise the reconstruction presented in Eq. (116). Due to the reconstruction, the condition for the non-equilibrium functions provided by Π_{yz}^{neq} becomes obsolete, i.e. it is automatically satisfied, and hence we have a total of nine conditions left.

Therefore, we increase the number of unknowns with three new variables denoted by k, l, and m:

$$
\begin{aligned}
f_C &= f_C^{eq} + a, \quad f_{NE} = f_{NE}^{eq} + b, \quad f_{BE} = f_{BE}^{eq} + c, \\
f_E &= f_E^{eq} + d, \quad f_{TE} = f_{TE}^{eq} + e, \quad f_{SE} = f_{SE}^{eq} + g, \\
f_N &= f_N^{eq} + k, \quad f_T = f_T^{eq} + l, \quad f_W = f_W^{eq} + m.
\end{aligned} \tag{117}
$$

This definition of the three new variables is certainly not the only choice available – many other definitions are equally valid. We choose to associate the variables with f_N^{eq}, f_T^{eq}, and f_W^{eq} because, in this way, the emerging linear system of equations is relatively easy to solve.

The nine conditions for the non-equilibrium functions, together with the nine unknown variables defined in Eq. (117) and with the reconstruction presented in Eq. (116), give rise to a linear system of equations:

$$
\begin{array}{rrrrrrrrrrl}
\rho: & a+b+c+d+e+g+k+l+m & = & -\left(f_{NW}^{neq}+f_{BW}^{neq}+f_{TW}^{neq}+f_{SW}^{neq}+f_{S}^{neq}+f_{B}^{neq}\right), \\
\rho_0 u_x: & b+c+d+e+g & -m & = & \left(f_{NW}^{neq}+f_{BW}^{neq}+f_{TW}^{neq}+f_{SW}^{neq}\right), \\
\rho_0 u_y: & b & -g+k & = & -\left(f_{NW}^{neq}-f_{SW}^{neq}-f_{S}^{neq}\right), \\
\rho_0 u_z: & -c & +e & +l & = & \left(f_{BW}^{neq}-f_{TW}^{neq}+f_{B}^{neq}\right), \\
\Pi_{xx}^{neq}: & b+c+d+e+g & +m & = & -\left(f_{NW}^{neq}+f_{BW}^{neq}+f_{TW}^{neq}+f_{SW}^{neq}\right)+\frac{1}{c_f^2}\Pi_{xx}^{visc}, \\
\Pi_{yy}^{neq}: & b & +g+k & & = & -\left(f_{NW}^{neq}+f_{SW}^{neq}+f_{S}^{neq}\right)+\frac{1}{c_f^2}\Pi_{yy}^{visc}, \\
\Pi_{zz}^{neq}: & +c & +e & +l & = & -\left(f_{BW}^{neq}+f_{TW}^{neq}+f_{B}^{neq}\right)+\frac{1}{c_f^2}\Pi_{zz}^{visc}, \\
\Pi_{xy}^{neq}: & b & -g & & = & \left(f_{NW}^{neq}-f_{SW}^{neq}\right)+\frac{1}{c_f^2}\Pi_{xy}^{visc}, \\
\Pi_{xz}^{neq}: & -c & +e & & = & -\left(f_{BW}^{neq}-f_{TW}^{neq}\right)+\frac{1}{c_f^2}\Pi_{xz}^{visc}.
\end{array}
$$

This system of equations is actually quite simple in structure, and it is not too difficult to determine its solution. For example, by subtracting the equation enforcing $\rho_0 u_x$ from the equation enforcing Π_{xx}^{visc}, an expression for m is obtained. Similarly, by subtracting the moment equation provided by Π_{xy}^{neq} from the equation provided by $\rho_0 u_y$, and the moment equation provided by Π_{xz}^{neq} from the equation provided by $\rho_0 u_z$, expressions for k and l are obtained, respectively. Then by substituting the expressions back to the system of equations, the remaining variables can be solved in the same way as in the case of six unknown variables. In summary, the boundary scheme is defined by Eq. (116) and by the expressions

found for the nine unknown variables:

$$
\begin{aligned}
a =& \; 2\left(f_{NW}^{neq} - f_{BW}^{neq} + f_{TW}^{neq} - f_{SW}^{neq} - f_{S}^{neq} - f_{B}^{neq}\right) - \frac{1}{c_r^2}\left(\Pi_{xx}^{visc} - \Pi_{xy}^{visc} - \Pi_{xz}^{visc}\right), \\
b =& \quad \left(f_{NW}^{neq} - 2f_{SW}^{neq} - f_{S}^{neq}\right) + \frac{1}{2c_r^2}\Pi_{yy}^{visc} + \frac{1}{c_r^2}\Pi_{xy}^{visc}, \\
c =& -\left(f_{BW}^{neq} + f_{B}^{neq}\right) + \frac{1}{2c_r^2}\Pi_{zz}^{visc}, \\
d =& -\left(f_{NW}^{neq} - 3f_{BW}^{neq} + f_{TW}^{neq} - 3f_{SW}^{neq} - 2f_{S}^{neq} - 2f_{B}^{neq}\right) + \frac{1}{c_r^2}\left(\frac{1}{2}\Pi_{xx}^{visc} - \Pi_{yy}^{visc}\right. \\
& \left. - \Pi_{zz}^{visc} - \Pi_{xy}^{visc} - \Pi_{xz}^{visc}\right), \\
e =& -\left(2f_{BW}^{neq} - f_{TW}^{neq} + f_{B}^{neq}\right) + \frac{1}{2c_r^2}\Pi_{zz}^{visc} + \frac{1}{c_r^2}\Pi_{xz}^{visc}, \\
g =& -\left(f_{SW}^{neq} + f_{S}^{neq}\right) + \frac{1}{2c_r^2}\Pi_{yy}^{visc}, \\
k =& -\left(2f_{NW}^{neq} - 2f_{SW}^{neq} - f_{S}^{neq}\right) - \frac{1}{c_r^2}\Pi_{xy}^{visc}, \\
l =& \quad \left(2f_{BW}^{neq} - 2f_{TW}^{neq} + f_{B}^{neq}\right) - \frac{1}{c_r^2}\Pi_{xz}^{visc}, \\
m =& -\left(f_{NW}^{neq} + f_{BW}^{neq} + f_{TW}^{neq} + f_{SW}^{neq}\right) + \frac{1}{2c_r^2}\Pi_{xx}^{visc}.
\end{aligned}
$$

APPENDIX 3 BIASED ONE-DIMENSIONAL CENTRAL DIFFERENCES

Some of the boundary schemes presented in Sec. 4.3 and Appendix 2, may require approximation of the partial derivatives of the fluid flow velocity at an open boundary. For example, the partial derivatives along the boundary are straightforwardly approximated with standard second-order central-difference schemes. However, at the open boundary lattice nodes located next to a fluid-solid interface, the approximation of the derivatives with a central difference scheme is somewhat delicate. Considered for example the one-dimensional configuration presented in Fig. 13 and, for a moment, let us assume that the fluid-solid interface is located at point A; points 0 and B belong to the fluid domain. Hence, the fluid flow velocities are available at these three points: $u_a \equiv u(-h_a), u_0 \equiv u(0)$, and $u_b \equiv u(h_b)$. Let us further assume that we are applying halfway reflection boundary conditions at the fluid-solid interfaces – here h denotes the lattice spacing. Then, $h_a = h/2 \neq h_b = h$. Hence, the fact that the information available is biased towards point A must be taken into account in the central difference scheme. Biased central difference schemes are nothing special either, but we prefer to be self-contained in the presentation of the boundary schemes and, for this reason, we provide here a general biased central-difference scheme. Moreover, from the general scheme we derive schemes for a few special cases.

We set out to construct a spatially second-order accurate finite-difference scheme for the general case $h_a \neq h_b$. To begin with, we assume that locally the function u is accurately approximated with a second-order polynomial,

$$p(x) = c_1 x^2 + c_2 x + c_3, \quad x \in [-h_a, h_b].$$

That is, the above definition interpolates the values of function u between points A, 0, and B with second-order accuracy. The dashed line in Fig. 13 represents polynomial p. The three unknown coefficients c_1, c_2, and c_3 are solved from linear system of equations which arises from the requirements $p(-h_a) = u_a$, $p(0) = u_0$, and $p(h_b) = u_b$:

$$\begin{cases} c_1 h_a^2 - c_2 h_a + c_3 = u_a, \\ \qquad\qquad\quad c_3 = u_0, \\ c_1 h_b^2 + c_2 h_b + c_3 = u_b. \end{cases}$$

The coefficient c_3 is immediately determined. The solutions to the other two coefficients are given by

$$c_1 = \frac{u_b - u_0 - r^2(u_a - u_0)}{h_a h_b + h_b^2} + \frac{u_a - u_0}{h_a^2},$$
$$c_2 = \frac{u_b - u_0 - r^2(u_a - u_0)}{h_b + h_b r},$$

where $r = h_b/h_a$ is the ratio between the distances from the origin (0) to points A and B.

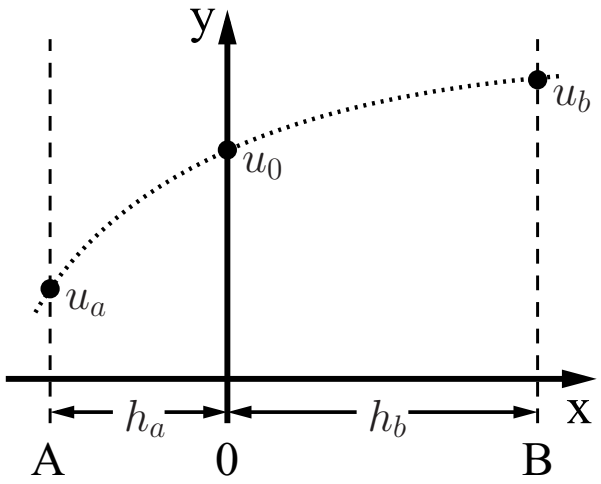

FIGURE 13 An illustration of the configuration for biased central-difference schemes in one dimension. The distance from the origin (0) to point A and B is $-h_a$ and h_b, respectively. It is assumed that the value of function u is known in a set of discrete points. In particular, the value of the function is avaible in the three points, A, 0, and B: $u_a \equiv u(-h_a), u_0 \equiv u(0)$, and $u_b \equiv u(h_b)$. In this configuration, the aim is to approximate the derivatives of u at the origin by utilising these three values. In this sense, a central finite-difference scheme is pursued. The term biased refers to the fact that in general $h_a \neq h_b$.

The solution for the three coefficients completely determines the second-order interpolation function p. The solution is not ideal: if the distances h_a or h_b approach zero, the expression for coefficient c_1 or c_2 may diverge – a common nuisance in computational schemes. Nonetheless, it is possible to analytically compute the derivatives of p: here the first and second derivatives are denoted by $p'(x)$ and $p''(x)$, respectively. Then, the values of the derivatives can be evaluated at a given point, in particular at the origin. Let us first consider the simplest example, where $h_a = h_b = h$:

$$p(x) = \left(\frac{u_b - 2u_0 + u_a}{2h^2}\right)x^2 + \left(\frac{u_b - u_a}{2h}\right)x + u_0.$$

By computing the first and second derivatives of the above function, and by evaluating the derivatives at the origin, we obtain very familiar finite-difference schemes:

$$p'(0) = \frac{u_b - u_a}{2h}, \quad p''(0) = \frac{u_b - 2u_0 + u_a}{h^2}. \tag{118}$$

These are the conventional second-order, central finite-difference approximations for the first and second derivative of function u at point 0. An alternative procedure for obtaining these approximations relies on a *Taylor series* expansion.

Next we consider special cases relevant for simulations where halfway reflection boundary conditions are utilised, i.e. the fluid-solid interfaces are assumed to locate halfway between the lattice nodes. In such simulations, and with the configuration presented in Fig. 13, the interface may locate at points A and B, corresponding to cases $h_a = h/2$ and $h_b = h/2$, respectively. For example, let $h_a = h/2$ and $h_b = h$:

$$p(x) = \left(\frac{2u_b - 6u_0 + 4u_a}{3h^2}\right)x^2 + \left(\frac{u_b + 3u_0 - 4u_a}{3h}\right)x + u_0.$$

By computing the first and second derivatives, and by evaluating them at the origin, we find biased central-difference schemes for approximating the derivatives of u at point 0:

$$p'(0) = \frac{u_b + 3u_0 - 4u_a}{3h}, \quad p''(0) = \frac{4u_b - 12u_0 + 8u_a}{3h^2}. \tag{119}$$

We find finite-difference schemes for the case $h_a = h$ and $h_b = h/2$ in a similar way:

$$\begin{aligned} p(x) &= \left(\frac{4u_b - 6u_0 + 2u_a}{3h^2}\right)x^2 + \left(\frac{4u_b - 3u_0 - u_a}{3h}\right)x + u_0, \\ p'(0) &= \frac{4u_b - 3u_0 - u_a}{3h}, \quad p''(0) = \frac{8u_b - 12u_0 + 4u_a}{3h^2}. \end{aligned} \tag{120}$$

Finally, in the case $h_a = h_b = h/2$:

$$\begin{aligned} p(x) &= \left(\frac{2u_b - 4u_0 + 2u_a}{h^2}\right)x^2 + \left(\frac{u_b - u_a}{h}\right)x + u_0, \\ p'(0) &= \frac{u_b - u_a}{h}, \quad p''(0) = \frac{4u_b - 8u_0 + 4u_a}{h^2}. \end{aligned} \tag{121}$$

Actually, the last expressions Eq. (121) can be obtained directly from Eq. (118) if h is formally replaced by $h/2$ – recall that h refers here to the lattice spacing.

APPENDIX 4 IMPLEMENTING THE D3Q19 MODEL: AN EXAMPLE

In order to promote modularity in the simulation software, it is necessary to clearly separate the implementations of the streaming and collision steps inherent in the lattice Boltzmann schemes. Here we provide an implementation example for the collision step of the D3Q19 model; the collision operator is modelled with the single-relaxation-time BGK model. The discrete equilibrium function is implemented with dimensionless variables, see Eq. (46) in Sec. 3.2.1. The example relies heavily on the concepts and techniques presented in Chapter 5 as well as in Refs [PI, PII]. First of all, the lattice nodes are enumerated, and the enumeration number is computed with the macro $N(i,j,k)$, where (i,j,k) are the spatial coordinates of the node. Secondly, the fluid nodes have an exclusive enumeration – no memory is allocated to the distribution functions of the solid nodes – and this enumeration is retrieved with the macro $ENUM\_N(n)$. The distribution functions of a fluid node are accessed from the global array with, e.g., the macro $F\_SW(nf)$, where nf is the fluid-node enumeration number. The discrete velocities are enumerated with the logic presented in Fig. 8. Also, the example does not include an assignment of body forces.

Special attention is devoted here to two issues: we have made some effort to reduce the number of floating-point operations in the implementation and, at the same time, we have attempted to avoid unnecessary dependences between instructions. With the latter objective we aim to promote *out of order execution* of the instructions, see Ref. [PI] for a more detailed discussion. Below the constants W_0, W_1, W_2, and $CS2$ refer to the equilibrium coefficients and to the speed of sound squared, respectively. The example is written in a C/C++ -style:

```
// ================================================
// RELAXATION (total of 159 floating-point operations)
// ================================================
// ------------------------------------------------
// Collect distribution values into a local array
// ------------------------------------------------
double f[Q];       // Q=19 for the D3Q19 model
int n = N(i,j,k);  // Enumeration for the node (i,j,k)
int nf = ENUM_N(n);// Fluid-node enumeration number

f[SW] = F_SW(nf); f[BW] = F_BW(nf); f[W]  = F_W(nf);
f[TW] = F_TW(nf); f[NW] = F_NW(nf);

f[BS] = F_BS(nf); f[S]  = F_S(nf);  f[TS] = F_TS(nf);
f[B]  = F_B(nf);  f[C]  = F_C(nf);  f[T]  = F_T(nf);
f[BN] = F_BN(nf); f[N]  = F_N(nf);  f[TN] = F_TN(nf);

f[SE] = F_SE(nf); f[BE] = F_BE(nf); f[E]  = F_E(nf);
f[TE] = F_TE(nf); f[NE] = F_NE(nf);
```

```
// ------------------------------------------------
// Density and momentum components with 33 operations
// ------------------------------------------------
double aw = f[SW]+f[BW]+f[W]+f[TW]+f[NW],
  ae = f[SE]+f[BE]+f[E]+f[TE]+f[NE],
  as = f[BS]+f[S]+f[TS], an = f[BN]+f[N]+f[TN],

  den = ae + aw + an + as + f[B] + f[C] + f[T],
  jx  = ae - aw,
  jy  = an - as + f[NE] + f[NW] - f[SE] - f[SW],
  jz  = f[TW] + f[TS] + f[T] + f[TN] + f[TE]
      - f[BW] - f[BS] - f[B] - f[BN] - f[BE];
//---------------------------------------
// Auxiliary variables with 29 operations
//---------------------------------------
double den1 = W1*den, inv_den1 = 1.0/(den1),
  // tx = (W2/CS2)*den*ux, HBFN = 0.5*(W1/CS2),
  tx = HBFN*jx, ty = HBFN*jy, tz = HBFN*jz,

  // tx_p_ty = W2*den*3.0*(ux-uy)
  tx_p_ty = (tx+ty), tx_p_tz = (tx+tz),
  ty_p_tz = (ty+tz), tx_m_ty = (tx-ty),
  tx_m_tz = (tx-tz), ty_m_tz = (ty-tz),

  // txx = W2*den*4.5*ux*ux, NOTE inv_den1
  txx = tx*tx*inv_den1,
  tyy = ty*ty*inv_den1,
  tzz = tz*tz*inv_den1,

  // tt = W2*den*1.5*(ux*ux+uy*uy+uz*uz)
  tt  = CS2*(txx + tyy + tzz),
  cmmn2 = W2*den - tt,
  cmmn1 = 2.0*cmmn2;

// tx = (W1/CS2)*den*ux
// txx = W1*den*4.5*ux*ux
tx *= 2.0; ty *= 2.0; tz *= 2.0;
txx *= 2.0; tyy *= 2.0; tzz *= 2.0;
//------------------------------------------------
// Update the distribution values with 97 operations
//------------------------------------------------
double cmmn_xpy = cmmn2 + inv_den1*tx_p_ty*tx_p_ty;
f[SW] = f[SW] - r1*(f[SW] - (cmmn_xpy - tx_p_ty));
f[NE] = f[NE] - r1*(f[NE] - (cmmn_xpy + tx_p_ty));
```

```
double cmmn_xpz = cmmn2 + inv_den1*tx_p_tz*tx_p_tz;
f[BW] = f[BW] - r1*(f[BW] - (cmmn_xpz - tx_p_tz));
f[TE] = f[TE] - r1*(f[TE] - (cmmn_xpz + tx_p_tz));

double cmmn_x = cmmn1 + txx;
f[W] = f[W] - r1*(f[W] - (cmmn_x - tx));
f[E] = f[E] - r1*(f[E] - (cmmn_x + tx));

double cmmn_xmz = cmmn2 + inv_den1*tx_m_tz*tx_m_tz;
f[TW] = f[TW] - r1*(f[TW] - (cmmn_xmz - tx_m_tz));
f[BE] = f[BE] - r1*(f[BE] - (cmmn_xmz + tx_m_tz));

double cmmn_xmy = cmmn2 + inv_den1*tx_m_ty*tx_m_ty;
f[NW] = f[NW] - r1*(f[NW] - (cmmn_xmy - tx_m_ty));
f[SE] = f[SE] - r1*(f[SE] - (cmmn_xmy + tx_m_ty));

double cmmn_ypz = cmmn2 + inv_den1*ty_p_tz*ty_p_tz;
f[BS] = f[BS] - r1*(f[BS] - (cmmn_ypz - ty_p_tz));
f[TN] = f[TN] - r1*(f[TN] - (cmmn_ypz + ty_p_tz));

double cmmn_y = cmmn1 + tyy;
f[S] = f[S] - r1*(f[S] - (cmmn_y - ty));
f[N] = f[N] - r1*(f[N] - (cmmn_y + ty));

double cmmn_ymz = cmmn2 + inv_den1*ty_m_tz*ty_m_tz;
f[TS] = f[TS] - r1*(f[TS] - (cmmn_ymz - ty_m_tz));
f[BN] = f[BN] - r1*(f[BN] - (cmmn_ymz + ty_m_tz));

double cmmn_z = cmmn1 + tzz;
f[B] = f[B] - r1*(f[B] - (cmmn_z - tz));
f[T] = f[T] - r1*(f[T] - (cmmn_z + tz));

f[C] = f[C] - r1*(f[C] - 6.0*cmmn1);
//-----------------------------------------------
// Store the new values back to the global array
//-----------------------------------------------
F_SW(nf) = f[SW]; F_BW(nf) = f[BW]; F_W(nf)  = f[W];
F_TW(nf) = f[TW]; F_NW(nf) = f[NW]; F_BS(nf) = f[BS];
F_S(nf)  = f[S];  F_TS(nf) = f[TS]; F_B(nf)  = f[B];
F_C(nf)  = f[C];  F_T(nf)  = f[T];  F_BN(nf) = f[BN];
F_N(nf)  = f[N];  F_TN(nf) = f[TN]; F_SE(nf) = f[SE];
F_BE(nf) = f[BE]; F_E(nf)  = f[E];  F_TE(nf) = f[TE];
F_NE(nf) = f[NE];
```

REFERENCES

[Abe97] Abe T, *Derivation of the Lattice Boltzmann Method by Means of the Discrete Ordinate Method for the Boltzmann Equation*, J. Comput. Phys. **131** (1): 241, 1997.

[Adl95] Adler C, Boghosian B, Flekkøy E, Margolus N, and Rothman D, *Simulating three-dimensional hydrodynamics on a cellular automata machine*, J. Statist. Phys. **81** (1–2): 105, 1995.

[Aid95] Aidun C and Lu Y, *Lattice Boltzmann simulation of solid particles suspended in fluid*, J. Statist. Phys. **81** (1–2): 49, 1995.

[Ale94] Alekseev B, *The Generalized Boltzmann Equation, Generalized Hydrodynamic Equations and their Applications*, Phil. Trans. R. Soc. Lond. A **349** (1691): 417, 1994.

[Ale00] Alekseev B, *Physical principles of the generalized Boltzmann kinetic theory of gases*, Phys. Usp. **43** (6): 601, 2000.

[Ale04] Alekseev B, *Generalized Boltzmann Physical Kinetics*, Elsevier, Amsterdam, 2004.

[Ale92] Alexander F, Chen H, Chen S, and Doolen G, *Lattice Boltzmann model for compressible fluids*, Phys. Rev. A **46** (4): 1967, 1992.

[Ale93] Alexander F, Chen S, and Sterling J, *Lattice Boltzmann thermohydrodynamics*, Phys. Rev. E **47** (4): R2249, 1993.

[Anc94] Ancona M, *Fully-Lagrangian and Lattice-Boltzmann Methods for Solving Systems of Conservation Equations*, J. Comput. Phys. **115** (1): 107, 1994.

[And00] Andries P, le Tallec P, Perlat J-P, and Perthame B, *The Gaussian-BGK model of Boltzmann equation with small Prandtl number*, Eur. J. Mech. B - Fluids **19** (6): 813, 2000.

[And01] Andries P and Perthame B, *The ES-BGK model equation with correct Prandtl number*, AIP Conf. Proc. **585**: 30, 2001.

[And02] Andries P, Bourgat J-F, le Tallec P, and Perthame B, *Numerical comparison between the Boltzmann and ES-BGK models for rarefied gases*, Comput. Methods Appl. Mech. Engrg. **191** (31): 3369, 2002.

[Ans02] Ansumali S and Karlin I, *Kinetic boundary conditions in the lattice Boltzmann method*, Phys. Rev. E **66** (2): 026311, 2002.

[Ans03] Ansumali S, Karlin I, and Öttinger H, *Minimal entropic kinetic models for hydrodynamics*, Europhys. Lett. **63** (6): 798, 2003.

[Ans05] Ansumali S and Karlin I, *Consistent Lattice Boltzmann Method*, Phys. Rev. Lett. **95** (26): 260605, 2005.

[Aok02] Aokui X, *Intrinsic instability of the lattice BGK model*, Acta Mech. Sin. Engl. Ser. **18** (6): 603, 2002.

[App90] Appert C and Zaleski S, *Lattice gas with a liquid-gas transition*, Phys. Rev. Lett. **64** (1): 1, 1990.

[Arg04] Argentini R, Bakker A, and Lowe C, *Efficiently using memory in lattice Boltzmann simulations*, Future Gener. Comput. Syst. **20** (6): 973, 2004.

[Arl02] Arlotti L, Bellomo N, and De Angelis E, *Generalized kinetic (Boltzmann) models: mathematical structures and applications*, Math. Models Methods Appl. Sci. **12** (4): 567, 2002.

[Asi09] Asinari P and Karlin I, *Generalized Maxwell state and H theorem for computing fluid flows using the lattice Boltzmann method*, Phys. Rev. E **79** (3): 036703, 2009.

[Axn08] Axner L, Bernsdorf J, Zeiser T, Lammers P, Linxweiler J, and Hoekstra A, *Performance evaluation of a parallel sparse lattice Boltzmann solver*, J. Comput. Phys. **227** (10): 4895, 2008.

[Bac78] Backus J, *Can programming be liberated from the von Neumann style? A functional style and its algebra of programs*, Commun. ACM **21** (8): 613, 1978.

[Bal87] Balasubramanian K, Hayot F, and Saam W, *Darcy's law from lattice-gas hydrodynamics*, Phys. Rev. A **36** (5): 2248, 1987.

[Ban06] Banda M, Yong W-A, and Klar A, *A Stability Notion for Lattice Boltzmann Equations*, SIAM J. Sci. Comput. **27** (6): 2098, 2006.

[Bao08] Bao J, Yuan P, and Schaefer L, *A mass conserving boundary condition for the lattice Boltzmann equation method*, J. Comput. Phys. **227** (18): 8472, 2008.

[Bar91] Bardos C, Golse F, and Levermore D, *Fluid dynamic limits of kinetic equations. I. Formal derivations*, J. Statist. Phys. **63** (1–2): 323, 1991.

[Bau89] Baudet C, Hulin J, Lallemand P, and d'Humières D, *Lattice-gas automata: A model for the simulation of dispersion phenomena*, Phys. Fluids A **1** (3): 507, 1989.

[Beh94] Behrend O, Harris R, and Warren P, *Hydrodynamic behavior of lattice Boltzmann and lattice Bhatnagar-Gross-Krook models*, Phys. Rev. E **50** (6): 4586, 1994.

[Beh95] Behrend O, *Solid-fluid boundaries in particle suspension simulations via the lattice Boltzmann method*, Phys. Rev. E **52** (1): 1164, 1995.

[Bel02] Bella G, Filippone S, Rossi N, and Ubertini S, *Using OpenMP on a hydrodynamic lattice-Boltzmann code*, in Proceedings of the Fourth European Workshop on OpenMP, Roma, Italy, 2002.

[Bel91a] Bellomo N and Gustafsson T, *The Discrete Boltzmann Equation: A Review of the Mathematical Aspects of the Initial and Initial-Boundary Value Problems*, Review Math. Phys. **3** (2): 137, 1991.

[Bel91b] Bellomo N and Longo E, *A new discretized model in nonlinear kinetic theory: the semicontinuous Boltzmann equation*, Math. Models Methods Appl. Sci. **1** (1): 113, 1991.

[Bel03] Bellomo N and Gatignol R, *Lecture notes on the discretization of the Boltzmann equation*, Ser. Adv. Math. Appl. Sci. **63**, World Scientific, Singapore, 2003.

[Ber99] Bernsdorf J, Durst F, and Schäfer M, *Comparison of cellular automata and finite volume techniques for simulation of incompressible flows in complex geometries*, Internat. J. Numer. Methods Fluids **29** (3): 251, 1999.

[Ber01] Bernaschi M, Succi S, and Chen H, *Accelerated Lattice Boltzmann Schemes for Steady-State Flow Simulations*, J. Sci. Comput. **16** (2): 135, 2001.

[Ber02] Bernaschi M, Succi S, Chen H, and Zhang R, *Computing steady state flows with an accelerated lattice Boltzmann technique*, Internat. J. Modern Phys. C **13** (5): 675, 2002.

[Ber03] Bernaschi M and Succi S, *Accelerated lattice Boltzmann scheme for steady-state flows*, Internat. J. Modern Phys. B **17** (1–2): 1, 2003.

[Ber09] Bernaschi M, Rossi L, Benzi R, Sbragaglia M, and Succi S, *Graphics processing unit implementation of lattice Boltzmann models for flowing soft systems*, Phys. Rev. E **80** (6): 066707, 2009.

[Ber10] Bernaschi M, Fatica M, Melchionna S, Succi S, and Kaxiras E, *A flexible high-performance Lattice Boltzmann GPU code for the simulations of fluid flows in complex geometries*, Concurrency Computat. Pract. Exper. **22** (1): 1, 2010.

[Bha54] Bhatnagar P, Gross E, and Krook M, *A Model for Collision Processes in Gases. I. Small Amplitude Processes in Charged and Neutral One-Component Systems*, Phys. Rev. **94** (3): 511, 1954.

[Bob95] Bobylev A, Palczewskii A, and Schneider J, *Discretization of the Boltzmann equation and discrete velocity models*, in Rarefied Gas Dynamics 19, eds. Harvey J and Lord G **2**: 857, 1995.

[Bog01] Boghosian B, Yepez J, Coveney P, and Wagner A, *Entropic Lattice Boltzmann Methods*, Proc. R. Soc. Lond. Ser. A Math. Phys. Eng. Sci. **457** (2007): 717, 2001.

[Bog03] Boghosian B, Love P, Coveney P, Karlin I, Succi S, and Yepez J, *Galilean-invariant lattice-Boltzmann models with H theorem*, Phys. Rev. E **68** (2): 025103(R), 2003.

[Bog04a] Boghosian B, Love P, Yepez J, and Coveney P, *Galilean-invariant multi-speed entropic lattice Boltzmann models*, Phys. D **193** (1–4): 169, 2004.

[Bog04b] Boghosian B, Love P, and Yepez J, *Entropic lattice Boltzmann model for Burgers's equation*, Philos. Trans. R. Soc. Lond. Ser. A Math. Phys. Eng. Sci. **362** (1821): 1691, 2004.

[Bol72] Boltzmann L, *Weitere Studien über das Wärme gleichgenicht unfer Gas-moläkuler*, Sitzungsberichte Akad. Wiss. **66**: 275, 1872. Translation in [Bru66]: *Further studies on the thermal equilibrium of gas molecules*.

[Bol96] Boltzmann L, *Lectures on gas theory*, University of California Press, Berkeley, 1964. Translated by Brush S, reprint of the 1896–1898 edition.

[Boo91] Boon J, *Statistical mechanics and hydrodynamics of lattice gas automata: An overview*, Phys. D **47** (1–2): 3, 1991.

[Bou01a] Bouzidi M, d'Humières D, Lallemand P, and Luo L-S, *Lattice Boltzmann Equation on a Two-Dimensional Rectangular Grid*, J. Comput. Phys. **172** (2): 704, 2001.

[Bou01b] Bouzidi M, Firdaouss M, and Lallemand P, *Momentum transfer of a Boltzmann-lattice fluid with boundaries*, Phys. Fluids **13** (11): 3452, 2001.

[Bro64a] Broadwell J, *Study of rarefied shear flow by the discrete velocity method*, J. Fluid Mech. **19** (3): 401, 1964.

[Bro64b] Broadwell J, *Shock Structure in a Simple Discrete Velocity Gas*, Phys. Fluids **7** (8): 1243, 1964.

[Bro07] Brownlee R, Gorban A, and Levesley J, *Stability and stabilization of the lattice Boltzmann method*, Phys. Rev. E **75** (3): 036711, 2007.

[Bru66] Brush S, *Kinetic Theory, Volume 2: Irreversible Processes*, Pergamon Press, Oxford, 1966.

[Bru72] Brush S, *Kinetic Theory, Volume 3: The Chapman-Enskog Solution of the Transport Equation for Moderately Dense Gases*, Pergamon Press, Oxford, 1972.

[Bui00] Buick J and Greated C, *Gravity in a lattice Boltzmann model*, Phys. Rev. E **61** (5): 5307, 2000.

[Bur87] Burges C and Zaleski S, *Buoyant Mixtures of Cellular Automaton Gases*, Complex Systems **1** (1): 31, 1987.

[Bur88] Burgess D, Hayot F, and Saam W, *Model for surface tension in lattice-gas hydrodynamics*, Phys. Rev. A **38** (7): 3589, 1988.

[Cai05] Caiazzo A, *Analysis of Lattice Boltzmann Initialization Routines*, J. Statist. Phys. **121** (1–2): 37, 2005.

[Cai09] Caiazzo A, Junk M, and Rheinländer M, *Comparison of analysis techniques for the lattice Boltzmann method*, Comput. Math. Appl. **58** (5): 883, 2009.

[Can90] Cancelliere A, Chang C, Foti E, Rothman D, and Succi S, *The permeability of a random medium: Comparison of simulation with theory*, Phys. Fluids A **2** (12): 2085, 1990.

[Cao97] Cao N, Chen S, Jin S, and Martínez D, *Physical symmetry and lattice symmetry in the lattice Boltzmann method*, Phys. Rev. E **55** (1): R21, 1997.

[Car33] Carleman T, *Sur la théorie de l'équation intégro-differentielle de Boltzmann*, Acta Math. **60**: 91, 1933.

[Car57] Carleman T, *Problèmes Mathématiques dans la Théorie Cinétique des Gaz*, Almqvist & Wiksell, Uppsala, 1957.

[Cer88] Cercignani C, *The Boltzmann equation and its applications*, Applied Mathematical Sciences **67**, Springer-Verlag, New York, 1988.

[Cer89] Cercignani C, *Kinetic theory with "bounce-back" boundary conditions*, Transport Theory. Stat. Phys. **18** (1): 125, 1989.

[Cer94] Cercignani C, Illner R, and Pulvirenti M, *The Mathematical Theory Of Dilute Gases*, Applied Mathematical Sciences **106**, Springer-Verlag, New York, 1994.

[Cer00] Cercignani C, *Rarefied gas dynamics: from basic concepts to actual calculations*, Cambridge texts in applied mathematics, Cambridge University Press, Cambridge, 2000.

[Cer09] Cercignani C, *The Boltzmann equation in the 20th century*, Discrete Contin. Dyn. Syst. **24** (1): 83, 2009.

[Cha16] Chapman S, *The Kinetic Theory of Simple and Composite Monatomic Gases: Viscosity, Thermal Conduction, and Diffusion*, Proc. R. Soc. Lond. A **93** (646): 1, 1916.

[Cha39] Chapman S and Cowling T, *The Mathematical Theory of Non-Uniform Gases*, Cambridge University Press, London, 1939.

[Cha67] Chapman S, *The kinetic theory of gases fifty years ago*, in Lectures in Theoretical Physics **90**: 1, ed. Brittin W, Gordon & Breach, New York, 1967. Reprinted in [Bru72].

[Cha09] Chang C, Liu C-H, and Lin C-A, *Boundary conditions for lattice Boltzmann simulations with complex geometry flows*, Comput. Math. Appl. **58** (5): 940, 2009.

[Che87] Chen H and Matthaeus W, *New cellular automaton model for magnetohydrodynamics*, Phys. Rev. Lett. **58** (18): 1845, 1987.

[Che89a] Chen H, Chen S, Doolen G, Lee Y, and Rose H, *Multithermodynamic phase lattice-gas automata incorporating interparticle potentials*, Phys. Rev. A **40** (5): 2850, 1989.

[Che89b] Chen S, Lee M, Zhao K, and Doolen G, *A lattice gas model with temperature*, Phys. D **37** (1–3): 42, 1989.

[Che89c] Chen S, Chen H, and Doolen G, *How the Lattice Gas Model for the Navier-Stokes Equation Improves When a New Speed is Added*, Complex Systems **3** (3): 243, 1989.

[Che89d] Chen S, She Z-S, Harrison L, and Doolen G, *Optimal initial condition for lattice-gas hydrodynamics*, Phys. Rev. A **39** (5): 2725, 1989.

[Che91a] Chen S, Chen H, Martínez D, and Matthaeus W, *Lattice Boltzmann model for simulation of magnetohydrodynamics*, Phys. Rev. Lett. **67** (27): 3776, 1991.

[Che91b] Chen S, Doolen G, and Matthaeus W, *Lattice gas automata for simple and complex fluids*, J. Statist. Phys. **64** (5–6): 1133, 1991.

[Che92] Chen H, Chen S, and Matthaeus W, *Recovery of the Navier-Stokes equations using a lattice-gas Boltzmann method*, Phys. Rev. A **45** (8): R5339, 1992.

[Che94] Chen Y, Ohashi H, and Akiyama M, *Thermal lattice Bhatnagar-Gross-Krook model without nonlinear deviations in macrodynamic equations*, Phys. Rev. E **50** (4): 2776, 1994.

[Che95a] Chen Y, Ohashi H, and Akiyama M, *Heat transfer in lattice BGK modeled fluid*, J. Statist. Phys. **81** (1–2): 71, 1995.

[Che95b] Chen S, Dawson S, Doolen G, Janecky D, and Lawniczak A, *Lattice methods and their applications to reacting systems*, Computers Chem. Engng **19** (6–7): 617, 1995.

[Che96] Chen S, Martínez D, and Mei R, *On boundary conditions in lattice Boltzmann methods*, Phys. Fluids **8** (9): 2527, 1996.

[Che97a] Chen Y, Ohashi H, and Akiyama M, *Two-Parameter Thermal Lattice BGK Model with a Controllable Prandtl Number*, J. Sci. Comput. **12** (2): 169, 1997.

[Che98a] Chen H, Teixeira C, and Molving K, *Realization of Fluid Boundary Conditions via Discrete Boltzmann Dynamics*, Internat. J. Modern Phys. C **9** (8): 1281, 1998.

[Che98b] Chen H, *Volumetric formulation of the lattice Boltzmann method for fluid dynamics: Basic concept*, Phys. Rev. E **58** (3): 3955, 1998.

[Che06a] Chen H, Zhang R, Staroselsky I, and Jhon M, *Recovery of full rotational invariance in lattice Boltzmann formulations for high Knudsen number flows*, Phys. A **362** (1): 125, 2006.

[Che06b] Chen H, Filippova O, Hoch J, Molvig K, Shock R, Teixeira C, and Zhang R, *Grid refinement in lattice Boltzmann methods based on volumetric formulation*, Phys. A **362** (1): 158, 2006.

[Che08] Chen H, Goldhirsch I, and Orszag S, *Discrete Rotational Symmetry, Moment Isotropy, and Higher Order Lattice Boltzmann Models*, J. Sci. Comput. **34** (1): 87, 2008.

[Chi06a] Chikatamarla S and Karlin I, *Entropy and Galilean Invariance of Lattice Boltzmann Theories*, Phys. Rev. Lett. **97** (19): 190601, 2006.

[Chi06b] Chikatamarla S, Ansumali S, and Karlin I, *Grad's approximation for missing data in lattice Boltzmann simulations*, Europhys. Lett. **74** (2): 215, 2006.

[Chi08] Chikatamarla S and Karlin I, *Complete Galilean invariant lattice Boltzmann models*, Comput. Phys. Comm. **179** (1–3): 140, 2008.

[Chi09] Chikatamarla S and Karlin I, *Lattices for the lattice Boltzmann method*, Phys. Rev. E **79** (4): 046701, 2009.

[Cho88] Chopard B and Droz M, *Cellular automata model for heat conduction in a fluid*, Phys. Lett. A **126** (8–9): 476, 1988.

[Cho03] Chopard B and Dupuis A, *A mass conserving boundary condition for lattice Boltzmann models*, Internat. J. Modern Phys. B **17** (1–2): 103, 2003.

[Chu07] Chun B and Ladd A, *Interpolated boundary condition for lattice Boltzmann simulations of flows in narrow gaps*, Phys. Rev. E **75** (6): 066705, 2007.

[Cla88] Clavin P, Lallemand P, Pomeau Y, and Searby G, *Simulation of free boundaries in flow systems by lattice-gas models*, J. Fluid Mech. **188**: 437, 1988.

[Coo04] Cook B, Noble D, and Williams J, *A direct simulation method for particle-fluid systems*, Eng. Comput. **21** (2–4): 151, 2004.

[Cor91] Cornubert R, d'Humières D, and Levermore D, *A Knudsen layer theory for lattice gases*, Phys. D **47** (1–2): 241, 1991.

[Cou28] Courant R, Friedrichs K, and Lewy H, *Über die partiellen Differenzengleichungen der mathematischen Physik*, Math. Annalen **100** (1): 32, 1928. Translation: *On the Partial Difference Equations of Mathematical Physics*, IBM J. Res. Dev. **11** (2): 215, 1967.

[Cro03] Crouse B, Rank E, Krafczyk M, and Tölke J, *A LB-Based Approach for Adaptive Flow Simulations*, Internat. J. Modern Phys. B **17** (1–2): 109, 2003.

[Dah87] Dahlburg J, Montgomery D, and Doolen G, *Noise and compressibility in lattice-gas fluids*, Phys. Rev. A **36** (5): 2471, 1987.

[Dar98a] Dardis O and McCloskey J, *Lattice Boltzmann scheme with real numbered solid density for the simulation of flow in porous media*, Phys. Rev. E **57** (4): 4834, 1998.

[Dar98b] Dardis O and McCloskey J, *Permeability porosity relationships from numerical simulations of fluid flow*, Geophys. Res. Lett. **25** (9): 1471, 1998.

[Del01] Dellar P, *Bulk and shear viscosities in lattice Boltzmann equations*, Phys. Rev. E **64** (3): 031203, 2001.

[Del02] Dellar P, *Compound waves in a thermohydrodynamic lattice BGK scheme using non-perturbative equilibria*, Europhys. Lett. **57** (5): 690, 2002.

[Del03] Dellar P, *Incompressible limits of lattice Boltzmann equations using multiple relaxation times*, J. Comput. Phys. **190** (2): 351, 2003.

[d'Hu86a] d'Humières D and Lallemand P, *Lattice Gas Models for 3D Hydrodynamics*, Europhys. Lett. **2** (4): 291, 1986.

[d'Hu86b] d'Humières D and Lallemand P, *Lattice gas automata for fluid mechanics*, Phys. A **140** (1–2): 326, 1986.

[d'Hu87a] d'Humières D and Lallemand P, *Numerical Simulations of Hydrodynamics with Lattice Gas Automata in Two Dimensions*, Complex Systems **1** (4): 599, 1987.

[d'Hu87b] d'Humières D, Lallemand P, and Searby G, *Numerical Experiments on Lattice Gases: Mixtures and Galilean Invariance*, Complex Systems **1** (4): 633, 1987.

[d'Hu89] d'Humières D, Qian Y, and Lallemand P, *Invariants in lattice gas models*, in [Mon89]: 102, 1989.

[d'Hu92] d'Humières D, *Generalized lattice-Boltzmann equations*, in *Rarefied gas dynamics: theory and simulations*, eds. Shizgal B and Weave D, Prog. Astronaut. Aeronaut. (AIAA Press, Washington, DC) **159**: 450, 1992.

[d'Hu01] d'Humières D, Bouzidi M, and Lallemand P, *Thirteen-velocity three-dimensional lattice Boltzmann model*, Phys. Rev. E **63** (6): 066702, 2001.

[d'Hu02] d'Humières D, Ginzburg I, Krafczyk M, Lallemand P, and Luo L-S, *Multiple-relaxation-time lattice Boltzmann models in three dimensions*, Phil. Trans. R. Soc. Lond. A **360** (1792): 437, 2002.

[d'Hu09] d'Humières D and Ginzburg I, *Viscosity independent numerical errors for Lattice Boltzmann models: From recurrence equations to "magic" collision numbers*, Comput. Math. Appl. **58** (5): 823, 2009.

[Dub88] Dubrulle B, *Method of computation of the Reynolds number for two models of lattice gas involving violation of semi-detailed balance*, Complex Systems **2** (5): 577, 1988.

[Dub90] Dubrulle B, Frisch U, Hénon M, and Rivet J-P, *Low-viscosity lattice gases*, J. Statist. Phys. **59** (5–6): 1187, 1990.

[Dup00] Dupuis A and Chopard B, *An object oriented approach to lattice gas modeling*, Future Gener. Comput. Syst. **16** (5): 523, 2000.

[Dup03] Dupuis A and Chopard B, *Theory and applications of an alternative lattice Boltzmann grid refinement algorithm*, Phys. Rev. E **67** (6): 066707, 2003.

[Dup08] Dupuis A, Chatelain P, and Koumoutsakos P, *An immersed boundary-lattice-Boltzmann method for the simulation of the flow past an impulsively started cylinder*, J. Comput. Phys. **227** (9): 4486, 2008.

[Düs06] Düster A, Demkowicz L, and Rank E, *High-order finite elements applied to the discrete Boltzmann equation*, Int. J. Numer. Meth. Engng **67** (8): 1094, 2006.

[Ens17] Enskog D, *Kinetische Theorie der Vorgänge in Mässig Verdünnten Gasen*, Doctoral Dissertation, Almqvist & Wiksell, Uppsala, 1917. Translation in [Bru72]: *Kinetic Theory of Processes in Dilute Gases*.

[Ens22] Enskog D, *Kinetische Theorie der Wärmeleitung, Reibung und Selbstdiffusion in Gewissen Verdichten Gasen und Flüssigkeiten*, Kungl. Svenska Veteenskapakad. Handl. **63** (4): 3, 1922. Translation in [Bru72]: *Kinetic Theory of Heat Conduction, Viscosity, and Self-Diffusion in Compressed Gases and Liquids*.

[Fah91] Fahner G, *A Multispeed Model for Lattice Gas Hydrodynamics*, Complex Systems **5** (1): 1, 1991.

[Fen04] Feng Z-G and Michaelides E, *The immersed boundary-lattice Boltzmann method for solving fluid-particles interaction problems*, J. Comput. Phys. **195** (2): 602, 2004.

[Fen10] Feng Y, Han K, and Owen D, *Combined three-dimensional lattice Boltzmann method and discrete element method for modelling fluid-particle interactions with experimental assessment*, Internat. J. Numer. Methods Fluids **81** (2): 229, 2010.

[Fer95] Ferréol B and Rothman D, *Lattice-Boltzmann simulations of flow through Fontainebleau sandstone*, Transp. Porous Media **20** (1–2): 3, 1995.

[Fil97] Filippova O and Hänel D, *Lattice-Boltzmann simulation of gas-particle flow in filters*, Comput. & Fluids **26** (7): 697, 1997.

[Fil98] Filippova O and Hänel D, *Grid Refinement for Lattice-BGK Models*, J. Comput. Phys. **147** (1): 219, 1998.

[Fil00] Filippova O and Hänel D, *Acceleration of Lattice-BGK Schemes with Grid Refinement*, J. Comput. Phys. **165** (2): 407, 2000.

[Fri86] Frisch U, Hasslacher B, and Pomeau Y, *Lattice-Gas Automata for the Navier-Stokes Equation*, Phys. Rev. Lett. **56** (14): 1505, 1986.

[Fri87] Frisch U, d'Humières D, Hasslacher B, Lallemand P, Pomeau Y, and Rivet J-P, *Lattice Gas Hydrodynamics in Two and Three Dimensions*, Complex Systems **1** (4): 649, 1987.

[Gal97] Gallivan M, Noble D, Georgiadis J, and Buckius R, *An evaluation of the bounce-back boundary condition for lattice Boltzmann simulations*, Internat. J. Numer. Methods Fluids **25** (3): 249, 1997.

[Gao94] Gao Y and Sharma M, *A LGA model for fluid flow in heterogeneous porous media*, Transp. Porous Media **17** (1): 1, 1994.

[Gat75] Gatignol R, *Théorie Cinétique des Gaz à Répartition Discrète de Vitesses*, Lectures Notes in Phys. **36**, Springer-Verlag, Berlin, 1975.

[Gat77] Gatignol R, *Kinetic theory boundary conditions for discrete velocity gases*, Phys. Fluids **20** (12): 2022, 1977.

[Gei06] Geier M, Greiner A, and Korvink J, *Cascaded digital lattice Boltzmann automata for high Reynolds number flow*, Phys. Rev. E **73** (6): 066705, 2006.

[Gei09] Geier M, Greiner A, and Korvink J, *A factorized central moment lattice Boltzmann method*, Eur. Phys. J. Special Topics **171** (1): 55, 2009.

[Gel06a] Geller S, Krafczyk M, Tölke J, Turek S, and Hron J, *Benchmark computations based on lattice-Boltzmann, finite element and finite volume methods for laminar flows*, Comput. & Fluids **35** (8–9): 888, 2006.

[Gel06b] Geller S, Tölke J, and Krafczyk M, *Lattice-Boltzmann Method on Quadtree-Type Grids for Fluid-Structure Interaction*, in Vol. **53** of Lect. Notes Comput. Sci. Eng., pp.270–293, Springer, Berlin, 2006.

[Gin94] Ginzbourg I and Adler P, *Boundary flow condition analysis for the three-dimensional lattice Boltzmann model*, J. Phys. II France **4** (2): 191, 1994.

[Gin96] Ginzburg I and d'Humières D, *Local second-order boundary methods for lattice Boltzmann models*, J. Statist. Phys. **84** (5–6): 927, 1996.

[Gin03] Ginzburg I and d'Humières D, *Multireflection boundary conditions for lattice Boltzmann models*, Phys. Rev. E **68** (6): 066614, 2003.

[Gin05] Ginzburg I, *Equilibrium-type and link-type lattice Boltzmann models for generic advection and anisotropic-dispersion equation*, Adv. Water Resour. **28** (11): 1171, 2005.

[Gin07] Ginzburg I, *Lattice Boltzmann modeling with discontinuous collision components: Hydrodynamic and Advection-Diffusion Equations*, J. Statist. Phys. **126** (1): 157, 2007.

[Gin08a] Ginzburg I, Verhaeghe F, and d'Humières D, *Two-relaxation-time Lattice Boltzmann scheme: About parametrization, velocity, pressure and mixed boundary conditions*, Commun. Comput. Phys. **3** (2): 427, 2008.

[Gin08b] Ginzburg I, Verhaeghe F, and d'Humières D, *Study of simple hydrodynamic solutions with the two-relaxation-times lattice Boltzmann scheme*, Commun. Comput. Phys. **3** (3): 519, 2008.

[Gra49a] Grad H, *On the Kinetic Theory of Rarefied Gases*, Comm. Pure Appl. Math. **2** (4): 331, 1949.

[Gra49b] Grad H, *Note on N-Dimensional Hermite Polynomials*, Comm. Pure Appl. Math. **2** (4): 325, 1949.

[Gra58] Grad H, *Principles of the kinetic theory of gases*, Handbuch der physik **12**: 205, ed. Flügge S, Springer-Verlag, Berlin, 1958.

[Gra85] Granger R, *Fluid Mechanics*, Holt-Saunders International Editions, 1985.

[Gro59] Gross E and Jackson E, *Kinetic Models and the Linearized Boltzmann Equation*, Phys. Fluids **2** (4): 432, 1959.

[Gru93] Grunau D, Chen S, and Eggert K, *A lattice Boltzmann model for multiphase fluid flows*, Phys. Fluids A **5** (10): 2557, 1993.

[Gun91] Gunstensen A and Rothman D, *Lattice Boltzmann model of immiscible fluids*, Phys. Rev. A **43** (8): 4320, 1991.

[Gun93] Gunstensen A and Rothman D, *Lattice-Boltzmann Studies of Immiscible Two-Phase Flow Through Porous Media*, J. Geophys. Res. **98** (B4): 6431, 1993.

[Guo00] Guo Z, Shi B, and Wang N, *Lattice BGK model for incompressible Navier-Stokes equation*, J. Comput. Phys. **165** (1): 288, 2000.

[Guo02a] Guo Z, Zheng C, and Shi B, *Discrete lattice effects on the forcing term in the lattice Boltzmann method*, Phys. Rev. E **65** (4): 046308, 2002.

[Guo02b] Guo Z, Zheng C, and Shi B, *An extrapolation method for boundary conditions in lattice Boltzmann method*, Phys. Fluids **14** (6): 2007, 2002.

[Guo04] Guo Z, Zhao T, and Shi Y, *Preconditioned lattice-Boltzmann method for steady flows*, Phys. Rev. E **70** (6): 066706, 2004.

[Guo07] Guo Z, Zheng C, Shi B, and Zhao T, *Thermal lattice Boltzmann equation for low Mach number flows: Decoupling model*, Phys. Rev. E **75** (3): 036704, 2007.

[Hal02] Halliday I, Hammond L, and Care C, *Enhanced closure scheme for lattice Boltzmann equation hydrodynamics*, J. Phys. A: Math. Gen. **35** (12): L157, 2002.

[Han07] Han K, Feng Y, and Owen D, *Coupled lattice Boltzmann and discrete element modelling of fluid-particle interaction problems*, Comput. Struct. **85** (11–14): 1080, 2007.

[Hao10] Hao J and Zhu L, *A lattice Boltzmann based implicit immersed boundary method for fluid-structure interaction*, Comput. Math. Appl. **59** (1): 185, 2010.

[Har72] Hardy J and Pomeau Y, *Thermodynamics and Hydrodynamics for a Modeled Fluid*, J. Math. Phys. **13** (7): 1042, 1972.

[Har73] Hardy J, Pomeau Y, and de Pazzis O, *Time evolution of a two-dimensional model system. I. Invariant states and time correlation functions*, J. Math. Phys. **14** (12): 1746, 1973.

[Har76] Hardy J, de Pazzis O, and Pomeau Y, *Molecular dynamics of a classical lattice gas: Transport properties and time correlation functions*, Phys. Rev. A **13** (5): 1949, 1976.

[Har66] Harris S, *Approach to Equilibrium in a Moderately Dense Discrete Velocity Gas*, Phys. Fluids **9** (7): 1328, 1966.

[Har04] Harris S, *An Introduction to the Theory of the Boltzmann Equation*, republication, Dover Publications, New York, 2004.

[Has87] Hasslacher B, *Discrete fluids*, Los Alamos Sci. **15**: 175, 1987.

[Ház03] Házi G, *Accuracy of the lattice Boltzmann method based on analytical solutions*, Phys. Rev. E **67** (5): 056705, 2003.

[Ház06] Házi G and Kávrán P, *On the cubic velocity deviations in lattice Boltzmann methods*, J. Phys. A: Math. Gen. **39** (12): 3127, 2006.

[He96] He X, Luo L-S, and Dembo M, *Some Progress in Lattice Boltzmann Method. Part I. Nonuniform Mesh Grids*, J. Comput. Phys. **129** (2): 357, 1996.

[He97a] He X and Luo L-S, *A priori derivation of the lattice Boltzmann equation*, Phys. Rev. E **55** (6): R6333, 1997.

[He97b] He X and Luo L-S, *Theory of the lattice Boltzmann method: From the Boltzmann equation to the lattice Boltzmann equation*, Phys. Rev. E **56** (6): 6811, 1997.

[He97c] He X and Luo L-S, *Lattice Boltzmann model for the incompressible Navier-Stokes equation*, J. Statist. Phys. **88** (3–4): 927, 1997.

[He97d] He X, Luo L-S, and Dembo M, *Some progress in the lattice Boltzmann method: Reynolds number enhancement in simulations*, Phys. A **239** (1–3): 276, 1997.

[He97e] He X, Zou Q, Luo L-S, and Dembo M, *Analytic solutions of simple flows and analysis of nonslip boundary conditions for the lattice Boltzmann BGK model*, J. Statist. Phys. **87** (1–2): 115, 1997.

[He98a] He X, Chen S, and Doolen G, *A Novel Thermal Model for the Lattice Boltzmann Method in Incompressible Limit*, J. Comput. Phys. **146** (1): 282, 1998.

[He98b] He X, Shan X, and Doolen G, *Discrete Boltzmann equation model for non-ideal gases*, Phys. Rev. E **57** (1): R13, 1998.

[He02] He X, Doolen G, and Clark T, *Comparison of the lattice Boltzmann method and the artificial compressibility method for Navier–Stokes equations*, J. Comput. Phys. **179** (1): 439, 2002.

[Hec10] Hecht M and Harting J, *Implementation of on-site velocity boundary conditions for D3Q19 lattice Boltzmann simulations*, J. Stat. Mech.: P01018, 2010.

[Hén87a] Hénon M, *Isometric Collision Rules for the Four-Dimensional FCHC Lattice Gas*, Complex Systems **1** (3): 475, 1987.

[Hén87b] Hénon M, *Viscosity of a Lattice Gas*, Complex Systems **1** (4): 763, 1987.

[Hén89] Hénon M, *Optimization of collision rules in the FCHC lattice gas, and addition of rest particles*, in [Mon89]: 146, 1989.

[Hén92] Hénon M, *Implementation of the FCHC lattice gas model on the Connection Machine*, J. Statist. Phys. **68** (3–4): 353, 1992.

[Hig89a] Higuera F and Jiménez J, *Boltzmann Approach to Lattice Gas Simulations*, Europhys. Lett. **9** (7): 663, 1989.

[Hig89b] Higuera F, *Lattice gas simulation based on the Boltzmann equation*, in [Mon89]: 162, 1989.

[Hig89c] Higuera F and Succi S, *Simulating the Flow Around a Circular Cylinder with a Lattice Boltzmann Equation*, Europhys. Lett. **8** (6): 517, 1989.

[Hig89d] Higuera F, Succi S, and Benzi R, *Lattice Gas Dynamics with Enhanced Collisions*, Europhys. Lett. **9** (4): 345, 1989.

[Hil12] Hilbert D, *Begründung der kinetischen Gastheorie*, Math. Annalen **72**: 562, 1912. Translation in [Bru72]: *Foundations of the Kinetic Theory of Gases*.

[Hil85a] Hillis W, *The Connection Machine*, MIT Press Series in Artificial Intelligence, Cambridge, Massachusetts, 1985.

[Hil89] Hillis W, *Richard Feynman and the Connection Machine*, Phys. Today **42** (2): 78, 1989.

[Hil85b] Hilts P, *Discovery in Flow Dynamics May Aid Car, Plane Design*, The Washington Post: Nov 19, 1985.

[Hol04] Holdych D, Noble D, Georgiadis J, and Buckius R, *Truncation error analysis of lattice Boltzmann methods*, J. Comput. Phys. **193** (2): 595, 2004.

[Hol06] Hollis A, Halliday I, and Care C, *Enhanced, mass-conserving closure scheme for lattice Boltzmann equation hydrodynamics*, J. Phys. A: Math. Gen. **39** (33): 10589, 2006.

[Hol08] Hollis A, Halliday I, and Care C, *An accurate and versatile lattice closure scheme for lattice Boltzmann equation fluids under external forces*, J. Comput. Phys. **227** (17): 8065, 2008.

[Hol66] Holway L, *New Statistical Models for Kinetic Theory: Methods of Construction*, Phys. Fluids **9** (9): 1658, 1966.

[Hou95] Hou S, Zou Q, Chen S, Doolen G, and Cogley A, *Simulation of Cavity Flow by the Lattice Boltzmann Method*, J. Comput. Phys. **118** (2): 329, 1995.

[Ima05] Imamura T, Suzuki K, Nakamura T, and Yoshida M, *Acceleration of steady-state lattice Boltzmann simulations on non-uniform mesh using local time step method*, J. Comput. Phys. **202** (2): 645, 2005.

[Ina95] Inamuro T, Yoshino M, and Ogino F, *A non-slip boundary condition for lattice Boltzmann simulations*, Phys. Fluids **7** (12): 2928, 1995.

[Ina97] Inamuro T, Yoshino M, and Ogino F, *Accuracy of the lattice Boltzmann method for small Knudsen number with finite Reynolds number*, Phys. Fluids **9** (11): 3535, 1997.

[Izq09] Izquierdo S, Martínez-Lera P, and Fueyo N, *Analysis of open boundary effects in unsteady lattice Boltzmann simulations*, Comput. Math. Appl. **58** (5): 914, 2009.

[Izq10] Izquierdo S and Fueyo N, *Momentum transfer correction for macroscopic-gradient boundary conditions in lattice Boltzmann methods*, J. Comput. Phys. **229** (7): 2497, 2010.

[Jeo10] Jeong H, Yoon H, Ha M, and Tsutahara M, *An immersed boundary-thermal lattice Boltzmann method using an equilibrium internal energy density approach for the simulation of flows with heat transfer*, J. Comput. Phys. **229** (7): 2526, 2010.

[Jun01] Junk M, *A finite difference interpretation of the lattice Boltzmann method*, Numer. Methods Partial Differential Equations **17** (4): 383, 2001.

[Jun05a] Junk M, Klar A, and Luo L-S, *Asymptotic analysis of the lattice Boltzmann equation*, J. Comput. Phys. **210** (2): 676, 2005.

[Jun05b] Junk M and Yang Z, *One-point boundary condition for the lattice Boltzmann method*, Phys. Rev. E **72** (6): 066701, 2005.

[Jun05c] Junk M and Yang Z, *Asymptotic Analysis of Lattice Boltzmann Boundary Conditions*, J. Statist. Phys. **121** (1–2): 3, 2005.

[Jun08a] Junk M and Rheinländer M, *Regular and multiscale expansions of a lattice Boltzmann method*, Progr. Comput. Fluid Dynam. Int. J. **8** (1–4): 25, 2008.

[Jun08b] Junk M and Yang Z, *Outflow boundary conditions for the lattice Boltzmann method*, Progr. Comput. Fluid Dynam. Int. J. **8** (1–4): 38, 2008.

[Jun09] Junk M and Yang Z, *Pressure boundary condition for the lattice Boltzmann method*, Comput. Math. Appl. **58** (5): 922, 2009.

[Kad86] Kadanoff L, *On two levels*, Phys. Today **39** (9): 7, 1986.

[Kad87] Kadanoff L, McNamara G, and Zanetti, *A Poiseuille Viscometer for Lattice Gas Automata*, Complex Systems **1** (4): 791, 1987.

[Kad89] Kadanoff L, McNamara G, and Zanetti G, *From automata to fluid flow: Comparisons of simulation and theory*, Phys. Rev. A **40** (8): 4527, 1989.

[Kan98] Kandhai D, Koponen A, Hoekstra A, Kataja M, Timonen J, and Sloot P, *Lattice-Boltzmann hydrodynamics on parallel systems*, Comput. Phys. Comm. **111** (1–3): 14, 1998.

[Kan99a] Kandhai D, Vidal D, Hoekstra A, Hoefsloot H, Iedema P, and Sloot P, *Lattice-Boltzmann and finite element simulations of fluid flow in a SMRX static mixer reactor*, Internat. J. Numer. Methods Fluids **31** (6): 1019, 1999.

[Kan99b] Kandhai D, Koponen A, Hoekstra A, Kataja M, Timonen J, and Sloot P, *Implementation Aspects of 3D Lattice-BGK: Boundaries, Accuracy, and a New Fast Relaxation Method*, J. Comput. Phys. **150** (2): 482, 1999.

[Kan00] Kandhai D, Soll W, Chen S, Hoekstra A, and Sloot P, *Finite-Difference Lattice-BGK methods on nested grids*, Comput. Phys. Comm. **129** (1–3): 100, 2000.

[Kan01] Kandhai D, Koponen A, Hoekstra A, and Sloot P, *Iterative momentum relaxation for fast lattice-Boltzmann simulations*, Future Gener. Comput. Syst. **18** (1): 89, 2001.

[Kao08] Kao P-H and Yang R-J, *An investigation into curved and moving boundary treatments in the lattice Boltzmann method*, J. Comput. Phys. **227** (11): 5671, 2008.

[Kar98a] Karlin I, Gorban A, Succi S, and Boffi V, *Maximum Entropy Principle for Lattice Kinetic Equations*, Phys. Rev. Lett. **81** (1): 6, 1998.

[Kar98b] Karlin I and Succi S, *Equilibria for discrete kinetic equations*, Phys. Rev. E **58** (4): R4053, 1998.

[Kar99] Karlin I, Ferrante A, and Öttinger H, *Perfect entropy functions of the Lattice Boltzmann method*, Europhys. Lett. **47** (2): 182, 1999.

[Kar10] Karlin I and Asinari P, *Factorization symmetry in the lattice Boltzmann method*, Phys. A **389** (8): 1530, 2010.

[Kau09] Kaufman A, Fan Z, and Petkov K, *Implementing the lattice Boltzmann model on commodity graphics hardware*, J. Stat. Mech.: P06016, 2009.

[Kea07] Keating B, Vahala G, Yepez J, Soe M, and Vahala L, *Entropic lattice Boltzmann representations required to recover Navier-Stokes flows*, Phys. Rev. E **75** (3): 036712, 2007.

[Kel48] Keller J, *On the Solution of the Boltzmann Equation for Rarefied Gases*, Comm. Pure App. Math. **1** (3): 275, 1948.

[Kim00] Kim I, *Second order bounce back boundary condition for the lattice Boltzmann fluid simulation*, KSME Int. J. **14** (1): 84, 2000.

[Kin92] Kingdon R, Schofield P, and White L, *A lattice Boltzmann model for the simulation of fluid flow*, J. Phys. A: Math. Gen. **25** (12): 3559, 1992.

[Kob03] Kobori T and Maruyama T, *A High Speed Computation System for 3D FCHC Lattice Gas Model with FPGA*, in Vol. **2778** of Lecture Notes in Comput. Sci., pp.755–765, Springer, Berlin, 2003.

[Koe91] Koelman J, *A Simple Lattice Boltzmann Scheme for Navier-Stokes Fluid Flow*, Europhys. Lett. **15** (6): 603, 1991.

[Kop98] Koponen A, Kandhai D, Hellén E, Alava M, Hoekstra A, Kataja M, Niskanen K, Sloot P, and Timonen J, *Permeability of Three-Dimensional Random Fiber Webs*, Phys. Rev. Lett. **80** (4): 716, 1998.

[Kos09] Kosuge S, *Model Boltzmann equation for gas mixtures: Construction and numerical comparison*, Eur. J. Mech. B - Fluids **28** (1): 170, 2009.

[Kow03] Kowarschik M and Weiß C, *An Overview of Cache Optimization Techniques and Cache-Aware Numerical Algorithms*, in Vol. **2625** of Lecture Notes in Comput. Sci., pp.213–232, Springer, Berlin, 2003.

[Kut06] Kutay M, Aydilek A, and Masad E, *Laboratory validation of lattice Boltzmann method for modeling pore-scale flow in granular materials*, Comput. Geotech. **33** (8): 381, 2006.

[Kuz10] Kuznik F, Obrecht C, Rusaouen G, and Roux J-J, *LBM based flow simulation using GPU computing processor*, Comput. Math. Appl.: Article in Press, 2010.

[Lad88] Ladd A, Colvin M, and Frenkel D, *Application of lattice-gas cellular automata to the Brownian motion of solids in suspension*, Phys. Rev. Lett. **60** (11): 975, 1988.

[Lad90] Ladd A and Frenkel D, *Dissipative hydrodynamic interactions via lattice-gas cellular automata*, Phys. Fluids A **2** (11): 1921, 1990.

[Lad93] Ladd A, *Short-time motion of colloidal particles: Numerical simulation via a fluctuating lattice-Boltzmann equation*, Phys. Rev. Lett. **70** (9): 1339, 1993.

[Lad94a] Ladd A, *Numerical simulations of particulate suspensions via a discretized Boltzmann equation. Part 1. Theoretical foundation*, J. Fluid Mech. **271**: 285, 1994.

[Lad94b] Ladd A, *Numerical simulations of particulate suspensions via a discretized Boltzmann equation. Part 2. Numerical results*, J. Fluid Mech. **271**: 311, 1994.

[Lad01] Ladd A and Verberg R, *Lattice-Boltzmann Simulations of Particle-Fluid Suspensions*, J. Statist. Phys. **104** (5–6): 1191, 2001.

[Lai01] Lai Y, Lin C-L, and Huang J, *Accuracy and efficiency study of Lattice Boltzmann method for steady-state flow simulations*, Numer. Heat Transfer Part B **39** (1): 21, 2001.

[Lal00] Lallemand P and Luo L-S, *Theory of the lattice Boltzmann method: Dispersion, dissipation, isotropy, Galilean invariance, and stability*, Phys. Rev. E **61** (6): 6546, 2000.

[Lal03a] Lallemand P and Luo L-S, *Theory of the lattice Boltzmann method: Acoustic and thermal properties in two and three dimensions*, Phys. Rev. E **68** (3): 036706, 2003.

[Lal03b] Lallemand P, and Luo L-S, *Lattice Boltzmann method for moving boundaries*, J. Comput. Phys. **184** (2): 406, 2003.

[Lav91] Lavallée P, Boon J, and Noullez A, *Boundaries in lattice gas flows*, Phys. D **47** (1–2): 233, 1991.

[Lee01] Lee T and Lin C-L, *A Characteristic Galerkin Method for Discrete Boltzmann Equation*, J. Comput. Phys. **171** (1): 336, 2001.

[Lee03] Lee T and Lin C-L, *An Eulerian description of the streaming process in the lattice Boltzmann equation*, J. Comput. Phys. **185** (2): 445, 2003.

[Lee09] Van Leemput P, Rheinländer M, and Junk M, *Smooth initialization of lattice Boltzmann schemes*, Comput. Math. Appl. **58** (5): 867, 2009.

[LeV02] LeVeque R, *Finite Volume Methods for Hyperbolic Problems*, Cambridge University Press, Cambridge, 2002.

[Li04] Li Y, LeBoeuf E, and Basu P, *Least-squares finite-element lattice Boltzmann method*, Phys. Rev. E **69** (6): 065701(R), 2004.

[Lia10] Liao C-C, Chang Y-W, Lin C-A, and McDonough J, *Simulating flows with moving rigid boundary using immersed-boundary method*, Comput. & Fluids **39** (1): 152, 2010.

[Lin96] Lin Z, Fang H, and Tao R, *Improved lattice Boltzmann model for incompressible two-dimensional steady flows*, Phys. Rev. E **54** (6): 6323, 1996.

[Lin00] Lin C-L and Lai Y, *Lattice Boltzmann method on composite grids*, Phys. Rev. E **62** (2): 2219, 2000.

[Liu08] Liu B and Khalili A, *Acceleration of steady-state lattice Boltzmann simulations for exterior flows*, Phys. Rev. E **78** (5): 056701, 2008.

[Lon93] Longo E, Preziosi L, and Bellomo N, *The semicontinuous Boltzmann equation: Towards a model for fluid dynamic applications*, Math. Models Methods Appl. Sci. **3** (1): 65, 1993.

[Luo98] Luo L-S, *Unified Theory of Lattice Boltzmann Models for Nonideal Gases*, Phys. Rev. Lett. **81** (8): 1618, 1998.

[Luo00a] Luo L-S, *Theory of the lattice Boltzmann method: Lattice Boltzmann models for nonideal gases*, Phys. Rev. E **62** (4): 4982, 2000.

[Luo00b] Luo L-S, *Some recent results on discrete velocity models and ramifications for lattice Boltzmann equation*, Comput. Phys. Comm. **129** (1–3): 63, 2000.

[Lät06] Lätt J and Chopard B, *Lattice Boltzmann method with regularized pre-collision distribution functions*, Math. Comput. Simulation **72** (2–6): 165, 2006.

[Lät08] Lätt J, Chopard B, Malaspinas O, Deville M, and Michler A, *Straight velocity boundaries in the lattice Boltzmann method*, Phys. Rev. E **77** (5): 056703, 2008.

[Mai96] Maier R, Bernard R, and Grunau D, *Boundary conditions for the lattice Boltzmann method*, Phys. Fluids **8** (7): 1788, 1996.

[Mar86] Margolus N, Toffoli T, and Vichniac G, *Cellular-Automata Supercomputers for Fluid-Dynamics Modeling*, Phys. Rev. Lett. **56** (16): 1694, 1986.

[Mar87] Margolus N and Toffoli T, *Cellular Automata Machines*, Complex Systems **1** (5): 967, 1987.

[Mar09] Marié S, Ricot D, and Sagaut P, *Comparison between lattice Boltzmann method and Navier-Stokes high order schemes for computational aeroacoustics*, J. Comput. Phys. **228** (4): 1056, 2009.

[Mar94] Martínez D, Matthaeus W, Chen S, and Montgomery D, *Comparison of spectral method and lattice Boltzmann simulations of two-dimensional hydrodynamics*, Phys. Fluids **6** (3): 1285, 1994.

[Mar96] Martys N and Chen H, *Simulation of multicomponent fluids in complex three-dimensional geometries by the lattice Boltzmann method*, Phys. Rev. E **53** (1): 743, 1996.

[Mar98] Martys N, Shan X, and Chen H, *Evaluation of the external force term in the discrete Boltzmann equation*, Phys. Rev. E **58** (5): 6855, 1998.

[Mar02] Martys N and Hagedorn J, *Multiscale modeling of fluid transport in heterogeneous materials using discrete Boltzmann methods*, Mater. Struct. **35** (10): 650, 2002.

[Mas02] Massaioli F and Amati G, *Achieving high performance in a LBM code using OpenMP*, in Proceedings of the Fourth European Workshop on OpenMP, Roma, Italy, 2002.

[Mav06] Mavriplis D, *Multigrid solution of the steady-state lattice Boltzmann equation*, Comput. & Fluids **35** (8–9): 793, 2006.

[Max60a] Maxwell J, *Illustrations of the Dynamical Theory of Gases. Part I. On the Motions and Collisions of Perfectly Elastic Spheres*, Lond. Edinb. Dubl. Phil. Mag. **19**: 19, 1860.

[Max60b] Maxwell J, *Illustrations of the Dynamical Theory of Gases. Part II. On the Process of Diffusion of Two or More Kinds of Moving Particles Among One Another*, Lond. Edinb. Dubl. Phil. Mag. **20**: 21, 1860.

[Max67] Maxwell J, *On the dynamical Theory of Gases*, Phil. Trans. R. Soc. Lond. **157**: 49, 1867.

[Max79a] Maxwell J, *On Stresses in Rarified Gases Arising from Inequalities of Temperature*, Phil. Trans. R. Soc. Lond. **170**: 231, 1879.

[Max79b] Maxwell J, *On Boltzmann's Theorem on the average distribution of energy in a system of material points*, Trans. Cambr. Phil. Soc. **12**: 547, 1879.

[McN88] McNamara G and Zanetti G, *Use of the Boltzmann Equation to Simulate Lattice-Gas Automata*, Phys. Rev. Lett. **61** (20): 2332, 1988.

[McN93] McNamara G and Alder B, *Analysis of the lattice Boltzmann treatment of hydrodynamics*, Phys. A **194** (1–4): 218, 1993.

[McN95] McNamara G, Garcia A, and Alder B, *Stabilization of thermal lattice Boltzmann models*, J. Statist. Phys. **81** (1–2): 395, 1995.

[McN97] McNamara G, Garcia A, and Alder B, *A hydrodynamically correct thermal lattice Boltzmann model*, J. Statist. Phys. **87** (5–6): 1111, 1997.

[McQ97] McQuarrie D and Simon J, *Physical Chemistry: A Molecular Approach*, University Science Books, Sausalito, CA, 1997.

[Mei99] Mei R, Luo L-S, and Shyy W, *An Accurate Curved Boundary Treatment in the Lattice Boltzmann Method*, J. Comput. Phys. **155** (2): 307, 1999.

[Mei00] Mei R, Shyy W, Yu D, and Luo L-S, *Lattice Boltzmann Method for 3-D Flows with Curved Boundary*, J. Comput. Phys. **161** (2): 680, 2000.

[Mei06] Mei R, Luo L-S, Lallemand P, and d'Humières D, *Consistent initial conditions for lattice Boltzmann simulations*, Comput. & Fluids **35** (8–9): 855, 2006.

[Mie00] Mieussens L, *Discrete velocity model and implicit scheme for the BGK equation of rarefied gas dynamics*, Math. Models Methods Appl.Sci. **10** (8): 1121, 2000.

[Mie04] Mieussens L and Struchtrup H, *Numerical comparison of Bhatnagar-Gross-Krook models with proper Prandtl number*, Phys. Fluids **16** (8): 2797, 2004.

[Mol89] Molvig K, Donis P, Myczkowski J, and Vichniac G, *Removing the Discreteness Artifacts in 3D Lattice-Gas Fluids*, in [Mon89]: 409, 1989.

[Mon89] Monaco R (ed.), Proceedings of Workshop *Discrete Kinematic Theory, Lattice Gas Dynamics and Foundations of Hydrodynamics*, World Scientific, Singapore, 1989.

[Mon91] Monaco R and Preziosi L, *Fluid dynamic applications of the discrete Boltzmann equation*, Ser. Adv. Math. Appl. Sci. **3**, World Scientific, Singapore, 1991.

[Mon87] Montgomery D and Doolen G, *Magnetohydrodynamic cellular automata*, Phys. Lett. A **120** (5): 229, 1987.

[Nan92] Nannelli F and Succi S, *The lattice Boltzmann equation on irregular lattices*, J. Statist. Phys. **68** (3–4): 401, 1992.

[Nie08a] Nie X, Shan X, and Chen H, *Galilean invariance of lattice Boltzmann models*, Europhys. Lett. **81** (3): 34005, 2008.

[Nie08b] Nie X, Shan X, and Chen H, *Thermal lattice Boltzmann model for gases with internal degrees of freedom*, Phys. Rev. E **77** (3): 035701(R), 2008.

[Niu06] Niu X, Shu C, Chew Y, and Peng Y, *A momentum exchange-based immersed boundary-lattice Boltzmann method for simulating incompressible viscous flows*, Phys. Lett. A **354** (3): 173, 2006.

[Nob95a] Noble D, Chen S, Georgiadis J, and Buckius R, *A consistent hydrodynamic boundary condition for the lattice Boltzmann method*, Phys. Fluids **7** (1): 203, 1995.

[Nob95b] Noble D, Georgiadis J, and Buckius R, *Direct assessment of lattice Boltzmann hydrodynamics and boundary conditions for recirculating flows*, J. Statist. Phys. **81** (1–2): 17, 1995.

[Nob96] Noble D, Georgiadis J, and Buckius R, *Comparison of accuracy and performance for lattice Boltzmann and finite difference simulations of steady viscous flow*, Internat. J. Numer. Methods Fluids **23** (1): 1, 1996.

[Nob98] Noble D and Torczynski J, *A Lattice-Boltzmann Method for Partially Saturated Computational Cells*, Internat. J. Modern Phys. C **9** (8): 1189, 1998.

[Ors86] Orszag S and Yakhot V, *Reynolds Number Scaling of Cellular-Automaton Hydrodynamics*, Phys. Rev. Lett. **56** (16): 1691, 1986.

[Pal97] Palczewski A, Schneider J, and Bobylev A, *A Consistency Result for a Discrete-Velocity Model of the Boltzmann Equation*, SIAM J. Numer. Anal. **34** (5): 1865, 1997.

[Pan04] Pan C, Prins J, and Miller C, *A high-performance lattice Boltzmann implementation to model flow in porous media*, Comput. Phys. Comm. **158** (2): 89, 2004.

[Pat09] Patil D and Lakshmisha K, *Finite volume TVD formulation of lattice Boltzmann simulation on unstructured mesh*, J. Comput. Phys. **228** (14): 5262, 2009.

[Pav98] Pavlo P, Vahala G, and Vahala L, *Higher Order Isotropic Velocity Grids in Lattice Methods*, Phys. Rev. Lett. **80** (18): 3960, 1998.

[Pen99] Peng G, Xi H, Duncan C, and Chou S-H, *Finite volume scheme for the lattice Boltzmann method on unstructured meshes*, Phys. Rev. E **59** (4): 4675, 1999.

[Pen04] Peng Y, Shu C, and Chew Y, *A 3D incompressible thermal lattice Boltzmann model and its application to simulate natural convection in a cubic cavity*, J. Comput. Phys. **193** (1): 260, 2004.

[Phi06] Philippi P, Hegele L, Jr., dos Santos L, and Surmas R, *From the continuous to the lattice Boltzmann equation: The discretization problem and thermal models*, Phys. Rev. E **73** (5): 056702, 2006.

[Pla88] Platkowski T and Illner R, *Discrete Velocity Models of the Boltzmann Equation: a Survey on the Mathematical Aspects of the Theory*, SIAM Rev. **30** (2): 213, 1988.

[Poh03] Pohl T, Kowarschik M, Wilke J, Iglberger K, and Rüde U, *Optimization and profiling of the cache performance of parallel lattice boltzmann codes*, Parallel Process. Lett. **13** (4): 549, 2003.

[Pra07] Prasianakis N and Karlin I, *Lattice Boltzmann method for thermal flow simulation on standard lattices*, Phys. Rev. E **76** (1): 016702, 2007.

[Pra09] Prasianakis N, Karlin I, Mantzaras J, and Boulouchos K, *Lattice Boltzmann method with restored Galilean invariance*, Phys. Rev. E **79** (6): 066702, 2009.

[Pre93] Preziosi L, *The semicontinuous Boltzmann equation for gas mixtures*, Math. Models Methods Appl. Sci. **3** (5): 665, 1993.

[Pre97] Preziosi L and Longo E, *On a conservative polar discretization of the Boltzmann equation*, Japan J. Indust. Appl. Math. **14** (3): 399, 1997.

[Pre09] Premnath K, Pattison M, and Banerjee S, *Steady state convergence acceleration of the generalized lattice Boltzmann equation with forcing term through preconditioning*, J. Comput. Phys. **228** (3): 746, 2009.

[Pun94] Punzo G, Massaioli F, and Succi S, *High-resolution lattice-Boltzmann computing on the IBM SP1 scalable parallel computer*, Comput. Phys. **8** (6): 705, 1994.

[Qia92] Qian Y, d'Humières D, and Lallemand P, *Lattice BGK Models for Navier-Stokes Equation*, Europhys. Lett. **17** (6): 479, 1992.

[Qia93a] Qian Y and Orszag S, *Lattice BGK Models for the Navier-Stokes Equation: Nonlinear Deviation in Compressible Regimes*, Europhys. Lett. **21** (3): 255, 1993.

[Qia93b] Qian Y, *Simulating thermohydrodynamics with lattice BGK models*, J. Sci. Comput. **8** (3): 231, 1993.

[Qia98] Qian Y and Zhou Y, *Complete Galilean-invariant lattice BGK models for the Navier-Stokes equation*, Europhys. Lett. **42** (4): 359, 1998.

[Raa04] Raabe D, *Overview of the lattice Boltzmann method for nano- and microscale fluid dynamics in materials science and engineering*, Modelling Simul. Mater. Sci. Eng. **12** (6): R13, 2004.

[Ree03] Reese J, Gallis M, and Lockerby D, *New Directions in Fluid Dynamics: Non-Equilibrium Aerodynamic and Microsystem Flows*, Philos. Trans. R. Soc. Lond. Ser. A Math. Phys. Eng. Sci. **361** (1813): 2967, 2003.

[Reg96] de Regt H, *Philosophy and the Kinetic Theory of Gases*, Brit. J. Phil. Sci. **47** (1): 31, 1996.

[Rei95] Reider M and Sterling J, *Accuracy of discrete-velocity BGK models for the simulation of the incompressible Navier-Stokes equations*, Comput. & Fluids **24** (4): 459, 1995.

[Rem89] Rem P and Somers J, *Cellular automata on a transputer network*, in [Mon89]: 268, 1989.

[Ren98] Renda A, Bella G, Succi S, and Karlin I, *Thermohydrodynamic lattice BGK schemes with non-perturbative equilibria*, Europhys. Lett. **41** (3): 279, 1998.

[Rei05] Rheinländer M, *A Consistent Grid Coupling Method for Lattice-Boltzmann Schemes*, J. Statist. Phys. **121** (1–2): 49, 2005.

[Rie09] Riegel E, Indinger T, and Adams N, *Implementation of a Lattice-Boltzmann method for numerical fluid mechanics using the nVIDIA CUDA technology*, Computer Science - R&D **23** (3–4): 241, 2009.

[Ris95] Risteen A, *Molecules and the Molecular Theory of Matter*, Ginn & Company, Boston, 1895.

[Riv88] Rivet J-P, Hénon M, Frisch U, and d'Humières D, *Simulating Fully Three-Dimensional External Flow by Lattice Gas Methods*, Europhys. Lett. **7** (3): 231, 1988.

[Roh02] Rohde M, Derksen J, and Van den Akker H, *Volumetric method for calculating the flow around moving objects in lattice-Boltzmann schemes*, Phys. Rev. E **65** (5): 056701, 2002.

[Roh03] Rohde M, Kandhai D, Derksen J, and Van den Akker H, *Improved bounce-back methods for no-slip walls in lattice-Boltzmann schemes: Theory and simulations*, Phys. Rev. E **67** (6): 066703, 2003.

[Roh06] Rohde M, Kandhai D, Derksen J, and Van den Akker H, *A generic, mass conservative local grid refinement technique for lattice-Boltzmann schemes*, Internat. J. Numer. Methods Fluids **51** (4): 439, 2006.

[Ros05] Rossi N, Ubertini S, Bella G, and Succi S, *Unstructured lattice Boltzmann method in three dimensions*, Internat. J. Numer. Methods Fluids **49** (6): 619, 2005.

[Rot88a] Rothman D, *Cellular-automaton fluids: A model for flow in porous media*, Geophysics **53** (4): 509, 1988.

[Rot88b] Rothman D and Keller J, *Immiscible cellular-automaton fluids*, J. Statist. Phys. **52** (2–3): 1119, 1988.

[Rot89a] Rothman D, *Negative-viscosity lattice gases*, J. Statist. Phys. **56** (3–4): 517, 1989.

[Rot89b] Rothman D, *Lattice-gas automata for immiscible two-phase flow*, in [Mon89]: 286, 1989.

[Rot97] Rothman D and Zaleski S, *Lattice-Gas Cellular Automata: Simple Models of Complex Hydrodynamics*, Cambridge University Press, Cambridge, UK, 1997.

[Rub08] Rubinstein R and Luo L-S, *Theory of the lattice Boltzmann equation: Symmetry properties of discrete velocity sets*, Phys. Rev. E **77** (3): 036709, 2008.

[Sbr05] Sbragaglia M and Succi S, *Analytical calculation of slip flow in lattice Boltzmann models with kinetic boundary conditions*, Phys. Fluids **17** (9): 093602, 2005.

[Sbr06] Sbragaglia M and Succi S, *A note on the lattice Boltzmann method beyond the Chapman-Enskog limits*, Europhys. Lett. **73** (3): 370, 2006.

[Sbr09] Sbragaglia M, Benzi R, Biferale L, Chen H, Shan X, and Succi S, *Lattice Boltzmann method with self-consistent thermo-hydrodynamic equilibria*, J. Fluid Mech. **628**: 299, 2009.

[Sch73] Schnute J and Shinbrot M, *Kinetic theory and boundary conditions for fluids*, Can. J. Math. **25** (6): 1183, 1973.

[Sch02] Schulz M, Krafczyk M, Tölke J, and Rank E, *Parallelization strategies and efficiency of CFD computations in complex geometries using lattice Boltzmann methods on high-performance computers*, in Vol. **21** of Lect. Notes Comput. Sci. Eng., pp.115–122, Springer, Berlin, 2002.

[Sea89] Searby G, Zenlé V, and Denet B, *Lattice gas mixtures and reactive flows*, in [Mon89]: 300, 1989.

[Ser08] Servan-Camas B and Tsai F, *Lattice Boltzmann method with two relaxation times for advection-diffusion equation: Third order analysis and stability analysis*, Adv. Water Resour. **31** (8): 1113, 2008.

[Set02] Seta T and Takahashi R, *Numerical Stability Analysis of FDLBM*, J. Statist. Phys. **107** (1–2): 557, 2002.

[Sha93] Shan X and Chen H, *Lattice Boltzmann model for simulating flows with multiple phases and components*, Phys. Rev. E **47** (3): 1815, 1993.

[Sha94] Shan X and Chen H, *Simulation of nonideal gases and liquid-gas phase transitions by the lattice Boltzmann equation*, Phys. Rev. E **49** (4): 2941, 1994.

[Sha98] Shan X and He X, *Discretization of the Velocity Space in the Solution of the Boltzmann Equation*, Phys. Rev. Lett. **80** (1): 65, 1998.

[Sha06] Shan X, Yuan X-F, and Chen H, *Kinetic Theory Representation of Hydrodynamics: A Way Beyond the Navier-Stokes Equation*, J. Fluid Mech. **550**: 413, 2006.

[Shi78] Shinbrot M, *Entropy change and the no-slip condition*, Arch. Rational Mech. Anal. **67** (4): 351, 1978.

[Shi03] Shi X, Lin J, and Z Yu, *Discontinuous Galerkin spectral element lattice Boltzmann method on triangular element*, Internat. J. Numer. Methods Fluids **42** (11): 1249, 2003 .

[Shu07] Shu C, Liu N, and Chew Y, *A novel immersed boundary velocity correction-lattice Boltzmann method and its application to simulate flow past a circular cylinder*, J. Comput. Phys. **226** (2): 1607, 2007.

[Sie08] Siebert D, Hegele L, Jr., and Philippi P, *Lattice Boltzmann equation linear stability analysis: Thermal and athermal models*, Phys. Rev. E **77** (2): 026707, 2008.

[Sko93] Skordos P, *Initial and boundary conditions for the lattice Boltzmann method*, Phys. Rev. E **48** (6): 4823, 1993.

[Soe98] Soe M, Vahala G, Pavlo P, Vahala L, and Chen H, *Thermal lattice Boltzmann simulations of variable Prandtl number turbulent flows*, Phys. Rev. E **57** (4): 4227, 1998.

[Sof03] Sofonea V and Sekerka R, *Viscosity of finite difference lattice Boltzmann models*, J. Comput. Phys. **184** (2): 422, 2003.

[Sof05] Sofonea V and Sekerka R, *Diffuse-reflection boundary conditions for a thermal lattice Boltzmann model in two dimensions: Evidence of temperature jump and slip velocity in microchannels*, Phys. Rev. E **71** (6): 066709, 2005.

[Sof06] Sofonea V, *Lattice Boltzmann approach to thermal transpiration*, Phys. Rev. E **74** (5): 056705, 2006.

[Som90] Somers J and Rem P, *The construction of efficient collision tables for fluid flow computations with cellular automata*, in vol. 46 of Springer Proceedings in Physics: *Cellular Automata and Modeling of Complex Physical Systems*, ed. Manneville P et al., Springer-Verlag, Berlin: 161, 1990.

[Som91] Somers J and Rem P, *Flow computation with lattice gases*, Appl. Sci. Res. **48** (3–4): 391, 1991.

[Som92] Somers J and Rem P, *Obtaining numerical results from the 3D FCHC-lattice gas*, in Vol. **398** of Lecture Notes in Phys., pp.59–78, Springer, Berlin, 1992.

[Ste96] Sterling J and Chen S, *Stability Analysis of Lattice Boltzmann Methods*, J. Comput. Phys. **123** (1): 196, 1996.

[Sti06] Stiebler M, Tölke J, and Krafczyk M, *An upwind discretization scheme for the finite volume lattice Boltzmann method*, Comput. & Fluids **35** (8–9): 814, 2006.

[Str07] Strack O and Cook B, *Three-dimensional immersed boundary conditions for moving solids in the lattice-Boltzmann method*, Internat. J. Numer. Methods Fluids **55** (2): 103, 2007.

[Str05] Struchtrup H, *Macroscopic Transport Equations for Rarefied Gas Flows: Approximation Methods in Kinetic Theory*, Springer, Heidelberg, 2005.

[Suc88] Succi S, Santangelo P, and Benzi R, *High-Resolution Lattice-Gas Simulation of Two-Dimensional Turbulence*, Phys. Rev. Lett. **60** (26): 2738, 1988.

[Suc89] Succi S, Foti E, and Higuera F, *Three-Dimensional Flows in Complex Geometries with the Lattice Boltzmann Method*, Europhys. Lett. **10** (5): 433, 1989.

[Suc01a] Succi S, *The lattice Boltzmann equation for fluid dynamics and beyond*, Oxford University Press, Oxford, 2001.

[Suc01b] Succi S, Filippova O, Smith G, and Kaxiras E, *Applying the lattice Boltzmann equation to multiscale fluid problems*, Computing in Sci. & Eng. **3** (6): 26, 2001.

[Suc02] Succi S, Karlin I, and Hudong C, *Colloquium: Role of the H theorem in lattice Boltzmann hydrodynamic simulations*, Rev. Mod. Phys. **74** (4): 1203, 2002.

[Suc08] Succi S, *Lattice Boltzmann across scales: from turbulence to DNA translocation*, Eur. Phys. J. B **64** (3–4): 471, 2008.

[Swi95] Swift M, Osborn W, and Yeomans J, *Lattice Boltzmann Simulation of Nonideal Fluids*, Phys. Rev. Lett. **75** (5): 830, 1995.

[Swi96] Swift M, Orlandini E, Osborn W, and Yeomans J, *Lattice Boltzmann simulations of liquid-gas and binary fluid systems*, Phys. Rev. E **54** (5): 5041, 1996.

[Tho04] Thornton S and Marion J, *Classical Dynamics of Particles and Systems*, 5th edition, Brooks/Cole, 2004.

[Tof84] Toffoli T, *CAM: A high-performance cellular-automaton machine*, Phys. D **10** (1–2): 195, 1984.

[Töl98] Tölke J, Krafczyk M, Schulz M, Rank E, and Berrios R, *Implicit discretization and nonuniform mesh refinement approaches for FD discretizations of LBGK Models*, Internat. J. Modern Phys. C **9** (8): 1143, 1998.

[Töl02] Tölke J, Krafczyk M, and Rank E, *A Multigrid-Solver for the Discrete Boltzmann Equation*, J. Statist. Phys. **107** (1–2): 573, 2002.

[Töl06] Tölke J, Freudiger S, and Krafczyk M, *An adaptive scheme using hierarchical grids for lattice Boltzmann multi-phase flow simulations*, Comput. & Fluids **35** (8–9): 820, 2006.

[Töl08] Tölke J and Krafczyk M, *TeraFLOP computing on a desktop PC with GPUs for 3D CFD*, Int. J. Comput. Fluid Dyn. **22** (7): 443, 2008.

[Töl10] Tölke J, *Implementation of a Lattice Boltzmann kernel using the Compute Unified Device Architecture developed by nVIDIA*, Comput. Visual. Sci. **13** (1): 29, 2010.

[Ube04] Ubertini S, Succi S, and Bella G, *Lattice Boltzmann Schemes without Coordinates*, Philos. Trans. R. Soc. Lond. Ser. A Math. Phys. Eng. Sci. **362** (1821): 1763, 2004.

[Ube06] Ubertini S, Bella G, and Succi S, *Unstructured lattice Boltzmann equation with memory*, Math. Comput. Simulation **72** (2–6): 237, 2006.

[Ube08] Ubertini S and Succi S, *A generalised Lattice Boltzmann equation on unstructured grids*, Commun. Comput. Phys. **3** (2): 342, 2008.

[Vel04] Velivelli A and Bryden K, *A cache-efficient implementation of the lattice Boltzmann method for the two-dimensional diffusion equation*, Concurrency Computat. Pract. Exper. **16** (14): 1415, 2004.

[Ver99] Verberg R and Ladd A, *Simulation of low-Reynolds-number flow via a time-independent lattice-Boltzmann method*, Phys. Rev. E **60** (3): 3366, 1999.

[Ver00] Verberg R and Ladd A, *Lattice-Boltzmann Model with Sub-Grid-Scale Boundary Conditions*, Phys. Rev. Lett. **84** (10): 2148, 2000.

[Ver01] Verberg R and Ladd A, *Accuracy and stability of a lattice-Boltzmann model with subgrid scale boundary conditions*, Phys. Rev. E **65** (1): 016701, 2001.

[Ver09a] Verhaeghe F, Luo L-S, and Blanpain B, *Lattice Boltzmann modeling of microchannel flow in slip flow regime*, J. Comput. Phys. **228** (1): 147, 2009.

[Ver09b] Verschaeve J, *Analysis of the lattice Boltzmann Bhatnagar-Gross-Krook no-slip boundary condition: Ways to improve accuracy and stability*, Phys. Rev. E **80** (3): 036703, 2009.

[Vic89] Vichniac G, *Cellular-Automata Fluids*, in *Instabilities and Nonequilibrium Structures II Dynamical Systems and Instabilities*, eds. Tirapegui E and Villarroel D, Kluwer Academic Publishers, 1989.

[Vid10] Vidal D, Roy R, and Bertrand F, *On improving the performance of large parallel lattice Boltzmann flow simulations in heterogeneous porous media*, Comput. & Fluids **39** (2): 324, 2010.

[Vil02] Villani C, *A Review of Mathematical Topics in Collisional Kinetic Theory*, Handbook of Mathematical Fluid Dynamics **1**: 71, ed. by Friedlander S and Serre D, Elsevier Science, Amsterdam, 2002.

[Wag98] Wagner A, *An H-theorem for the lattice Boltzmann approach to hydrodynamics*, Europhys. Lett. **44** (2): 144, 1998.

[Wal09] Walsh S, Burwinkle H, and Saar M, *A new partial-bounceback lattice-Boltzmann method for fluid flow through heterogeneous media*, Comput. Geosci. **35** (6): 1186, 2009.

[Wan05] Wang J, Zhang X, Bengough A, and Crawford J, *Domain-decomposition method for parallel lattice Boltzmann simulation of incompressible flow in porous media*, Phys. Rev. E **72** (1): 016706, 2005.

[Wel54] Welander P, *On the temperature jump in a rarefied gas*, Ark. Fys. **7** (44): 507, 1954.

[Wel06] Wellein G, Zeiser T, Hager G, and Donath S, *On the single processor performance of simple lattice Boltzmann kernels*, Comput. & Fluids **35** (8–9): 910, 2006.

[Whi03] White F, *Fluid Mechanics*, 5th edition, McGraw-Hill, New York, 2003.

[Wol00] Wolf-Gladrow D, *Lattice-Gas Cellular Automata and Lattice Boltzmann Models: An Introduction*, Lecture Notes in Mathematics **1725**, Springer-Verlag, Berlin, 2000.

[Wol86] Wolfram S, *Cellular automaton fluids 1: Basic theory*, J. Statist. Phys. **45** (3–4): 471, 1986.

[Wor97] Worthing R, Mozer J, and Seeley G, *Stability of lattice Boltzmann methods in hydrodynamic regimes*, Phys. Rev. E **56** (2): 2243, 1997.

[Wu09] Wu J and Shu C, *Implicit velocity correction-based immersed boundary-lattice Boltzmann method and its applications*, J. Comput. Phys. **228** (6): 1963, 2009.

[Wu10a] Wu J and Aidun C, *A method for direct simulation of flexible fiber suspensions using lattice Boltzmann equation with external boundary force*, Int. J. Multiphase Flow **36** (3): 202, 2010.

[Wu10b] Wu J and Aidun C, *Simulating 3D deformable particle suspensions using lattice Boltzmann method with discrete external boundary force*, Internat. J. Numer. Methods Fluids **62** (7): 765, 2010.

[Xi99] Xi H, Peng G, and Chou S-H, *Finite-volume lattice Boltzmann method*, Phys. Rev. E **59** (5): 6202, 1999.

[Xu98] Xu K and Luo L-S, *Connection Between Lattice-Boltzmann Equation and Beam Scheme*, Internat. J. Modern Phys. C **9** (8): 1177, 1998.

[Xu03] Xu K and He X, *Lattice Boltzmann method and gas-kinetic BGK scheme in the low-Mach number viscous flow simulations*, J. Comput. Phys. **190** (1): 100, 2003.

[Yon03] Yong W-A and Luo L-S, *Nonexistence of H theorems for the athermal lattice Boltzmann models with polynomial equilibria*, Phys. Rev. E **67** (5): 051105, 2003.

[Yon05] Yong W-A and Luo L-S, *Nonexistence of H Theorem for Some Lattice Boltzmann Models*, J. Statist. Phys. **121** (1–2): 91, 2005.

[Yon09] Yong W-A, *An Onsager-like relation for the lattice Boltzmann method*, Comput. Math. Appl. **58** (5): 862, 2009.

[Yu02] Yu D, Mei R, and Shyy W, *A multi-block lattice Boltzmann method for viscous fluid flows*, Internat. J. Numer. Methods Fluids **39** (2): 99, 2002.

[Yu05] Yu D, Mei R, and Shyy W, *Improved treatment of the open boundary in the method of Lattice Boltzmann equation*, Progr. Comput. Fluid Dynam. Int. J. **5** (1–2): 3, 2005.

[Zal89] Zaleski S, *Weakly compressible fluid simulations at high Reynolds numbers*, in [Mon89]: 384, 1989.

[Zan89] Zanetti G, *Hydrodynamics of lattice-gas automata*, Phys. Rev. A **40** (3): 1539, 1989.

[Zei08] Zeiser T, Wellein G, Nitsure A, Iglberger K, Rüde U, and Hager G, *Introducing a parallel cache oblivious blocking approach for the lattice Boltzmann method*, Progr. Comput. Fluid Dynam. Int. J. **8** (1–4): 179, 2008.

[Zha06] Zhang R, Shan X, and Chen H, *Efficient kinetic method for fluid simulation beyond the Navier-Stokes equation*, Phys. Rev. E **74** (4): 046703, 2006.

[Zha07] Zhang R, Staroselsky I, and Chen H, *Realization of isotropy of the lattice Boltzmann method via rotation of lattice velocity bases*, J. Comput. Phys. **225** (2): 1262, 2007.

[Zha08] Zhao Y, *Lattice Boltzmann based PDE solver on the GPU*, Visual Comput. **24** (5): 323, 2008.

[Zhe04] Zheng Y, *Analysis of Kinetic Models and Macroscopic Continuum Equations for Rarefied Gas Dynamics*, PhD Thesis, Dept. Mech. Eng., Univ. of Victoria, Canada, 2004.

[Zie93] Ziegler D, *Boundary conditions for lattice Boltzmann simulations*, J. Statist. Phys. **71** (5–6): 1171, 1993.

[Zou95a] Zou Q, Hou S, Chen S, and Doolen G, *An improved incompressible lattice Boltzmann model for time-independent flows*, J. Statist. Phys. **81** (1–2): 35, 1995.

[Zou95b] Zou Q, Hou S, and Doolen G, *Analytical solutions of the lattice Boltzmann BGK model*, J. Statist. Phys. **81** (1–2): 319, 1995.

[Zou97] Zou Q and He X, *On pressure and velocity boundary conditions for the lattice Boltzmann BGK model*, Phys. Fluids **9** (6): 1591, 1997.

YHTEENVETO (FINNISH SUMMARY)

Laskennallinen virtausdynamiikka on tutkimusala, jossa tietokonesimulaatioilla pyritään jäljittelemään todellisia virtausilmiöitä. Yleisesti ottaen tavoitteena on, että näiden simulaatioiden avulla saavutetaan laajempi tai syvällisempi ymmärrys todellisten virtausten käyttäytymisestä. Tietokonesimulaatiot pohjautuvat lähtökohtaisesti matemaattisesti esitettyihin virtausmalleihin: nämä matemaattiset mallit ovat yksikäsitteisiä, mutta toisaalta myös yksinkertaistettuja kuvauksia todellisten virtausten käyttäytymiselle. On myös huomionarvoista, että matemaattisen mallin laatiminen edellyttää aina perustavanlaatuista valintaa. Nimittäin, yhtä luonnonilmiötä voi fysikaalisesti kuvata monen eri mittakaavan malleilla. Esimerkiksi virtaus on pohjimmiltaan atomien ja molekyylien liikettä suuressa mittakaavassa; atomien ja molekyylien skaalassa operoiva malli on mikroskooppisen tason kuvaus. Toisaalta, meidän arkipäiväinen kokemus virtauksista on toisenlainen: virtaus on nesteen yhtenäistä, katkeamatonta liikettä – tosin liike voi ajoittain olla hyvinkin kaoottista. Tällaiseen jatkumoperiaatteeseen nojautuva malli on makroskooppisen tason kuvaus virtauksille.

Tässä väitöskirjassa, jonka otsikko on *Virtausdynamiikan tietokonesimulaatioita Hila-Boltzmann –menetelmällä: implementointi ja reunaehdot*, keskitytään mesoskooppisen tason kuvauksiin virtauksille. Mittakaavoissa tämä taso sijoittuu mikroskooppisen ja makroskooppisen tason väliin. Yleisesti ilmaistuna tässä väitöskirjassa perehdytään keinoihin, joilla mesoskooppisen tason matemaattisesta mallista edetään laskennallisen virtausmenetelmän tietokonetoteutukseen. Lyhyesti selitettynä, kun kaikki matemaattiseen malliin liittyvät yksityiskohdat on kiinnitetty, kuten esimerkiksi niin sanotut reunaehdot ja materiaaliparametrit, mallin muodostaville yhtälöille on olemassa yksikäsitteinen ratkaisu. Tämä ratkaisu on mallin ennustama kuvaus nesteen tai kaasun käyttäytymiselle kulloisessakin virtaustilanteessa. Laskennallinen menetelmä puolestaan on kuvaus mekaanisesta menettelytavasta, jota noudattamalla voidaan laskea likiarvo alkuperäisen mallin ratkaisulle. Menettelytapa on niin mekaaninen, että se voidaan ohjelmoida tietokoneelle – tällöin puhutaan laskennallisen menetelmän tietokonetoteutuksesta. Toisin sanoen, tietokonesimulaatioilla lasketaan likiarvoja alkuperäisen matemaattisen mallin ratkaisuille.

Täsmällisesti ilmaistuna tämä väitöskirja käsittelee tutkimustyömme sitä osaa, jossa olemme vertailleet ja kehittäneet erilaisia vaihtoehtoja Hila-Boltzmann –laskentamenetelmän tietokonetoteutukselle; Hila-Boltzmann –menetelmä perustuu Boltzmannin yhtälöön, joka on mesoskooppisen tason matemaattinen malli sekä statistisen mekaniikan tunnetuimpia kuljetusyhtälöitä. Edellisen aihepiirin lisäksi tämä väitöskirja käsittelee myös Hila-Boltzmann –menetelmän reunaehtoja: tutkimustyössämme olemme kehittäneet niin sanottuja massavuopohjaisia sisään- ja ulosvirtausreunaehtoja. Väitöskirjan alkuosa on laajennettu johdanto yllä mainituille tutkimusaiheille.

A closed mind is like a closed book – just a block of wood.

Chinese Proverb

JYVÄSKYLÄ STUDIES IN COMPUTING

1 Ropponen, Janne, Software risk management - foundations, principles and empirical findings. 273 p. Yhteenveto 1 p. 1999.
2 Kuzmin, Dmitri, Numerical simulation of reactive bubbly flows. 110 p. Yhteenveto 1 p. 1999.
3 Karsten, Helena, Weaving tapestry: collaborative information technology and organisational change. 266 p. Yhteenveto 3 p. 2000.
4 Koskinen, Jussi, Automated transient hypertext support for software maintenance. 98 p. (250 p.) Yhteenveto 1 p. 2000.
5 Ristaniemi, Tapani, Synchronization and blind signal processing in CDMA systems. - Synkronointi ja sokea signaalinkäsittely CDMA järjestelmässä. 112 p. Yhteenveto 1 p. 2000.
6 Laitinen, Mika, Mathematical modelling of conductive-radiative heat transfer. 20 p. (108 p.) Yhteenveto 1 p. 2000.
7 Koskinen, Minna, Process metamodelling. Conceptual foundations and application. 213 p. Yhteenveto 1 p. 2000.
8 Smolianski, Anton, Numerical modeling of two-fluid interfacial flows. 109 p. Yhteenveto 1 p. 2001.
9 Nahar, Nazmun, Information technology supported technology transfer process. A multi-site case study of high-tech enterprises. 377 p. Yhteenveto 3 p. 2001.
10 Fomin, Vladislav V., The process of standard making. The case of cellular mobile telephony. - Standardin kehittämisen prosessi. Tapaustutkimus solukkoverkkoon perustuvasta matkapuhelintekniikasta. 107 p. (208 p.) Yhteenveto 1 p. 2001.
11 Päivärinta, Tero, A genre-based approach to developing electronic document management in the organization. 190 p. Yhteenveto 1 p. 2001.
12 Häkkinen, Erkki, Design, implementation and evaluation of neural data analysis environment. 229 p. Yhteenveto 1 p. 2001.
13 Hirvonen, Kullervo, Towards better employment using adaptive control of labour costs of an enterprise. 118 p. Yhteenveto 4 p. 2001.
14 Majava, Kirsi, Optimization-based techniques for image restoration. 27 p. (142 p.) Yhteenveto 1 p. 2001.
15 Saarinen, Kari, Near infra-red measurement based control system for thermo-mechanical refiners. 84 p. (186 p.) Yhteenveto 1 p. 2001.
16 Forsell, Marko, Improving component reuse in software development. 169 p. Yhteenveto 1 p. 2002.
17 Virtanen, Pauli, Neuro-fuzzy expert systems in financial and control engineering. 245 p. Yhteenveto 1 p. 2002.
18 Kovalainen, Mikko, Computer mediated organizational memory for process control. Moving CSCW research from an idea to a product. 57 p. (146 p.) Yhteenveto 4 p. 2002.
19 Hämäläinen, Timo, Broadband network quality of service and pricing. 140 p. Yhteenveto 1 p. 2002.
20 Martikainen, Janne, Efficient solvers for discretized elliptic vector-valued problems. 25 p. (109 p.) Yhteenveto 1 p. 2002.
21 Mursu, Anja, Information systems development in developing countries. Risk management and sustainability analysis in Nigerian software companies. 296 p. Yhteenveto 3 p. 2002.
22 Seleznyov, Alexandr, An anomaly intrusion detection system based on intelligent user recognition. 186 p. Yhteenveto 3 p. 2002.
23 Lensu, Anssi, Computationally intelligent methods for qualitative data analysis. 57 p. (180 p.) Yhteenveto 1 p. 2002.
24 Ryabov, Vladimir, Handling imperfect temporal relations. 75 p. (145 p.) Yhteenveto 2 p. 2002.
25 Tsymbal, Alexey, Dynamic integration of data mining methods in knowledge discovery systems. 69 p. (170 p.) Yhteenveto 2 p. 2002.
26 Akimov, Vladimir, Domain decomposition methods for the problems with boundary layers. 30 p. (84 p.). Yhteenveto 1 p. 2002.
27 Seyukova-Rivkind, Ludmila, Mathematical and numerical analysis of boundary value problems for fluid flow. 30 p. (126 p.) Yhteenveto 1 p. 2002.
28 Hämäläinen, Seppo, WCDMA Radio network performance. 235 p. Yhteenveto 2 p. 2003.
29 Pekkola, Samuli, Multiple media in group work. Emphasising individual users in distributed and real-time CSCW systems. 210 p. Yhteenveto 2 p. 2003.
30 Markkula, Jouni, Geographic personal data, its privacy protection and prospects in a location-based service environment. 109 p. Yhteenveto 2 p. 2003.
31 Honkaranta, Anne, From genres to content analysis. Experiences from four case organizations. 90 p. (154 p.) Yhteenveto 1 p. 2003.
32 Raitamäki, Jouni, An approach to linguistic pattern recognition using fuzzy systems. 169 p. Yhteenveto 1 p. 2003.
33 Saalasti, Sami, Neural networks for heart rate time series analysis. 192 p. Yhteenveto 5 p. 2003.
34 Niemelä, Marketta, Visual search in graphical interfaces: a user psychological approach. 61 p. (148 p.) Yhteenveto 1 p. 2003.
35 You, Yu, Situation Awareness on the world wide web. 171 p. Yhteenveto 2 p. 2004.
36 Taatila, Vesa, The concept of organizational competence – A foundational analysis. - Perusteanalyysi organisaation kompetenssin käsitteestä. 111 p. Yhteenveto 2 p. 2004.

37 LYYTIKÄINEN, VIRPI, Contextual and structural metadata in enterprise document management. - Konteksti- ja rakennemetatieto organisaation dokumenttien hallinnassa. 73 p. (143 p.) Yhteenveto 1 p. 2004.
38 KAARIO, KIMMO, Resource allocation and load balancing mechanisms for providing quality of service in the Internet. 171 p. Yhteenveto 1 p. 2004.
39 ZHANG, ZHEYING, Model component reuse. Conceptual foundations and application in the metamodeling-based systems analysis and design environment. 76 p. (214 p.) Yhteenveto 1 p. 2004.
40 HAARALA, MARJO, Large-scale nonsmooth optimization variable metric bundle method with limited memory. 107 p. Yhteenveto 1 p. 2004.
41 KALVINE, VIKTOR, Scattering and point spectra for elliptic systems in domains with cylindrical ends. 82 p. 2004.
42 DEMENTIEVA, MARIA, Regularization in multistage cooperative games. 78 p. 2004.
43 MAARANEN, HEIKKI, On heuristic hybrid methods and structured point sets in global continuous optimization. 42 p. (168 p.) Yhteenveto 1 p. 2004.
44 FROLOV, MAXIM, Reliable control over approximation errors by functional type a posteriori estimates. 39 p. (112 p.) 2004.
45 ZHANG, JIAN, Qos- and revenue-aware resource allocation mechanisms in multiclass IP networks. 85 p. (224 p.) 2004.
46 KUJALA, JANNE, On computation in statistical models with a psychophysical application. 40 p. (104 p.) 2004.,
47 SOLBAKOV, VIATCHESLAV, Application of mathematical modeling for water environment problems. 66 p. (118 p.) 2004.
48 HIRVONEN, ARI P., Enterprise architecture planning in practice. The Perspectives of information and communication technology service provider and end-user. 44 p. (135 p.) Yhteenveto 2 p. 2005.
49 VARTIAINEN, TERO, Moral conflicts in a project course in information systems education. 320 p. Yhteenveto 1p. 2005.
50 HUOTARI, JOUNI, Integrating graphical information system models with visualization techniques. - Graafisten tietojärjestelmäkuvausten integrointi visualisointitekniikoilla. 56 p. (157 p.) Yhteenveto 1p. 2005.
51 WALLENIUS, EERO R., Control and management of multi-access wireless networks. 91 p. (192 p.) Yhteenveto 3 p. 2005.
52 LEPPÄNEN, MAURI, An ontological framework and a methodical skeleton for method engineering – A contextual approach. 702 p. Yhteenveto 2 p. 2005.
53 MATYUKEVICH, SERGEY, The nonstationary Maxwell system in domains with edges and conical points. 131 p. Yhteenveto 1 p. 2005.
54 SAYENKO, ALEXANDER, Adaptive scheduling for the QoS supported networks. 120 p. (217 p.) 2005.
55 KURJENNIEMI, JANNE, A study of TD-CDMA and WCDMA radio network enhancements. 144 p. (230 p.) Yhteenveto 1 p. 2005.
56 PECHENIZKIY, MYKOLA, Feature extraction for supervised learning in knowledge discovery systems. 86 p. (174 p.) Yhteenveto 2 p. 2005.
57 IKONEN, SAMULI, Efficient numerical methods for pricing American options. 43 p. (155 p.) Yhteenveto 1 p. 2005.
58 KÄRKKÄINEN, KARI, Shape sensitivity analysis for numerical solution of free boundary problems. 83 p. (119 p.) Yhteenveto 1 p. 2005.
59 HELFENSTEIN, SACHA, Transfer. Review, reconstruction, and resolution. 114 p. (206 p.) Yhteenveto 2 p. 2005.
60 NEVALA, KALEVI, Content-based design engineering thinking. In the search for approach. 64 p. (126 p.) Yhteenveto 1 p. 2005.
61 KATASONOV, ARTEM, Dependability aspects in the development and provision of location-based services. 157 p. Yhteenveto 1 p. 2006.
62 SARKKINEN, JARMO, Design as discourse: Representation, representational practice, and social practice. 86 p. (189 p.) Yhteenveto 1 p. 2006.
63 ÄYRÄMÖ, SAMI, Knowledge mining using robust clustering. 296 p. Yhteenveto 1 p. 2006.
64 IFINEDO, PRINCELY EMILI, Enterprise resource planning systems success assessment: An integrative framework. 133 p. (366 p.) Yhteenveto 3 p. 2006.
65 VIINIKAINEN, ARI, Quality of service and pricingin future multiple service class networks. 61 p. (196 p.) Yhteenveto 1 p. 2006.
66 WU, RUI, Methods for space-time parameter estimation in DS-CDMA arrays. 73 p. (121 p.) 2006.
67 PARKKOLA, HANNA, Designing ICT for mothers. User psychological approach. – Tieto- ja viestintätekniikoiden suunnittelu äideille. Käyttäjäpsykologinen näkökulma. 77 p. (173 p.) Yhteenveto 3 p. 2006.
68 HAKANEN, JUSSI, On potential of interactive multiobjective optimization in chemical process design. 75 p. (160 p.) Yhteenveto 2 p. 2006.
69 PUTTONEN, JANI, Mobility management in wireless networks. 112 p. (215 p.) Yhteenveto 1 p. 2006.
70 LUOSTARINEN, KARI, Resource , management methods for QoS supported networks. 60 p. (131 p.) 2006.
71 TURCHYN, PAVLO, Adaptive meshes in computer graphics and model-based simulation. 27 p. (79 p.) Yhteenveto 1 p.
72 ZHOVTOBRYUKH, DMYTRO, Context-aware web service composition. 290 p. Yhteenveto 2 p. 2006.

73 KOHVAKKO, NATALIYA, Context modeling and utilization in heterogeneous networks. 154 p. Yhteenveto 1 p. 2006.
74 MAZHELIS, OLEKSIY, Masquerader detection in mobile context based on behaviour and environment monitoring. 74 p. (179 p). Yhteenveto 1 p. 2007.
75 SILTANEN, JARMO, Quality of service and dynamic scheduling for traffic engineering in next generation networks. 88 p. (155 p.) 2007.
76 KUUVA, SARI, Content-based approach to experiencing visual art. - Sisältöperustainen lähestymistapa visuaalisen taiteen kokemiseen. 203 p. Yhteenveto 3 p. 2007.
77 RUOHONEN, TONI, Improving the operation of an emergency department by using a simulation model. 164 p. 2007.
78 NAUMENKO, ANTON, Semantics-based access control in business networks. 72 p. (215 p.) Yhteenveto 1 p. 2007.
79 WAHLSTEDT, ARI, Stakeholders' conceptions of learning in learning management systems development. - Osallistujien käsitykset oppimisesta oppimisympäristöjen kehittämisessä. 83 p. (130 p.) Yhteenveto 1 p. 2007.
80 ALANEN, OLLI, Quality of service for triple play services in heterogeneous networks. 88 p. (180 p.) Yhteenveto 1 p. 2007.
81 NERI, FERRANTE, Fitness diversity adaptation in memetic algorithms. 80 p. (185 p.) Yhteenveto 1 p. 2007.
82 KURHINEN, JANI, Information delivery in mobile peer-to-peer networks. 46 p. (106 p.) Yhteenveto 1 p. 2007.
83 KILPELÄINEN, TURO, Genre and ontology based business information architecture framework (GOBIAF). 74 p. (153 p.) Yhteenveto 1 p. 2007.
84 YEVSEYEVA, IRYNA, Solving classification problems with multicriteria decision aiding approaches. 182 p. Yhteenveto 1 p. 2007.
85 KANNISTO, ISTO, Optimized pricing, QoS and segmentation of managed ICT services. 45 p. (111 p.) Yhteenveto 1 p. 2007.
86 GORSHKOVA, ELENA, A posteriori error estimates and adaptive methods for incompressible viscous flow problems. 72 p. (129 p.) Yhteenveto 1 p. 2007.
87 LEGRAND, STEVE, Use of background real-world knowledge in ontologies for word sense disambiguation in the semantic web. 73 p. (144 p.) Yhteenveto 1 p. 2008.
88 HÄMÄLÄINEN, NIINA, Evaluation and measurement in enterprise and software architecture management. - Arviointi ja mittaaminen kokonais- ja ohjelmistoarkkitehtuurien hallinnassa. 91 p. (175 p.) Yhteenveto 1 p. 2008.
89 OJALA, ARTO, Internationalization of software firms: Finnish small and medium-sized software firms in Japan. 57 p. (180 p.) Yhteenveto 2 p. 2008.
90 LAITILA, ERKKI, Symbolic Analysis and Atomistic Model as a Basis for a Program Comprehension Methodology. 321 p. Yhteenveto 3 p. 2008.
91 NIHTILÄ, TIMO, Performance of Advanced Transmission and Reception Algorithms for High Speed Downlink Packet Access. 93 p. (186 p.) Yhteenveto 1 p. 2008.
92 SETÄMAA-KÄRKKÄINEN, ANNE, Network connection selection-solving a new multiobjective optimization problem. 52 p. (111p.) Yhteenveto 1 p. 2008.
93 PULKKINEN, MIRJA, Enterprise architecture as a collaboration tool. Discursive process for enterprise architecture management, planning and development. 130 p. (215 p.) Yhteenveto 2 p. 2008.
94 PAVLOVA, YULIA, Multistage coalition formation game of a self-enforcing international environmental agreement. 127 p. Yhteenveto 1 p. 2008.
95 NOUSIAINEN, TUULA, Children's involvement in the design of game-based learning environments. 297 p. Yhteenveto 2 p. 2008.
96 KUZNETSOV, NIKOLAY V., Stability and oscillations of dynamical systems. Theory and applications. 116 p. Yhteenveto 1 p. 2008.
97 KHRIYENKO, OLEKSIY, Adaptive semantic Web based environment for web resources. 193 p. Yhteenveto 1 p. 2008.
98 TIRRONEN, VILLE, Global optimization using memetic differential evolution with applications to low level machine vision. 98 p. (248 p.) Yhteenveto 1 p. 2008.
99 VALKONEN, TUOMO, Diff-convex combinations of Euclidean distances: A search for optima. 148 p. Yhteenveto 1 p. 2008.
100 SARAFANOV, OLEG, Asymptotic theory of resonant tunneling in quantum waveguides of variable cross-section. 69 p. Yhteenveto 1 p. 2008.
101 POZHARSKIY, ALEXEY, On the electron and phonon transport in locally periodical waveguides. 81 p. Yhteenveto 1 p. 2008.
102 AITTOKOSKI, TIMO, On challenges of simulation-based globaland multiobjective optimization. 80 p. (204 p.) Yhteenveto 1 p. 2009.
103 YALAHO, ANICET, Managing offshore outsourcing of software development using the ICT-supported unified process model: A cross-case analysis. 91 p. (307 p.) Yhteenveto 4 p. 2009.
104 KOLLANUS, SAMI, Tarkastuskäytänteiden kehittäminen ohjelmistoja tuottavissa organisaatioissa. - Improvement of inspection practices in software organizations. 179 p. Summary 4 p. 2009.
105 LEIKAS, JAANA, Life-Based Design. 'Form of life' as a foundation for ICT design for older adults. - Elämälähtöinen suunnittelu. Elämänmuoto ikääntyville tarkoitettujen ICT tuotteiden ja palvelujen suunnittelun lähtökohtana. 218 p. (318 p.) Yhteenveto 4 p. 2009.

106 VASILYEVA, EKATERINA, Tailoring of feedback in web-based learning systems: Certitude-based assessment with online multiple choice questions. 124 p. (184 p.) Yhteenveto 2 p. 2009.

107 KUDRYASHOVA, ELENAV., Cycles in continuous and discrete dynamical systems. Computations, computer assisted proofs, and computer experiments. 79 p. (152 p.) Yhteenveto 1 p. 2009.

108 BLACKLEDGE, JONATHAN, Electromagnetic scattering and inverse scattering solutions for the analysis and processing of digital signals and images. 297 p. Yhteenveto 1 p. 2009.

109 IVANNIKOV, ANDRIY, Extraction of event-related potentials from electroencephalography data. - Herätepotentiaalien laskennallinen eristäminen EEG-havaintoaineistosta. 108 p. (150 p.) Yhteenveto 1 p. 2009.

110 KALYAKIN, IGOR, Extraction of mismatch negativity from electroencephalography data. - Poikkeavuusnegatiivisuuden erottaminen EEG-signaalista. 47 p. (156 p.) Yhteenveto 1 p. 2010.

111 HEIKKILÄ, MARIKKA, Coordination of complex operations over organisational boundaries. 265 p. Yhteenveto 3 p. 2010.

112 FEKETE, GÁBOR, Network interface management in mobile and multihomed nodes. 94 p. (175 p.) Yhteenveto 1 p. 2010.

113 KUJALA, TUOMO, Capacity, workload and mental contents - Exploring the foundations of driver distraction. 146 p. (253 p.) Yhteenveto 2 p. 2010.

114 LUGANO, GIUSEPPE, Digital community design - Exploring the role of mobile social software in the process of digital convergence. 253 p. (316 p.) Yhteenveto 4 p. 2010.

115 KAMPYLIS, PANAGIOTIS, Fostering creative thinking. The role of primary teachers. - Luovaa ajattelua kehittämässä. Alakoulun opettajien rooli. 136 p. (268 p.) Yhteenveto 2 p. 2010.

116 TOIVANEN, JUKKA, Shape optimization utilizing consistent sensitivities. - Muodon optimointi käyttäen konsistentteja herkkyyksiä. 55 p. (130 p.) Yhteenveto 1 p. 2010.

117 MATTILA, KEIJO, Implementation techniques for the lattice Boltzmann method. - Virtausdynamiikan tietokonesimulaatioita Hila-Boltzmann -menetelmällä: implementointi ja reunaehdot. 177 p. (233 p.) Yhteenveto 1 p. 2010.